FACTORS DETERMINING THE THERMOLUMINESCENCE OF CHRONOLOGICALLY SIGNIFICANT MATERIALS

by

Ann Grace Wintle

Thesis submitted for the degree of

Doctor of Philosophy

at the

University of Oxford

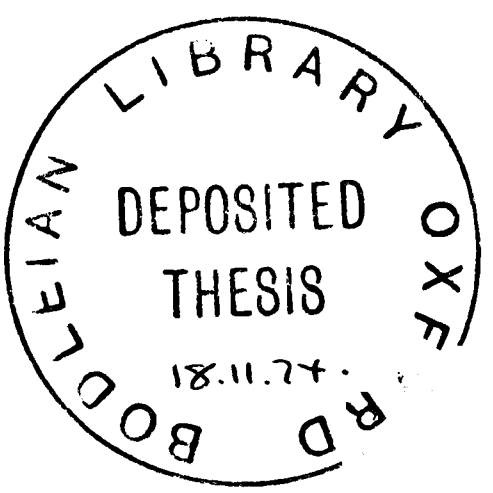

Linacre College,
Oxford.

Hilary Term,
1974.

FACTORS DETERMINING THE THERMOLUMINESCENCE OF CHRONOLOGICALLY SIGNIFICANT MATERIALS

A B S T R A C T

Thermoluminescence has been successfully applied to the dating of pottery from archaeological sites and the good agreement obtained between the TL dates and the archaeologically known dates suggested that the basic assumptions concerning the build up and release of trapped charges were correct. In this thesis I report the results of a test programme I carried out on recent volcanic lava of known age: the TL ages were all far too young and hence it was apparent that at least one of the assumptions used in the dating of pottery was invalid when applied to lava.

The most obvious differences between pottery and lava dating were studied, such as the effect of crushing such a hard material to obtain fine grains and the influence of the known occurrence of radioactive disequilibrium in recent lavas, but the cause of the low ages was found to be the breakdown of a far more basic assumption. The assumption that electrons in deep traps are capable of remaining in the traps over archaeological time is the basic tenet upon which the whole of TL dating is based. In the case of lava it is shown in this thesis that this does not hold; there was a loss of high temperature TL during storage at room temperature for a few hours. This effect was called 'anomalous fading' as it is in disagreement with thermal untrapping of electrons predicted by kinetic

theory and widely accepted in the literature.

The third part of this thesis describes the experiments carried out in an attempt to elucidate this phenomenon which was found to be exhibited by a variety of minerals that would normally be considered suitable for the application of TL dating. The same phenomenon has since been reported in the study of the TL of lunar samples and similar effects in other materials are also reported in the final chapter. Two models are suggested which are consistent with the experimental evidence accumulated. They both involve the tunnelling of an electron at low temperatures but differ in their explanation of the thermal dependence observed in experiments at room temperature. The implications of these models with regard to testing for anomalous fading are discussed and it is concluded that, when contemplating the application of TL dating to a new material, a test programme should be carried out on samples of known age and, furthermore, the agreement of the archaeological stability of electrons with that predicted by kinetic analysis of the TL peaks should also be demonstrated.

Kinetic analysis carried out on one of the high temperature peaks in limestone agreed with the stability suggested by the geological age of the sample. This confirmed the absence of anomalous fading in this mineral as had been suggested by short-term fading tests. In similar studies on quartz the archaeological stability was found to be greater than that predicted by kinetic analysis using the initial rise method. This discrepency is shown to be due to the inapplicability of the initial rise method to samples in which thermal quenching is occurring. In the past the initial rise has been the most frequently used method of trap depth determination because of its independence of the untrapping kinetics; what has been completely overlooked is that in thermoluminescence the signal will also

be affected by any temperature dependence of the luminescence centres. Once this had been allowed for the predicted stability again confirmed the absence of anomalous fading in quartz and hence its suitability for dating. .

.....

C O N T E N T S

PART I

PART I

This section outlines the basic principles of TL dating as developed for pottery. The problems of radioactive disequilibrium are discussed and the methods of kinetic analysis used in Part II are explained. A dating programme on recent lava is reported; the failure to obtain meaningful dates led to the discovery of 'anomalous fading' which was investigated in detail as described in Part III.

CHAPTER 1 INTRODUCTION

1.1 THERMOLUMINESCENT DATING OF POTTERY

The property of thermoluminescence (TL) exhibited by certain minerals which are commonly found in pottery has enabled a dating technique to be established (Aitken and Fleming, 1973). The TL process can be thought of in naive terms as due to the production of charge carriers (electrons or holes) by naturally occurring ionizing radiation, their subsequent trapping at defects in the crystal and their eventual recombination at luminescent centres in the crystal after thermal activation out of the traps by the application of heat. The traps that have been filled during geological time are emptied, in the case of pottery, by man firing the pot and they then start to fill again at a rate that is proportional to the radiation dose rate experienced. When the sample is subsequently heated in the laboratory a plot of light emission measured with a photomultiplier versus temperature is obtained and this is termed a TL glow curve. The deeper the trap the more resistant it is to thermal activation and hence the charge carriers that are most stable over archaeological time are also those that are associated with the TL occurring at a higher temperature during a glow curve. The intensity of the light at any given temperature and heating rate is proportional to the absorbed dose of ionizing radiation.

The natural dose rate is of the order of one rad per year. It is made up of:

(a) an internal dose rate due to the radioactive impurities in the pottery, typically a few parts per million of uranium and thorium and a few parts per hundred of potassium;

(b) an environmental dose rate due to the same impurities but in the surrounding soil, and

(c) a small cosmic dose rate.

The basic equation used for dating is

$$\text{Age} = \frac{\text{Accumulated TL}}{(\text{TL per rad}) \times (\text{rads per year})} \qquad (1.1)$$

where the accumulated TL is obtained from the first glow curve, the (TL per rad) is the sensitivity determined by measuring the TL induced by a known absorbed dose of radiation and the (rads per year) is the absorbed dose rate as calculated from radioactivity measurements of the pottery and the surrounding soil. The accumulated TL as described above is that light which is associated with the emptying of deep traps i.e. those which are considered to retain their charges over archaeological time as implied by the kinetic equations discussed in Chapter 3. In general, for a heating rate of about 10°C/second these traps empty at glow curve temperatures of about 350°C and above. Measurement of traps emptying above 450°C is not usually possible due to the dominance of thermal emission from the sample: this is commonly termed 'black body radiation'.

1.2 GRAIN SIZE DOSIMETRY AND ASSOCIATED TL

Two methods of dating pottery have been developed using grain sizes that are particularly suited to the microdosimetry applicable to TL sensitive grains in pottery.

(a) Fine Grain Dating

Grains of 1-8 μ diameter in an homogenous radioactive matrix are fully irradiated by the α radiation from the uranium and thorium chains as well as the β and γ radiation from the sherd and the environmental radiation.

One important feature that must be taken into account is that although for typical pottery the α dose makes up the majority of the dose it has been found that the relative effectiveness of α radiation in producing TL is down by about an order of magnitude when compared with β and γ radiation. This effectiveness is conveniently expressed for a given sample as the 'k value'.

TL sensitivity measurements are made by depositing the grains on aluminium discs 1 cm in diameter and irradiating them with a $^{90}Sr/^{90}Y$ β source and a ^{244}Cm α source (Zimmerman, 1971a). It is convenient to rewrite equation (1.1) as

$$\text{Age} = \frac{(ED)_{FG}}{k\,D\alpha + D\beta + D\gamma + Dc} \qquad (1.2)$$

where

$$(ED)_{FG} = \frac{\text{Accumulated TL}}{(\text{TL per rad})\,\beta}$$

and is termed the 'equivalent dose' and where

$$k = \frac{(\text{TL per rad})\,\alpha}{(\text{TL per rad})\,\beta} \quad \text{as defined above.}$$

$D\alpha$, $D\beta$, $D\gamma$ and Dc are the annual dose rates of alpha, beta, gamma and cosmic radiations.

(b) Inclusion Dating

Quartz grains found in pottery have negligible self radioactivity and hence quartz grains of 90-105 μ diameter receive the full γ dose, a slightly attenuated β dose and a severely attenuated α dose. If the outer α irradiated layer is removed by etching with hydrofluoric acid, the α ray contribution to the TL observed becomes negligible (Fleming, 1970).

In this case the age equation becomes

$$\text{Age} = \frac{(ED)\ \text{Incl}}{D\beta + D\gamma + Dc} \qquad (1.3)$$

where the equivalent dose has been obtained from measurements on such etched inclusions.

1.3 DOSE RATE EVALUATION

The major contributors to the dose rate are the ^{238}U and ^{232}Th chains and ^{40}K. The routine measurement of ^{238}U and ^{232}Th is done by the technique of thick source alpha counting (Tite and Waine) using a ZnS screen and photomultiplier; about 1 gramme of material is needed and a typical measurement time is 12 hours. This method has the advantage that it is far less susceptible to disequilibrium effects than chemical analysis and is relatively simple to set up; the major disadvantage is due to the effect of emanation of the gaseous decay product ^{222}Rn. The extent of its emanation during burial is also a likely source of error in determining the appropriate dose rate.

The ^{40}K dose rate (β and γ only) is deduced from the total potassium content, determined by the standard technique of flame photometry. Mrs. G. Huxtable carried out such measurements for the work in this thesis.

The environmental dose rate can be determined by similar measurements on a sample of the surrounding soil, but is best measured by leaving a capsule containing a suitable TL phosphor (e.g. natural CaF_2 or $CaSO_4$: Dy) in the same archaeological context as the pottery for about a year. This makes allowance for seasonal fluctuations as may be caused by changes in γ attenuation by water and radon migration.

A discussion of the problems involved in TL dating and the method of assessment of the error limits in dating pottery has been presented by

Aitken and Alldred and these considerations are borne in mind throughout the thesis (Aitken and Alldred).

1.4 EXTENSION OF TL DATING TO MATERIAL OTHER THAN POTTERY

There is a very great need for an absolute dating method which would cover the Pleistocene period i.e. the last million years. Figure 1.1 shows some of the various dating methods that have been used to date events in the last million years; the broken lines indicate where the methods have been applied in exceptional circumstances. In the case of potassium-argon dating the youngest rocks that can be satisfactorily dated are usually within the age range 50,000 - 500,000 years BP.* In exceptional circumstances, large pure samples of potassium rich minerals have yielded reproducible ages as young as 10,000 years BP (Dalrymple), but material suitable for such an analysis is very rare. The youngest age that can be measured by the fission track method depends upon the uranium content of the material for study; much younger zircon, with high uranium content, than mica can be dated (Fleischer and Hart). The sources of error in the radiocarbon and uranium series disequilibrium dating have been extensively discussed, particularly when more than one method has been used to date the same sample (Broecker and Bender). A method that is not dependent on a radioactive decay constant would do much to alleviate present dating problems (Vita-Finzi).

When the use of TL as a tool for dating was first suggested, two of the possible fields of application were volcanic lava and carbonate formations. But the lack of knowledge about such effects as the low α efficiency and non-radiation induced light due to heating in air (termed 'spurious TL') led to errors in experimental attempts to obtain meaningful dates.

However, with ten years experience of overcoming such problems in pottery dating, the time seemed ripe for moving TL dating into new fields;

* BP = before present

in particular there was a need for dating volcanic lava which retains information about the Earth's magnetic field at the time of formation of the lava and a stimulus for the initial direction of this thesis was the need for more precise dating of the so-called Laschamp polarity event bracketed between 8,000 and 20,000 years BP by radiocarbon and potassium-argon dating (Bonhommet and Zahringer).

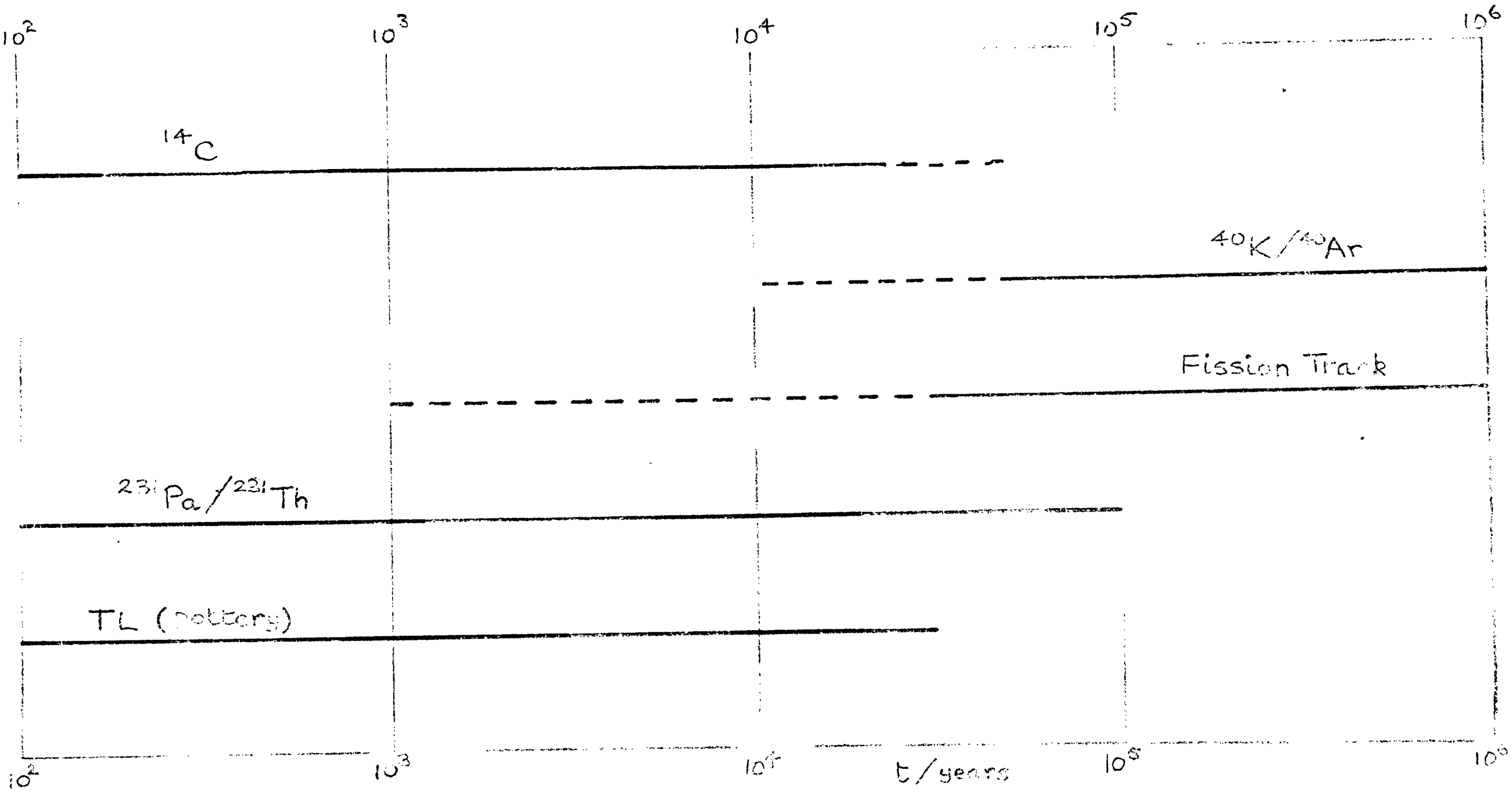

Fig. 1.1 Approximate range of dating techniques applicable to the last million years

CHAPTER 2 SPECIAL PROBLEMS IN DATING NON-POTTERY MATERIALS

2.1 INTRODUCTION

Thermoluminescent (TL) dating of archaeological ceramics has been developed over the past ten years to the extent that a dating accuracy of about ± 7% is now possible for pottery fragments collected from satisfactory burial contexts. The good agreement obtained for samples of known archaeological age (Zimmerman, 1971(a); Fleming, 1970) confirmed the basic assumptions of the dating method -

(a) that the electrons in deep traps that give rise to the high temperature part of the glow curve are stable over archaeological time;

(b) that the calculated radiation dosimetry for the two grain sizes (1-8 μ and 90-105 μ) used for the dating techniques is correct;

(c) that the dose rate received by the pottery over archaeological time is not significantly different from that calculated from laboratory measurements of the present day radioactivity.

In considering the extension of the TL dating method to non-pottery samples, both geological and archaeological, the validity and applicability of these tenets has to be studied in theory and by experiment. Other problems connected with the individual materials are also considered.

2.2 SAMPLE PREPARATION

(a) Effect of crushing sample for alpha counting

When using fine grains from the ground mass for TL measurement, one needs to know whether the uranium and thorium is distributed uniformly in

the ground mass or whether there are any radioactive inclusions with a diameter of the order of the α particle ranges because if so, the dose received by the fine grains will be attenuated. Zimmerman found few such inclusions; using induced fission track studies of 6 pieces of pottery and by considering α counts on viced and powdered samples he decided that in the sherds studied there was on average only a 6% increase for the powdered sample. This might however be affected by the change in counting geometry as in the viced sample most of it is still large compared to the alpha particle range (~ 25 microns); if so, the effect of radioactive inclusions would have been even less.

Only two lava samples have been studied for this effect and the results are shown in Table 2.1. Because there was little difference between the viced and powdered α counts for these two lavas (22 h4 from Etna; 132 a1 from the Massif Central), the effect of any radioactive inclusions was considered negligible compared to the errors suggested in Chapter 4 and no further work was done. The results quoted are all within the statistical error of the unsealed alpha counts.

(b) Effect of crushing on the TL measurement

In the extraction from pottery of 1-8 μ and 90-150 μ grains for TL measurements, various methods of breaking up the piece of pot were considered and vicing was found to be the best method to retain the grain size distribution. This is important as the addition to the naturally occurring fine grains of crystals broken off large grains will reduce the equivalent dose obtained; the larger grains have a smaller equivalent dose because they have received far less alpha radiation from the clay matrix.

Lava ground mass is very much harder than the relatively weak fired clay matrix. It is very difficult to crush in a vice and other more violent

TABLE 2.1

ALPHA COUNTS OBTAINED FOR LAVAS

(a) viced and immediately sealed
(b) viced, sealed and left 10 days
(c) powdered and immediately sealed

} counts / k sec

lava	a	b	c
22 h4	14.7	14.9	14.5
132 a1	6.46	6.56	6.45

methods of crushing were tried; a hydraulic jack and a roller mill in the Department of Mineralogy, Oxford, were used. Fine grains (1-8 μ) were collected after the sample had been fed into the mill once, 4-6 times and 6-8 times. The 'equivalent beta dose' obtained for each set of fine grain discs is shown in Table 2.2 along with those obtained by extracting fine grains after vicing two pieces from the same lump of lava. The equivalent dose for fine grains if the sample is 35,000 years old should be 11.5 krads. Apart from the general level being altogether too low, it can be seen from the variation that preparation of fine grain samples from lava must be given further thought.

Severe crushing could give rise to a reduced equivalent dose for several reasons other than the above radiation dosimetry problem -

(i) Lava flows that are covered by more recent flows or sediments sometimes contain secondary minerals which are either washed in as fine grains or are redeposited e.g. quartz and calcium carbonate respectively. A thin section was made of the lava and no evidence for secondary minerals was seen under the microscope. Also, as both of the minerals have distinctive glow curves their presence would be noticed in the TL measurements; neither were considered present in the fine grain measurements.

(ii) The crushing might produce new traps, which would give rise to an increase in the TL sensitivity as measured by a subsequent laboratory irradiation, Fig. 2.1. To study this, a piece of the same lava was thermally drained for an hour at 500°C, cooled and given a 3.9 krad γ dose. Various sets of fine grain discs were prepared from the sample over the fortnight following the irradiation by vicing and by crushing in the roller mill. They all gave an equivalent dose between 1.1 and 1.9 krads. This suggested that the sensitivity to the monitor irradiations might have been increased

TABLE 2.2

THE VARIATION OF "EQUIVALENT DOSE BETA" FOR FINE GRAIN DISCS AS A RESULT OF CRUSHING LAVA 132 a1 BY VICING AND USING A ROLLER MILL

Sample number	method	ED beta/krad
1.2	mill x 1	6.9 ± .2
1.3	mill x 4-6	2.0
1.5	mill x 4-6	2.0
1.6	mill x 6-8	2.0
1.7	viced	0.6
1.9	viced	1.5

compared with its sensitivity prior to crushing. However subsequent work showed the explanation to be due to 'anomalous fading', Chapter 7.

2.3 LAVA RADIOACTIVITY MEASUREMENTS

(a) Disequilibrium due to gaseous radionuclides

The uranium and thorium activity are measured by the technique of thick source α-counting (Cherry): the pot is crushed in a vice and spread uniformly on a zinc sulphide screen which is placed on a photomultiplier tube; this method is used in preference to chemical analysis or activation analysis because it minimises the effect of any disequilibrium in the uranium or thorium decay chains. Table 2.3 shows the major aspects of the two decay chains.

In pottery the major source of disequilibrium that must be taken into account in TL dating is the escape of the gas ^{222}Rn (radon)(Desai and Aitken). Radon has a half life of 3.8 days and is capable of moving through soil (Tanner), about 200 cm if the soil is dry but only 2 cm if the soil is saturated. The rate of escape of radon is thought to depend on three factors -

(i) the concentration of ^{226}Ra in the soil,

(ii) the fraction of the total number of ^{226}Ra atoms that are located on or near the surface of mineral grains and soil particles in a position that favours the escape of the newly formed daughter atoms into the soil gas;

(iii) the physical characteristics of the near surface soil which determine the rate of diffusion of radon within the soil gas and the rate of transport of radon across the earth-air interface.

In a study of ^{222}Rn exhalation on the island of Hawaii the lava was found to have an emanating power about 3% that of the deep, agricultural soils on the island which had originated from volcanic ash. This indicated

TABLE 2.3

^{238}U series

Isotope	Classical name	half life	Primary decay mode
$^{238}_{92}U$	Uranium 1	4.5×10^{9} yr.	α
$^{234}_{90}Th$	Uranium X_1	24.1 days	β^-
$^{234}_{91}Pa$	Uranium X_2	1.17 min	β^-
$^{234}_{91}Pa$	Uranium Z	6.75 hrs.	β^-
$^{234}_{92}U$	Uranium 11	2.47×10^{5} yr.	α
$^{230}_{90}Th$	Ionium	8×10^{4} yr.	α
$^{226}_{88}Ra$	Radium	1,602 yr.	α
$^{222}_{86}Rn$	Radon	3.82 days	α
$^{218}_{84}Po$	Radium A	3.05 min	α
$^{214}_{82}Pb$	Radium B	26.8 min	β^-
$^{214}_{83}Bi$	Radium C	19.7 min	α, β^{-} *
$^{214}_{84}Po$	Radium C'	1.64×10^{-4} sec	α
$^{210}_{81}Tl$	Radium C''	1.32 min	β^-
$^{210}_{82}Pb$	Radium D	22 yr.	β^-
$^{210}_{83}Bi$	Radium E	5.01 days	β^-
$^{210}_{84}Po$	Radium F	138.4 days	α
$^{206}_{82}Pb$	Radium G	stable	

TABLE 2.3 continued

^{232}Th series

Isotope	Classical name	Half life	Primary decay mode
$^{232}_{90}$Th	Thorium	1.41×10^{10} yr.	α
$^{228}_{88}$Ra	Mesothorium 1	6.7 yr.	β^-
$^{228}_{89}$Ac	Mesothorium 2	6.13 hrs.	β^-
$^{228}_{90}$Th	Radiothorium	1.91 yr.	α
$^{224}_{88}$Ra	Thorium X	3.64 days	α
$^{220}_{86}$Rn	Thoron	55.3 sec	α
$^{216}_{84}$Po	Thorium A	0.145 sec	α
$^{212}_{82}$Pb	Thorium B	10.64 hrs.	β^-
$^{212}_{83}$Bi	Thorium C	60.6 mins	α, β^- *
$^{212}_{84}$Po	Thorium C^1	3.0×10^{-7} secs	α
$^{208}_{81}$Tl	Thorium C^{11}	3.10 mins	β^-
$^{208}_{82}$Pb	Thorium D	Stable	

* The decay branches here.

that although ^{226}Ra was present in the volcanic materials the ^{222}Rn atoms were trapped in the crystalline and glassy minerals (Wilkening). This was confirmed for the lavas studied in Chapter 4; there was no significant increase in the α-count made on a sample that had been stored for 14 days in a sealed container to allow ^{222}Rn to reach equilibrium compared with an α-count immediately after sealing. Also, in spite of their porous appearance, the lava samples studied had saturation water contents of less than 5% and hence diffusion was not thought to be a problem in lava.

The thorium 232 series does not present a problem in disequilibrium; all the decay products have short half lives, the longest being that of ^{228}Ra which is 6.7 years. The gaseous radionuclide ^{220}Rn, thoron, has a mean life less than 1 minute and hence its diffusion is unimportant.

Escape of gaseous radionuclides, at formation or subsequently, was not thought to be a problem in TL dating of lava.

(b) Disequilibrium at formation

Recent volcanic rocks have been found to exhibit considerable disequilibrium of the ^{238}U series (Nishimura; Oversby and Gast). Disequilibrium ratios of ^{238}U, ^{230}Th, ^{226}Ra and ^{210}Pb were found to vary according to the geographical location of the samples and type, viz. acid, intermediate or basic, and were attributed to chemical fractionation during magmatic processes. An earlier study of historic basalts from Hawaii showed excess ^{230}Th content of between 10% and 50% and amounts of ^{210}Pb that varied from 60% to 220% of their equilibrium value (Somayajulu et al); some of their measurements are shown in Table 2.4. The variation of these results suggests that the disequilibrium was created in the magma prior to eruption.

Within a very limited volcanic area, e.g. Vesuvius, the excess ^{226}Ra seems to be a constant for each eruption and its decay has been used for

TABLE 2.4

CONCENTRATION OF URANIUM AND THORIUM AND THEIR DAUGHTER NUCLIDE

ACTIVITIES FOR HISTORIC HAWAIIAN VOLCANIC ROCKS

(reproduced after Somayajulu et al)

Sample	description	Th	U	$\frac{U}{Th}$	$\frac{^{210}Pb}{238\ U}$	$\frac{^{230}Th}{^{238}U}$
		(ppm)	(ppm)		(activity ratios)	
1963	Alae Crater	1.14	0.40	0.35	0.66	1.29
1926	Mauna Loa	0.60	0.21	0.35	1.07	1.51
1921	Halemaumau	1.24	0.44	0.35	0.72	1.14
1907	Mauna Loa	0.53	0.19	0.36	2.14	1.30
1801	Hualalai	1.90	0.54	0.28	1.00	1.27

dating lava samples less than 2,500 years old (Rapolla and Vitozzi).

Local fractionation of uranium and thorium, between minerals within a sample of igneous rock at the time of crystallization has been used to date its solidification using the ionium disequilibrium (Kigoshi).

(c) Disequilibrium due to leaching

Fractionation of ^{234}U does not occur during magmatic processes but is seen as a result of weathering (Thurber; Somayajulu et al). Uranium is relatively soluble in water and ground water leaching is responsible for its mobility in surface rocks (Talibudeen). In the dense, crystallized, ground mass of volcanic rock 10^7 years old, up to 80% loss of total uranium was found compared with that in the non-hydrated volcanic glass from the same rocks by Rosholt and Noble, who surmised from their measurements of $^{230}Th/^{234}U$ ratios that most of the loss took place soon after the rocks cooled but that leaching could be continuing at a much slower rate over a longer time (Rosholt and Noble). If there is loss of ^{238}U and ^{234}U due to their leaching soon after cooling, then the radioactive decay will take place as if ^{230}Th was the parent and hence would proceed with a half life of 8×10^4 years.

(d) Effect of such disequilibrium on dating by TL

Let us consider the effect of disequilbrium of ^{226}Ra occurring at the formation of the lava. I will assume that the earlier radionuclides are in equilibrium with the parent ^{238}U. ^{226}Ra is of particular interest because

(i) it is the last long lived member of the ^{238}U decay chain;

(ii) its half life (1,602 years) is comparable with the ages being observed;

(iii) it is often found to be in disequilibrium in young lava.

If there is disequilibrium at the time of laboratory measurement and this is defined in terms of the activity ratio

$$F(t) = \frac{(Ra)}{(U)}$$

then the fractional error, E, in the total dose rate obtained using the activity (U) determined by α counting can be calculated (Appendix A). Fig. 2.1 shows a plot of E versus t for a present day activity ratio F(t) = 1.1. For example, if a sample is 4,800 years old, E = 0.37 if F(t) = 1.1 and this gives an age that is 18% too old if the uranium chain is responsible for half the dose.

If the initial disequilibrium, F(0), is known and if we let F(0)-1 = m, then the observed α count = 8(U) + 5m(U) exp $(-A/\tau)$ where A is the age of the sample and τ is the mean life of ^{226}Ra. The dose received by the sample in time A is however proportional to

$$(U) + 5m(U)\,\frac{\tau}{A}\left\{1-\exp\left[-\frac{A}{\tau}\right]\right\}$$

Hence the ratio of T/A, where T is the age determined using the observed α count, is given by

$$\frac{T}{A} = \frac{8 + 5\ m\ \tau/A\left\{1 - \exp(-A/\tau)\right\}}{8 + 5\ m\ \exp(-A/\tau)} \qquad (2.1)$$

and hence the error in the fractional error in the age is given by

$$\frac{T-A}{A} = \frac{5\ m\left\{\tau/A - \tau/A\ \exp(-A/\tau) - \exp(-A/\tau)\right\}}{8 + 5\ m\ \exp(-A/\tau)} \qquad (2.2)$$

This function is shown plotted as a function of (A/τ) in Fig. 2.2 for various values of m. It must be noted that the errors are obtained assuming

(i) that the total dose is due only to the decay of the uranium chain;

(ii) that the dose is due purely to the alpha particles.

Using the above equations one is able to draw a few simple conclusions about the effect of disequilibrium of ^{226}Ra:-

(i) if <u>all</u> the ^{226}Ra is missing at t = 0, the maximum error that could occur is a -22% error in the age for A = 2,000 years;

(ii) if the initial values of F(0), the activity ratios are 1.5 and 2.5, as found by Oversby and Gast for recent lava from Tristan da Cunha and the Azores respectively, the maximum errors in the TL ages that could be obtained are + 9% and + 25% respectively;

(iii) if the initial value is F(0) = 11, as found for a recent lava from Vesuvius (Oversby and Gast), the maximum value of the fractional error $\frac{T-A}{A}$ is 1.28; this means that the TL age will be 128% too large. This is the largest reported excess of ^{226}Ra (Nishimura) and hence the TL age should never be more than 2.3 x the true age.

At this point it should be pointed out that in the course of the test programme carried out on lava in Chapter 4, the TL ages of the lava samples were up to an order of magnitude too young and were never too old. Hence it is impossible for an initial depletion of ^{226}Ra to account for the error in the TL dating. Further theoretical considerations of disequilibrium, e.g. for ^{230}Th and ^{234}U depletion, were stopped when experimental work on lava showed a more basic problem connected with the TL itself to be the cause of the dates being too young.

2.4 RADIOACTIVE DISEQUILIBRIUM IN CALCIUM CARBONATE

(a) Marine strand lines

Living corals incorporate about 3 parts per million uranium and negligible amounts of post ^{234}U daughters. When the system becomes closed the build up of the daughter products of ^{238}U and ^{235}U begins and this is the basis of the uranium series method for dating fossil corals (Mesolella, Mathews, Broecker and Thurber). Marine fossil molluscs have also been

studied but have been found to be less suitable for uranium series dating (Thurber); during this study it was noted that aragonitic molluscs had a higher uranium content than calcitic molluscs and that molluscs take in only about 2% of the uranium taken in by coral.

(b) Ocean sediments

In relatively young deep sea sediments, formed by the deposition of calcareous foraminifera, ^{230}Th is known to be in excess and dating methods based on its decay have been developed (Volchok and Kulp; Rosholt et al, 1961). In considering the TL dating of such sediments it is obvious that accurate knowledge of the state of disequilibrium must be obtained; determination by alpha spectrometry is feasible, but the TL properties of the sediments must be shown to be satisfactory before the radioactive disequilibrium is studied and TL dating attempted.

(c) Dripstones

Similar disequilibrium studies have also been carried out on stalactites and stalagmites (Duplessy et al). No ^{230}Th is present at formation but errors are introduced in the dating by the $^{230}Th/^{234}Th$ method if particles of clay were deposited during precipitation of the calcite (Fornaca-Rinaldi). Also the $^{234}U/^{238}U$ ratio for water from limestone regions was not found to be 1.15 as in the oceans but anywhere between 1.0 and 3.0 times this value (Ford, Thompson and Schwarcz). This means that the present day $^{234}U/^{238}U$ ratio must be measured for each sample as well as determining the build up of ^{230}Th as in the case of ocean sediments. There is also the worry that radium, being an alkaline earth element, will be precipitated at the same time as calcium carbonate. This would be extremely important if one was considering a recent dripstone.

2.5 THERMOLUMINESCENT RESPONSE OF CALCIUM CARBONATE

(a) Limestone

Much of the early work done on geological TL was carried out on carbonates. They were more TL sensitive than most other minerals but were also susceptible to misinterpretation due to spurious (i.e. non-radiation induced) TL. The method of sample preparation has been studied in conjunction with the effects of pressure (d'Albissin and Fornaca - Rinaldi), but the most important source of spurious TL was that induced by glowing in air. Aitken et al (1968(b)) showed that most of the spurious signal could be removed by using large grains to lessen the surface area, washing the grains in Calgon and glowing in oxy-free nitrogen; glowing the sample under vacuum was suggested by Bettinali and Ferraresso, but this is not practical for heating rates greater than about $1^{o}C$/second because of bad thermal contact with the heating plate.

Other problems encountered have been -

(a) sensitivity changes on heating (Hutchison), which was overcome by use of UV drainage to obtain the dose growth curve;

(b) trap creation by alpha particles during the first 100 million years (Medlin, 1968(b));

(c) the observation of TL in a freshly precipitated calcium carbonate that has not been exposed to radioactivity (Zeller, Wray and Daniels);

(d) recrystallization can take place and has been shown in radiocarbon studies of calcium carbonate nodules (Williams and Polach).

(b) Shells

Johnson (1960) studied the TL properties of biogenic $CaCO_3$ in recent and fossil shells; he found that the aragonitic shells had very low intrinsic TL sensitivity compared to the calcitic shells (Table 2.5). Aragonite and calcite are the two principal polymorphs of $CaCO_3$; the former is metastable

TABLE 2.5

CHARACTERISTIC POLYMORPHIC CONSTITUTION

OF CALCAREOUS SKELETAL MATERIAL (FROM JOHNSON, 1960)

Calcite	Calcite-aragonite mixture	Aragonite
Algae Corallinaceae	Mollusca Gastropoda (rare cases) Cephlopoda Pelecypoda Pectinacea	Algae Chlorophyceae
Protozoa Foraminifera		Coelenterata Zoantharia
Mollusca Pelecypoda Anomiacea Ostreacea		Mollusca Gastropoda Scaphopoda Pelecypoda
Bryozoa		
Brachiopoda Articulata		
Echinodermata		

and can become calcite whenever sufficient activation energy is available (Jamieson). Johnson also found light emission connected with the phase transition of aragonite into calcite at temperatures above 400°C. For reliable measurements original calcitic shells must be used.

Further work suggested that shells less than 10^7 years old had a peak at 230°C but because of its relatively short mean life at 20°C, ~ 10^5 years, it could only be used for very recent age determinations unless the ambient temperature was well known (Johnson and Blanchard; Bothner and Johnson). A higher temperature peak at 300°C was seen in older shells.

(c) Bone

Much effort has been put into attempting to date bone; the main problem has been found to be the difficulty in removing the organic matter which gives rise to a spurious TL signal (Christodoulides and Fremlin).

2.6 SUMMARY

The first non-pottery material to be considered experimentally was volcanic lava. The major sources of concern were the likelihood of radioactive disequilibrium and the effect of sample preparation on radiation dosimetry. The TL dates obtained for lavas of known age were found to be far too young, Chapter 4, but the reason was found to be an entirely unexpected phenomenon, the loss of electrons from deep traps on storage at ambient temperature, now termed 'anomalous fading' (Wintle). Because of its obvious importance in TL age determinations, most of the rest of the thesis concentrates on this factor.

Limestone and quartz were found to be free of anomalous fading. In Chapter 6 dates are obtained for archaeologically and geologically heated limestone samples where disequilibrium is not a problem because the limestone

was old enough before heating for the dose rate during the period of interest to be the same as that measured in the laboratory. Spurious TL was not found to be a problem even though fine grain samples were used; this is because measurements were carried out in oxy-free nitrogen.

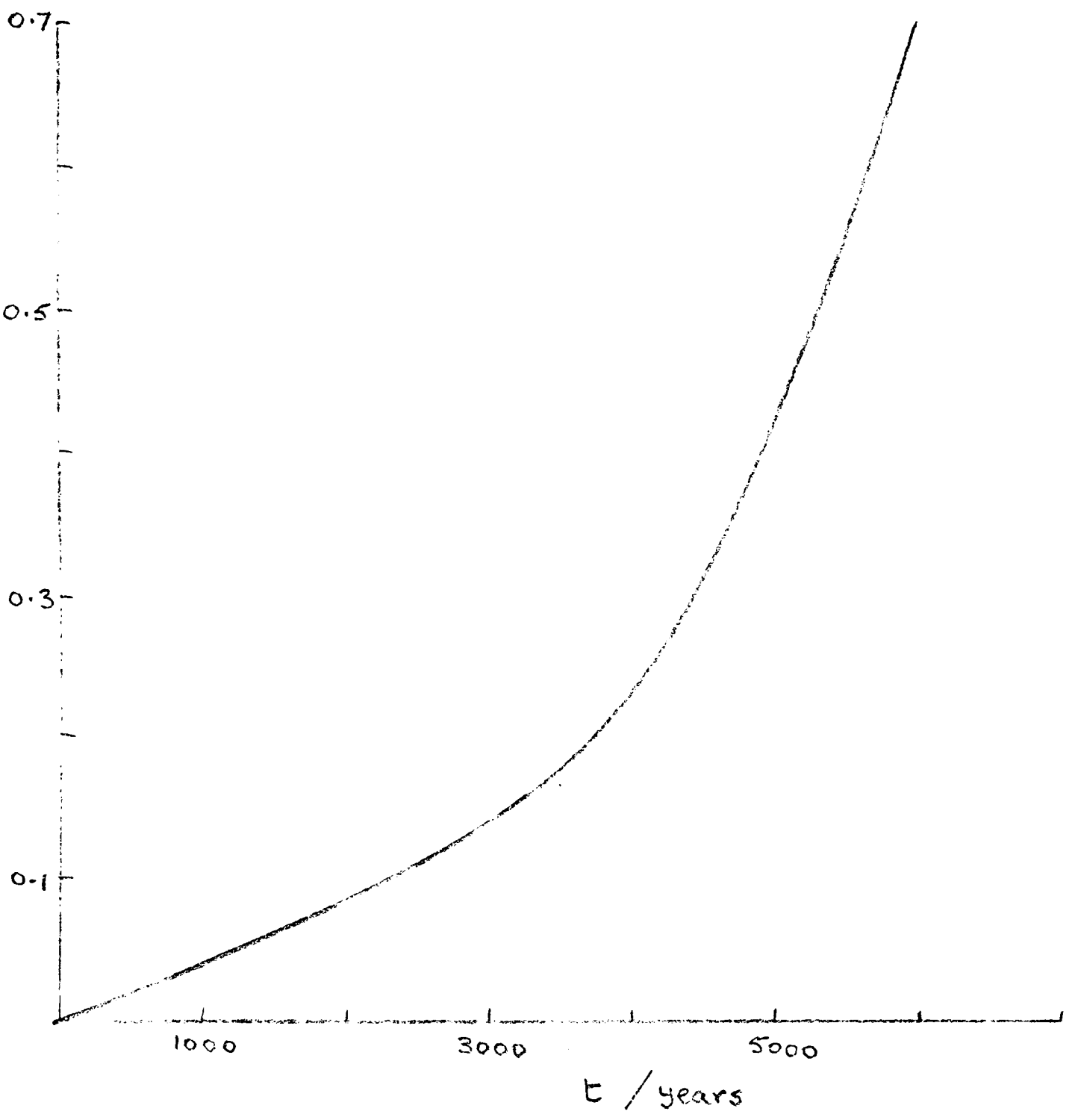

Fig. 2.1 Fractional error as a function of true age

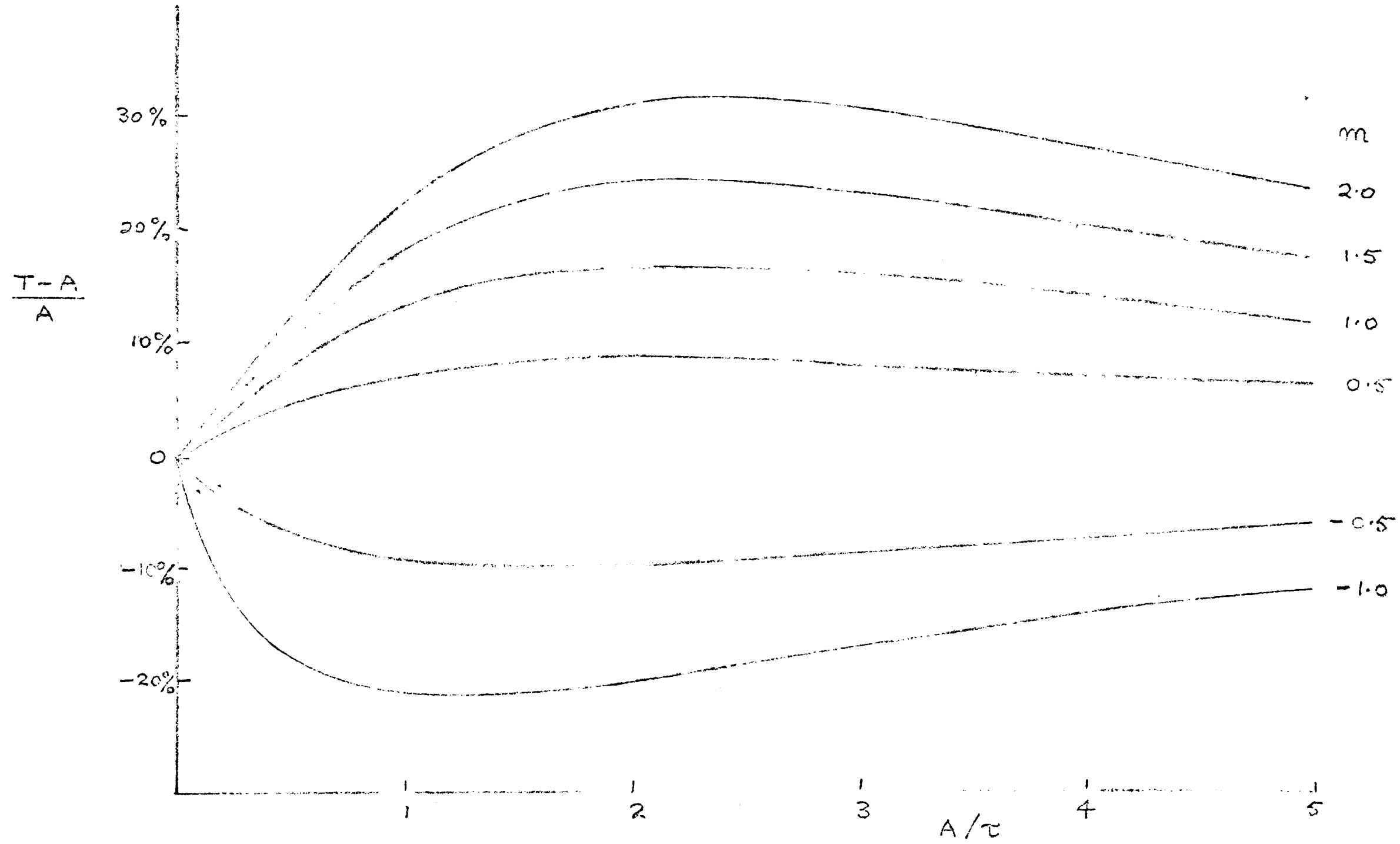

Fig. 2.2 Percentage error (T-A)/A as a function of A/T

CHAPTER 3 THE THERMOLUMINESCENT PROCESS

3.1 INTRODUCTION

Thermoluminescent (TL) dating is based on the measurement of trapped electrons that have accumulated in pottery over archaeological time or, in the case of lava and limestone, since their formation. Free electrons (or holes) are produced in the mineral constituents of the sample by naturally occurring ionizing radiation and these electrons become trapped at defects in the crystal. Electrons in shallow traps which are close to the conduction band, are thermally unstable and an electron trapped at such a trap will be ejected into the conduction band and may then recombine at a luminescence centre with subsequent emission of a photon, whose wavelength is characteristic of the luminescence centre.

Deeper traps retain their electrons for longer at ambient temperatures but if the sample is heated sufficiently the electrons are ejected at a temperature characteristic of the trap. Luminescence measurements made at elevated temperatures on artificially irradiated samples enable one to obtain values for two characteristic parameters, the trap depth E and an associated frequency factor s. In this chapter I shall discuss first the various methods of determination of E and s and the implied stability of an electron in such a trap at ambient temperature. I shall then discuss the recombination centres and the probabilities of radiative and non-radiative recombination.

3.2 MODELS FOR THE THERMOLUMINESCENT PROCESS

(a) Recombination dominant

The simplest model for TL is that using first order kinetic theory which was first discussed by Randall and Wilkins. It assumes that once an electron has been ejected from its trap it has negligible probability of being retrapped. The probability per unit time p (sec^{-1}) of an electron in a trap of depth E (eV) escaping at a temperature T (K) and undergoing a radiative recombination is given by the equation

$$p = s \exp (- E/kT) \qquad (3.1)$$

where s is a constant in units of $seconds^{-1}$ and is commonly known as the frequency factor.

If n is the number of filled traps at a time t, then the rate of emptying of electrons from traps is

$$- \frac{dn}{dt} = ns \exp (- E/kT) \qquad (3.2)$$

This represents an exponential decay with a half life

$$\tau_{\frac{1}{2}} = \ln 2 \; s^{-1} \exp (E/kT) \qquad (3.3)$$

Hence, once E and s have been obtained for a particular trap, the half life at any temperature T can be obtained. Two points to be noted about equation (3.3) are

(i) the strong temperature dependence of τ for given E and s as shown in Fig. 3.1, e.g. a factor of X 4 between storage at 10°C and 20°C;

(ii) any small error in determination of E will give rise to a large error in τ, which is made worse by the fact that s is usually determined from that value of E also.

Such first order kinetics are applicable in systems where recombination dominates over retrapping; this can happen both for localized systems where the trap and centre are spatially related and where the untrapped electron

moves via the conduction band to an unassociated recombination centre.

(b) Retrapping and Recombination allowed

If there is a finite probability of retrapping then the monomolecular kinetics described above is no longer valid. The kinetics of the process is characterized by the retrapping factor $R = \beta/\gamma$, where β is the coefficient for retrapping and γ that for recombination (Fig. 3.2). The monomolecular kinetics described earlier is the limiting case when $R = 0$.

When $R = 1$ and the electron is ejected via the conduction band we obtain a second order kinetic process such that the rate of trap emptying is given by

$$- \frac{dn}{dt} = n^2 s^1 \exp \left\{ - \frac{E}{kT} \right\} \qquad (3.4)$$

This model was developed by Garlick and Gibson. The same kinetics are obtained for a localized process if retrapping is dominant (Halperin and Braner). Conduction band processes can be differentiated from localized processes as the former give a decrease in the temperature of the glow peak maximum with increasing dose.

More complicated systems have been analysed mathematically with particular regard to the methods of determining trap depth from TL data (Braunlich, 1968) but they are not considered here as, except in a few instances, naturally occurring TL minerals do not have well defined single glow peaks.

3.3 DETERMINATION OF TRAP DEPTHS

Several recent papers have given comprehensive reviews on the various methods that have been developed to determine trap depths from the study of TL glow curves (Braunlich, 1968; Nicholas and Woods; Shalgaonkar and

Narlikar). The methods vary from rough estimates based on the temperature of the peak maximum T_m to more complex methods utilizing the peak shapes, but I shall consider here only those methods I actually use in subsequent chapters.

(a) The initial rise method

The most widely used technique is the initial rise method developed by Garlick and Gibson. Its advantage is that, provided the density of unoccupied recombination centres is very much greater than the density of trapped electrons, the method is independent of the recombination kinetics (Braunlich, 1967).

The reason that this method is independent of the kinetics is because at the start of the glow curve the intensity of luminescence I is given by

$$I = - C \frac{dn}{dt} = C f(n) \exp (- E/kT) \qquad (3.5)$$

where C is a constant connected with the luminescence efficiency. For $n_o - n \ll n_o$, i.e. where there has been negligible loss of electrons, f(n) may be treated as a constant and hence a plot of log I versus T^{-1} yields a straight line with a slope of (- E/k).

If there are overlapping peaks on the lower edge of the peak under study, they may be removed by thermal washing similar to that advocated by Hoogenstraaten. If a distribution of traps is expected the fractional glow technique used by Gobrecht and Hofmann for ZnS and by Halperin, Braner, Ben-Zvi and Kristianpoller for NaCl can be used. By subsequent heatings and coolings following irradiation initial rise curves can be obtained and the various activation energies can be plotted against the average temperature of the range used for finding the energy. This was used by Halperin, Chu, Haber and Dropkin for determining trap depths in ZnS (ErF_3, NH_4F).

(b) Hoogenstraaten's method

For a glow peak obeying first order kinetics the trap depth may be determined from its relationship to the peak temperature and the heating rate (Hoogenstraaten). During a glow curve when n_o is the initial number of trapped electrons and β is the heating rate (^oC/second), the number of electrons remaining trapped is obtained from equation (3.2) to be

$$n = n_o \exp\left[-\frac{s}{\beta}\int_{To}^{T} \exp\left\{-\frac{E}{kT}\right\} dT\right] \qquad (3.6)$$

The intensity of the glow curve is given by

$$I = C\, n_o\, s \exp\left\{-\frac{E}{kT}\right\} \exp\left[-\frac{s}{\beta}\int_{To}^{T} \exp\left\{-\frac{E}{kT}\right\} dT\right] \qquad (3.7)$$

At the glow curve peak $T = T_m$ and $\frac{dI_m}{dT} = 0$; differentiation of equation (3.7) yields

$$\frac{E}{k\,T_m^{\,2}} = \frac{s}{\beta} \exp\left\{-\frac{E}{k\,T_m}\right\} \qquad (3.8)$$

and hence

$$\log\left\{\frac{T_m^{\,2}}{\beta}\right\} = \frac{E}{k\,T_m} - \log\frac{sk}{E} \qquad (3.9)$$

Thus a plot of $\log\left\{\frac{T_m^{\,2}}{\beta}\right\}$ versus $T_m^{\,-1}$ is linear and has a slope E/k.

Such a method is also useful when the peak is not 'clean' as only quantities at the peak are measured (T_m, I_m). It is more advantageous for low intensity peaks than the initial rise method as the latter involves intensity measurements which can only go up to about 5% of the maximum intensity (Chen and Haber). This method has been generalised for higher order peaks (Chen and Winer).

(c) Isothermal decay method

For a first order peak the decay of TL at a temperature T is exponential with a mean life

$$\tau = s^{-1} \exp (E/kT) \qquad (3.10)$$

If the mean lives at various temperatures are experimentally determined, a plot of log τ versus T^{-1} will yield a straight line of slope E/k and having an intercept of log s^{-1}.

(d) Phosphorescent decay method

Phosphorescent decay curves are obtained by irradiating a sample at a given temperature and observing the light emitted at that temperature as a function of time. The phosphorescent intensity I_φ for a first order peak is given by the equation

$$I_\varphi = C \frac{dn}{dt} = \frac{C\, n_o}{\tau} \exp \left\{ - \frac{t}{\tau} \right\} \qquad (3.11)$$

where n_o is the number of trapped electrons at the end of the irradiation. Hence a plot of ln I_φ versus t will yield a straight line of slope - τ. This method is thus similar to the isothermal decay method, but has the advantage that τ can be obtained from a single experiment. Its disadvantage is that it can only be used for high levels of luminescence.

If there are several trap depths present, then a plot of log I_φ versus t will yield a curve which can be analysed as a sum of exponentials

$$I = \sum_i I_i \exp (- t_i/\tau) \qquad (3.12)$$

This analysis can be done provided that the traps are not too close together, i.e. at a given temperature the mean lives differ from each other by an order of magnitude. This method has been used to determine E and s for traps in CaF_2 with peaks between - 20°C and 100°C (Rao and Bose).

Medlin found that the general decay of phosphorescence could be expressed as

$$I = I_o \left\{ \frac{b}{b+t} \right\}^m \qquad (3.13)$$

where b and m are constants for the trap under consideration and are related to the excitation time (Medlin, 1961) but not to E and s. He found a similar power law for the phosphorescence of a distribution (Medlin, 1968a).

3.4 DETERMINATION OF KINETIC ORDER

For a first order peak the phosphorescence decay is exponential whereas second order decay is hyperbolic. A second order peak shifts to a lower temperature as the dose is increased whereas the position of a first order peak is independent of dose.

Another method of determining whether the peak obeys first or second order kinetics involves plotting log I/n and log I/n^2 versus T^{-1}, where I is the intensity of the TL glow curve at a given temperature abscissa, and n is the number of trapped electrons remaining and is proportional to the area beneath the glow curve beyond T. Before obtaining the glow curve the irradiated sample must be held at a temperature well below its peak to empty any shallower traps present; allowance must also be made for any overlap from a higher temperature glow peak. If the peak is first order then a plot of log I/n (versus T^{-1}) will be linear right through the temperature range of the glow curve; log I/n^2 will be parallel to log 1/n until f(n) in equation (3.5) deviates significantly from $f(n_o)$, see Fig. 3.3. Also shown is log I versus T^{-1}, the initial rise plot, which deviates at the same ordinate.

In fact no pure second order peak has been observed in TL studies of naturally occurring minerals. Slight downward shifts (~ 8°C) were observed

for the 375°C peak in quartz when the concentration of filled traps was changed from 5% to complete saturation, whereas a 50°C shift would be predicted theoretically for a pure second order peak at that temperature (Aitken and Fleming, 1973). Because of the dominance of first order kinetics for isolated peaks the following sections in this chapter are concerned with first order kinetic theory only.

3.5 DETERMINATION OF s

The frequency factor s can be obtained for a first order peak from extrapolation of the plots used in 3.3(b) and 3.3(c). It can also be calculated directly from equation (3.8)

$$\frac{E}{k T_m^2} = \frac{s}{\beta} \exp\left\{-\frac{E}{k T_m}\right\}$$

once E has been determined. A useful graphical approximation is given in Fig. 3.4.

3.6 ELECTRONIC STABILITY PREDICTED FROM E AND s VALUES

In thermoluminescent dating the assumption is made that electrons in traps giving rise to the high temperature TL are stable over archaeological time i.e. negligible drainage of the traps has taken place, $n(t) \approx n_o$ and $e^{-t/\tau} \approx 1$. For example if it is assumed that n_o electrons were trapped at time $t = 0$ then by the time $t = \tau/20$, $\frac{n(t)}{n_o} = 0.95$ i.e. 5% of the electrons initially trapped have been thermally activated out of the traps. The dependence of τ upon E, s and T has been studied theoretically (Christodoulides and Ettinger) and graphs such as they obtained may be used to judge whether a peak is suitable for dating studies. Figure 3.5 is a plot of mean lives at 20°C versus trap depths that give rise to $T_m = 300$°C at a heating rate of 10°C/second.

As glow curves from pottery do not contain well defined peaks that can be analysed as described in sections 3.3 and 3.5, a method was developed to determine the region of thermal stability suitable for dating (Aitken, Tite and Reid). This plateau technique involves plotting against glow curve temperature ordinates the ratio of the natural TL glow for one sample divided by the TL for a second sample that was given an artificial irradiation before glowing. This method assumes that a constant ratio is a sufficient criterion for a thermally stable region. Figure 3.6 gives an example for fine grains extracted from pottery and shows that for this sample only electrons in traps that give rise to TL above 350°C (for this heating rate of 10°C/second) are thermally stable over archaeological time and can be used for dating.

The sharp edge on the plot is caused by the rapid variation of mean life with TL emission temperature. This can be seen in Fig. 3.7 where the fraction of trapped electrons remaining in a trap of depth E after storage at a temperature T for a time t is given in first order kinetics as

$$\frac{n}{n_o} = \exp\left[- s \exp\left\{-\frac{E}{kT}\right\}t\right] \qquad (3.14)$$

The graph is plotted assuming $s = 10^{13}$ sec^{-1} for all E and the storage temperature is taken as 27°C.

From the graph it can be seen that a peak of depth 1.6 eV and having a frequency factor 10^{13} sec^{-1} can be used for dating archaeological material < 10,000 years old, but a trap deeper than 1.7 eV is needed to date material up to a million years old if it has the same frequency factor.

3.7 LUMINESCENCE CENTRES

The emission centres in calcite, anhydrite and quartz have been studied in natural and doped samples and the activating and quenching impurities have to some extent been identified (Chapters 5 and 6). In calcite Mn^{++}

ions are responsible for most of the luminescence; it has been shown that the Mn^{++} is excited by a non-radiative energy transfer from a recombination event at a nearby colour centre (Medlin, 1968a). Medlin has also been able to establish the observed emission spectrum in calcite in terms of the configurational coordinate diagram.

A simple configuration coordinate diagram as drawn in Fig. 3.8 enables us to explain qualitatively various characteristics of the luminescence centres. After recombination has taken place the luminescence centre is left in an excited state; the length of time it remains there depends upon the probability of the optical transition which gives rise to a photon of energy $E = h\nu$. One can see that an increase in temperature would give rise to an increase in amplitude of oscillation of the centre with a corresponding broadening of the emission band. This has been shown for quartz emission in the ultraviolet which is thought to be due to de-excitation of a lattice defect luminescence centre (Medlin, 1963b).

3.8 THERMAL QUENCHING

The configurational coordinate diagram also shows how a radiationless transition can take place from the excited state to the ground state. The curves for these two states approach each other closely at T and if sufficient energy U is provided the centre can make this transition without emitting radiation; all the energy is dissipated non-radiatively as the centre relaxes to the minimum of the ground state curve. The increased probability of such a transition with increasing temperature gives rise to a decrease in luminescence efficiency known as 'thermal quenching' (Curie).

The luminescence efficiency η of a phosphor may be written as the ratio

$$\eta = \frac{P_r}{P_r + P_{nr}} \qquad (3.15)$$

where P_r is the probability of radiative emission, assumed independent of temperature, and P_{nr} is the probability of a non-radiative transition, rising with increasing temperature. If there is only one luminescence centre, equation (3.15) simplifies to

$$\eta = \frac{1}{1 + K \exp(-W/kT)}$$

where W is the characteristic energy and K is a dimensionless constant.

Such thermal quenching has been observed in K Cl : Tl (Johnson and Williams) and in ZnS : Cu (Curie).

3.9 SUMMARY

At the beginning of this chapter techniques to determine E and s for particular traps were discussed. In circumstances where the values of these parameters indicated short lifetimes, these predictions have been confirmed by laboratory experiments lasting for weeks and even months. But no experiments have been sought to confirm their validity in the case of much longer lifetimes spanning centuries or millenia. In Chapters 5 and 6 such studies have been carried out on quartz and limestone which have suitable peaks.

I have also mentioned the plateau test which has been considered the sole criterion for stability of trapped electrons; if there was a plateau within $\pm$ 5% then the sample could be included in a dating programme. In Chapters 4 and 7 it will be shown that the long term stability suggested by the plateau test on minerals commonly encountered in lava and some types of pottery is not valid.

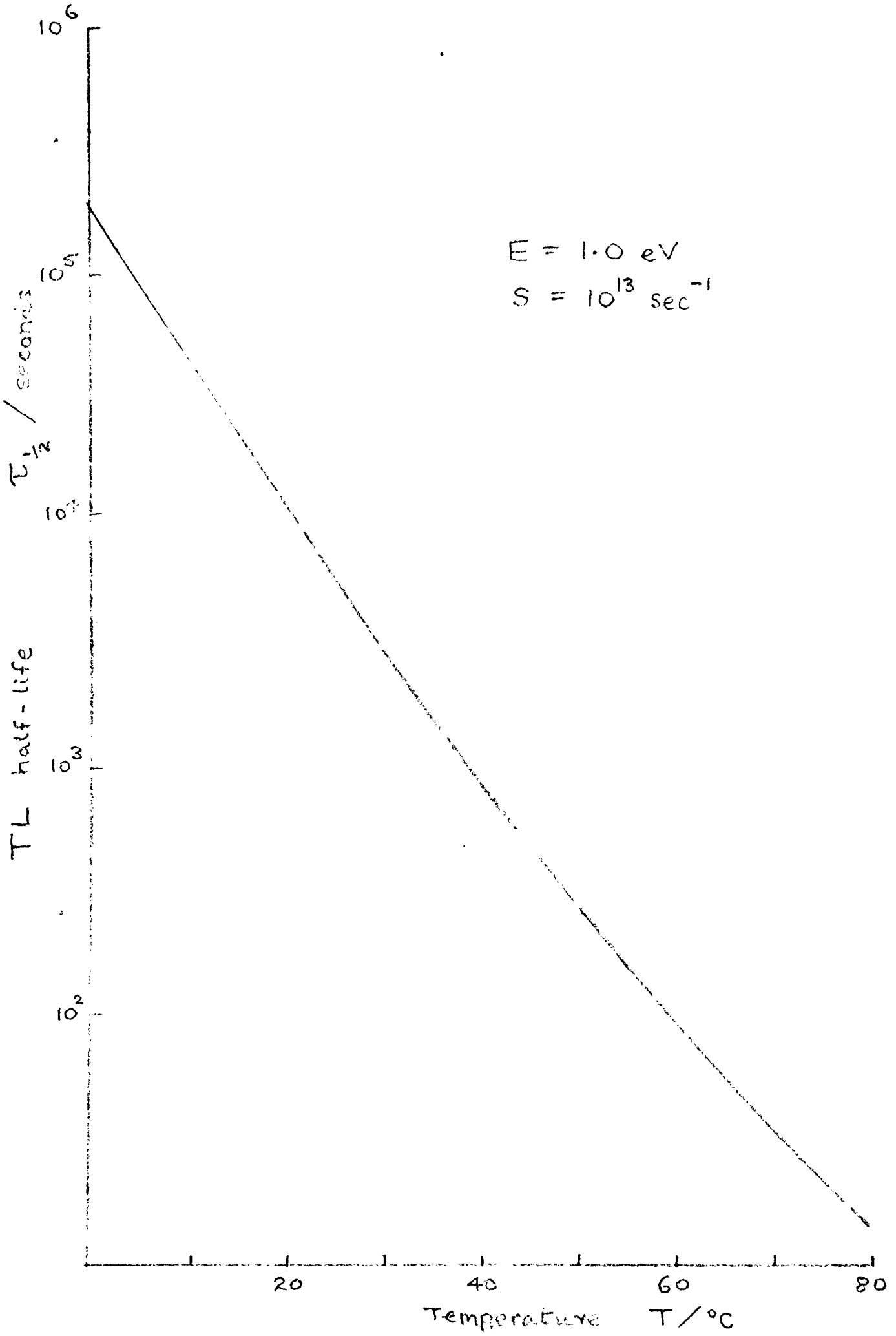

Fig. 3.1 TL half-life versus storage temperature

(a) First order kinetic processes
(recombination dominates)

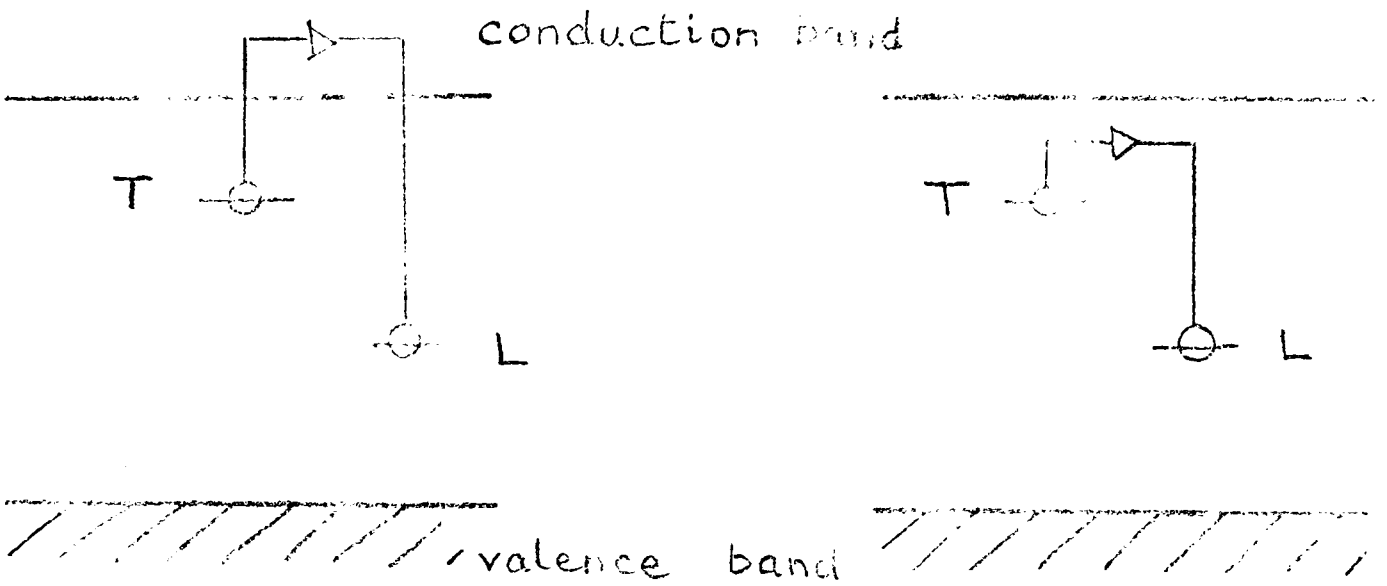

(b) Second order kinetic processes
(retrapping occurs)

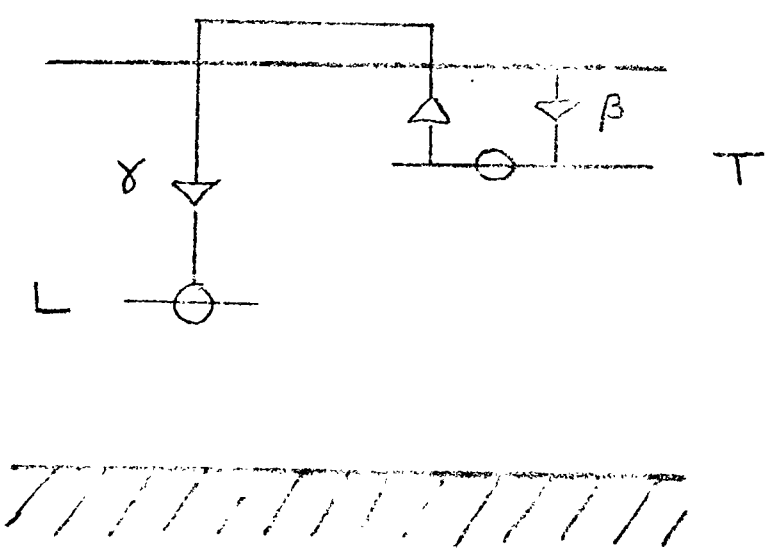

Fig. 3.2 Simplified TL models

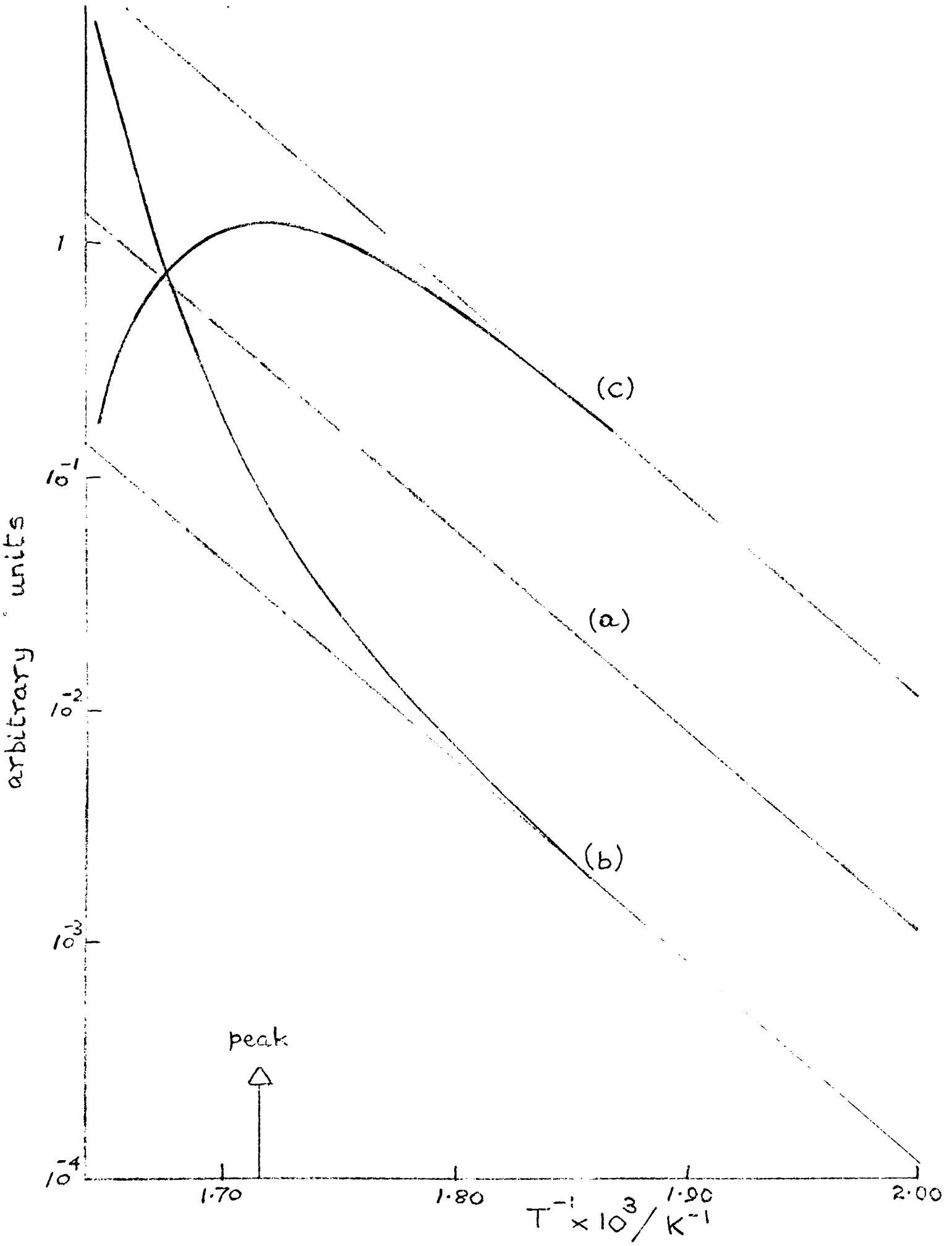

Fig. 3.3 Theoretical plots for a first order kinetic peak

(a) $\log I_r/n$ v T^{-1}

(b) $\log I_r/n^2$ v T^{-1}

(c) $\log I_r$ v T^{-1}

E = 1.69 eV

s = 10^{14} sec^{-1}

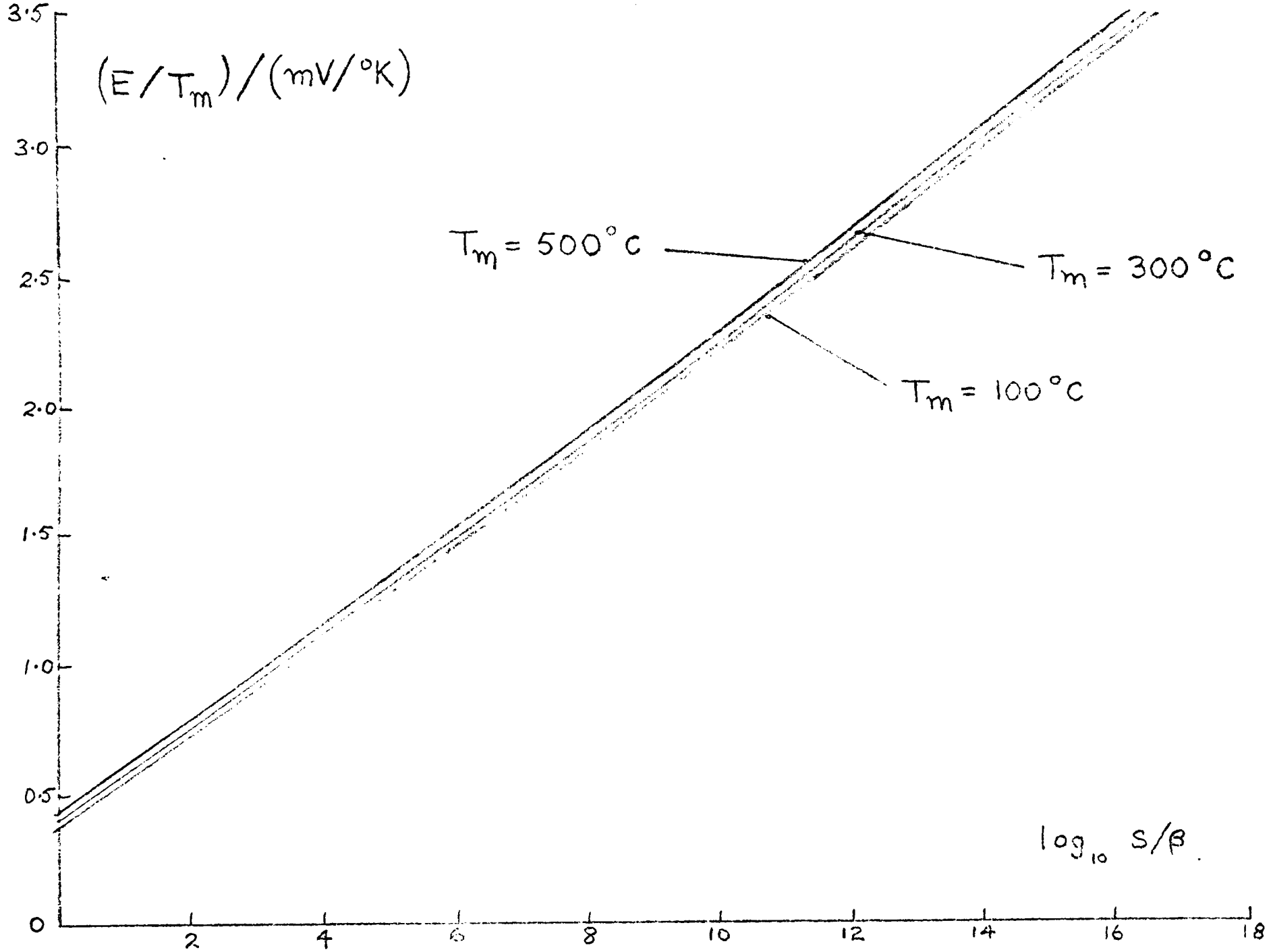

Fig. 3.4 Graphical evaluation of c using T_m and β

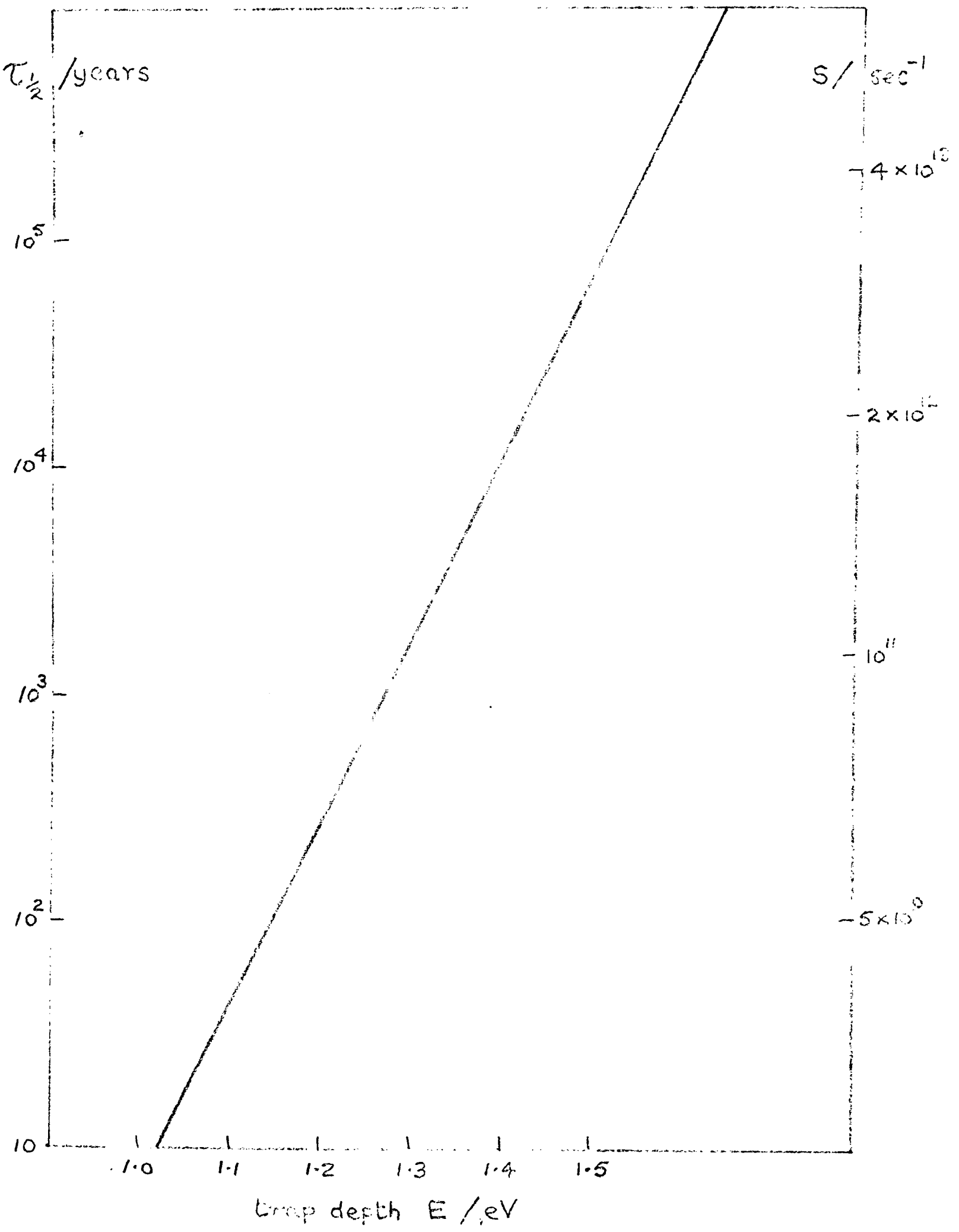

Fig. 3.5 Half-life at 20°C as a function of trap depth

Tm = 300°C, β = 10°C/sec

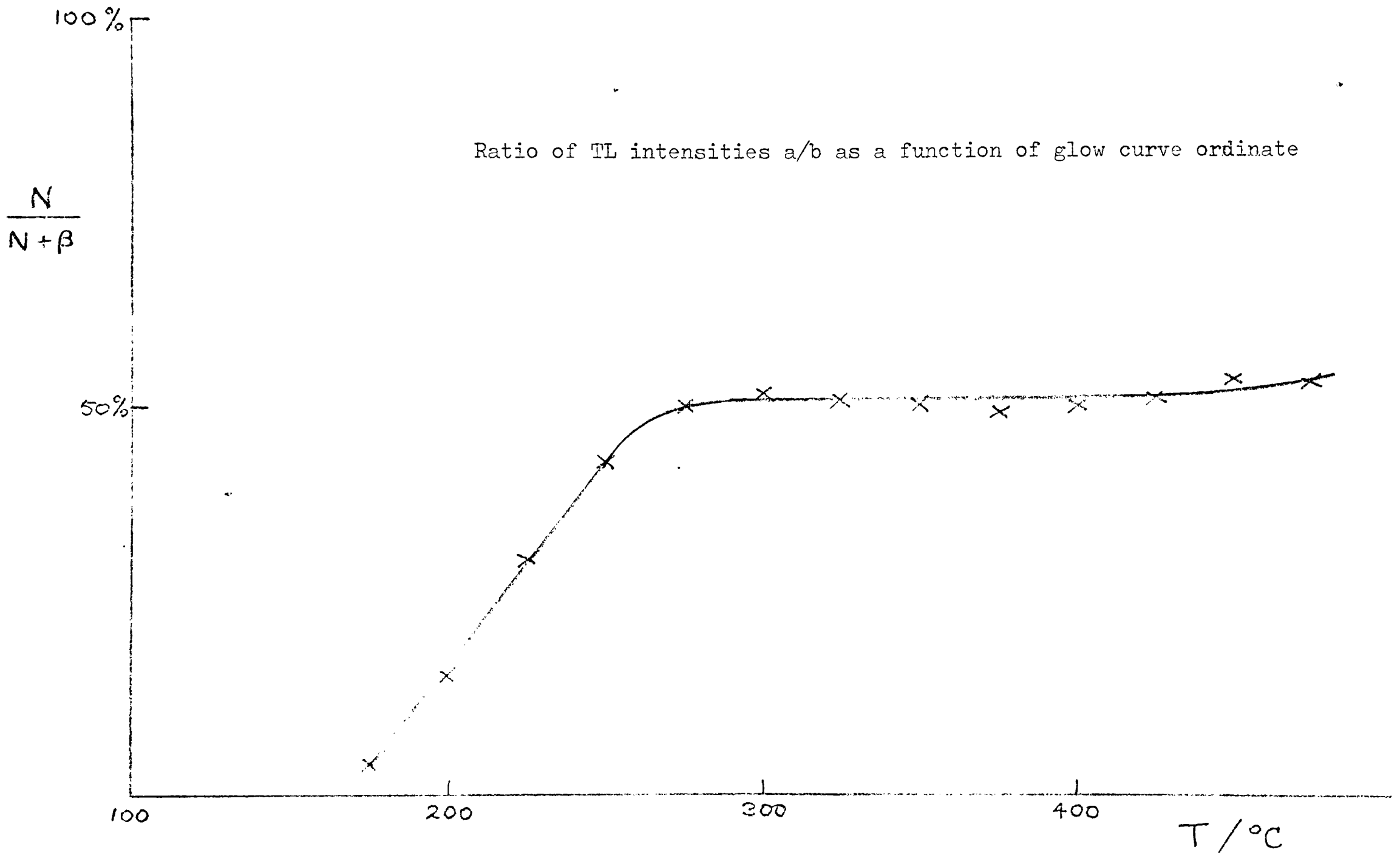

Fig. 3.6 Plateau test

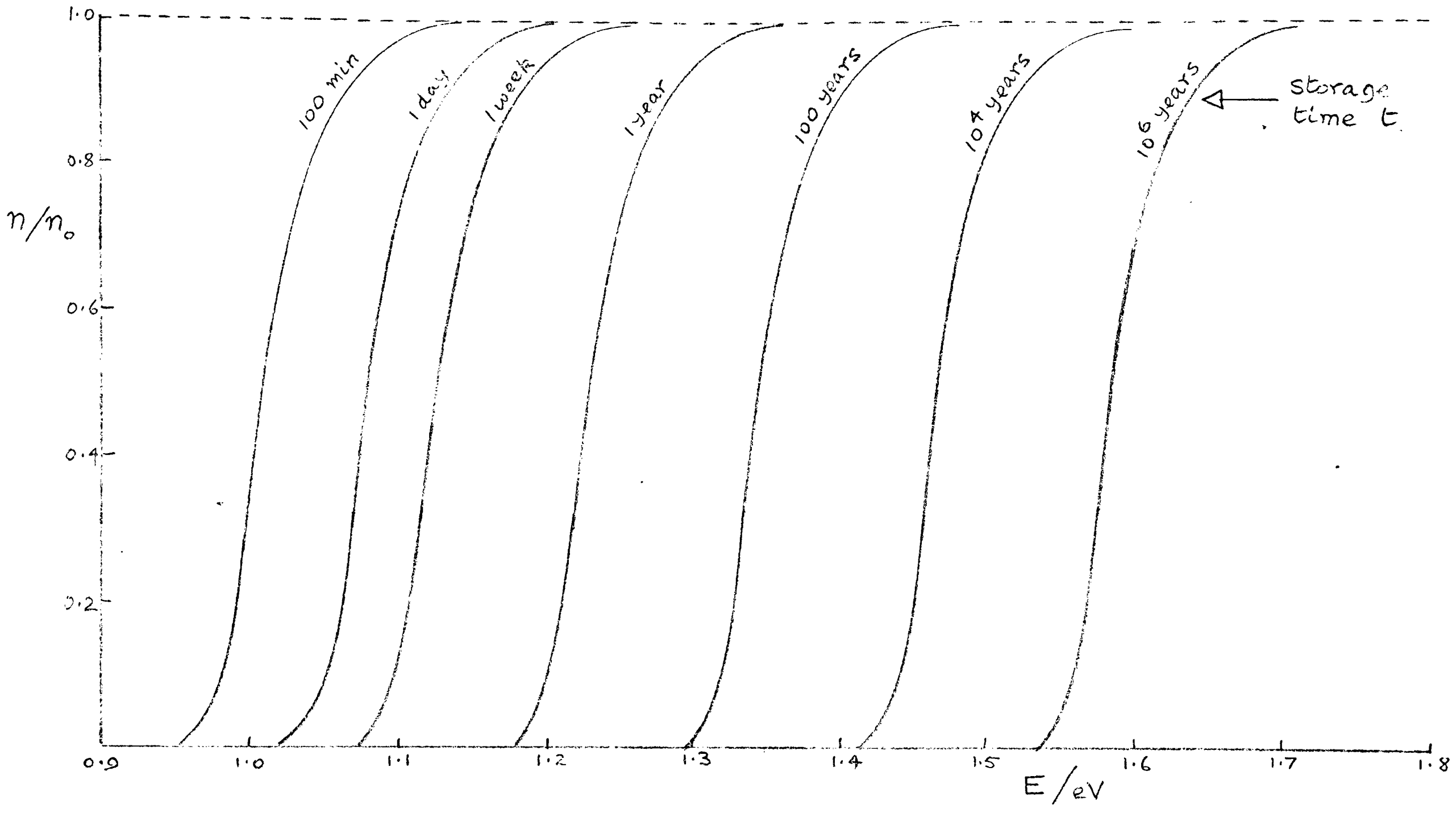

Fig. 3.7 Trap emptying. n/n_o vs E for various storage times at 27°C, with $s = 10^{13}$ sec^{-1}

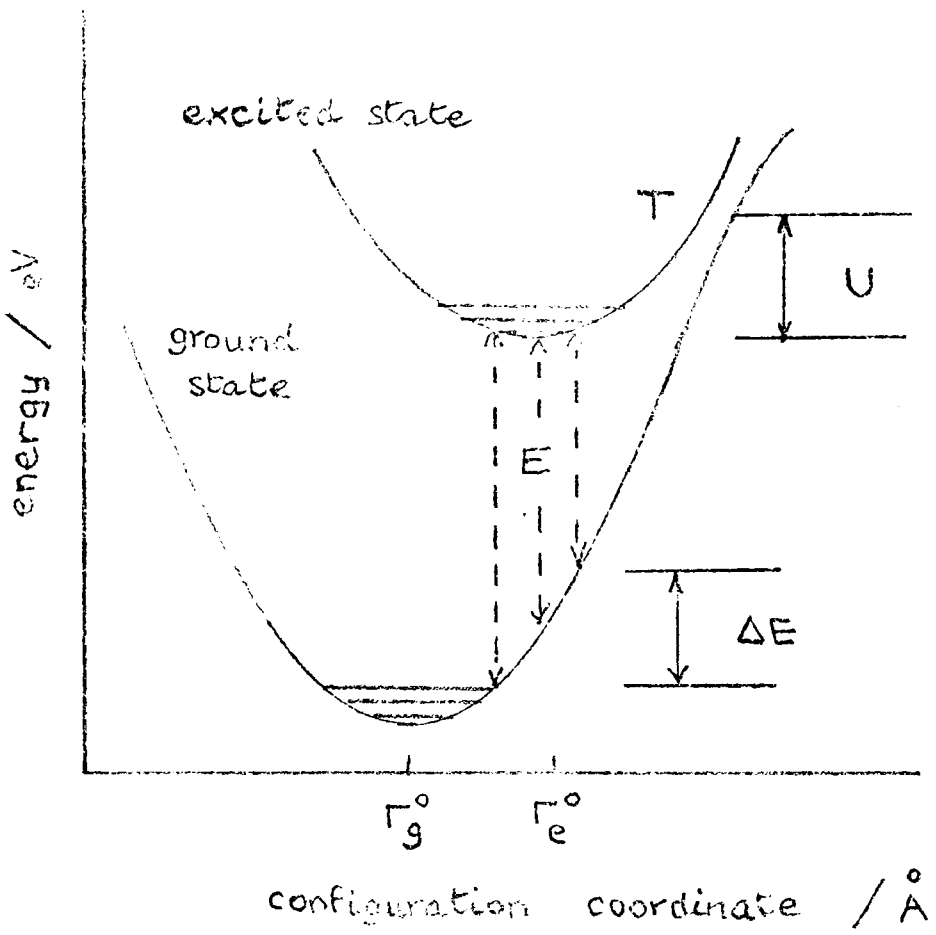

Fig. 3.8 Schematic configuration coordinate diagram of a luminescent centre

CHAPTER 4 THERMOLUMINESCENT DATING STUDY OF VOLCANIC LAVA

4.1 GEOLOGICAL INTRODUCTION

There is a serious gap in the dating of lava flows between those for which dates are written in historical records and those whose age is at least 10^5 years, the minimum for which suitable isotope ratio dating (i.e. K/Ar and Rb/Sr) can successfully be applied. The intervening period has seen volcanic activity in a variety of countries, notably Iceland, France, New Zealand and Italy. During this time the Earth's magnetic field has changed considerably in direction and intensity and palaeomagnetic studies have been carried out on many flows, particularly in France from which a geomagnetic reversal within the last 20,000 years has been inferred (Bonhommet and Zahringer). Radiocarbon dating has been applied to carbon fragments found beneath flows when they have been exposed by a stream or by quarrying, but these examples are not common. The extension of TL dating to lava would span the gap and be directly applicable to the flow itself and hence enable the changes in the Earth's magnetic field to be charted over the past 10,000 years.

4.2 EARLY WORK ON LAVA

The earliest application of TL to feldspars in lava was made by Sabels in 1962; he was able to establish rough ages for the basalts he studied in spite of the simplicity of the dating method at that time. A more recent study was undertaken by Aitken, Fleming, Doell and Tanguy on historically dated flows from Mount Etna. The results were not very encouraging; measurement of whole rock samples gave equivalent doses that were far too

low and mineral separates, that had been ground in mechanical pulverizers and split on the basis of magnetic susceptibility differences using a Franz-type magnetic separator, had equivalent doses that ranged from 0.1 to 9 x the expected values. The anomalously high values were shown to be due to the crushing giving rise to spurious TL i.e. triboluminescence (Aitken, Fleming, Reid and Tite); the low values for the whole rock measurements could not however be explained.

More encouraging results have been reported using fine grains on a piece of lava from Thera (Aitken and Fleming, 1971) and using single crystals 1 mm in diameter on a single sample of lava from Pompeii (Hwang); however the experience obtained during the present research suggests these are exceptions to the general rule and were encountered by chance.

In the most recently reported study of TL in volcanic lava, Berry showed that in general the 'specific TL' defined to be

$$\frac{\text{natural TL}}{\text{artificial TL}} \Big/ \text{annual dose rate},$$

was proportional to age (Berry). It is significant to note that although all the information was available, no actual dates were given and out of eight samples studied only four showed linearity of specific TL with known age.

4.3 LAVA SAMPLES STUDIED

Lava samples were collected from Iceland by the author with the help of Professor Sigugeirsson of the Geology Department, Reykjavik University, and from the Central Massif region of France by Dr. M.J. Aitken with the help of Dr. N. Bonhommet of the University of Strasbourg. The Italian samples were collected by Dr. G. Walker of Imperial College, London and Dr. G.W. Grindley from New Zealand.

The French and Icelandic flows were basalts containing plagioclase feldspar (andesine/labradorite/bytownite) as the major TL minerals. The Italian flows from near Naples were trachytic flows containing the alkali feldspar sanidine, and a little quartz.

4.4 SAMPLE PREPARATION

The whole of the handling process was conducted under subdued red light to prevent bleaching or generation of TL. Each sample was crushed in a vice and sieved - no further mechanical crushing was used. The 50 - 150 μ grains were washed in acetone to remove fine grains adhering to them and dried in an oven below 50°C. A Franz magnetic separator was then used, the sample being vibrated along a chute between the pole pieces of an electro-magnet of variable strength. The non-magnetic grains were collected and found to be mainly feldspar and/or quartz. In the case of the trachytic flows containing both quartz and sanidine, bromoform (< 2.6 gm/cc) was used to try and separate the grains but this was difficult as the quartz was less than 1% of the non-magnetic separate and the quartz grains were often intergrown with the feldspar.

To show the presence of feldspar in a separate various staining techniques were used (Van der Plas; Allman and Lawrence). The alkali feldspar grains were stained yellow after immersing in HF and then washing in sodium cobaltinitrite solution. Plagioclase feldspars were stained red by washing in $BaCl_2$ and potassium rhodizonate after etching. More detailed mineral identification was carried out if necessary using X-ray diffraction with a Debye-Scherrer powder camera.

Besides using the 100 μ feldspar grains for TL analysis, the fine grains (2 - 8 μ) were also collected by sedimentation in acetone and deposited

on 1 cm diameter aluminium discs for TL analysis.

Radioactive analysis for U and Th was done by thick source α-counting of the crushed whole rock and potassium analysis by flame photometry was done on the ground rock and also on some of the alkali feldspar inclusions.

4.5 RESULTS

Seven lava samples were studied in detail, three from France, three from Italy and one from Iceland. The detailed results are given here and summarized in the following section. 132 al - this sample was taken from a basalt flow at Prenal in the Massif Central and had an associated radiocarbon date of 35,000 years (Gif - 1408)(Delibrias, Guillier and Labeyrie).

Table 4.1 contains the results of six separate sets of fine grain discs made from the sample. The equivalent doses, obtained by plotting the first and second glow growth curves, vary from 0.6 to 6.9 krad and hence are well below the value expected. A typical glow curve and plateau are shown in Fig. 4.1 along with the first and second glow growth curves. There is a plateau to within 10% above 300°C ; the beta dose response curves are linear and parallel up to a dose that is 3 x natural equivalent dose. Similar behaviour was obtained for the other fine grain measurements with the exception of 1.7.

The results of the radioactive analysis, assuming equilibrium in the uranium and thorium chains, are shown in Table 4.2. The total dose rate per year for fine grains, using the experimentally determined $k_{eff} = 0.11$, is 0.34 rad/year and for inclusions of 100 μ diameter the total dose rate is 0.23 rad/year (allowing for 5% beta attenuation). Given an age of 35,000 years the equivalent doses for the fine grains should be about 12 krads and that for inclusions about 8 krads.

TABLE 4.1

FINE GRAIN RESULTS FOR 132 a1

sample	equivalent dose/krads	plateau
1.2	6.9	yes, above 300 °C
1.3	2.2	yes
1.5	2.7	yes, above 400 °C
1.6	2.3	yes, 350-450 °C
1.7	0.6	no
1.9	1.5	yes, after thermal washing at 250 °C

Notes

(1) The equivalent dose is obtained at 450 °C ordinate if there is no plateau.

(2) Supralinearity was not significant in the equivalent dose determinations.

The non-magnetic 100 μ separate was small and hence equivalent dose determination by additional doses was not possible. The equivalent doses obtained by comparison of the natural glow intensity at 400°C with that after a laboratory irradiation of the same portion varied from 8 to 14 krads but sensitivity changes could not be checked and there was no plateau.

132 il - this sample was taken from the St. Saturnin flow in the same region which has an associated radiocarbon date of 7,700 ± 180 years (Gif - 1625). The radioactive analysis is shown in Table 4.3 and hence the fine grain dose rate (using the experimentally determined k_{eff} = 0.22) is calculated to be 0.35 rad/year; thus the total dose received should be about 2.6 krad.

The inclusions exhibited spurious TL and gave no plateau but the two sets of fine grain discs had plateaux above 400°C and gave equivalent doses of 2.1 krad and 1.48 krad. There appeared to be a sensitivity increase after glowing but the second glow growth curve was linear and passed through the origin, Fig. 4.2(c).

132 hl - this sample was taken from a layer of domite from the Puy de Dome and it had an associated radiocarbon date of 8,400 ± 300 (Gif - 1498). The rock differs from samples 132 al and 132 il in that it contains alkali feldspar and is much more radioactive. The radioactive analysis is given in Table 4.4 and hence the fine grain dose rate is 1.09 rad/year, using the experimentally determined k_{eff} = 0.114, and this suggests an equivalent dose of 9.2 krads.

The TL glow curves for the fine grains gave a plateau above 325°C , Fig. 4.3(b), and the first and second beta growth curves obtained for the plateau region are linear but not parallel, Fig. 4.3(c). The equivalent dose is 3.0 krad.

129 e7 - this sample is a lava inclusion from a tephra deposit near Naples

TABLE 4.2

RADIOACTIVE ANALYSIS OF LAVA 132 a1

% K_2O	1.30

immediately sealed α-count (42 mm ring)

	counts	time/ksec	count rate/ksec^{-1}
background	5	25	0.20
total count + background	2265	340	6.66
pairs count	37	340	0.109

counts due to Th = 2.35 counts/ksec

" " " U = 6.46 - 2.35 = 4.11 c/ksec

Uranium gives 63% of the α-count

delayed sealed α-count

total count	1530	227	6.74
pairs count	25	227	0.110

only 1% increase in total counts on delaying measurement for 14 days.

Dose rates obtained from above analysis in millirads/year

	α	β	γ	α eff	cosmic
U	612	28	27	67	
Th	327	11	31	36	
^{40}K	-	93	28	-	
Total		132	86	103	15

TABLE 4.3

RADIOACTIVE ANALYSIS OF LAVA 132 i1

% K_2O 1.26

immediately sealed α-count (42 mm ring)

	counts	time/ksec	count rate/ksec^{-1}
background	6	49	0.12
total count + background	1487	317	4.69
pairs count	22	317	0.069

counts due to Th = 1.51 c/ksec

" " " U = 3.06 c/ksec

Uranium gives 67% of the α-count

delayed sealed α-count

total count	1057	261	4.05
pairs count	27	261	.103

There has been an apparent decrease of 14% in the total count.

Dose rate (m rad yr^{-1}) obtained from immediately sealed count

	α	β	γ	α eff	cosmic
U	456	21	20	100	
Th	210	7	20	46	
^{40}K	-	90	27	-	
Total		118	67	146	15

TABLE 4.4

RADIOACTIVE ANALYSIS OF DOMITE 132 h1

$\%.K_2O$ 4.65

immediately sealed α-count (42 mm ring)

	counts	time/ksec	count rate/ksec^{-1}
background	9	70	0.13
total count + background	1759	87	20.22
pairs count	42	87	0.483

counts due to Th = 9.2 c/ksec

" " " U = 10.9 c/ksec

Uranium gives 54% of the α-count

Dose rate obtained from immediately sealed count

	α	β	γ	αeff	cosmic
U	1624	74	71	185	
Th	1279	42	121	146	
^{40}K	-	332	100	-	
Total		448	292	331	15

TABLE 4.5

RADIOACTIVE ANALYSIS OF LAVA 129 e7

$\%\ K_2O$ powdered whole rock 8.2

non-magnetic crystals 14

immediately sealed α-count (42 mm ring)

	counts	time/ksec	count rate/ksec^{-1}
background	60	76	0.79
total count + background	8444	234	36.1
pairs count	212	234	0.91

counts due to Th = 14.6 c/ksec

" " " U = 20.7 c/ksec

Uranium gives 59% of the α-count

delayed sealed α-count

total count	3072	87	35.3
pairs count	95	87	1.1

There is no significant change in the total count rate.

Dose rates obtained from above analysis in millirads/year.

	α	β	γ	α eff*	cosmic
U	3084	141	135	308	
Th	2029	67	191	203	
^{40}K	-	586	177	-	
Total		794	503	511	15

*(keff = 0.1 is assumed)

TABLE 4.6

RADIOACTIVE ANALYSIS OF LAVA 129 e14

% K_2O powdered whole rock 8.7

immediately sealed α-count (42 mm ring)

	counts	time/ksec	count rate/ksec^{-1}
background	4	30	0.13
total counts + background	2580	69	37.4
pairs	76	69	1.10

counts due to Th = 16.0 c/ksec

" " " U = 21.3 c/ksec

uranium gives 57% of the α-count

Dose rate obtained from immediately sealed count

	α	β	γ	α_{eff}*	cosmic
U	3174	145	138	317	
Th	2224	73	210	222	
^{40}K	-	622	188	-	
Total		840	536	539	15

(k_{eff} = 0.1 is assumed)

TABLE 4.7

RADIOACTIVE ANALYSIS OF LAVA 129 e15

% K_2O powdered whole rock 9.5

immediately sealed α-count (42 mm ring)

	counts	time/ksec	count rate/ksec^{-1}
background	3	20	0.15
total counts + background	3324	78	42.6
pairs count	78	78	1.0

counts due to Th = 13.9 c/ksec

" " " U = 28.5 c/ksec

uranium gives 67% of the α-count.

Dose rate obtained from immediately sealed count

	α	β	γ	α_{eff}	cosmic
U	4246	194	185	603	
Th	1932	64	182	274	
^{40}K	-	679	205	-	
Total		937	572	877	15

TABLE 4.8

RADIOACTIVITY ANALYSIS ON LAVA 129 a4

% K_2O 0.16

immediately sealed α-count (42 mm ring)

	counts	time/ksec	count rate/ksec^{-1}
background	1	12	0.08
total counts + background	110	125	0.88
pairs count	3	125	0.024

The pairs count is not statistically meaningful and a 50% U activity is assumed in determination of the dose rate.

Dose rate using above measurements obtained for 100 μ inclusions.

	β	γ	cosmic
U + Th	4.3	8.0	
^{40}K	11.4	3.4	
Total	15.7	11.4	22

and the tephra has an associated radiocarbon date of 4,000 years. It was described by the geologist as a quartz bearing trachyte containing sanidine and hornblende. The radioactive analysis is given in Table 4.5; the fine grains are likely to have a dose rate of about 1.8 rad/year but the α sensitivity was not determined; the inclusions which are rich in potassium will have a correspondingly high dose rate, about 1.3 rad/year. The fine grain equivalent dose for this 4,000 year old sample is likely to be about 7 krads.

The fine grain TL did not give a plateau, Fig. 4.4, and was therefore considered unsuitable for dating. Comparing the natural glow curve with the second glow it can be seen that the lack of plateau above $400^{\circ}C$ is due to non-radiation induced TL in the natural glow curve above $400^{\circ}C$. In the temperature region $275^{\circ}C$ - $400^{\circ}C$ the TL intensity ratio is changing slowly with temperature and the equivalent dose obtained for the various ordinates varies from 0.3 to 1.1 krads; these are well below the estimated 7 krad.

The 100 μ non-magnetic grains also failed to exhibit a plateau. Etching with HF for 20 mins did not remove the alkali feldspar and no improvement in the plateau was obtained after this treatment.

129 e14 - this sample is also from the Naples area and is between 50,000 and 10,000 years old. The radioactive analysis is given in Table 4.6 and hence the equivalent dose should be between 19.3 krad and 96.5 krad. The TL from the fine grain discs did not give a plateau, Fig. 4.5(b), but at the $400^{\circ}C$ abscissa the equivalent dose was found to be only 0.3 krad.

129 e15 - this sample from Mount Olibano near Naples is 4,000 to 10,000 years old. The radioactive analysis given in Table 4.7 suggests the equivalent dose of the fine grains, using the experimental value $k_{eff} = 0.142$, should be between 9.6 krad and 24 krad.

The fine grain TL gave a plateau above 300°C , Fig. 4.7(b), and the first and second glow beta growth curves were parallel and gave an equivalent dose of 1.25 krads, Fig. 4.7(c).

129 a4 - this sample was collected in Iceland and was said to be at least 60,000 years old by Professor Sigugeirsson but no precise date was available. The TL sensitivity was about 2 orders of magnitude less than for the other lavas studied above. The fine grain TL was spurious and could not be used for dating but it was possible to extract sufficient 100 μ non-magnetic crystals to make measurements with 10 milligramme samples. A typical natural glow curve and associated plateau are shown in Fig. 4.8(a) and (b). The beta growth curves for the 400°C abscissa are shown in Fig. 4.8(c). The equivalent dose is 0.33 krad.

The radioactive analysis is given in Table 4.8 and for 100 μ inclusions the total dose rate is only 0.05 rad/year. (The cosmic dose is 22 mrad/year because the sample was 5-5½ inches from the surface of the lava flow.) This gives an age of about 6,700 years.

4.6 DISCUSSION OF LAVA DATING RESULTS

The results of dating seven different lava flows are shown in Table 4.9, where the equivalent doses obtained from TL measurements using fine grains (except for 129 a4) are compared with those calculated from the radioactivity measurements and the known age. There is no agreement even though satisfactory plateaux were obtained for samples 132 a1, 132 i1, 132 h1 and 129 e15 and the equivalent doses for the other samples were obtained using the TL at the 400°C abscissa. Being able to obtain a plateau implies that there has been no thermal untrapping of electrons from the deep traps which give rise to the high temperature TL (see Chapter 3.6). A bad plateau may

TABLE 4.9

LAVA DATING RESULTS

	Geological Age/yrs	Measured ED/krad	Measured ED / Calculated ED using known age	Plateau
FRANCE				
132 a1	35,000	0.6 to 6.9	0.05 to 0.58	yes
132 il	7,500	1.48 to 2.1	0.58 to 0.81	yes
132 hl	8,500	3.0	0.33	yes
ITALY				
129 e7	4,000	0.3 to 1.1	0.04 to 0.16	no
129 e 14	10-50,000	0.3	0.003 to 0.015	no
129 e15	4-10,000	1.25	0.05 to 0.13	yes
ICELAND (inclusions)				
129 a4	> 60,000	0.33	< 11	poor

result from the presence of non-radiation induced TL in the natural glow curve, but this usually gives rise to an overestimate of the natural dose and could not account for the low equivalent doses in Table 4.9. A bad plateau can also be caused by sensitivity changes at the different glow curve ordinates, but again this could not give rise to such large discrepancies.

Initially the disagreement was thought likely to be connected with radioactive disequilibrium at the formation of the lava as discussed in Chapter 2, but a factor of x 20 between the results as in 132 a1, 129 e7 and 129 e15 is too large to be accounted for in this way as it would imply gross disequilibrium many times greater than any so far reported. However, during the experiment described in Chapter 2.3, it was noticed that samples from the same set of fine grain discs yielded higher doses glowed immediately after preparation than thcse glowed a few days later.

The far reaching implications of this observation were followed up using beta irradiations on the same set of disc samples, the following experimental procedure being carried out after thermal drainage to 500 ^{o}C to remove the TL due to the gamma dose,

(i) irradiate

(ii) store in darkness at room temperature

(iii) measure TL

(iv) irradiate

(v) measure TL immediately

A check was made that there was no change in sensitivity between measurements. Two of the same set of disc samples were subjected to the following repetitive procedure -

(i) irradiate

(ii) measure TL immediately

(iii) irradiate

(iv) measure TL immediately

The result of the storage experiment for lava 132 a1 is shown in Fig. 4.9. Above 350°C the % loss of TL was independent of the glow curve abscissa such loss of TL, which is a complete contradiction of the kinetic theory of TL as discussed in Chapter 3, is termed 'anomalous fading'.

4.7 ANOMALOUS FADING OF LAVA TL

As a result of the discovery of 45% loss of TL at the 400°C abscissa in sample 132 a1 after storage for three days at room temperature, other lavas were studied using the same procedure and Table 4.10 summarizes the results for five different lavas. Some of the TL intensity ratio plots are shown in Fig. 4.10(a)(b)(c) and (d). The samples were given doses of about 1 krad and the delayed curve was compared with the mean of the monitor glow curves taken before storage and immediately after the delayed readout. This procedure also makes allowance for a change of sensitivity in the TL response which was not more than 5% between measurements for any of these samples.

All the lavas studied show a loss of high temperature TL on storage at room temperature and hence the assumption that TL occurring above the 400°C abscissa is stable is invalid. The ratio curves for 132 a1 and 129 a4 are of particular interest because they show how samples that exhibit anomalous fading can still pass the plateau test as noted in Table 4.9. Similarly 129 e7 and 129 e14 showed greater fading at lower glow curve abscissae in the laboratory experiments and these samples did not pass the plateau test as applied to the natural TL. However, such agreement of long

TABLE 4.10

ROOM TEMPERATURE FADING IN LAVA

Reference	Lava Type	Temp. ordinate ^{o}C	% TL lost	Time/hours
129 e14	Naples:	400	60	96
129 e7	Trachytic flows	400	35	16
129 a4	Iceland: Plagioclase basalt	350	5	18
132 1	Massif Central: basalt	350	38	150
132 a1		400	45	70

term and short term fading as shown by the ratio tests may not always hold true; 132 il had a good plateau above the 400°C ordinate, Fig. 4.2(b), but this could not have been predicted by the delayed ratio test, Fig. 4.10(a).

In an attempt to predict the fading that might have occurred in a geological sample, long term fading experiments were carried out on four lavas, 129 e7, 129 e14, 129 e15 and 129 a4 and the results are shown in Figs. 4.11(a)(b)(c) and (d); the error bars represent the error on the two measurements made for each point. It can be seen that even if room temperature storage experiments are carried out over several months then the age could still be only obtained within an order of magnitude, always assuming that such extrapolation is valid. For the three fine grain Italian samples the extrapolated log (% TL left) versus log t plots were in agreement with the age data given and the range of equivalent doses obtained, Table 4.11. These results indicate for these lavas that although there is rapid initial fading, there is no long term 'levelling-off' of the fading as suggested by Fleming (Fleming, 1974). Possible mechanisms that could give rise to decays as shown in Figs. 4.11(a)(b) and (c) are discussed in Chapter 8.

4.8 SINGLE GRAIN TL

In view of the results of the previous section the practical conclusion seems to be that anomalous fading is an insurmountable barrier to the dating of lava by conventional fine grain or inclusion techniques. One attempt to get round the problem that was considered however was the study of single grains. In the study of the TL of lunar material it has been reported that the natural TL is due mainly to feldspars but that for a given sample of feldspar grains the natural TL is produced by about 1 grain in 15 (Hoyt, Walker, Zimmerman and Zimmerman). There were also grains that gave very

TABLE 4.11

COMPARISON OF ED_{FG} WITH EXTRAPOLATED VALUES FROM LABORATORY FADING EXPERIMENTS

	Age/10^3 years	ED_{FG}/krad	Measured ED / Calculated ED/%	Extrapolated values of TL left/%
129 e7	4	0.3 - 1.1	4 - 16	10
129 e14	10 - 50	0.3	0.3 - 2	0.5 - 0.8
129 e15	4 - 10	1.25	5 - 13	15 - 23

little natural TL but that gave a considerable amount of TL when given a subsequent artificial irradiation. Although Hoyt et al (1972) do not study anomalous fading, one interpretation is that the grains that have little natural TL are grains that could be shown to exhibit anomalous fading, whereas the remaining grains may not have faded at all. If this is the correct interpretation and if the same situation pertains in lavas then by separating out these non-fading grains dating might be possible.

To be able to study single grains the signal-to-noise ratio and the signal-to-thermal radiation ratio had to be improved. To increase the signal-to-noise ratio the optical system was modified; an annular magnet (EMI C121/6) was placed against the face of the photomultiplier to reduce the active area and by this means the dark current was reduced from 150 counts/second to less than 10 counts/second. The efficiency of the light collection was maintained by using a miniature pyrex light guide 7 mm in diameter; this together with a 7 mm Chance-Pilkington (HA-3) filter and a 7 mm Corning colour filter were held in position with an aluminium tube as shown in Fig. 4.12. Using this system the limitation was due to statistical fluctuation in the TL signal; for a TL intensity of 600 counts/second and with a rate meter time constant of 0.15 seconds, there was a noise level of $\pm$ 50 counts/second, i.e. much greater than the dark count of 4/second. Observations on the 110°C peak in quartz showed this optical system to be only four times less sensitive than one without an annular magnet but with 44 mm diameter filters of the same thickness.

When observing TL above 350°C there is considerable thermal radiation from both the sample and the nichrome heating strip. When using this type of heating for a single grain, the heating plate emission must be masked from the photomultiplier. The best mask was found to be a piece of mica

0.1 mm thick which had been silvered on both sides and had a 0.5 mm diameter hole drilled through the centre to expose the crystal sample which was placed in a depression in the heater plate. Good thermal contact was ensured by a small drop of silicon oil in the depression. Using a 7 mm diameter Corning (5-60) colour filter the thermal radiation at 450°C was 50 ± 20 counts/second.

Colourless, non-magnetic crystals 150 - 400 μ diameter were separated from lava 129 e15 after crushing and were subsequently handled using a vacuum pick-up (model No. VP-50, Henes Manufacturing Co., Arizona) connected to a square ended hypodermic needle with an inside diameter of 50 μ. A Grey Five-Forty binocular microscope was used in sorting the crystals.

Typical smoothed glow curves are shown in Fig. 4.13; when compared with the second glow TL induced by a 10 minute beta irradiation, the natural equivalent dose at the 400°C ordinate is less than 0.4 krad, whereas the equivalent dose calculated from the known age and radioactivity measurements should be in the range 6-15 krad. Only twenty crystals were looked at; the mean equivalent dose obtained was 0.5 ± 0.3 krad. This result agrees with the fine grain results reported in section 4.5, see Table 4.12.

Although a good statistical survey was not carried out, it was thought unlikely that further work would show up grains that did not show anomalous fading. For the lunar sample reported by Hoyt et al it must be emphasised that bulk samples of lunar fines were being studied and hence the initial sources of the two types of feldspar grains found are likely to be quite different. In the case of lava, the crystals come from the same piece of rock and are likely to have cooled at the same rate and contain the same impurities; it is therefore unlikely that any one grain should have completely different fading properties.

TABLE 4.12

129 e15 COMPARISON OF FINE GRAIN AND SINGLE CRYSTAL RESULTS

	(a) Calculated ED/krad	(b) Measure ED/krad	(b)/(a)
Fine Grain 1 - 8 μ	9.6 - 24	1.25	5 - 13%
Single crystals 150 - 400 μ	6 - 15	0.5 ± 0.3	3 - 8%

There is however one possible refinement of the study of single crystals that could permit dating of certain lavas. When the magma erupts it can pick up crystals, e.g. quartz, from the surrounding older rock; subject to their lack of anomalous fading, such crystals could be dated.

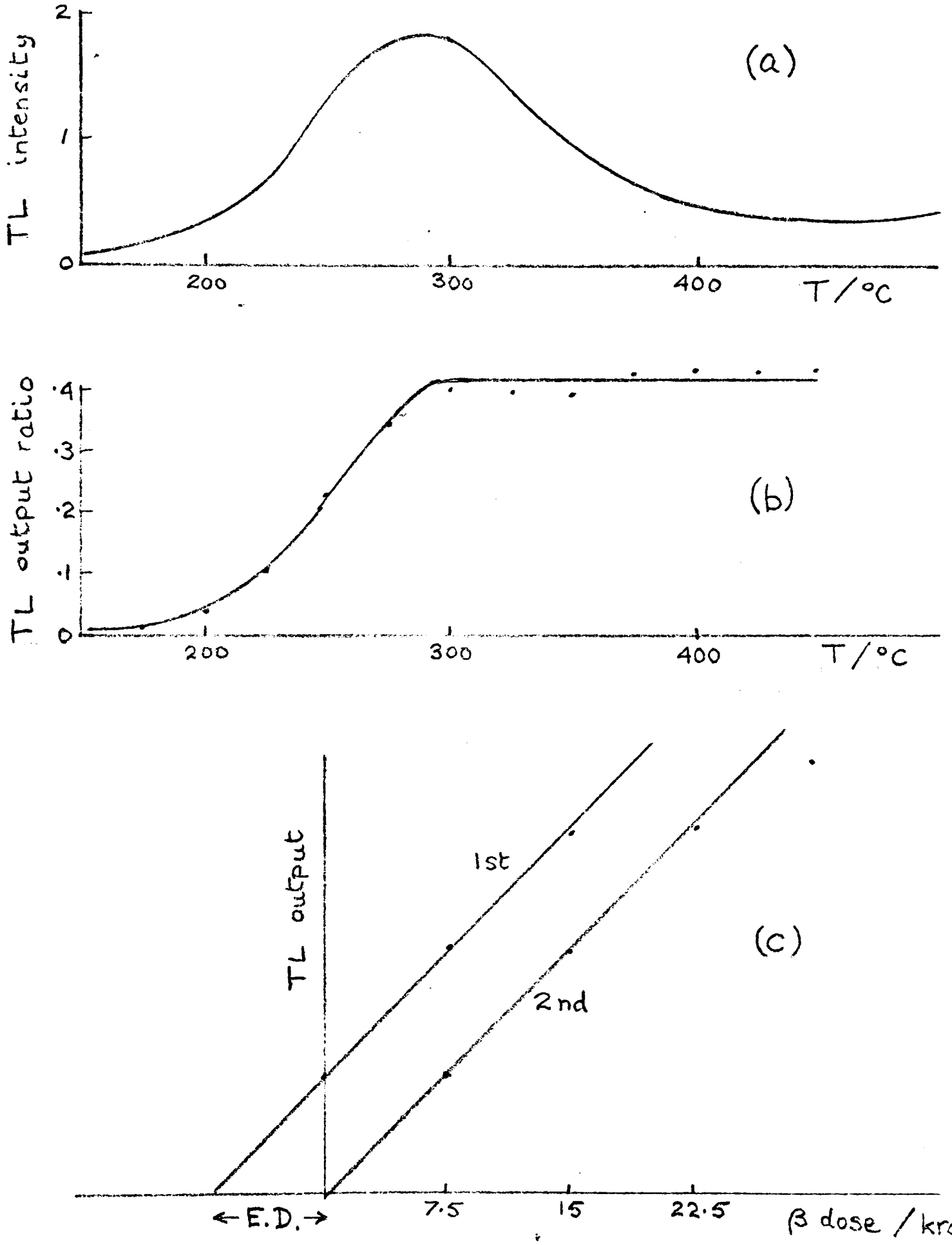

Fig. 4.1 132a 12 Fine grain TL

(a) natural glow curve

(b) plateau test N/N+β

(c) β dose growth curves for 400°C ordinate

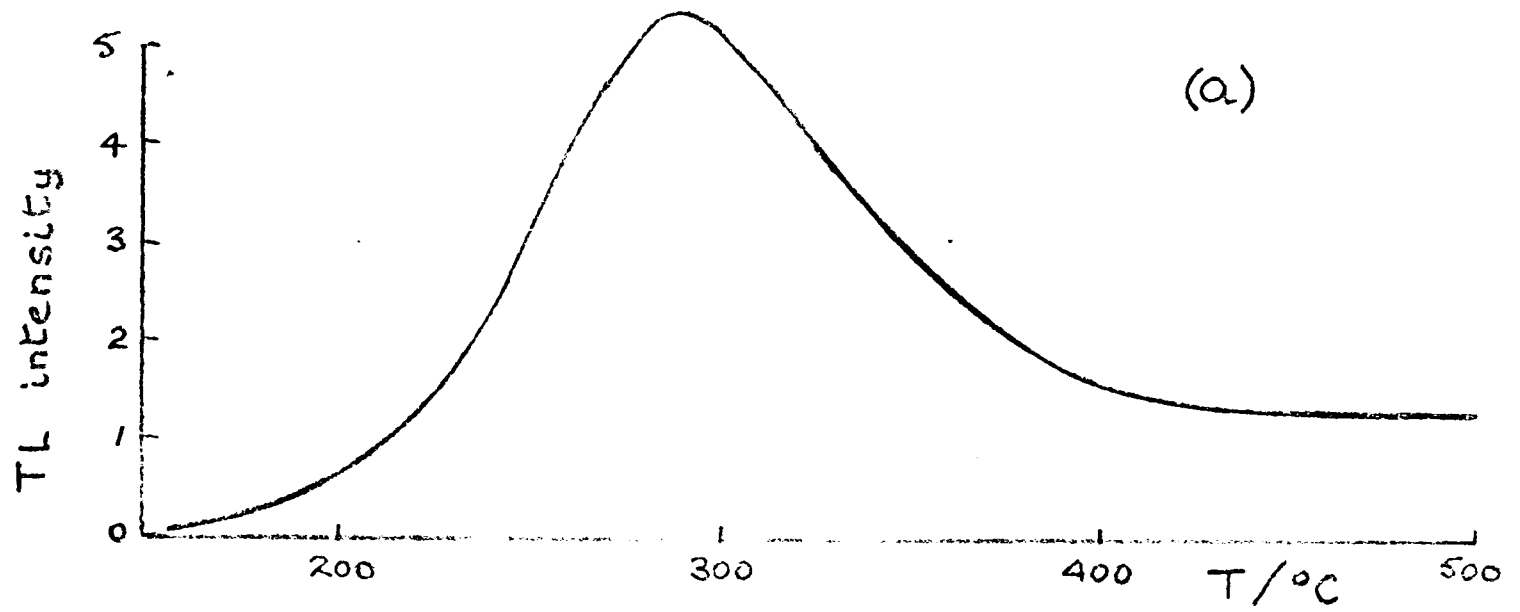

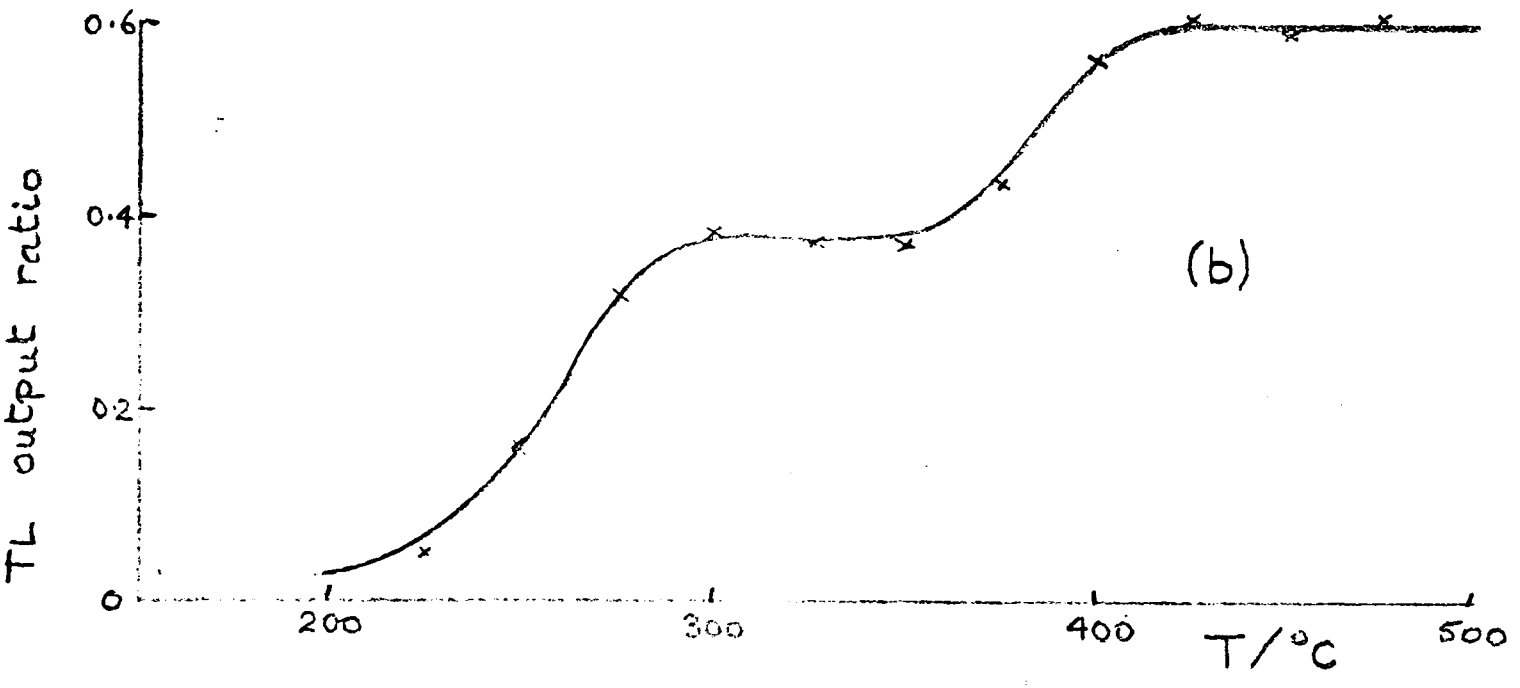

Fig. 4.2 132 i 1.1 Fine grain TL

(a) natural glow curve

(b) plateau test $N/N+\beta$

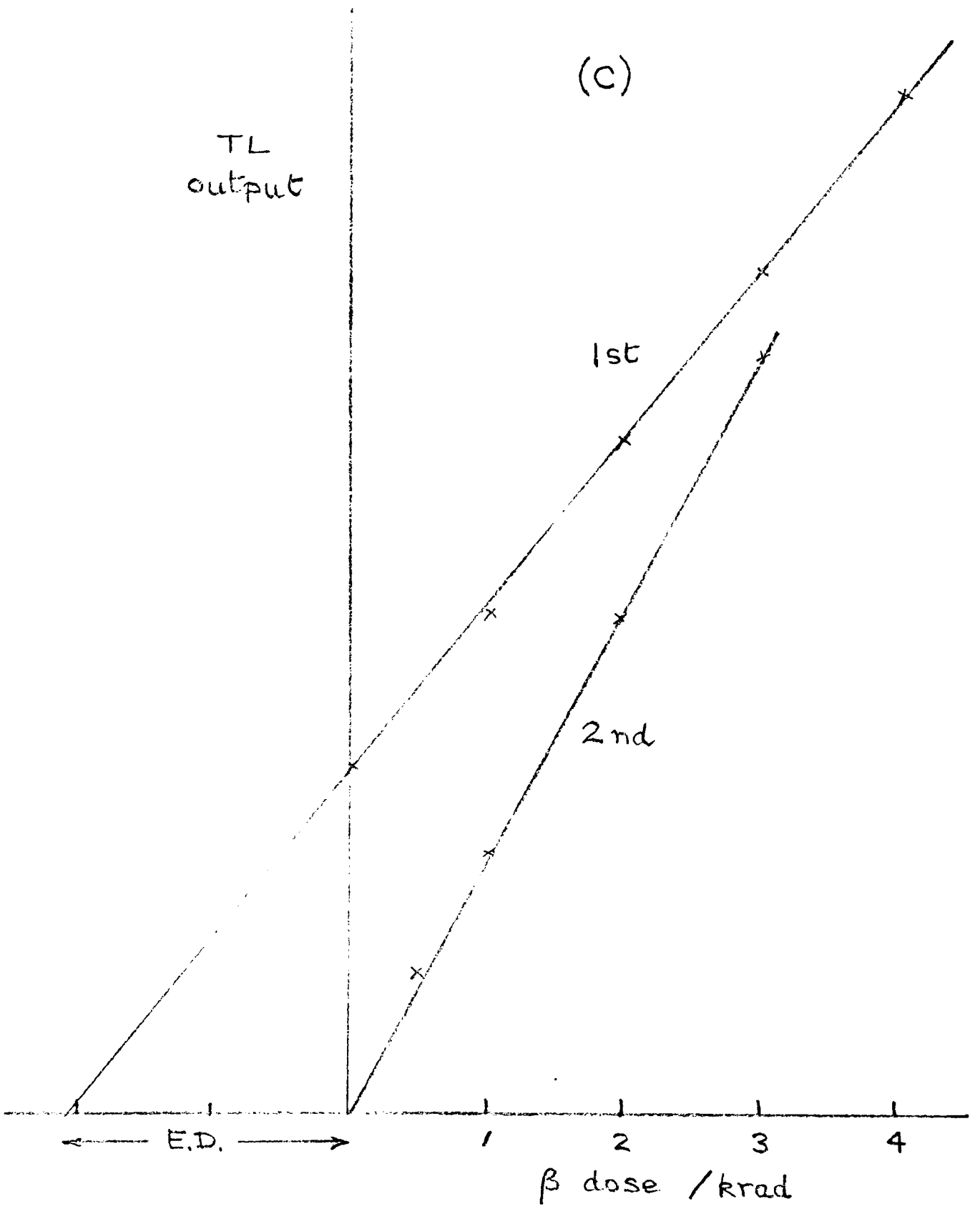

Fig. 4.2 132 i 1.1 Fine grain TL

(c) β dose growth curves for 450°C ordinate

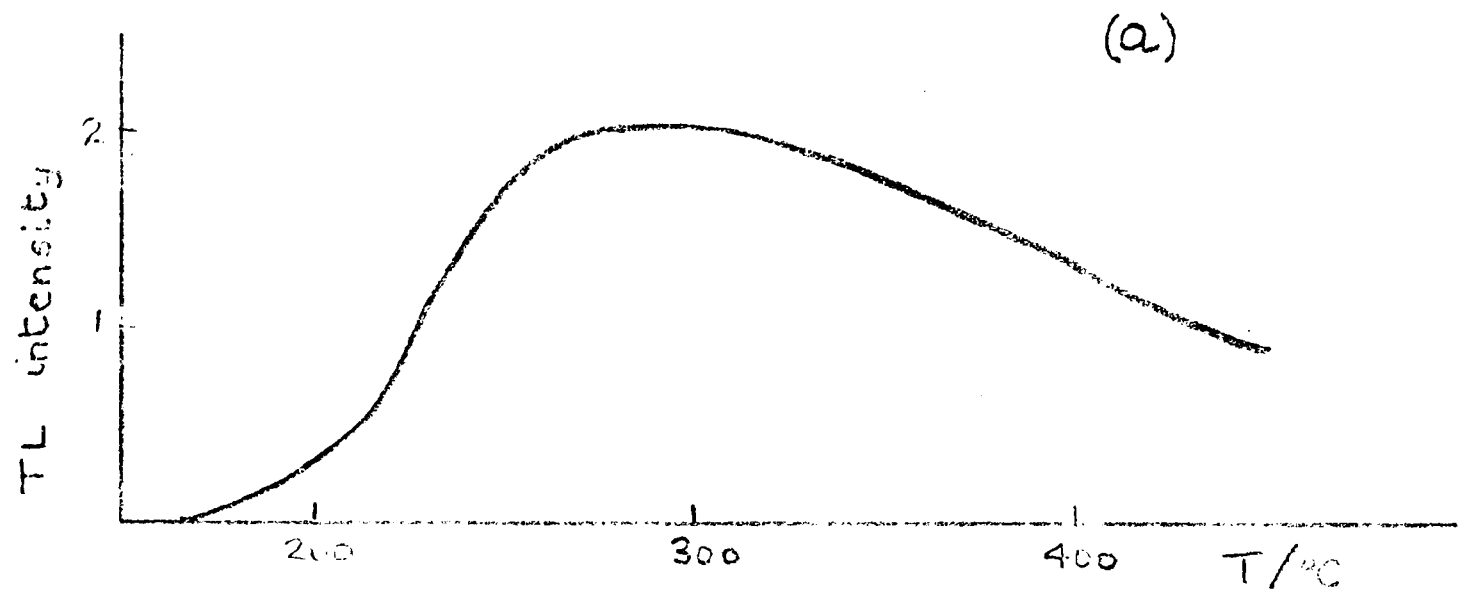

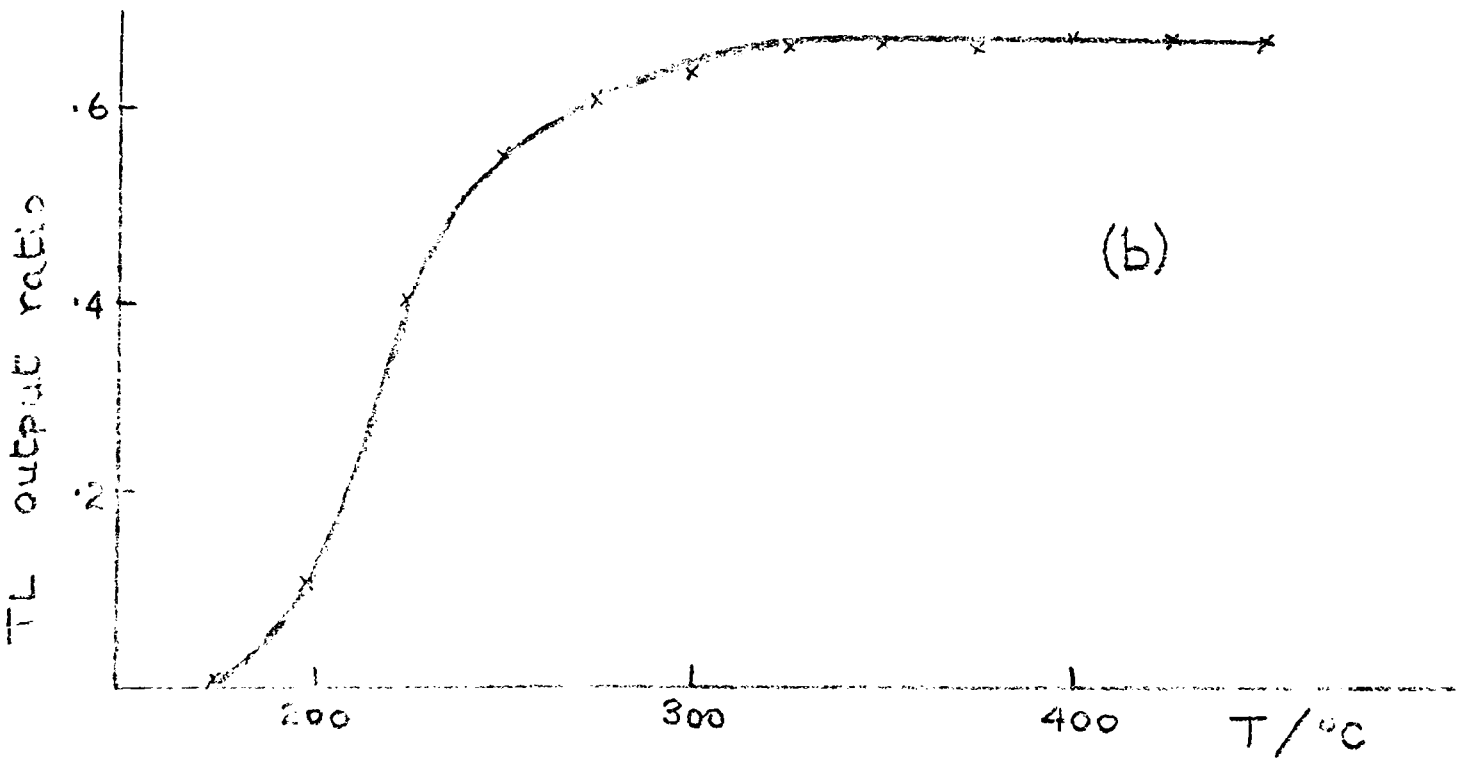

Fig. 4.3 132 h 1.1 Fine grain TL

(a) natural glow curve

(b) plateau test N/N+β

(C)

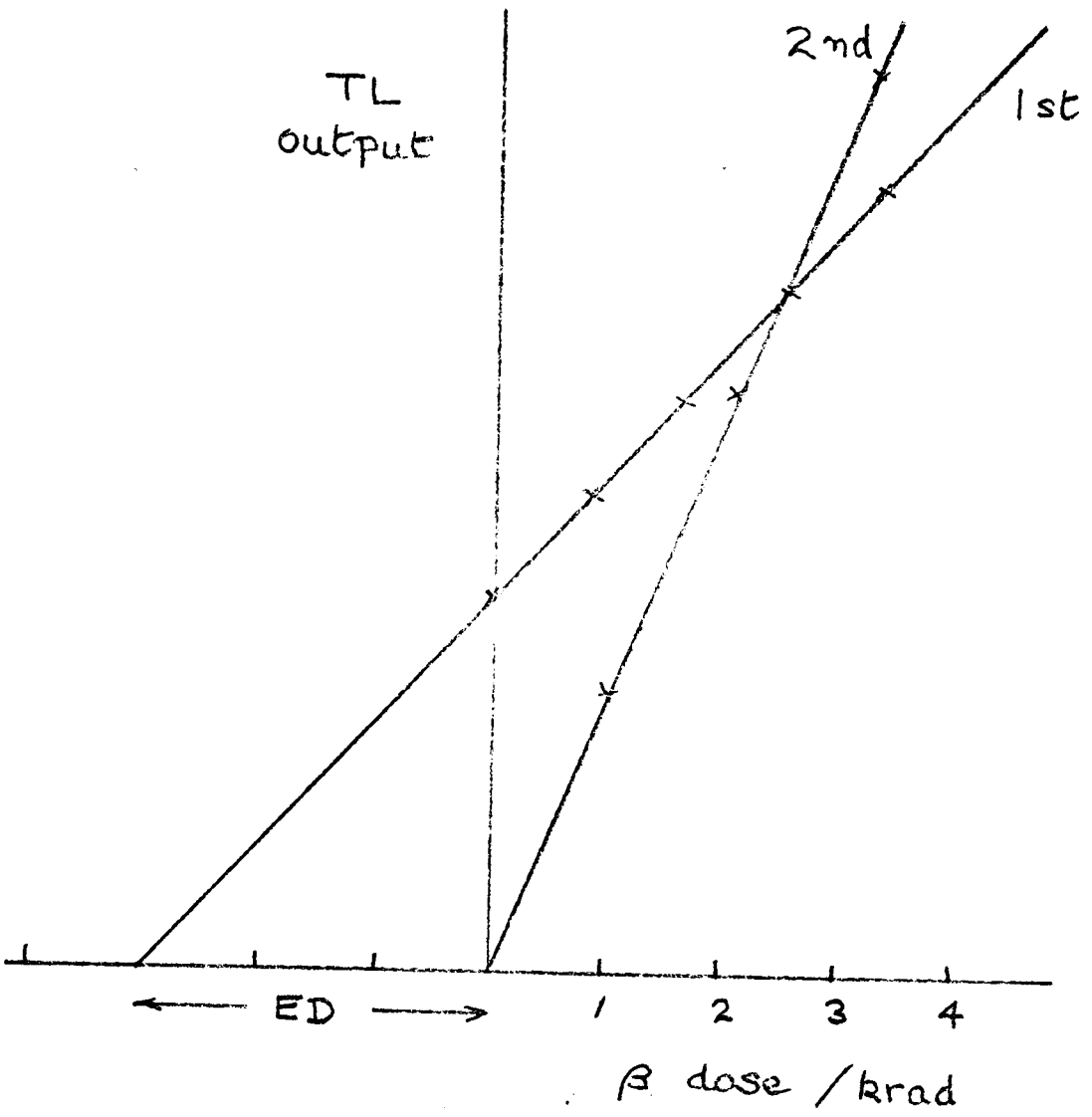

Fig. 4.3 132 h 1.1 Fine grain TL

(c) β dose growth curves for 350°C ordinate

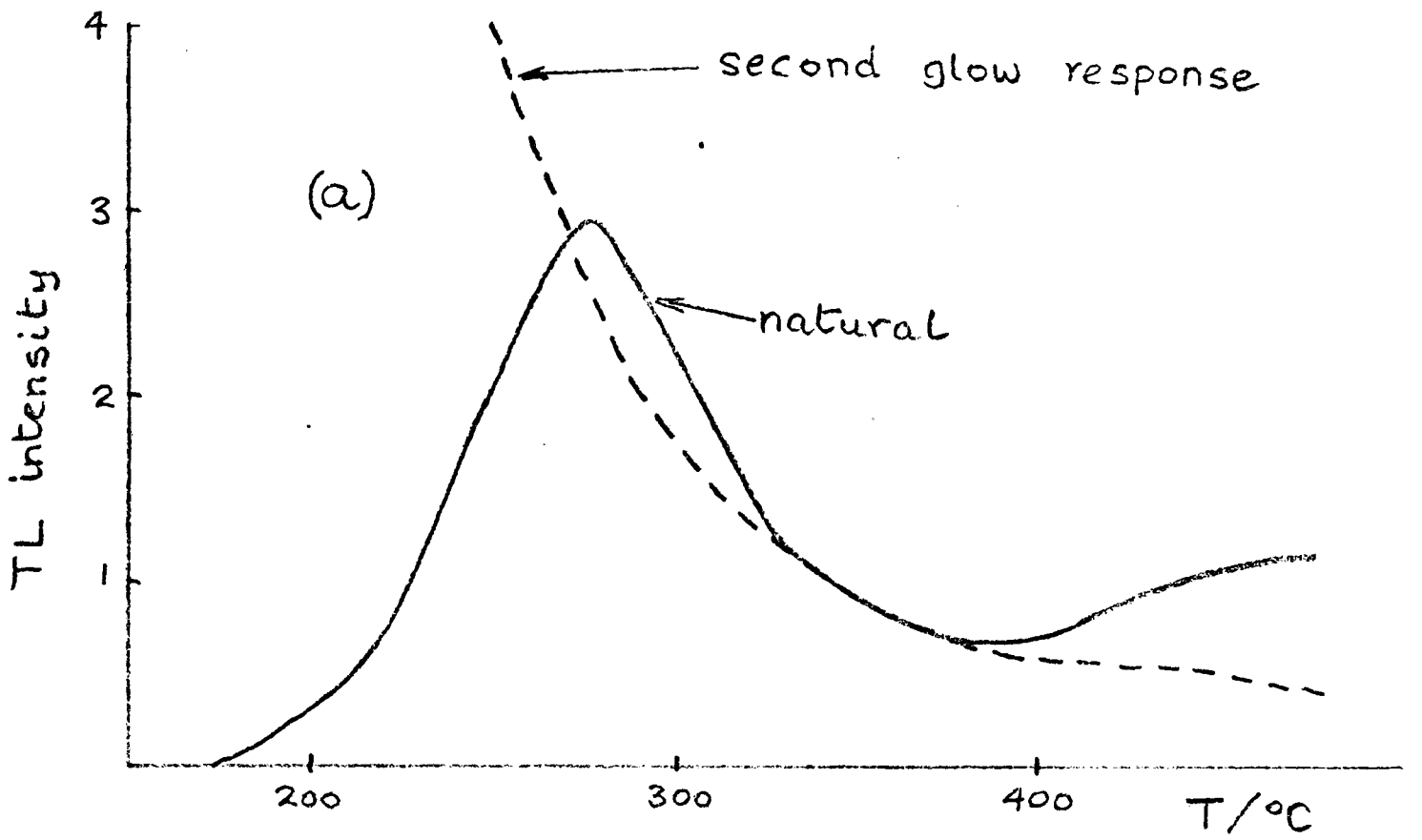

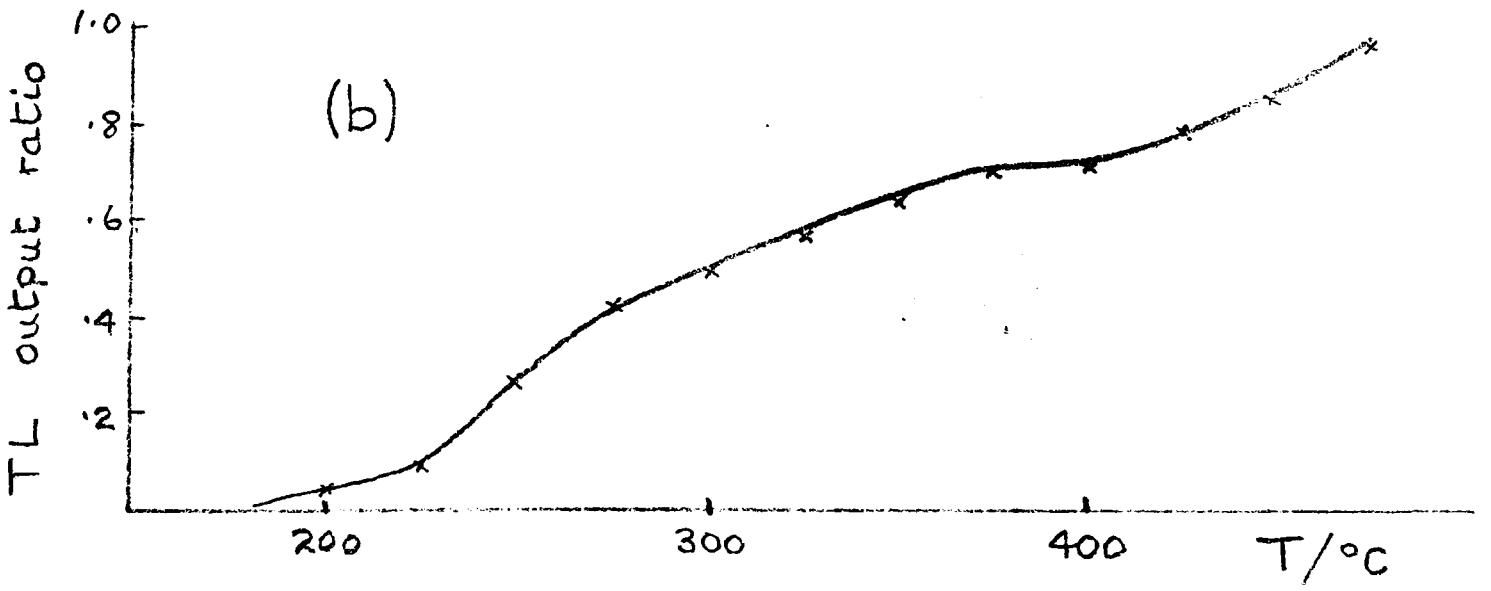

Fig. 4.4 129 e 7 Fine grain TL

(a) glow curves

(b) plateau test N/N+β

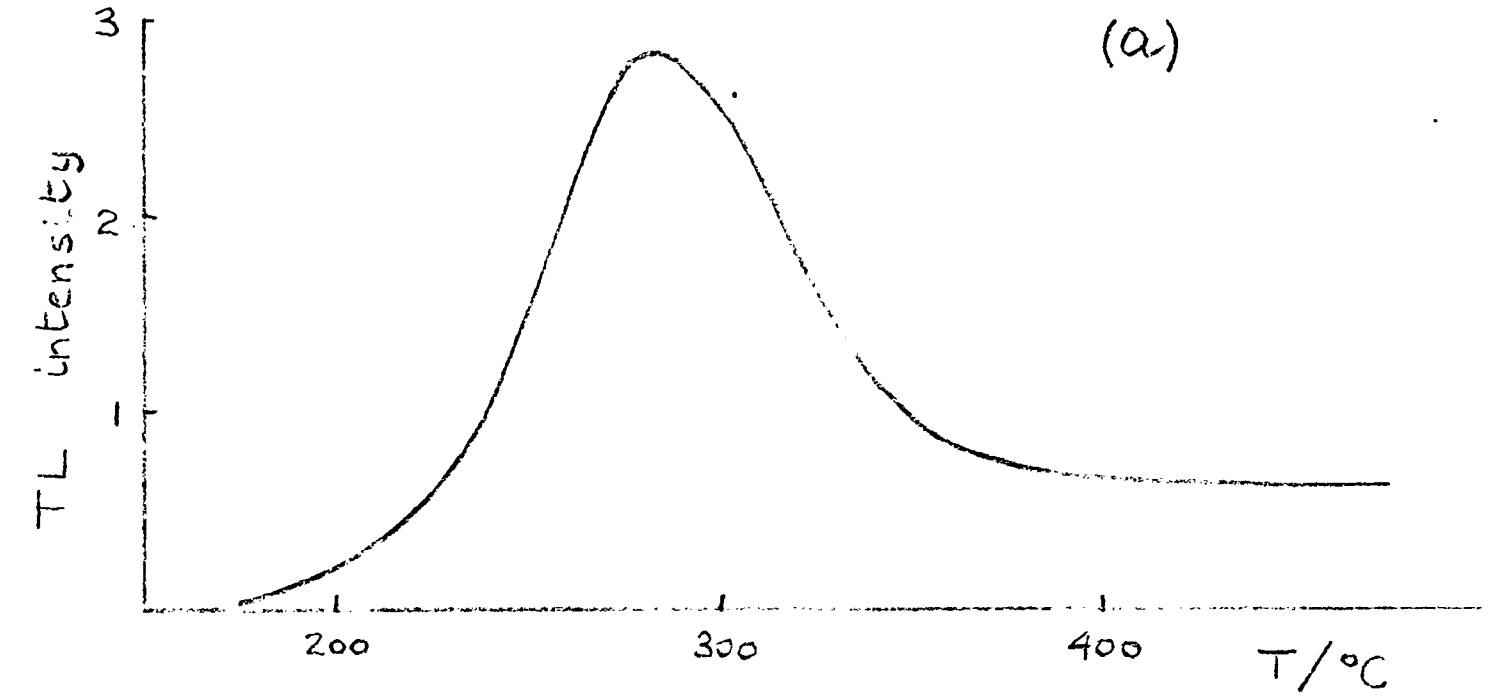

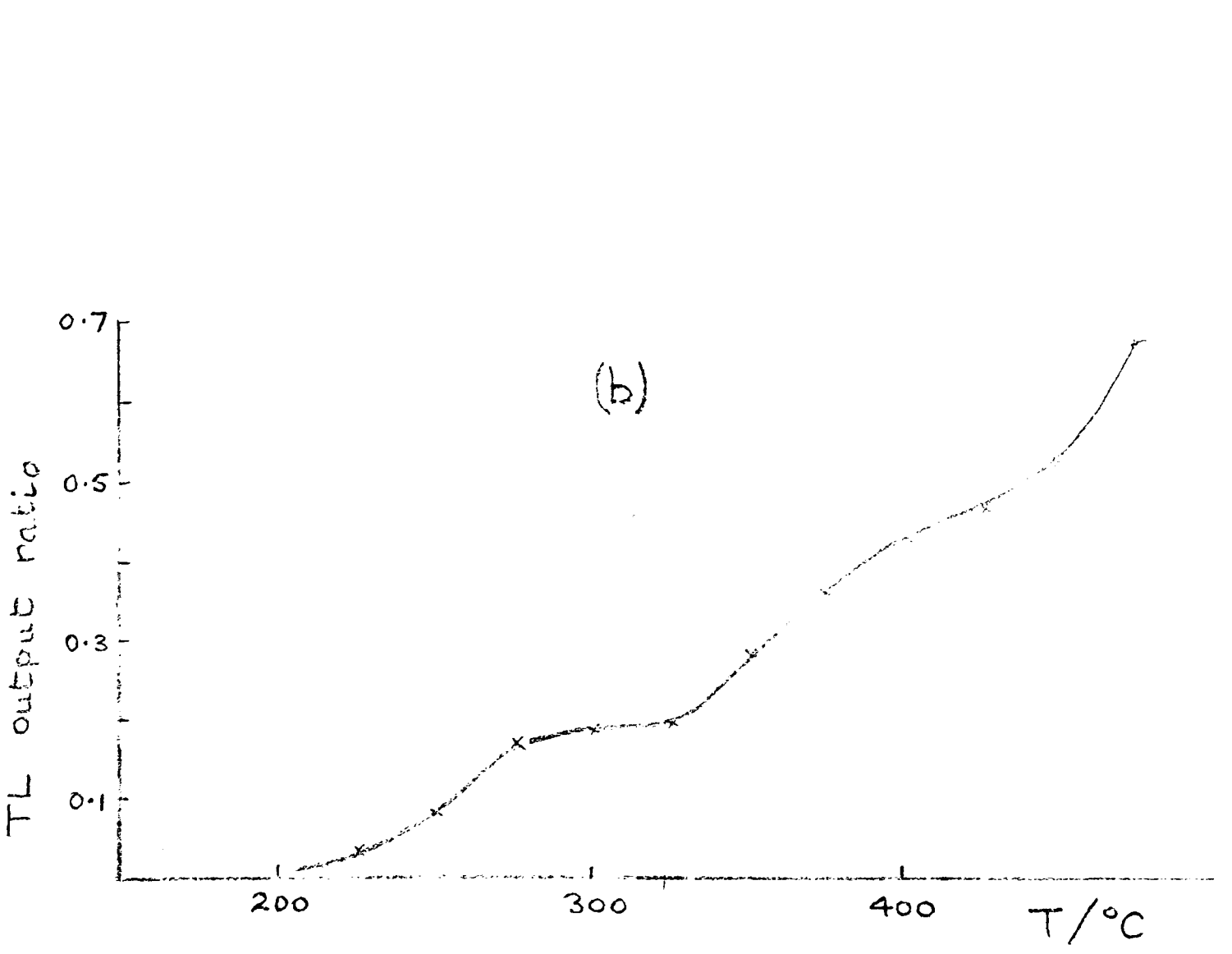

Fig. 4.5 129 e 14.1 Fine grain TL

(a) natural glow curve

(b) plateau test N/N+β

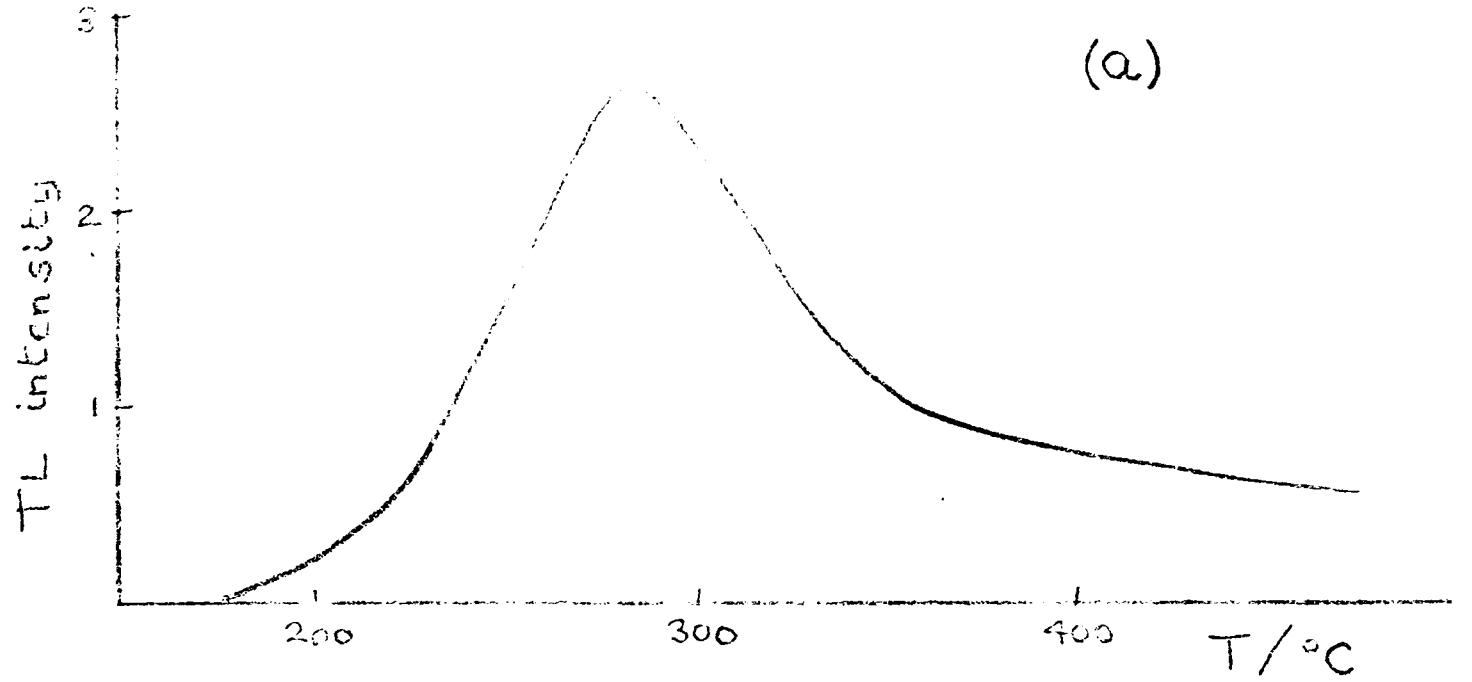

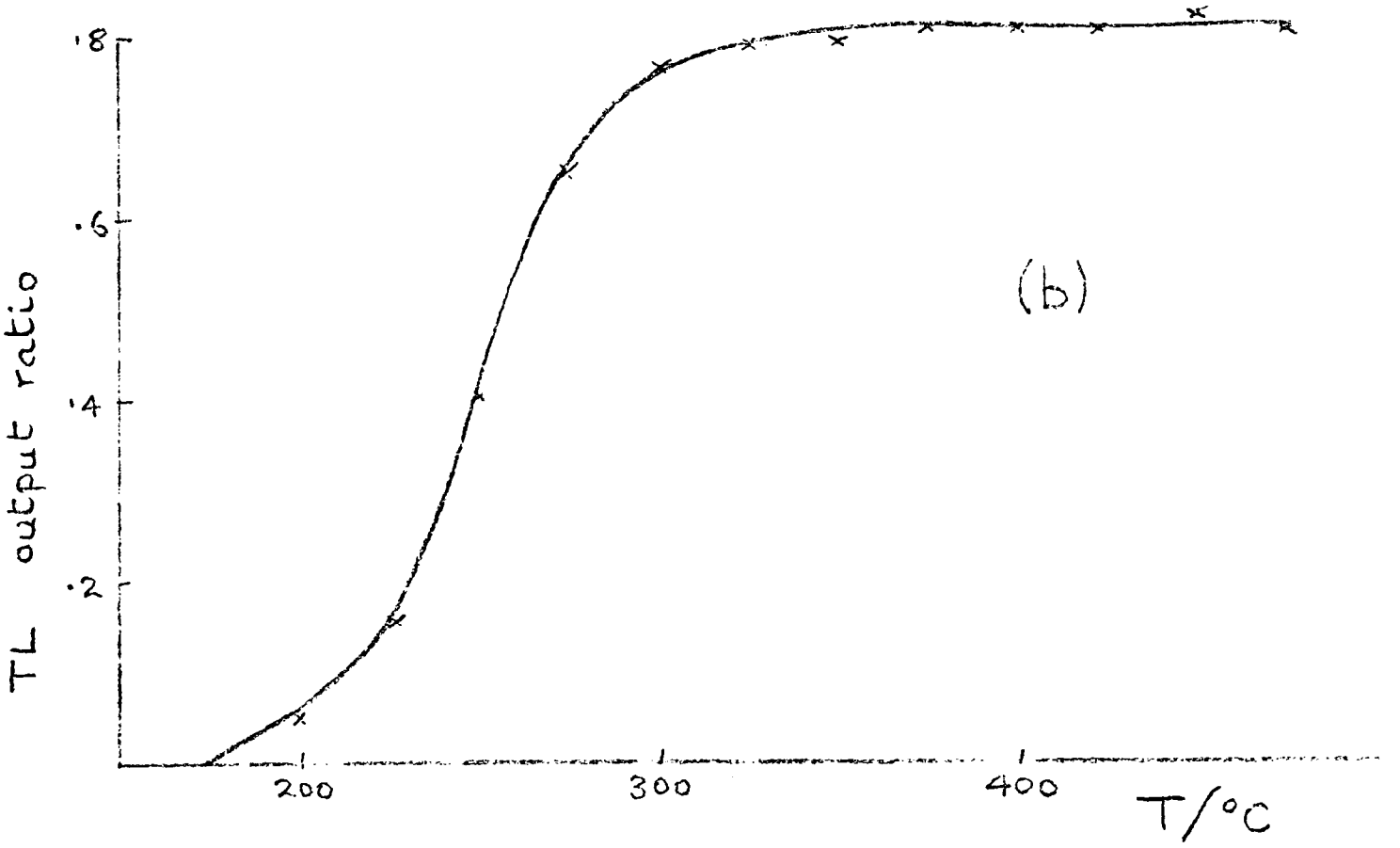

Fig. 4.7 129 e 15.1 Fine grain TL

(a) natural glow curve

(b) plateau test N/N+β

(c)

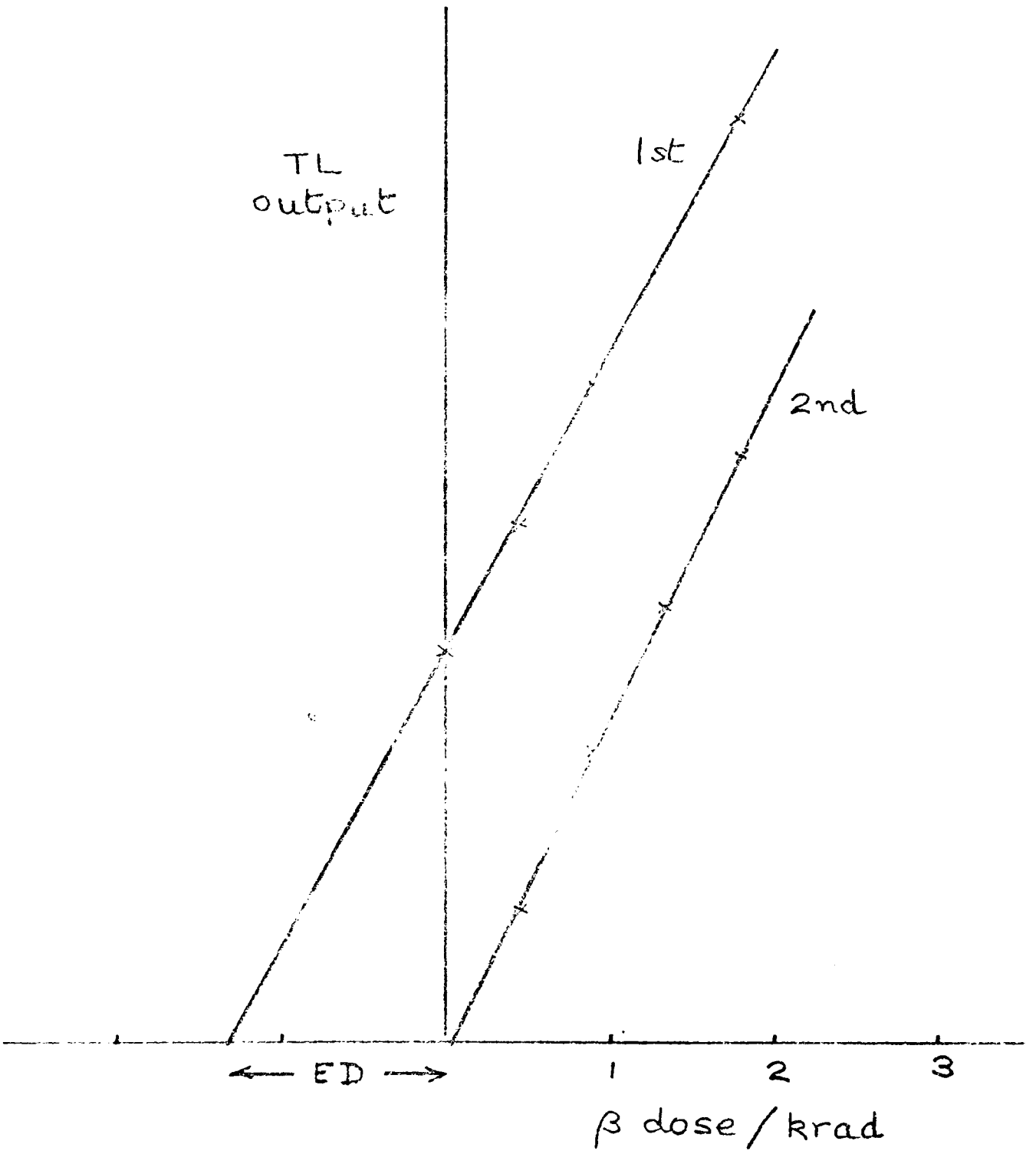

Fig. 4.7 129 e 15.1 Fine grain TL

(c) beta dose growth curves for 400°C ordinate

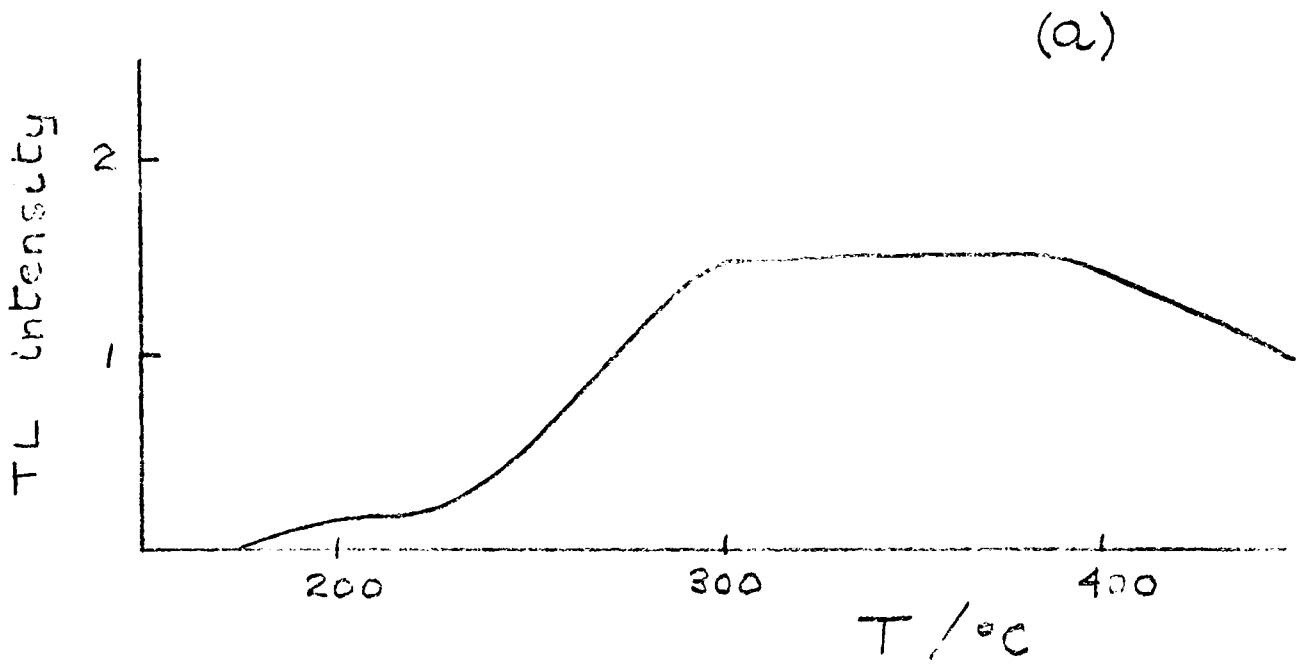

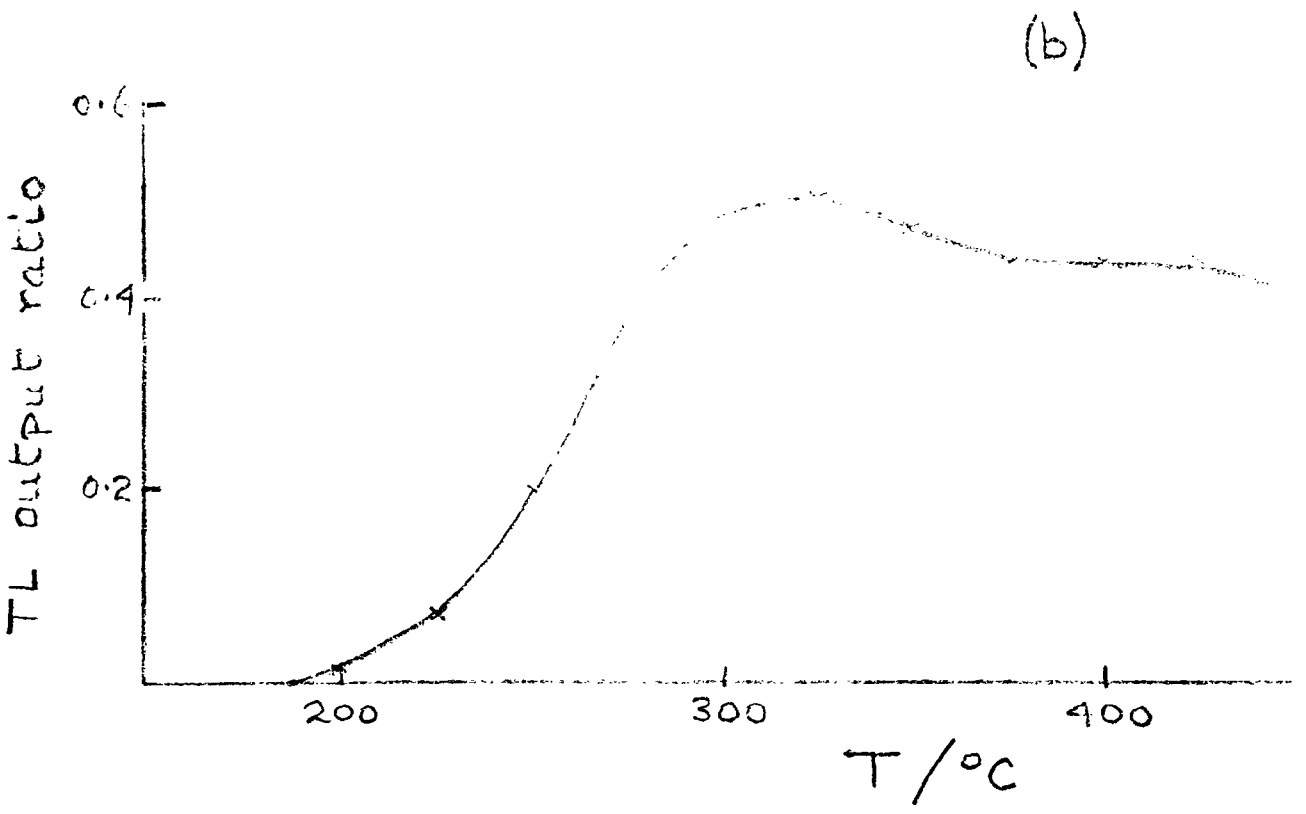

Fig. 4.8 129 a 4.2 Inclusion TL

(a) natural glow curve

(b) plateau test N/N+β

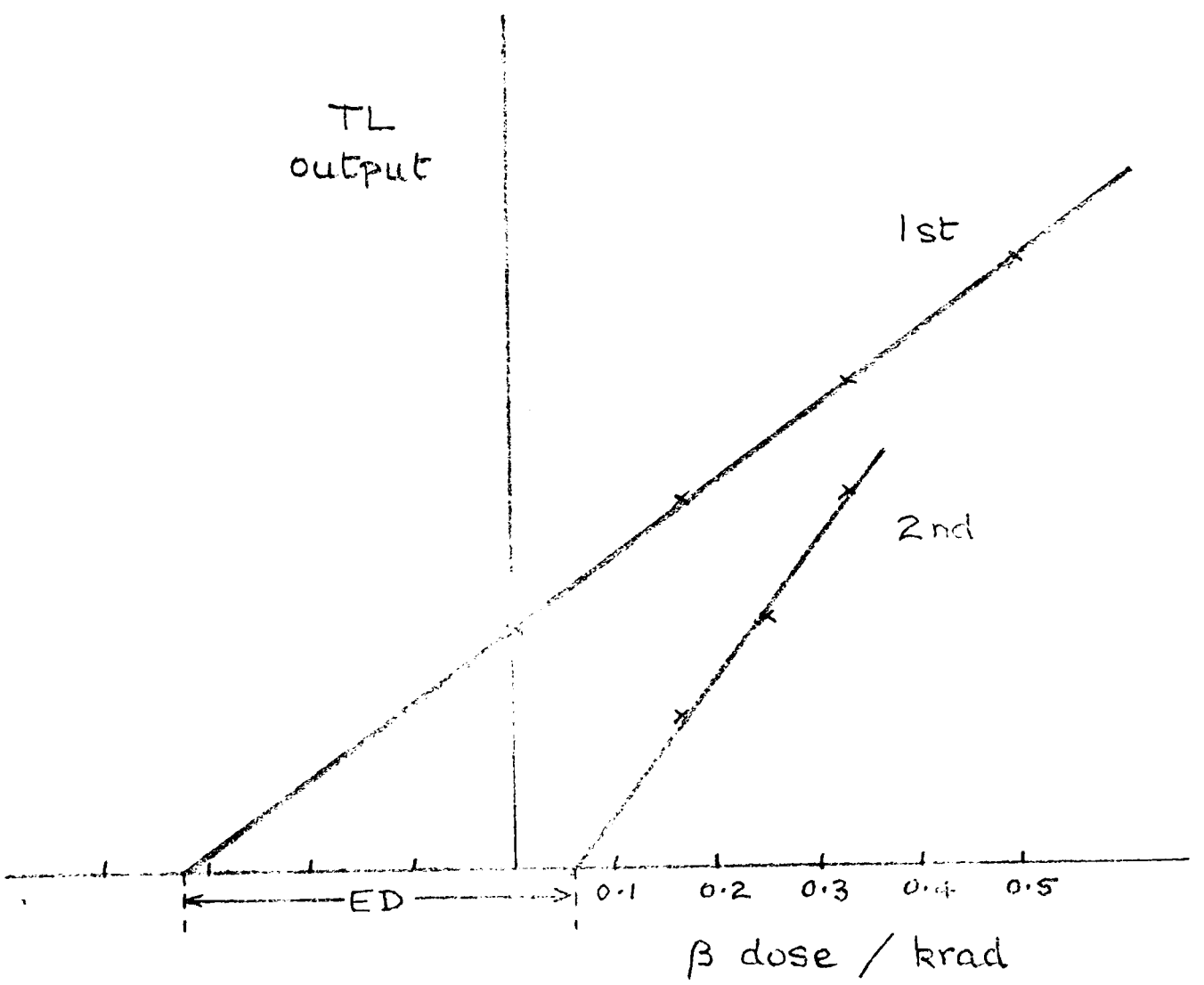

Fig. 4.8 129 a 4.2 Inclusion TL

(c) beta dose growth curves for the 400°C ordinate

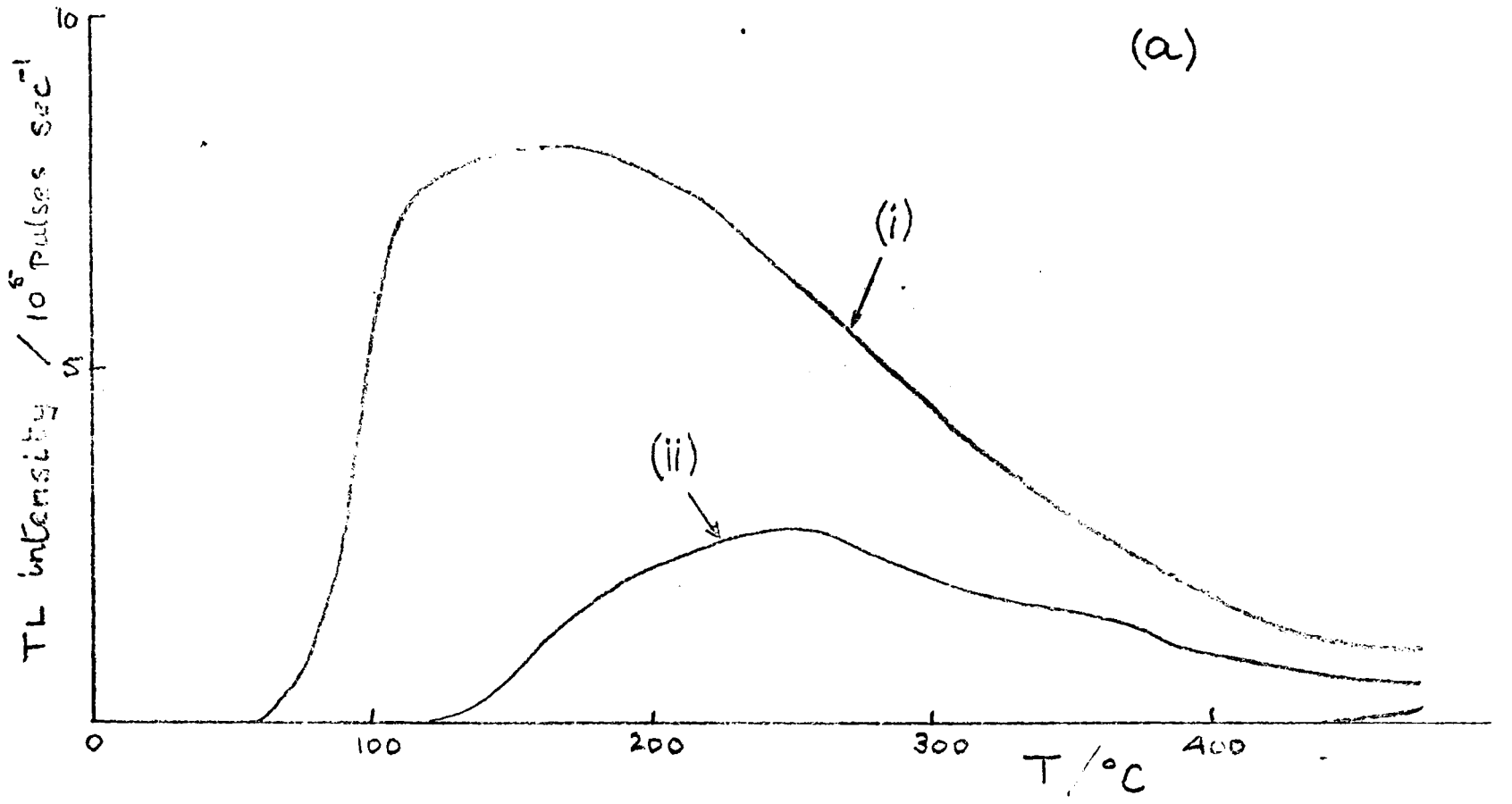

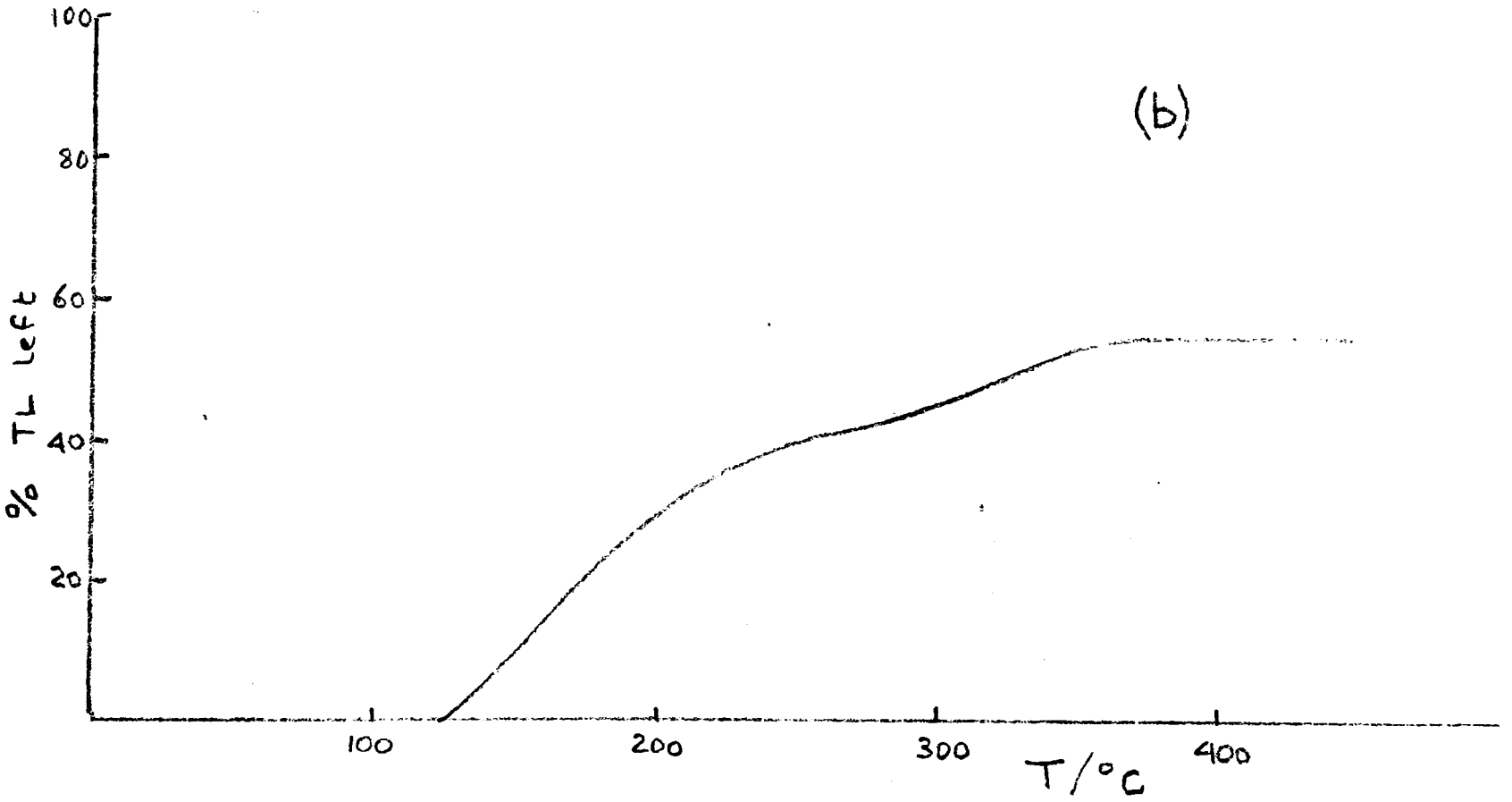

Fig. 4.9 (a) TL glow curves for 132 al

(i) immediately after irradiation

(ii) after storage for 3 days at room temperature

(b) TL intensity ratio curve derived from (a)

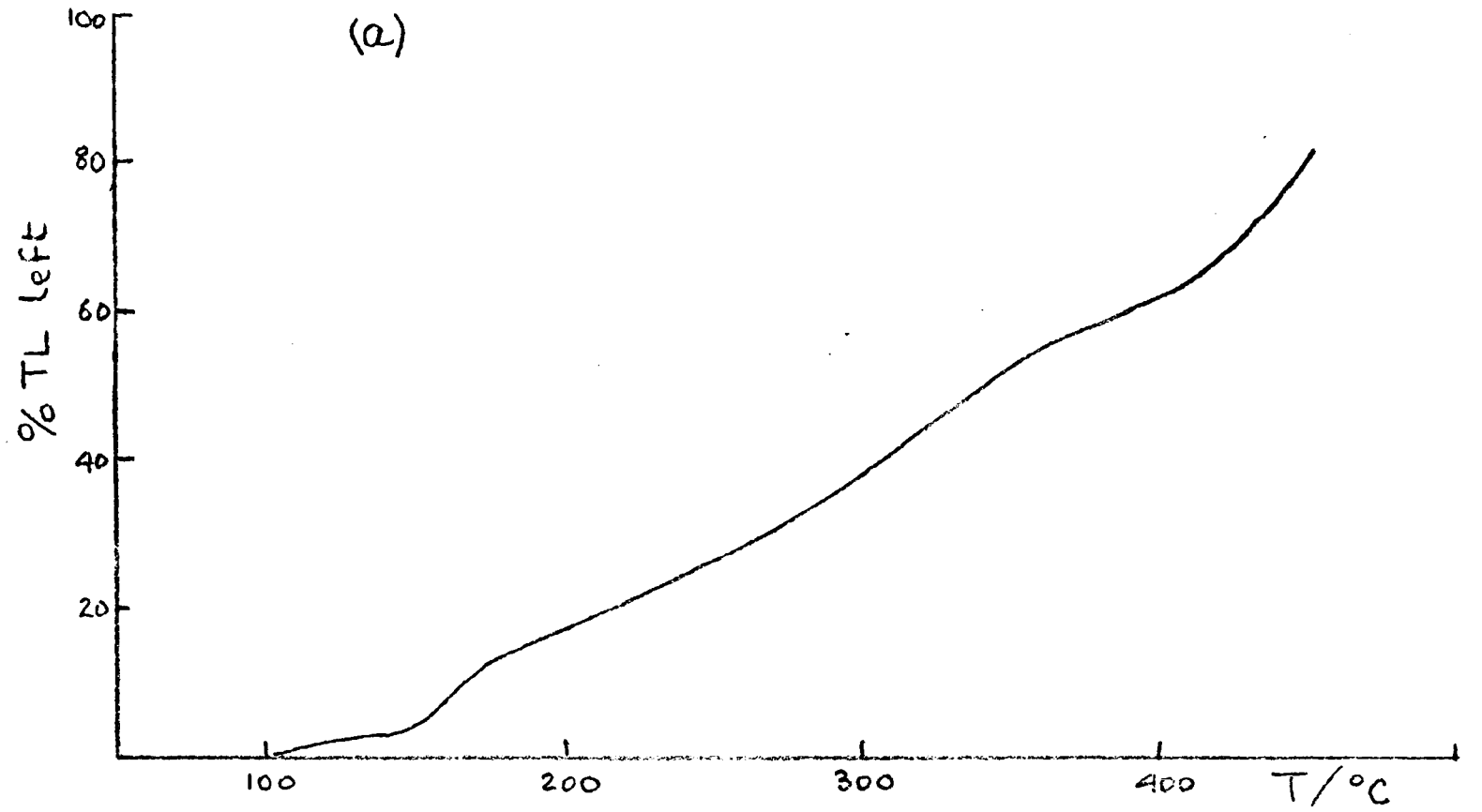

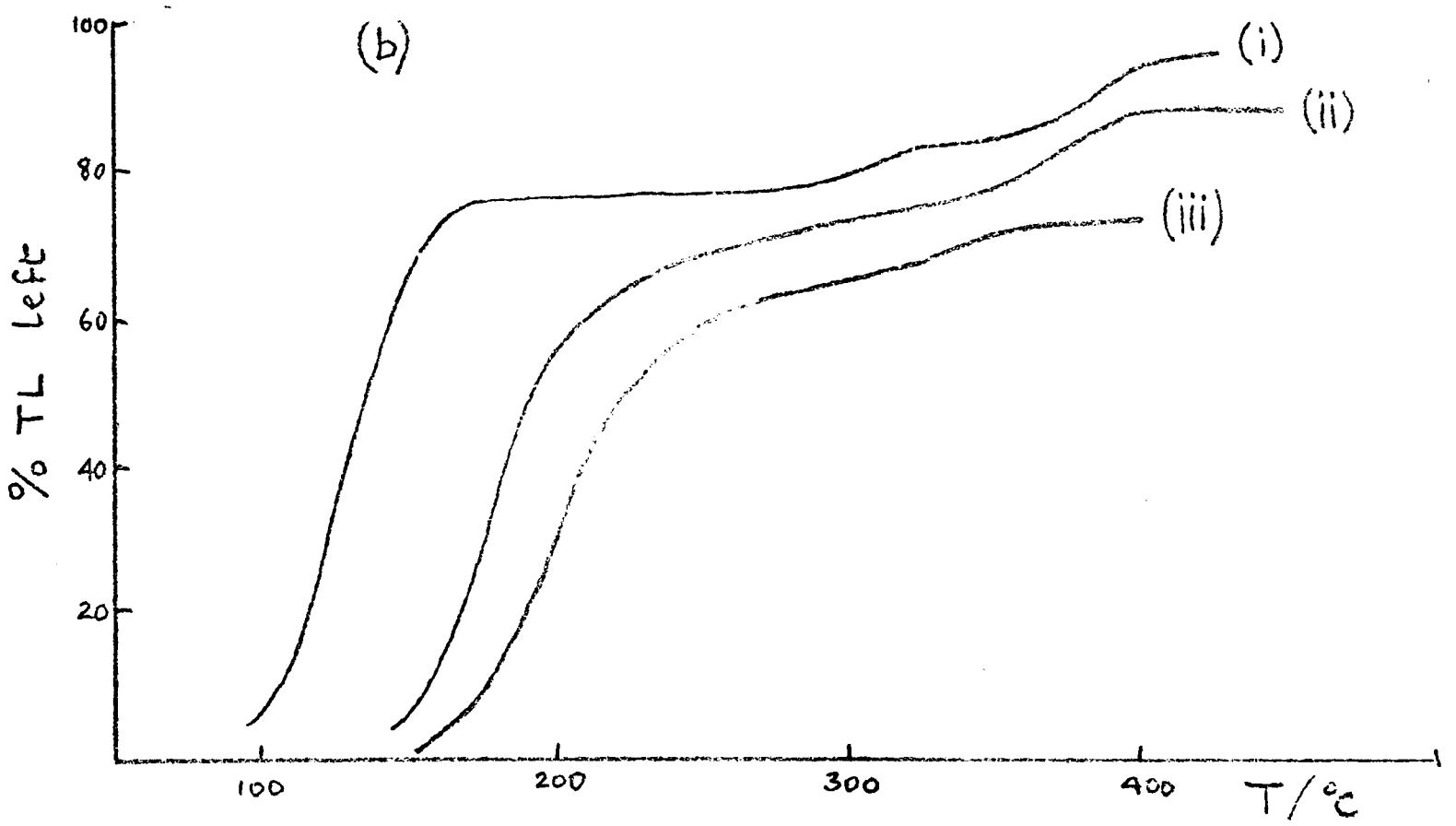

Fig. 4.10 Fading at room temperature

(a) Sample 132 i1, storage time t = 147 hours

(b) Sample 129 a4, (i) t = 18 hours (ii) t = 5, 7 and 18 days (iii) t = 8 months

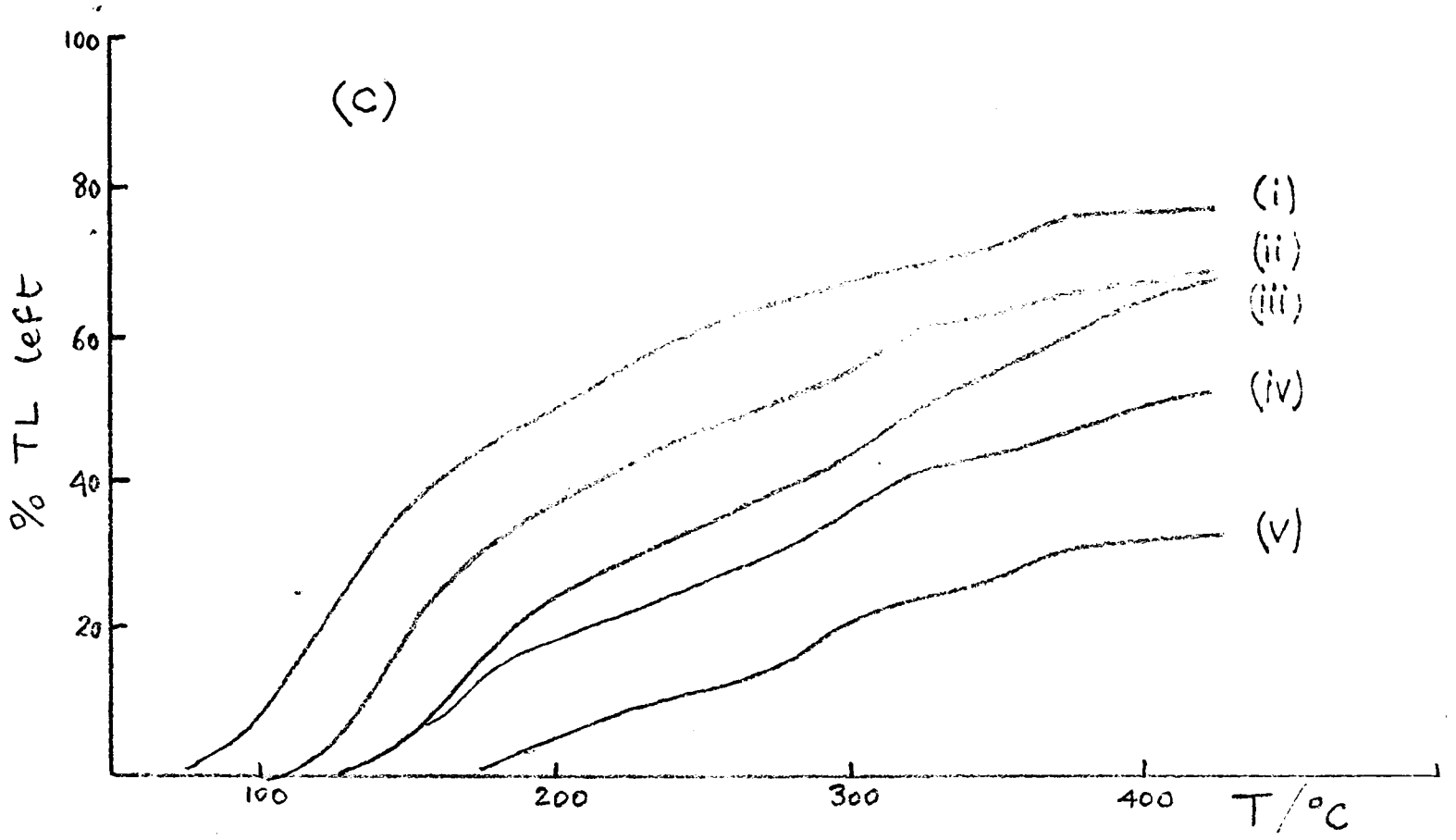

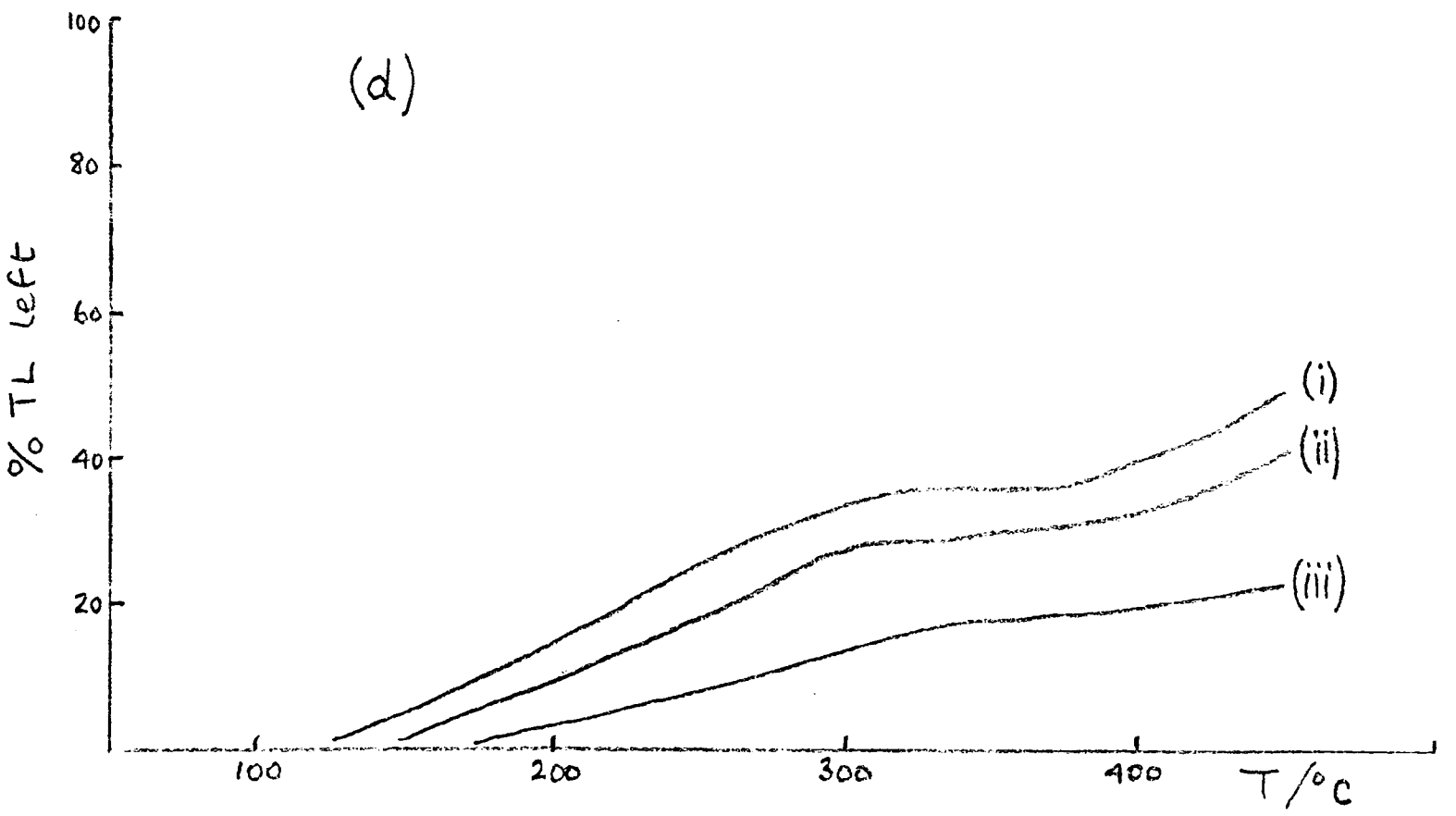

Fig. 4.10 Fading at room temperature

(c) Sample 129 e7, storage times t (i) $3\frac{1}{4}$ hours (ii) 16 hours (iii) 60 hours (iv) 220 hours (v) 8 months

(d) Sample 129 e14, storage times t (i) 96 hours (ii) 9 days (iii) 76 days

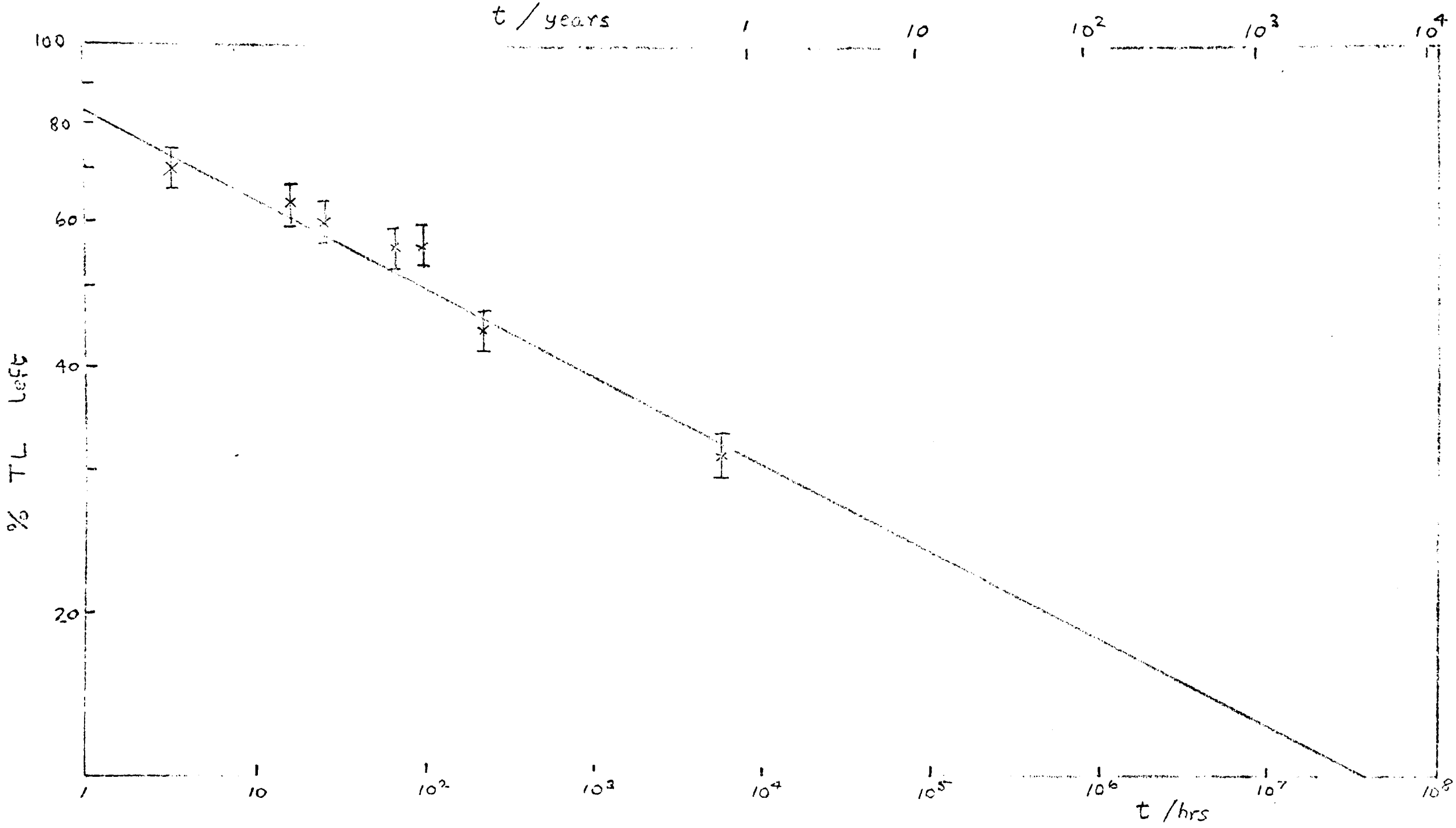

Fig. 4.11(a) Sample 129 e 7: Fine grains, decay of TL at 375°C ordinate

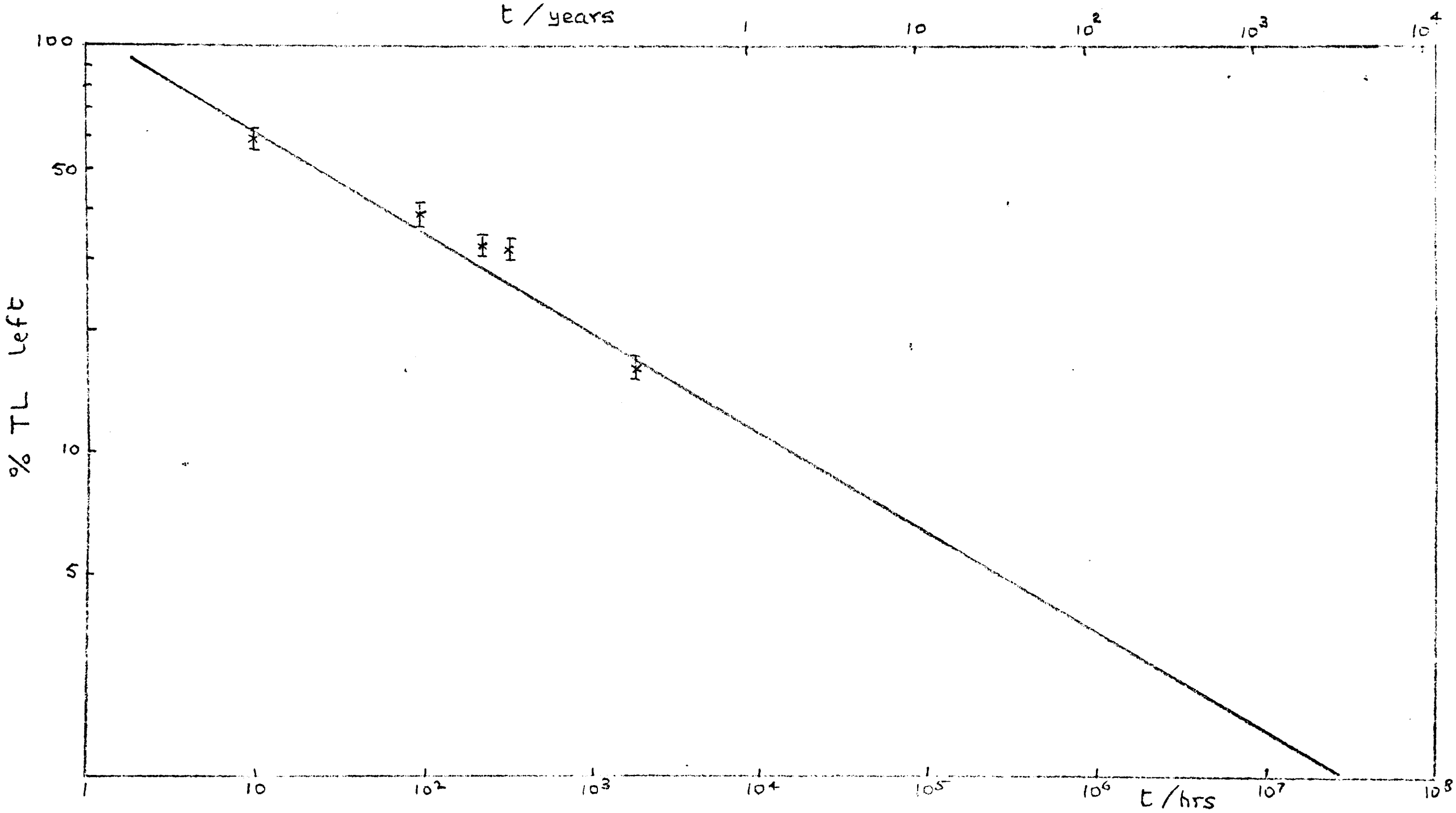

Fig. 4.11(b) Sample 129 e 14: Fine grains, decay of TL at 400°C ordinate

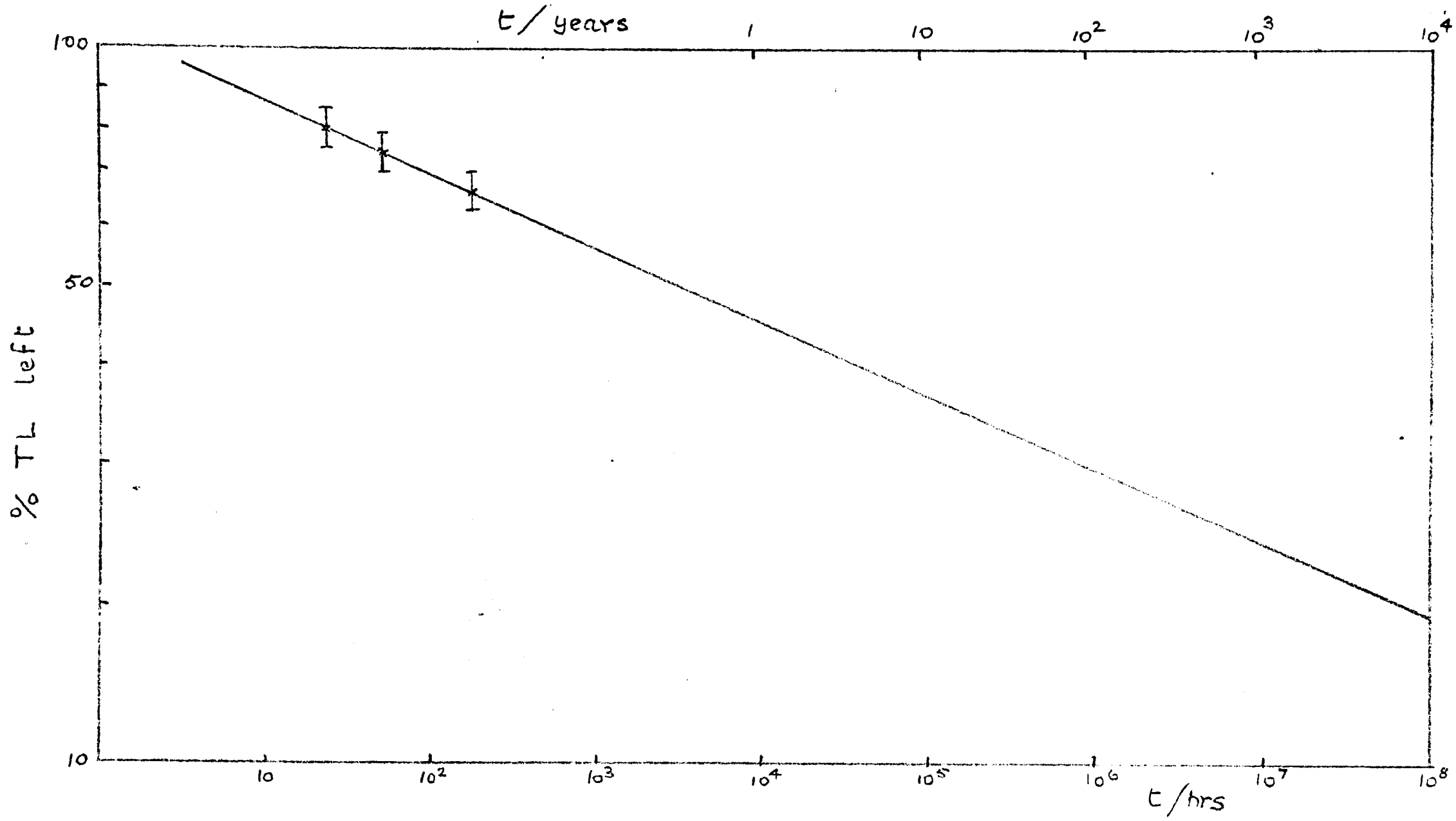

Fig. 4.11(c) Sample 129 e 15.1: Fine grains, decay of TL at 400°C ordinate

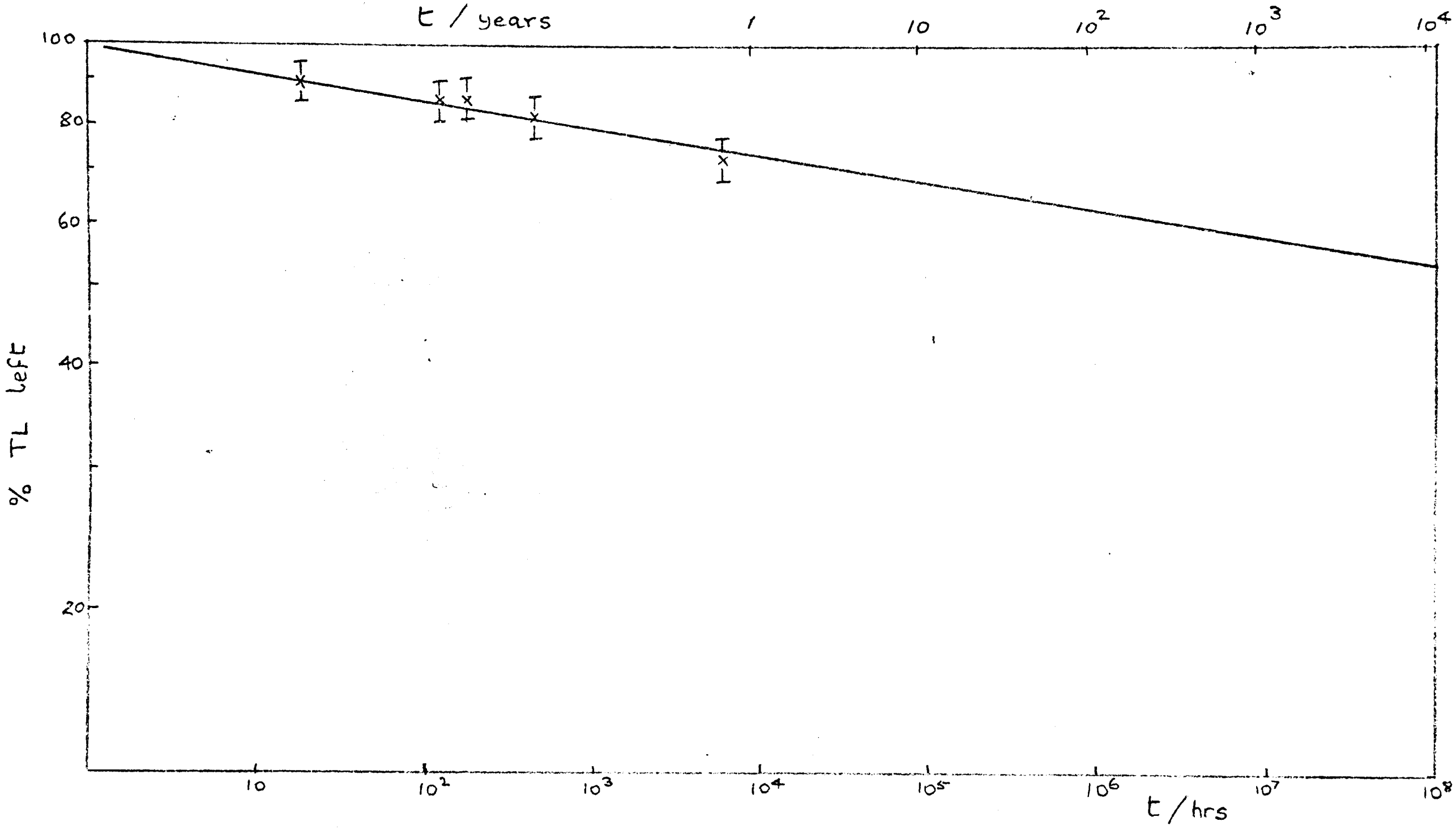

Fig. 4.11(d) Sample 129 a 4.2: Inclusions, decay of TL at 400°C ordinate

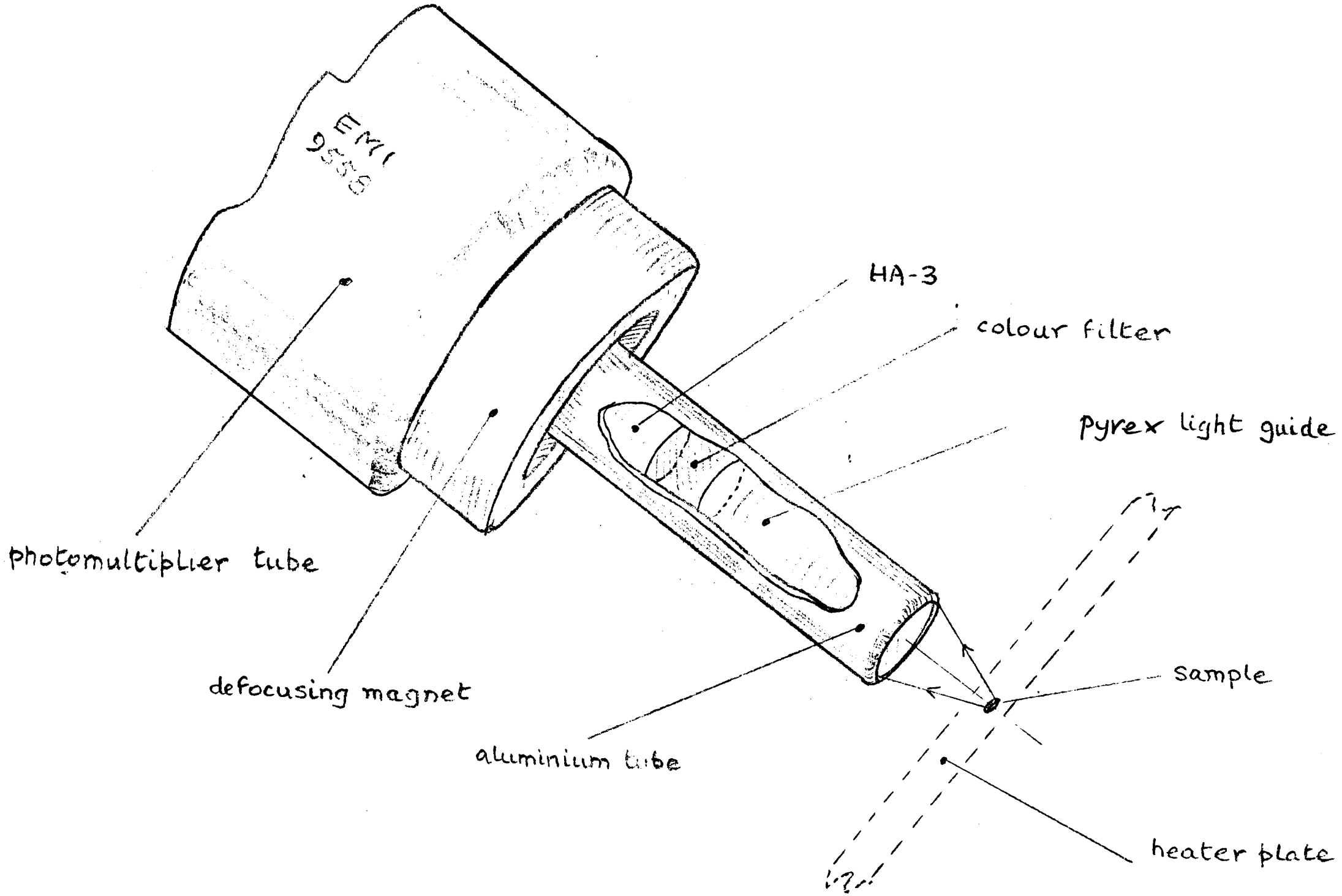

Fig. 4.12 Optical system for single crystal work

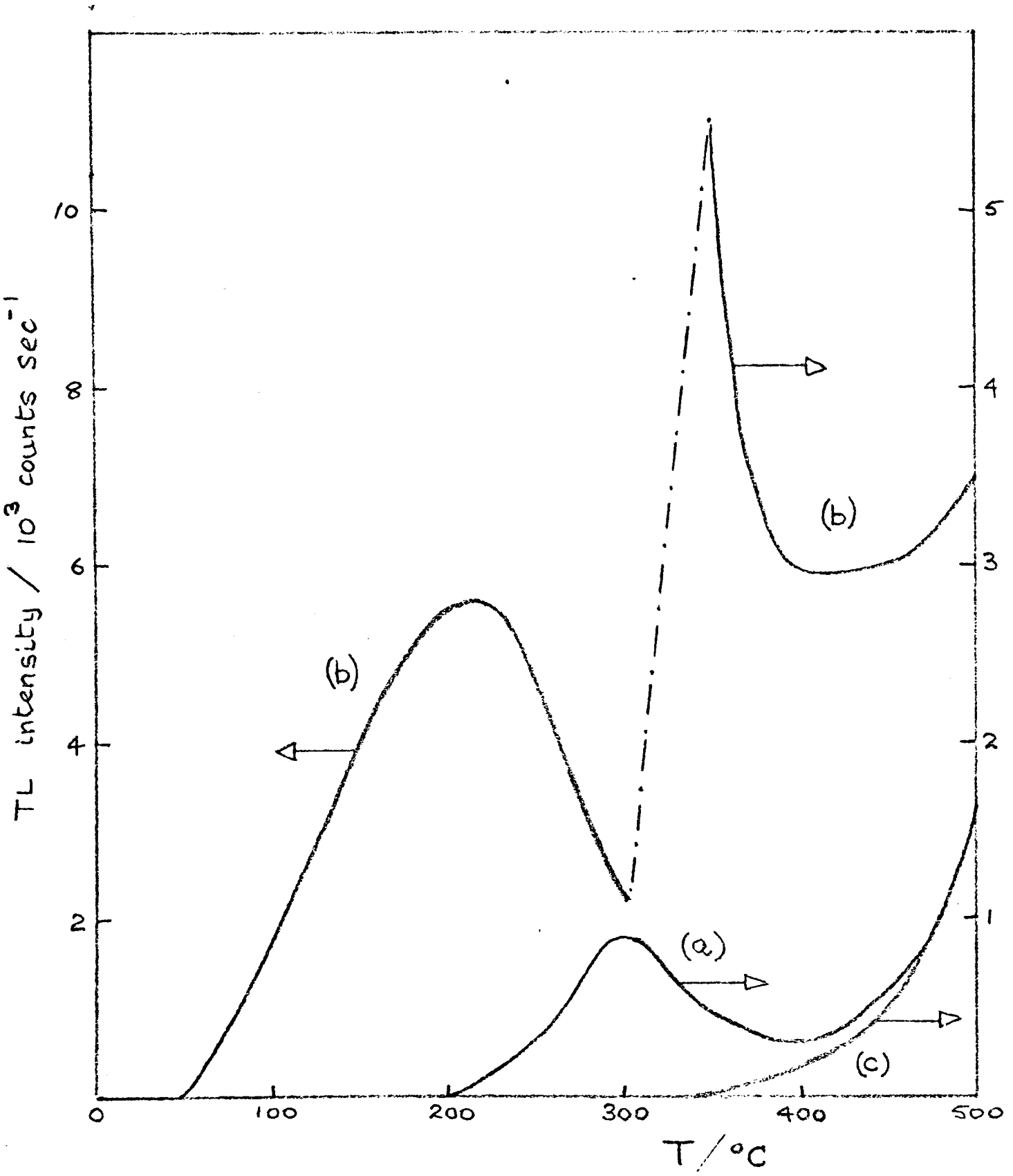

Fig. 4.13 Sample 129 e 15: Single grain TL glow curve

(a) natural

(b) artificial, induced by β dose of 10 krad

(c) thermal radiation

PART II

Following this discovery of instability of the high temperature TL in lava and its serious effect on the dating of lava, the question as to whether any mineral has the expected stability has to be answered. The stability is predicted using measured values of the trap depth E and the pre-exponential (frequency) factor s, and since all previous work in checking such predictions involved time periods not exceeding a year, it seemed possible that the kinetic theory on which the predictions are based may not be adequate when extended to time periods of thousands of years; this is quite apart from its failure for time periods of a few days in the case of particular minerals present in volcanic lava.

A variety of TL sensitive minerals were tested for fading, see Chapter 7; only two of those tested did not show any loss in high temperature TL, quartz and limestone. The kinetic parameters for these two minerals were then studied and the mean lives of electrons in the various TL glow peaks were calculated. To see how well these predicted values agreed with the archaeological stability, case studies were made of archaeologically heated quartz and a geologically heated limestone; they both had high temperature peaks in their natural glow curves, the upper one being completely thermally stable over the periods of interest and the lower one having a mean life only slightly larger than the time that had elapsed since the sample had been heated. The mean lives determined for these lower peaks were consistent with the mean lives predicted from the kinetic parameters, thereby justifying the terminology 'anomalous' in describing the fading observed in volcanic lava.

CHAPTER 5 KINETIC STUDIES ON QUARTZ

5.1 INTRODUCTION

In using the quartz inclusion technique of TL dating, it is assumed that the relevant traps are deep enough to retain all their trapped electrons over the archaeological period. A typical TL glow curve of quartz grains that have been irradiated after heating to 500°C to remove their natural TL is shown in Fig.5.1; the main peaks that occur when heating at 20°C/second are at about 110°C, 170°C, 230°C, 325°C and 375°C. Various studies have been made of these and other peaks (Fleming, 1969; Hwang and Goksu; Kaul, Ganguli and Hess) by the initial rise and isothermal decay methods, but no attempt has been made to check that the predicted mean lives are meaningful by comparing them with those obtained from archaeological samples of quartz of known age. This chapter is concerned with comparisons carried out for the 210°C and 325°C peaks; several different methods of trap depth determination were used and it was found that the commonly used initial rise method was highly unsatisfactory.

THE 375°C PEAK

5.2 THE 375°C PEAK

The 375°C peak has been studied extensively by Fleming and is thought satisfactory for dating up to 10^5 years as its trap depth was determined as 1.66 eV and the mean life at 20°C was calculated to be 4×10^7 years (Fleming, 1969; Aitken and Fleming, 1973). The limiting factor is more likely to be the deviation from linearity of the TL growth curve due to saturation; the

actual dose at which the onset of saturation occurs varies and samples must be considered individually. As an example this peak was used in the dating of a piece of burnt rock crystal (Wintle and Oakley). The growth curve started to saturate at a total dose of 2 krad but, as the equivalent dose was less than 1 krad because of the low internal activity of the sample, it was possible to evaluate an age (6,500 $\pm$ 700 years BP).

Later in the chapter this peak is reported as having been used for dating quartz inclusions from aboriginal hearths in Australia that are about 30,000 years old. The dates obtained are consistent with the stability of the trapped electrons as quoted above and reinforce the absence of 'anomalous fading' in quartz.

THE 325°C PEAK

5.3 INTRODUCTION

In some pottery the 325°C peak dominates the glow curve above the 300°C ordinate. In his Romano-British dating programme, Fleming has shown that for these samples the naturally acquired TL dose obtained for the 325°C peak was within 5% of that obtained at higher glow curve abscissae (Fleming, 1970). This suggests that negligible emptying of the traps which give rise to the 325°C peak has taken place during archaeological time i.e. about 2,000 years. However, determination of the trap depth and associated frequency factor for this peak suggested a mean life at 20°C of only 3,000 years (Aitken and Fleming, 1973), suggesting that for quartz the predictions of the E and s values were again in error but, in this case, contrary to the situation in feldspars in the previous chapter, the actual meanlife was at least an order of magnitude greater than predicted. To study this anomaly, quartz was extracted from a Romano-British sherd, 51 a2, that

had been studied by Fleming; its high temperature glow curve is shown in Fig.5.2.

5.4 DETERMINATION OF E AND PREDICTED STABILITY

(a) Isothermal decay

A typical isothermal decay curve is shown in Fig.5.3; the sample was held at 202°C for various lengths of time and the % TL left at the peak was plotted as a function of time. The simple exponential decay suggests that the peak obeys first order kinetics. Table 5.1 gives the half life, experimentally determined for various storage temperatures. Fig. 5.4 shows a plot of log $\tau_{\frac{1}{2}}$ versus T^{-1}; the slope (= E/k) gives E = 1.7 $\pm$ .1 eV.

(b) Hoogenstraaten's method

The variation of peak temperature T_m with heating rate β is shown in Table 5.2 and a plot of log T_m^2/β versus T_m^{-1} is given in Fig. 5.5. This has a slope = E/k and the value of E obtained is 1.69 $\pm$ .02 eV.

(c) Initial rise

For the initial rise measurements the quartz was given a 15 kilorad dose, held for five minutes at a temperature below the peak to remove overlapping low temperature TL peaks and then glowed with an expanded temperature axis on the chart recorder. A typical plot of log I(T) versus T^{-1} is shown in Fig. 5.6; the slope is - E/k and hence E = 1.05 $\pm$ .03 eV. The values obtained from 12 measurements varied from 1.02 to 1.10 eV and were independent of the heating rates used or the doses received by the samples prior to measurement; the temperature range was from 210°C to 265°C.

(d) Discussion

The two methods of trap determination based on first order kinetics yield a trap depth of 1.69 eV, quite different to that obtained by the

TABLE 5.1

EXPERIMENTALLY DETERMINED HALF LIVES AT VARIOUS TEMPERATURES FOR THE 325 ^{o}C PEAK IN QUARTZ (51 a2)

holding temperature/^{o}C	half life/mins
240	5.5
217	40
202	145
182	880

TABLE 5.2

EXPERIMENTALLY DETERMINED VARIATION OF PEAK TEMPERATURE Tm WITH HEATING RATE β FOR THE 325 ^{o}C PEAK IN QUARTZ (51 a2)

β/^{o}C sec^{-1}	Tm/^{o}C	Tm/K
1.35	287	560
3.38	302	575
5.5	310	583
10.8	321	594
21.8	335	606

initial rise method 1.05 eV; neither agree with the value of 1.26 eV determined by Aitken and Fleming, who also used the initial rise method.

(e) Determination of kinetic order

Plots of log I, log I/n and log I/n^2 versus T^{-1} in Fig. 5.7 show the first order kinetic nature of the peak as discussed theoretically in section 3.4; I is the TL intensity at the glow curve above T and n is the area under the glow curve above T and is proportional to the number of electrons still trapped. Log I/n is linear with T^{-1} up to the peak temperature, whereas log I/n^2 deviates from linearity at the same value of T^{-1} as the initial rise log I versus T^{-1} plot. The deviation of log I/n above the peak is partly due to error in the assumed shape of the glow peak after subtraction of overlapping higher temperature TL peaks; the curve used is shown in Fig. 5.8. Another cause is the effect of the thermal quenching on the value of n i.e. the glow curve area.

(f) Predicted stabilities for various values of E

Using the previously derived equation

$$\frac{E}{kT_m^2} = \frac{s}{\beta} \exp\left\{-\frac{E}{kT_m}\right\}$$

values of s were determined for the three values of E; they are shown in Table 5.3(a) along with the mean lives at 20°C that are predicted. The mean lives connected with the two lower values of E, both determined by the initial rise method, are in disagreement with the known stability over archaeological time as shown in section 5.3. This suggests that the initial rise method should not be applied to this material; in the following sections the cause of the disagreement is studied. Table 5.3(b) shows the variation of τ over the error range of E.

TABLE 5.3

(a) CALCULATED VALUES OF s AND τ AT 20 °C FOR THE DIFFERENT TRAP DEPTHS OBTAINED THAT WOULD GIVE RISE TO THE 325 °C PEAK

E/eV	s/sec^{-1}	τ_{20}/years
1.69	$\sim 10^{14}$	3×10^{7}
1.05	$\sim 10^{8}$	200
1.26	$\sim 10^{10}$	3,000

(b) VARIATION IN MEAN LIFE AT 20 °C DUE TO ERROR IN DETERMINATION OF E

E/eV	s/sec	τ_{20}/years
1.67	8.5×10^{13}	2×10^{7}
1.69	1.3×10^{14}	3×10^{7}
1.71	1.9×10^{14}	4×10^{7}

5.5 LUMINESCENCE EFFICIENCY

(a) Suggested temperature dependence of intensity

The fact that the first order kinetic plot, log I/n versus T^{-1} has the same slope as log I versus T^{-1} measured during the initial rise suggests that the kinetics of the trap emptying are indeed first order but the luminescence efficiency is decreasing with increasing temperature during an initial rise measurement. Since the plot of log I versus T^{-1} is linear, the luminescence efficiency η would have to be of the form

$$\eta = A \exp(B/kT) \qquad (5.1)$$

where A is a dimensionless constant and B is the characteristic energy (eV); comparing the values of E obtained experimentally suggests that B = 0.64 $\pm$ 0.03 eV.

A temperature dependent luminescence efficiency does not affect the isothermal decay method because, although intensities are being measured, intensity ratios are plotted. For Hoogenstraaten's peak shift method it can be shown that the appropriate equation is

$$\log\left\{\frac{\beta}{T_m^2}\right\} = \log\left\{\frac{sk}{E-B}\right\} - \frac{E}{kT_m} \qquad (5.2)$$

instead of

$$\log\left\{\frac{\beta}{T_m^2}\right\} = \log\left\{\frac{sk}{E}\right\} - \frac{E}{kT_m}$$

and hence a plot of $\log(\beta/T_m^2)$ versus T_m^{-1} gives the trap depth = E; only the intercept is affected by the temperature dependent luminescence efficiency as given in equation (5.1).

(b) Confirmation of temperature dependence

Another way of observing a temperature dependent luminescence efficiency using TL is to study the peak intensity I_m as a function of (β/T_m^2) for

constant n_m i.e. when the initial radiation is constant. When η is constant, the intensity at the peak I_m is given by the equation

$$I_m = \frac{n_m E}{k} \frac{\beta}{T_m^2} \tag{5.3}$$

when η is of the form given in equation (5.1) then the observed intensity is given by the equation

$$I_m = \frac{n_m}{k} A \exp\left\{\frac{B}{kT_m}\right\}\{E - B\} \frac{\beta}{T_m^2} \tag{5.4}$$

Figure 5.9 shows that a plot of log I_m versus (β/T_m^2) is not linear, but when the values of I_m are multiplied by exp $(- B/kT_m)$, where B = 0.64 eV as determined in the previous section, and plotted against (β/T_m^2) there is agreement with equation (5.4) as shown in Fig. 5.10. This confirms exponential luminescence efficiency in this temperature range, 286°C to 334°C. This does not cover the temperature region of the initial rise method, but as will be seen later there is evidence that the exponential dependence does extend into that region.

(c) Temperature dependence due to thermal quenching

A similar approach was used by Gorbics et al to show the presence of thermal quenching in various TL phosphors, but not quartz (Gorbics, Nash and Attix, 1968(b)). They had already attempted to study the luminescence centres alone by observing the prompt luminescence, RL, at various temperatures during continuous X-ray exposure, but discontinuities in the vicinity of the TL glow peak temperatures made it impossible to study the thermal quenching (Gorbics, Nash and Attix, 1968(a)). However RL studies by Aitken et al suggest that in the case of quartz there were no such discontinuities and hence for this substance RL studies were in fact a useful tool for studying thermal quenching (Aitken, Thompson and Fleming, 1968).

5.6 RADIO LUMINESCENCE (RL)

(a) Equipment

Prompt luminescence, RL, during irradiation with a 40 millicurie $^{90}Sr/^{90}Y$ beta source (dose rate $\approx$ 10 rad/minute) was observed using an EMI 6256 photomultiplier tube in conjunction with several different broad band interference filters; this is shown schematically in Fig. 5.11. The RL intensity was recorded continuously whilst heating at a steady rate, 5.5°C/second, and also whilst cooling; this ensures that the RL is due to the recombination of conduction band electrons at the luminescence centres. Corrections were necessary for scintillations in the photomultiplier tube caused by the source, even though the latter was encased in thick brass.

(b) RL using optical system centred on 465 nm

A typical RL curve is shown in Fig. 5.12(a); the intensity starts to drop just below 100°C and levels off above 275°C. In the simple thermal quenching equation discussed earlier η decreases exponentially with T and hence the emission above 275°C was thought to be due to the presence of different luminescence centres which are not affected by thermal quenching; in Fig. 5.12(b) the steady component has been subtracted. It must be remembered that this subtraction is only valid if more than one luminescence centre is involved; in the case of some single emission centres η does not fall to a very small value at high T and the η value becomes constant = A^{-1}. However in the example shown in Fig. 5.12, the ratio of $\eta(T)/\eta(T\rightarrow 0) = 0.2$; the value of A is determined to be 2.8×10^{7} at the temperature where the RL curve has half its initial intensity i.e. when $A \exp(-B/kT) = 1$. Since $A^{-1} = 3.6 \times 10^{-8}$ is much less than $\eta(T)/\eta(T\rightarrow 0) = 0.2$, we may deduce that we are not dealing with a single emission centre and that subtracting the steady component of the RL is valid.

Fig. 5.13 shows a theoretical curve for log η versus T^{-1} for

$$\eta = \frac{1}{1 + A \exp(-B/kT)}$$

where B = 0.64 eV, obtained from the difference between the initial rise determination of E and that obtained for first order kinetic analysis, and $A = 2.8 \times 10^7$ as determined above. The experimental points are those obtained by replotting curve (b) from Fig. 5.12 after normalizing with respect to the initial intensity.

(c) RL at other wavelengths

RL measurements were also made using broad band interference filters centred at 310, 370, 410 and 495 nm; the results are shown in Fig. 5.14. Thermal quenching can be seen in all the curves but Fig. 5.12(e) suggests that the steady component luminescence is dominant at longer wavelengths. This suggests that if the initial rise trap depth determination was carried out using an optical system with a longer wavelength response then the value of E obtained would be greater than 1.05 eV.

Thermal quenching analyses similar to those carried out in the previous section for the 465 nm emission were also carried out for the 370 nm and 410 nm RL emission curves. The values of B obtained are given in Table 5.4.

The RL measurements also enable us to compare the luminescence spectra of the two RL components. Table 5.5 shows the results for the RL at 50°C for the thermally quenched emission and for the steady emission; Fig. 5.15 shows the relative intensities of the two components and Fig. 5.16(a) shows the spectra after normalizing to the highest intensity measured. (It must be remembered that using broad band filters loses all the fine structure of the spectra and only broad comparisons may be drawn.)

(d) Further initial rise measurements

As a result of the RL study initial rise measurements were carried out

TABLE 5.4

WAVELENGTH DEPENDENCE OF THE ACTIVATION ENERGY B OBTAINED FROM RL

λ/nm	B/eV
370	0.70 ± .03
410	0.64 ± .03
465	0.65 ± .05

TABLE 5.5

MEASUREMENTS OF RL EMISSION SPECTRA AT 50 ^{o}C

Filter λ/nm	RL intensity	filter efficiency	normalized RL	RL relative to maximum as 100
(a) component that shows thermal quenching				
310	1.45	26	5.5	23
370	5.7	33	17.3	74
410	23.5	100	23.5	100
465	4.5	64	7	30
495	.35	65	.54	2.3
(b) steady component				
310	.1	26	.39	22
370	.25	33	.76	43
410	1.35	100	1.35	77
465	1.12	64	1.75	100
495	.65	65	1.0	57

using an EMI 9558 photomultiplier tube in conjunction with a Corning (4-96) blue/green filter and a Corning (3-70) sharp cut filter. The characteristics of this tube and filters and those used for the earlier measurements are shown in Figs. 5.17(a) and 5.17(b). The initial rise curves gave a trap depth of 1.25 $\pm$ .02 eV for the 325°C peak which was greater than the earlier value of 1.05 eV; it was still less than the value obtained by first order kinetics of 1.69 eV, and hence some thermal quenching was still occurring.

Looking at the RL curves of Fig. 5.14, one would expect the steady luminescence component to dominate in all experiments above 250°C, i.e. those involving the peak maximum intensity. But this is not so, as is demonstrated in Fig. 5.9 and this suggests that in the TL process a smaller fraction of the electrons that undergo radiative recombination go to these luminescence centres than during RL measurements. This is also suggested by the fact that there is still a considerable discrepancy in the value of E obtained using the luminescence which the RL suggested was predominantly unaffected by thermal quenching. This is certainly likely if the traps and luminescence centres are spatially related for the TL process; in the RL measurements the electrons in the conduction band have a choice of recombination centres.

5.7 IMPLICATIONS

(a) For TL dating

If thermal quenching is occurring in the region of a peak in a mineral that is being considered for dating, or in a phosphor that is being considered for on-site monitor measurements, the mean life of trapped electrons giving rise to that peak will be grossly underestimated. For the 325°C peak in quartz the difference in mean lives for the two values of E, one deter-

mined by initial rise analysis and the other determined by first order kinetic methods, was at least a factor of 10^4 (see Table 5.3). It is therefore suggested that the suitability of a peak should not be based on its trap depth as determined by the initial rise method unless RL measurements have been done to confirm the absence of thermal quenching. In the case of the 325°C peak in quartz the initial rise method erroneously indicates a mean life that is too short for archaeological dating; the true value is more than adequate.

Although it was not checked by studying peak shift with temperature, thermal quenching is also likely to extend into the region of the 375°C peak discussed in section 5.2. Here the trap depth may be increased from 1.66 eV to 2.1 eV (using the value of Aitken and Fleming) and thus the 375°C peak mean life will also be increased, by as much as 4 orders of magnitude.

(b) For sensitivity changes

In his paper on the quartz inclusion dating method, Fleming describes the behaviour of the 325°C peak as 'malign' because there is an increase in the sensitivity of the linear response region after heating to 500°C to obtain the natural TL (Fleming, 1970). This gives rise to uncertainty in the determination of the supralinearity correction. An incidental observation of spectra during the RL measurements combined with other observations (Zimmermann, 1971(b)) suggested that this sensitivity change might be removed by suitable treatment.

In Fig. 5.15(b) the normalized TL emission spectra of the 110°C and 325°C peak are given and they may be compared with the two RL spectra in Fig. 5.16(a). If the similarities between the curves are taken to imply that the luminescence centres used in the 110°C glow peak exhibit thermal quenching and that the higher peak uses a mixture of the two types of

luminescence centres, then the TL properties of the 110°C peak that are due to the recombination centres should also occur but to a lesser extent in the 325°C peak. One of the most important properties of the 110°C peak is the radiation induced TL sensitivity, which has been shown to be due primarily to an increase in the number of activated luminescence centres (Zimmerman, 1971(b)); a related sensitivity increase would therefore be expected for the 325°C peak and it should also be possible to reduce the sensitivity of these centres by the method used for the 110°C peak i.e. 240 nm UV irradiation. A more thorough experimental study is needed however to confirm the initial comparison and to test the predictions and this suggestion should be regarded as tentative.

(c) <u>For thermal quenching theories as applied to quartz</u>

In Chapter 3 thermal quenching was described in terms of the probability of a radiationless transition to the ground state for an excited luminescence centre and it was shown schematically in a configurational coordinate diagram. This approach was used by Johnson and Williams who were able to obtain theoretically the configurational coordinate diagram for KCl:Tl and found that the activation energy thus derived was in agreement with that obtained experimentally.

Another explanation of thermal quenching has been put forward by Klasens with particular reference to ZnS phosphors (Klasens). He considers the luminescence centre to be W eV above the valence band and hence if the temperature of the phosphor is high enough then electrons may be raised from the valence band into the empty ground states of these luminescence centres; the resulting holes migrate through the lattice until they are trapped at defects and create competing non-radiative recombination centres. This theory also gives rise to a similar expression for the temperature dependence of

the luminescence efficiency, but W, the activation energy, has a completely different significance.

In the experimental study of quartz reported in the previous sections, the activation energy was determined as about 0.64 eV. Zimmerman suggested however that the luminescence centres responsible for the 110°C peak were about 2.7 eV above the valence band and that electrons could be excited from the valence band into these centres by UV irradiation of 240 nm (Zimmerman, 1971(b)). If these are considered to be the same luminescence centres, as is implied by the TL and RL emission spectra reported in section 5.7(b), then the second theory for thermal quenching is invalid in the case of quartz i.e. the thermal quenching observed is due to radiationless transitions to the ground state at the excited luminescence centre.

5.8 ARCHAEOLOGICAL STABILITY

In section 5.3 it was mentioned that negligible emptying of the traps giving rise to the 325°C peak had occurred in sample 51 a2 which had an archaeologically known age of 1900 ± 10 years. Confirmation of the much longer stability suggested by the trap depth of 1.69 eV, Table 5.6, was looked for in samples obtained from early hearths in Australia; a fireplace from Lake Mungo had an associated radiocarbon age of

30,750 ± 520 years BP (ANU 680)

Inclusion dating was carried out by Mrs. G. Huxtable and ages of

37,600 ± 3,000 BP

38,900 ± 4,000 BP

35,200 ± 3,000 BP

were obtained on samples from the same hearth giving an average age of

37,200 ± 2,700 BP

TABLE 5.6

VARIATION OF MEAN LIFE WITH STORAGE TEMPERATURE

FOR A TRAP OF DEPTH 1.69 eV AND WITH $s = 10^{14}\ sec^{-1}$

T/°C	mean-life/million years
10	300
15	100
20	30
25	10

NB The mean life at 20 °C storage temperature for a trap of depth E = 1.05 eV and having its peak at 325 °C is 200 years (Table 5.3a).

The discrepancy between this age and the radiocarbon ages is thought to be due to a high atmospheric C-14 concentration due to the effect of the reduced intensity of the Earth's magnetic field at that time.

The above TL dating was carried out on the 375°C peak using optical filters which discriminated against the 325°C peak. However, before this optimization was carried out, the equivalent doses were obtained by the method of additional doses for both the peaks; the equivalent dose for the lower peak was shown to be not less than 10% that of the higher peak with an experimental uncertainty in the equivalent doses of $\pm$ 10% (personal communication, M.J. Aitken).

If the number of electrons built up in the 365°C peak as a function of time is

$$n_1(t) = \alpha t \qquad (5.5)$$

and those built up in the 325°C peak, which has a mean life $\tau = \beta^{-1}$, is

$$n_2(t) = \frac{\alpha}{\beta}(1 - e^{-\beta t}) \qquad (5.6)$$

then the ratio of the two peaks is

$$\frac{n_2(t)}{n_1(t)} = \frac{1}{\beta t}(1 - e^{-\beta t}) \qquad (5.7)$$

This function is shown in Fig. 5.18 for small values of βt i.e. when the mean life is a few orders of magnitude greater than the archaeological age of the sample. This graph emphasises the impossibility of obtaining a mean life even within a few orders of magnitude when the value of $\frac{n_2(t)}{n_1(t)} > 0.95$.

For the above archaeological example the maximum value of βt is 0.44 and hence, given the average TL age of 37,200 years, the least possible value of the mean life of the 325°C peak at the archaeological storage temperature is 85,000 years. This result is not incompatible with the laboratory determinations of the trap depth E = 1.69 eV, see Table 5.6; it confirms that

the value of 1.05 eV obtained by the initial rise method is invalid.

THE 210°C PEAK

5.9 Trap depth determinations and predicted stability

The depth of the traps giving rise to the 210°C peak in quartz was determined for sample 51 a2 by the initial rise method to be E = 1.10 ± .05 eV and from a plot of log (T_m^2/β) versus T_m^{-1} to be E = 1.79 ± .03 eV. Presumably the difference between the values of E is again due to thermal quenching and evidence that E = 1.79 eV is the correct value is provided by

(a) the RL curves of Fig. 5.14

(b) the evidence of the archaeological stability given in the next section.

The values of s and the half lives at 20°C for the various values of E are are given in Table 5.7.

5.10 ARCHAEOLOGICAL STABILITY

The low temperature natural TL of sample 51 a2 had been affected by pre-heating to 150°C for other reasons but natural TL glow curves were available for another sample, 71 a2, which had a similar archaeologically known age, 1850 ± 30 years. The quartz extract had a similar glow curve and gave the same value of trap depth for the 210°C peak as 51 a2. The natural TL glow curve and $N/(N + \beta)$ plateau are shown in Figs. 5.19(a) and 5.19(b)(i); Fig. 5.19(b)(ii) shows the plot of $N/\{(N + \beta) - N\}$ and the ratio of the two plateaux gives $\frac{n_1(t)}{n_2(t)} = 0.89$; this gives $\beta t = 0.24$. The archaeological age being 1850 years gives $\tau = \beta^{-1} = 7{,}700$ years. Comparing this value with the calculated variation of mean life with temperature for a trap of 1.79 eV, Table 5.8, suggests an effective archaeological storage temperature of 27°C. As sample 71 a2 was from a British site an effective temperature of 15°C is more likely and this would predict a mean life of 130,000 years

TABLE 5.7

CALCULATED VALUES OF s AND τ AT 20 ^{o}C FOR THE TRAP DEPTHS OBTAINED FOR THE PEAK THAT OCCURS AT 202 ^{o}C AT A HEATING RATE OF 5.5 ^{o}C/SECOND

E/eV	s/sec^{-1}	τ_{20}/years
1.76	2×10^{18}	25×10^{3}
1.79	5×10^{18}	38×10^{3}
1.82	10^{19}	60×10^{3}
1.05	4×10^{10}	1
1.10	10^{11}	2
1.15	5×10^{11}	4

TABLE 5.8

VARIATION OF MEAN LIFE WITH STORAGE TEMPERATURE

FOR A TRAP OF DEPTH E = 1.79 eV

AND WITH $s = 5 \times 10^{18}\ sec^{-1}$

T/°C	mean-life/millenia
10	467
15	131
20	38
21	30
23	19
25	12
27	7

and a loss of less than 1% in the equivalent dose obtained for the 210°C peak.

However this analysis does not take supralinearity into account and also the growth curves obtained for the 210°C peak were subject to interference. However the evidence of Fig. 5.19 does show the mean life derived from the initial rise method to be invalid.

THE 110°C PEAK

5.11 Trap depth determination

To conclude the study of the validity of τ as predicted by laboratory measurements of E in quartz, similar experiments were carried out on the 110°C peak. The initial rise method yielded a trap depth E = 0.99 ± .02 eV, in agreement with that reported by Aitken and Fleming and in agreement with the value obtained from a plot of log T_m^2/β versus T_m^{-1}, E = 1.0 ± .1 eV. A plot of I_m versus β/T_m^2 is linear for this peak, Fig. 5.20. This confirms the RL results which imply only slight thermal quenching below 100°C.

5.12 PHOSPHORESCENCE

The high sensitivity of the 110°C peak and its first order kinetics as shown by a plot of log I/n versus T^{-1} (Fleming, 1969) make it suitable for study by phosphorescence as described in Chapter 3.3(d). A typical phosphorescent decay is shown in Fig. 5.21; the sample has been irradiated for a minute at 57°C (β dose rate $\simeq$ 500 rad/minute) and the photomultiplier dark current has been subtracted before plotting the intensity as a function of the time after the end of the irradiation. Phosphorescent decay curves were obtained at various temperatures for periods of up to 15 minutes. Table 5.9 gives the experimental half lives of the decays at various

TABLE 5.9

EXPERIMENTALLY DETERMINED HALF LIVES OF THE PHOSPHORESCENT DECAY OF THE 110 ^{o}C PEAK

T/^{o}C	$\tau_{\frac{1}{2}}$/min
13	180.0
25	35.0
36	10.5
40	7.0
43	4.1
51	2.0
57	1.07

temperatures and in Fig. 5.22 the plot of ln $\tau_{\frac{1}{2}}$ versus T^{-1} gives E = 0.99 $\pm$ .02 eV, in agreement with the results quoted in section 5.11 above; s is given $\approx 2 \times 10^{13}$ sec^{-1}. These results are also in agreement with those quoted by Hwang and Goksu who used the isothermal decay method (Hwang and Goksu).

5.13 CONCLUSIONS

In this chapter two peaks have been studied in detail and the stability of their trapped electrons as predicted by kinetic analysis has been compared with the stability of these electrons in samples of known age. In the few papers published on natural quartz the trap depths obtained by the initial rise method seemed to indicate that the peaks were fairly shallow and that the associated TL would have relatively short mean lives when compared to traps giving rise to peaks at the same temperature in other materials (Aitken and Fleming, 1973; Kaul, Ganguli and Hess), but no comment had been made concerning this.

In this study initial rise trap depth determinations also gave low values of E; other methods relying on the first order kinetic nature of the peaks, as established experimentally for the 325°C peak, gave higher values however. This discrepancy was confirmed by studies of the prompt luminescence, RL, as a function of temperature, to be due to thermal quenching. The higher value of E for the 325°C peak was consistent with its presence in samples over 30,000 years old and the value for the 210°C peak with its presence in a sample 1,850 years old, but it was not possible to obtain a more precise correlation of the mean lives. However, these studies do show, in agreement with the one year storage check reported in Chapter 7, that there is at least one mineral in which the

deep traps exhibit mean lives that are not inconsistent with laboratory determinations of E and s.

The study of the 110°C peak showed that, as predicted by the RL studies, thermal quenching was not occurring below about 100°C and hence the initial rise measurement agreed with the other methods used. It is also the only peak in naturally occurring minerals for which trap characteristics have been obtained by means of measurement of phosphorescence.

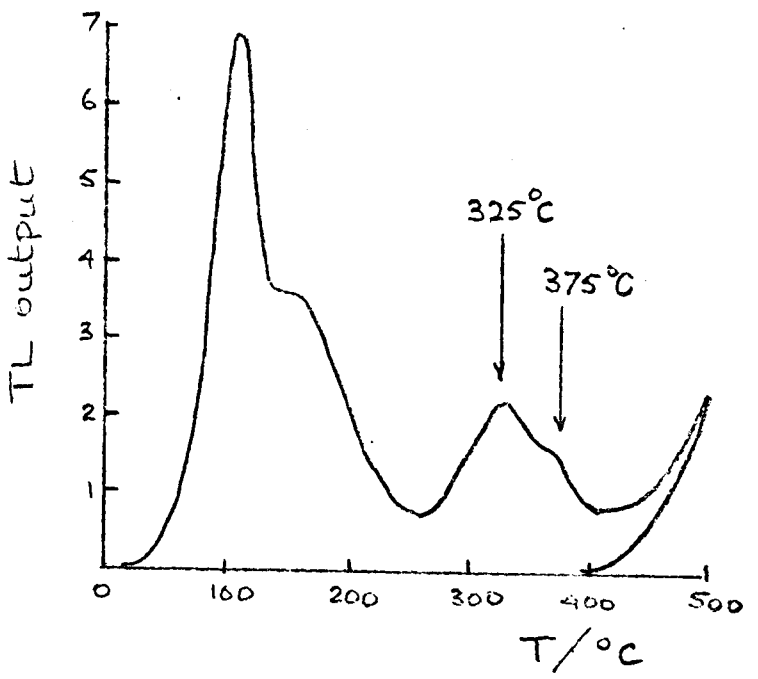

Fig. 5.1 Quartz extract from pottery glow curve after β dose of 550 rads

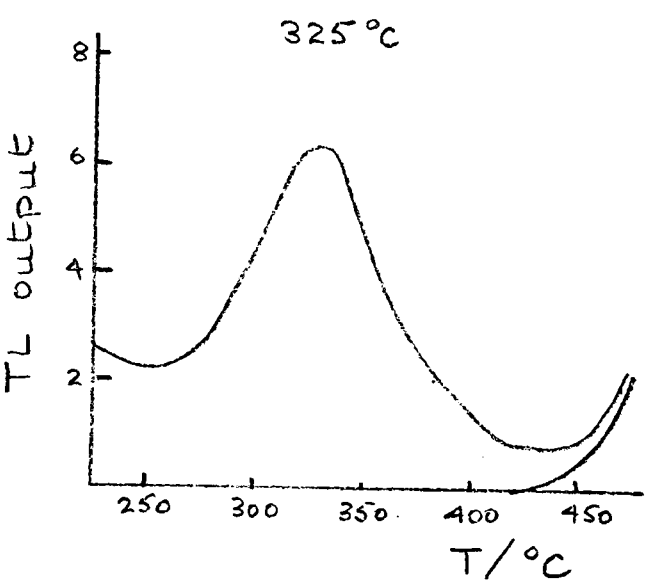

Fig. 5.2 Quartz extract 51 a2 high temperature glow curve.

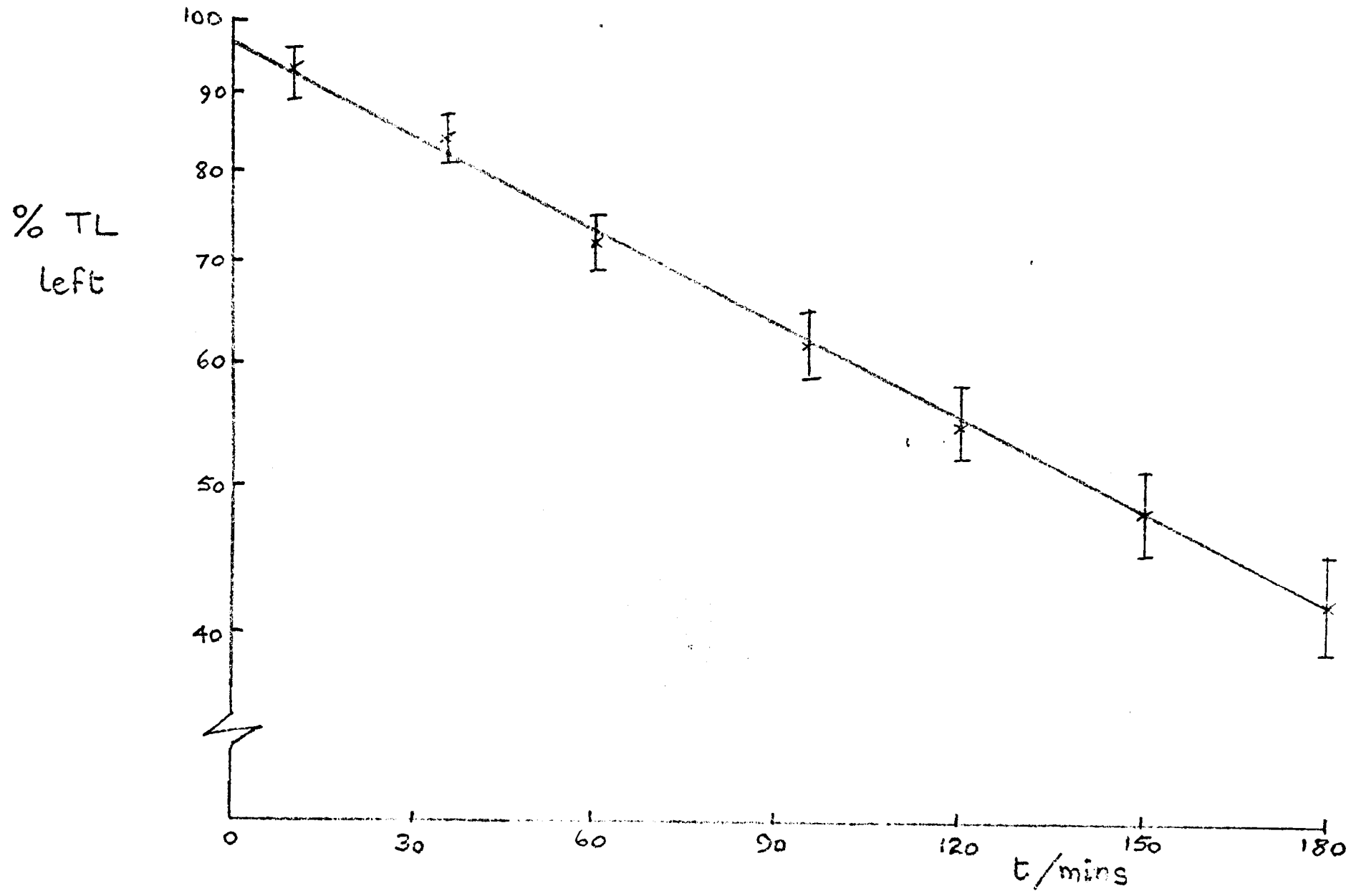

Fig. 5.3 Isothermal decay of TL in quartz (51 a 2)

Decay of 325°C peak with sample held at 202°C; $\tau_{\frac{1}{2}}$ = 145 mins

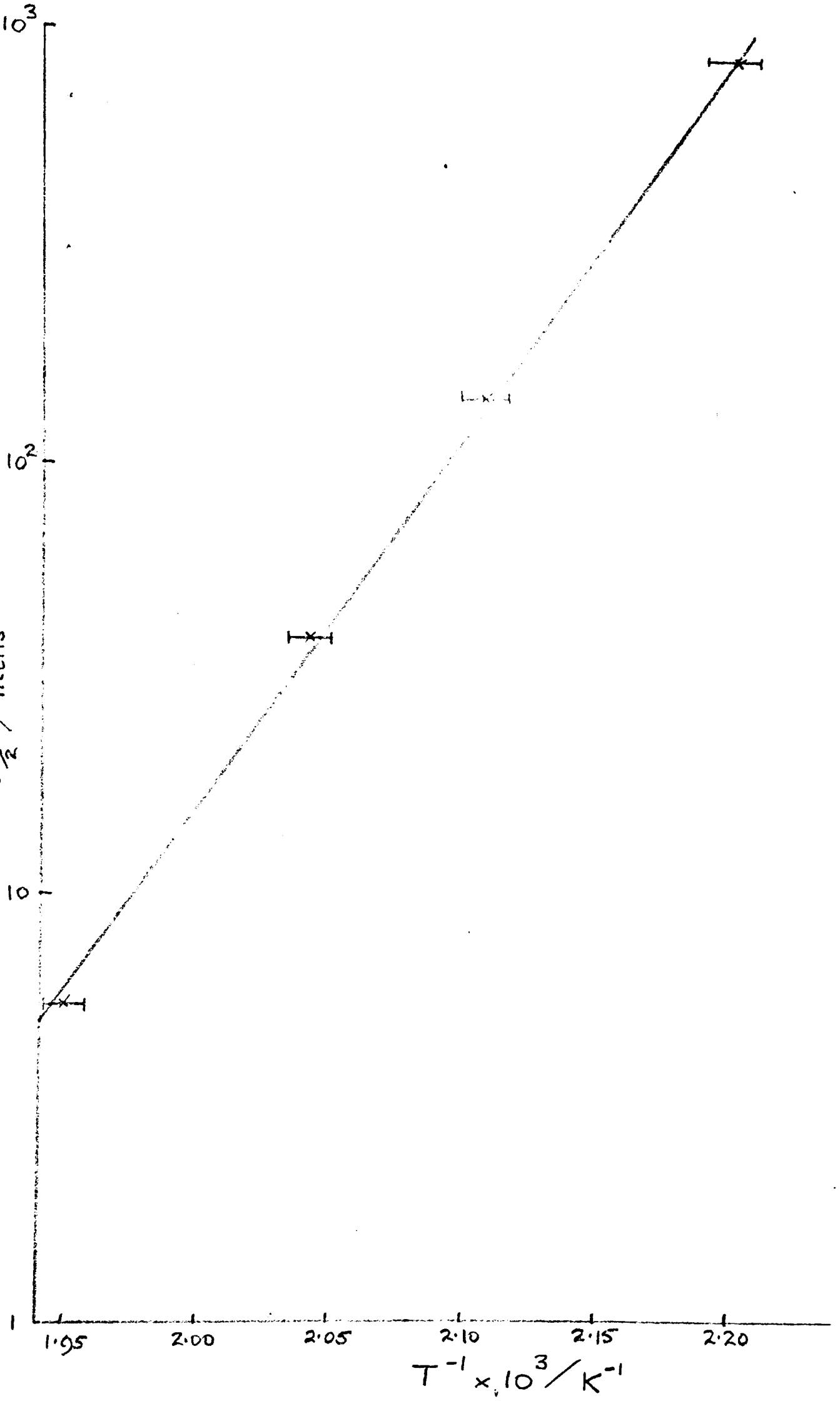

Fig. 5.4 Isothermal decay in quartz

$T_{\frac{1}{2}}$ versus T^{-1} for 325^{o} peak,

slope = E/k, whence E = 1.7 $\pm$ 0.1 eV

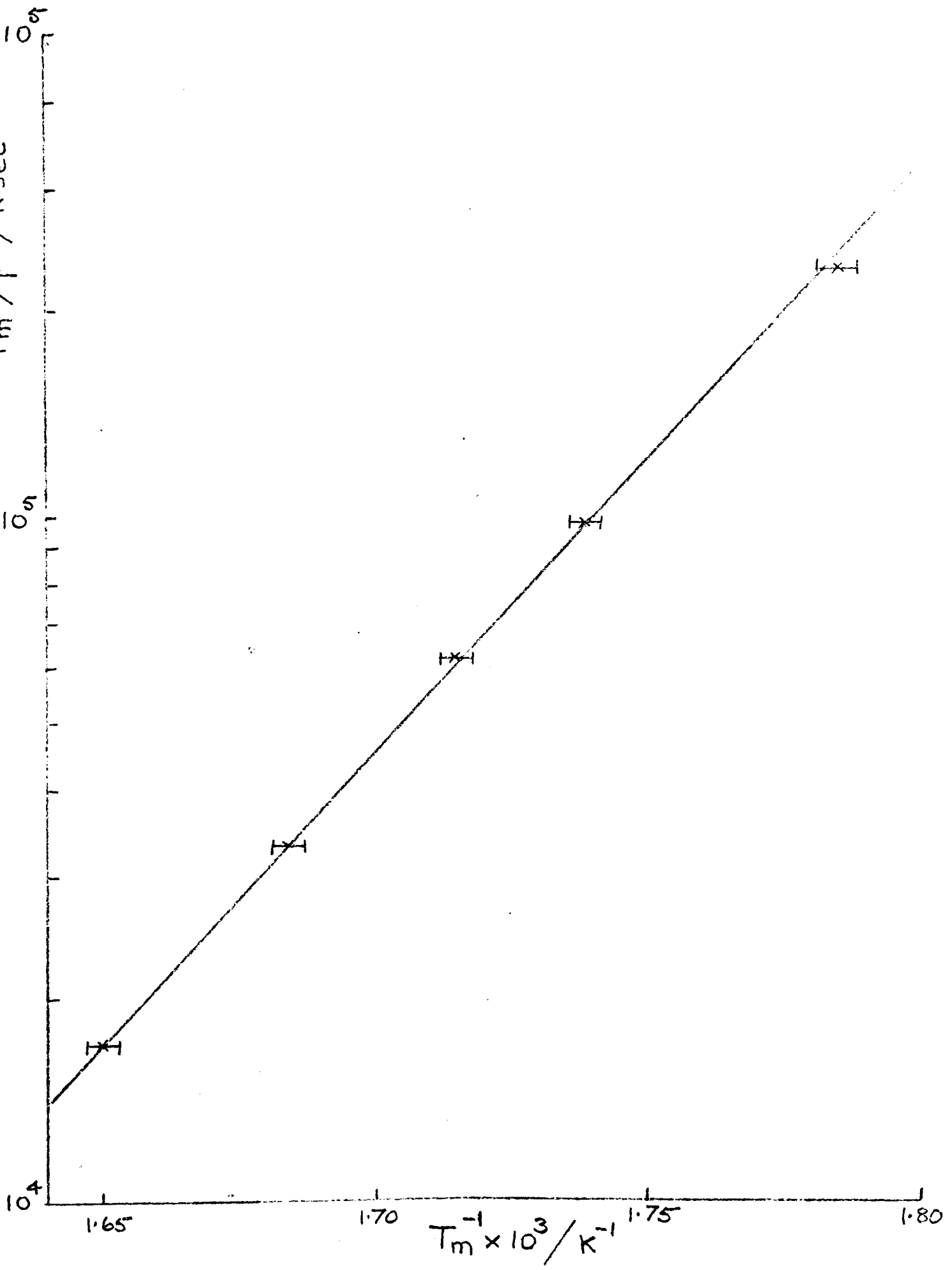

Fig. 5.5 Variation of peak temperature with heating rate

log T_m^2/β versus T_m^{-1} for 325°C peak,

slope = E/k, whence E = 1.69 ± 0.02 eV

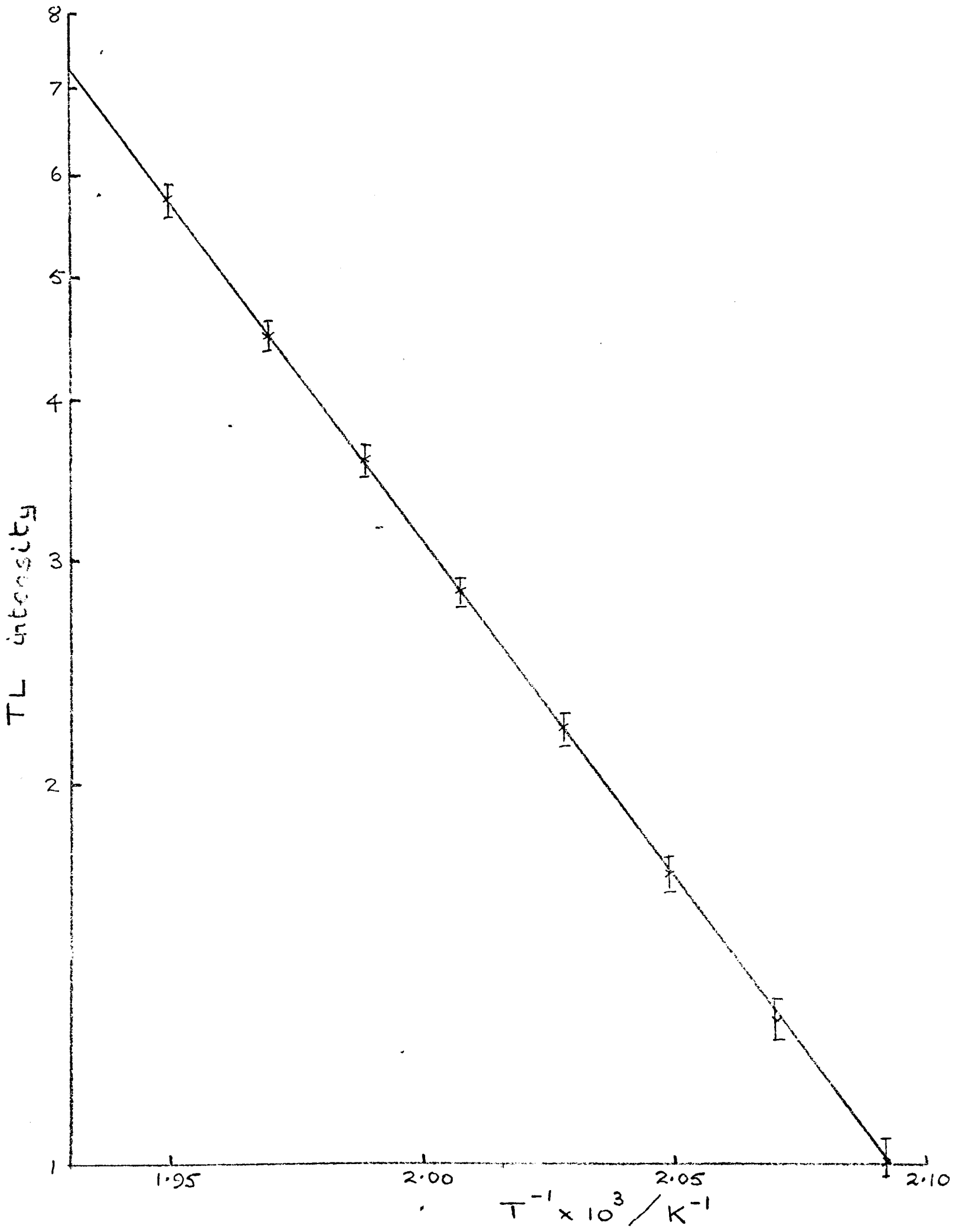

Fig. 5.6 Initial rise plot for 325°C peak, after sample held at 215°C for 5 minutes. slope = -E/k, whence E = 1.05 ± .03 eV

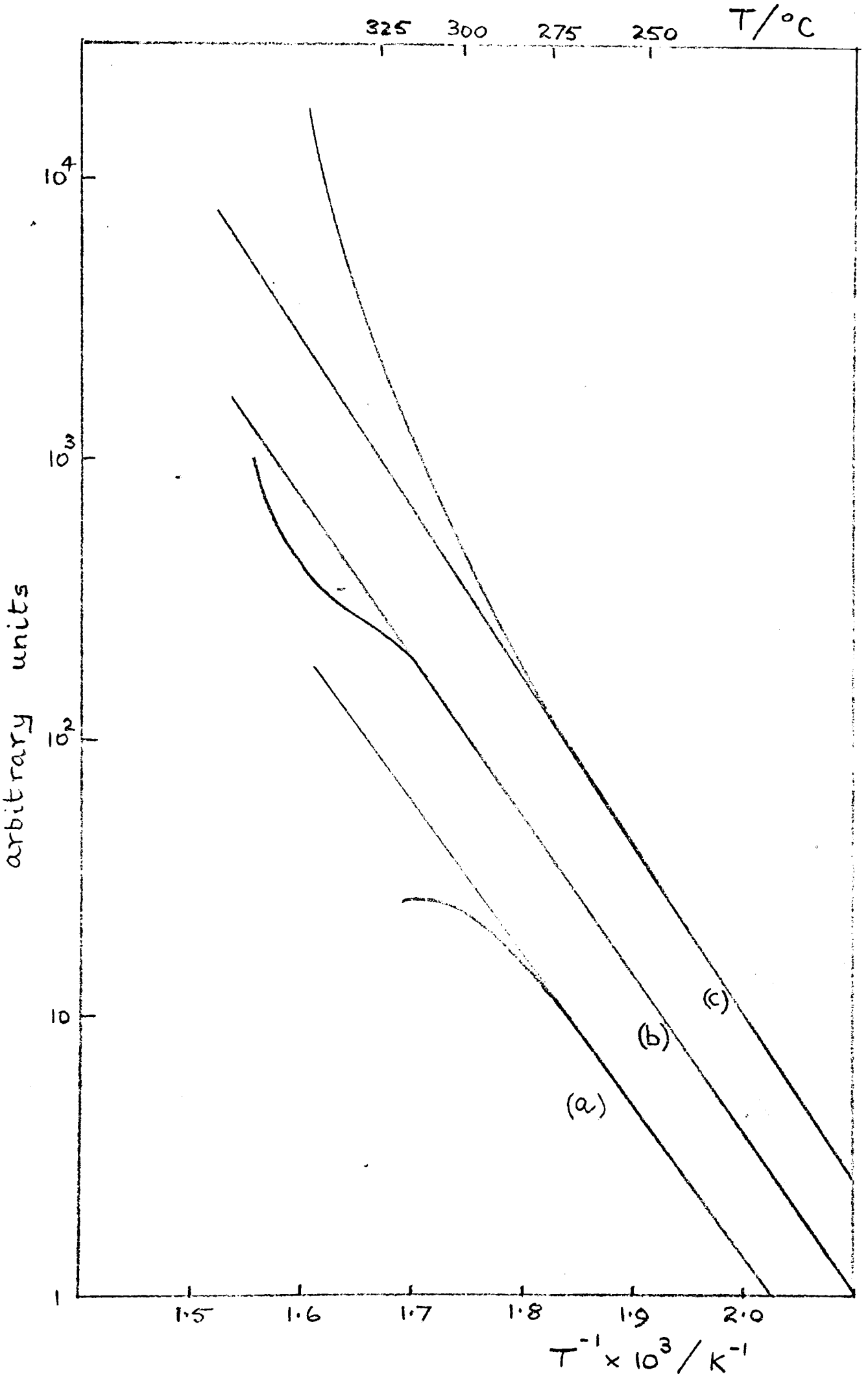

Fig. 5.7 Kinetics of the 325°C peak

(a) log I vs T^{-1}

(b) log I/n vs T^{-1}

(c) log I/n^2 vs T^{-1}

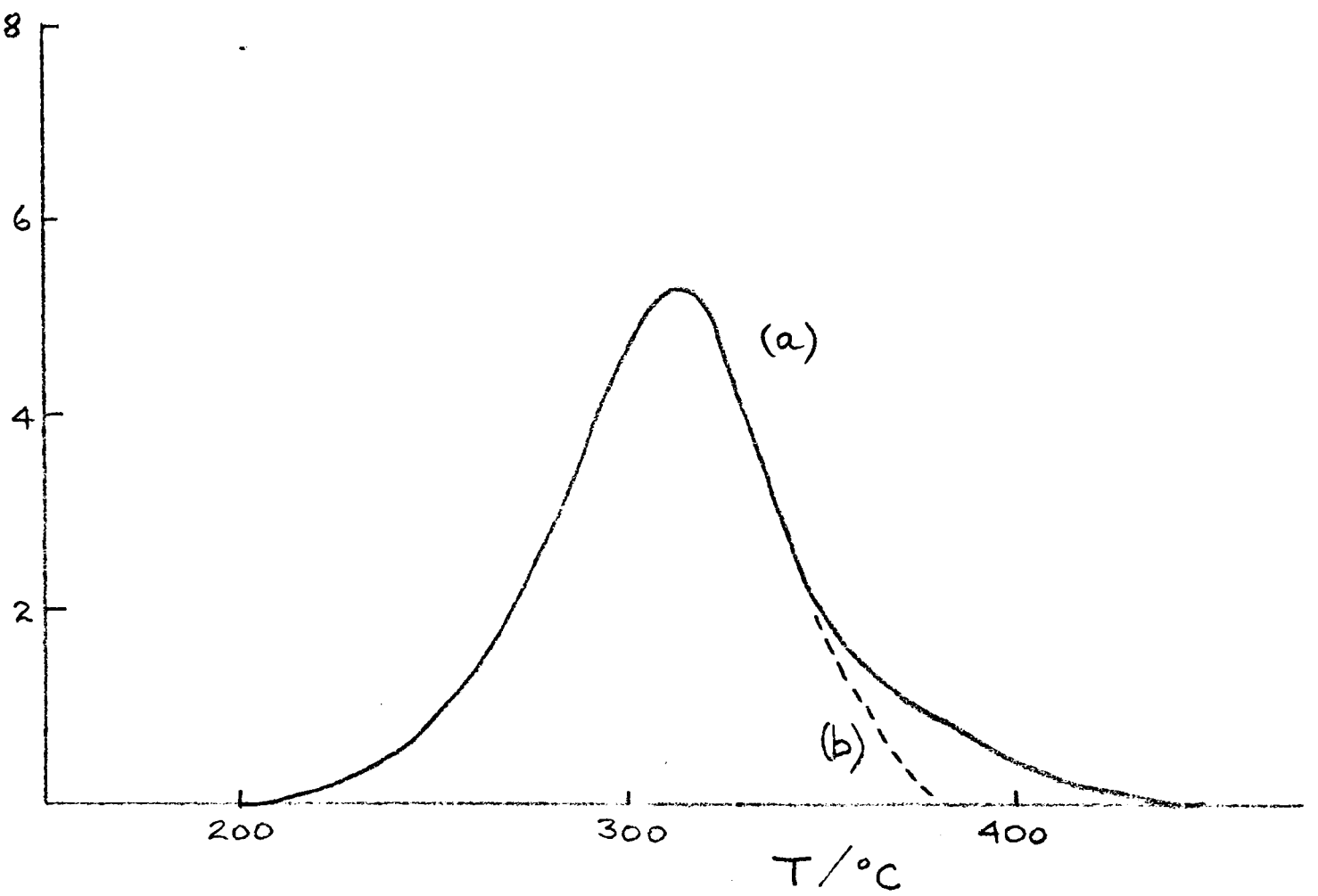

Fig. 5.8 Shape of 325°C peak

(a) glow curve after holding at 202°C for 35 min; heating rate 5.5°C/sec

(b) dotted line - peak shape assumed for kinetic analysis

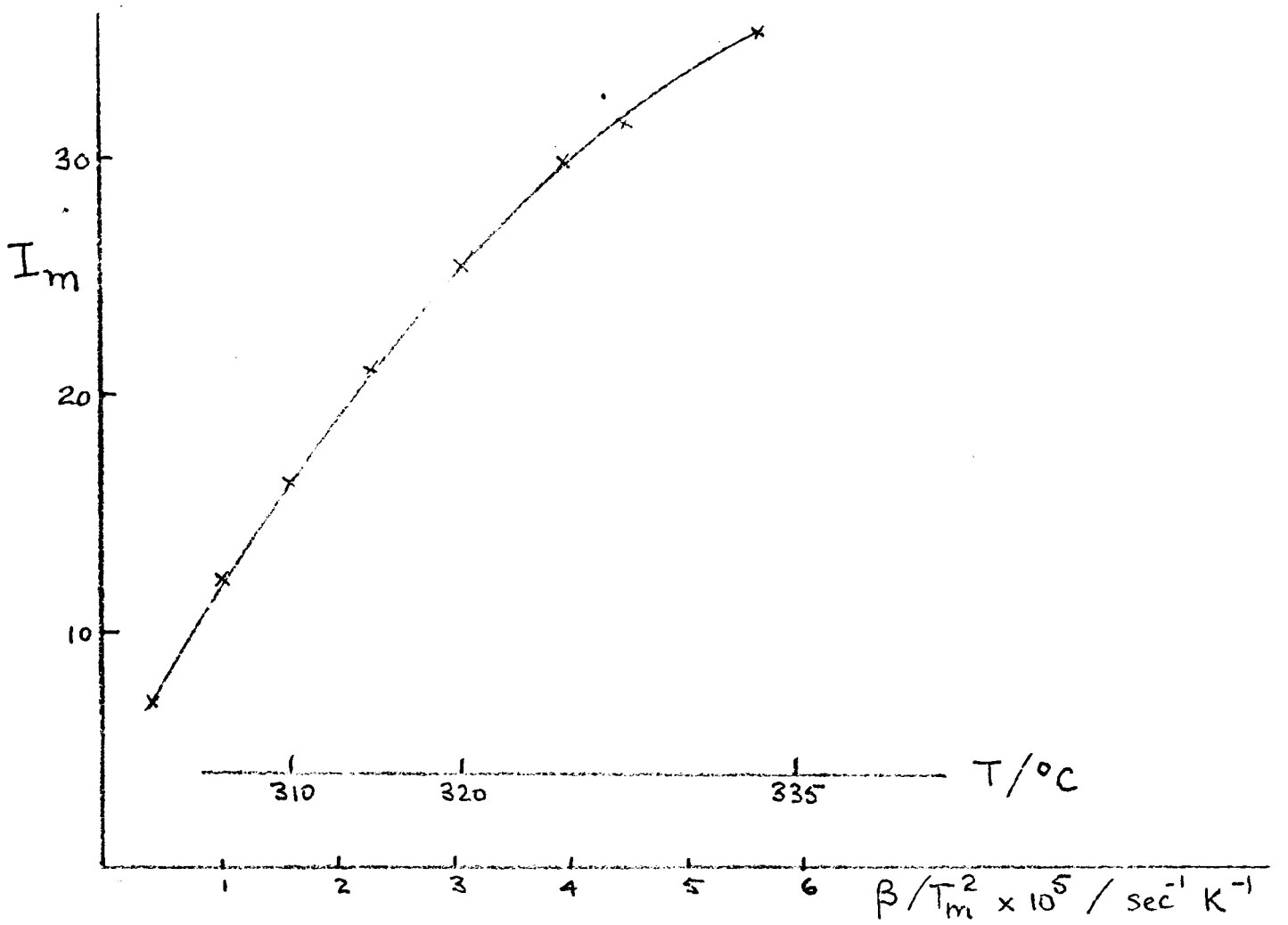

Fig. 5.9 325°C glow peak, I_m vs β/T_m^2, n constant

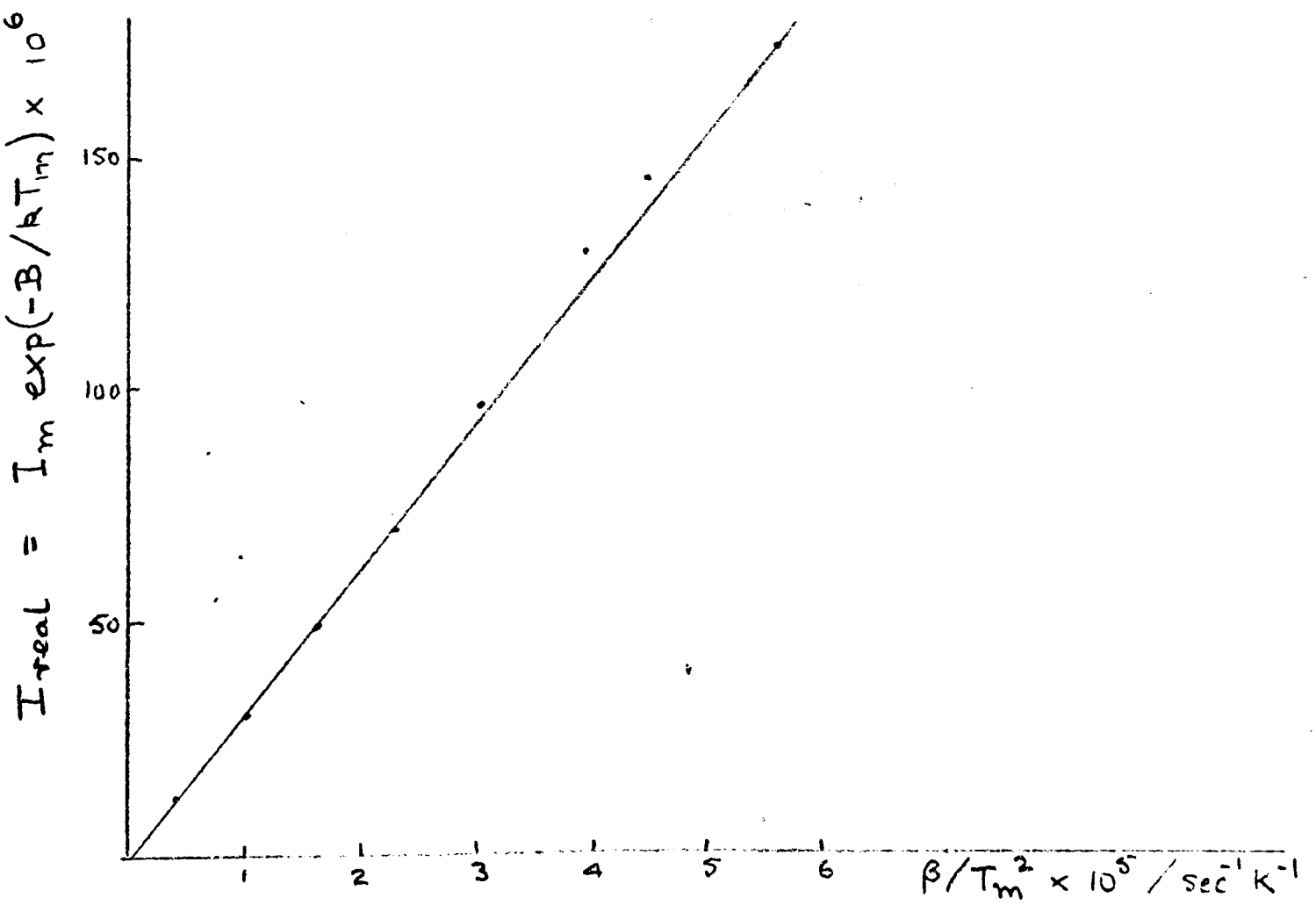

Fig. 5.10 325°C glow peak, $I_m \exp(-B/kT_m)$ vs β/T_m^2

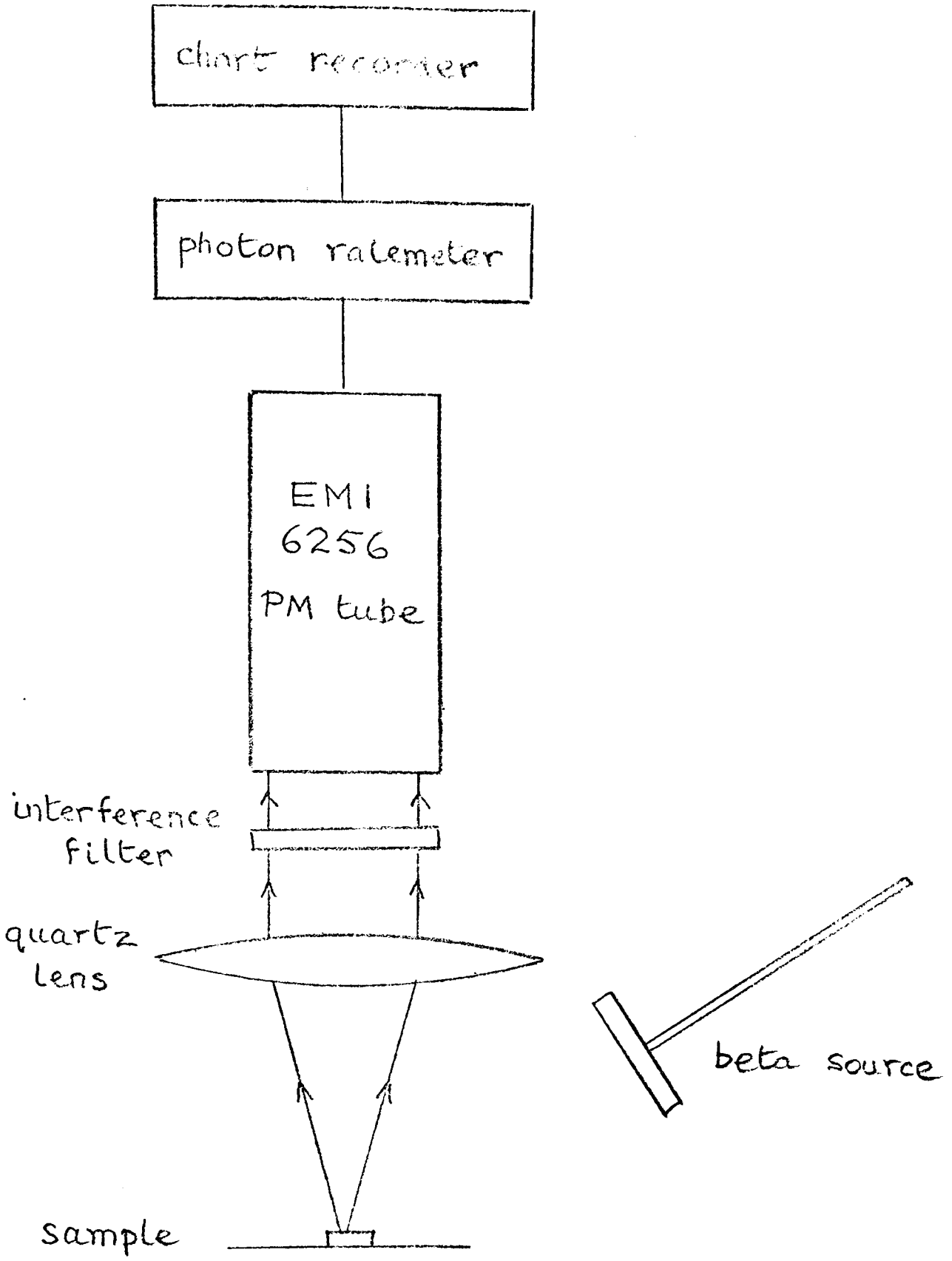

Fig. 5.11 Radioluminescence equipment

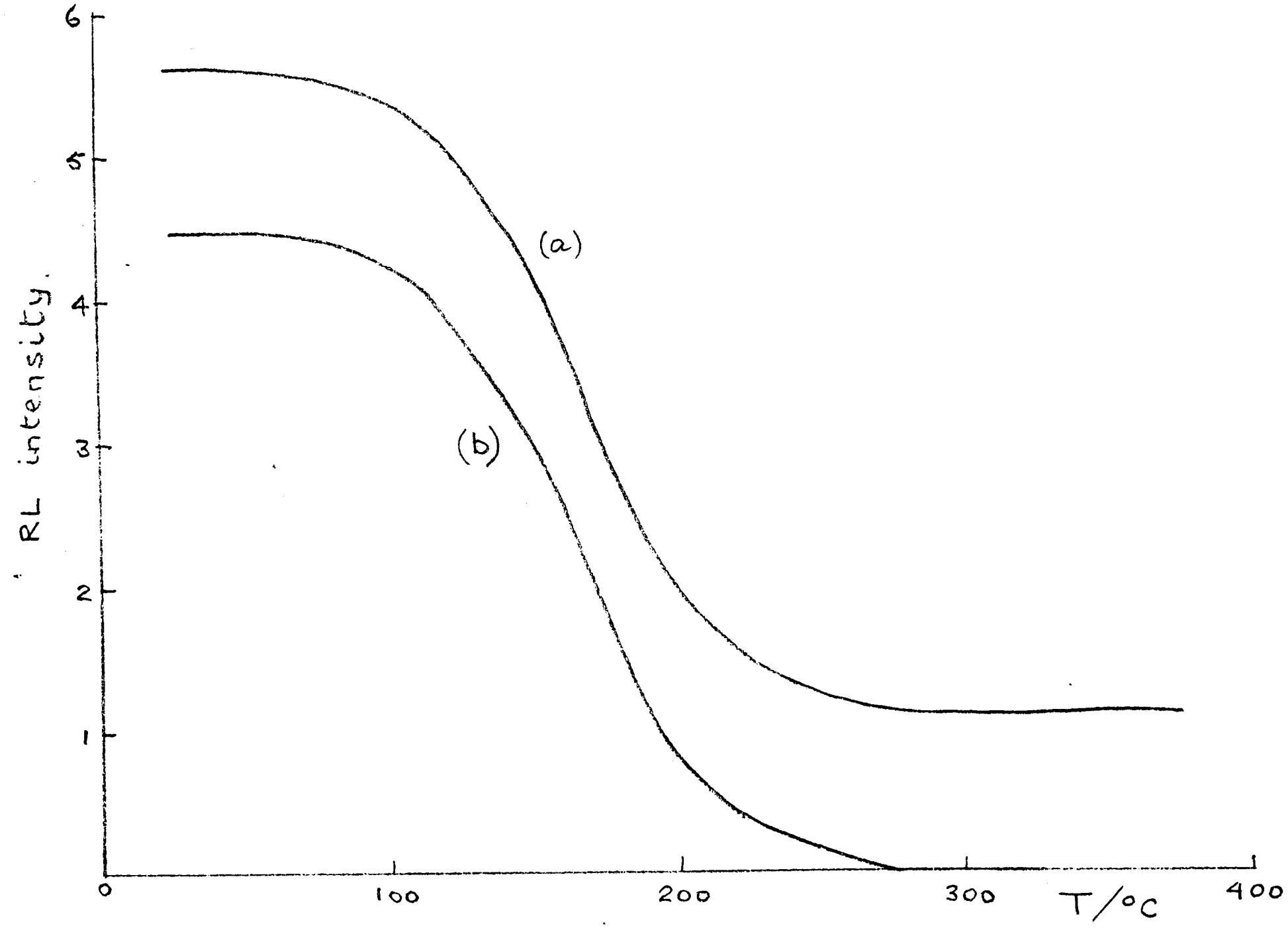

Fig. 5.12 Radioluminescence, (a) as observed, (b) after subtraction of steady emission. (A broad band filter centred on 465 nm was used)

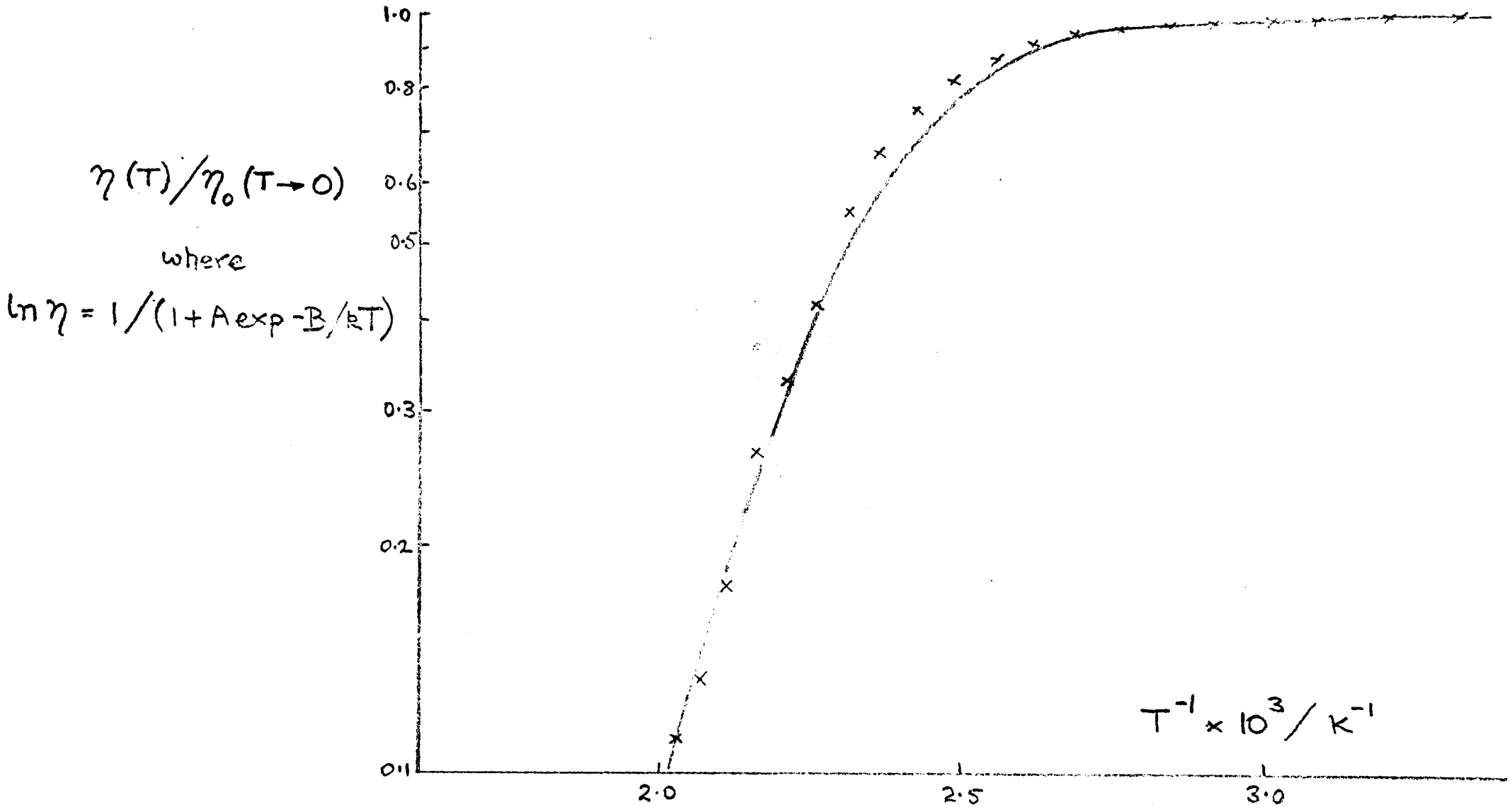

Fig. 5.13 Theoretical plot of ln η vs. T^{-1} for A = 2.8×10^7 and B = 0.64 eV; the crosses are experimental points for RL (465 nm)

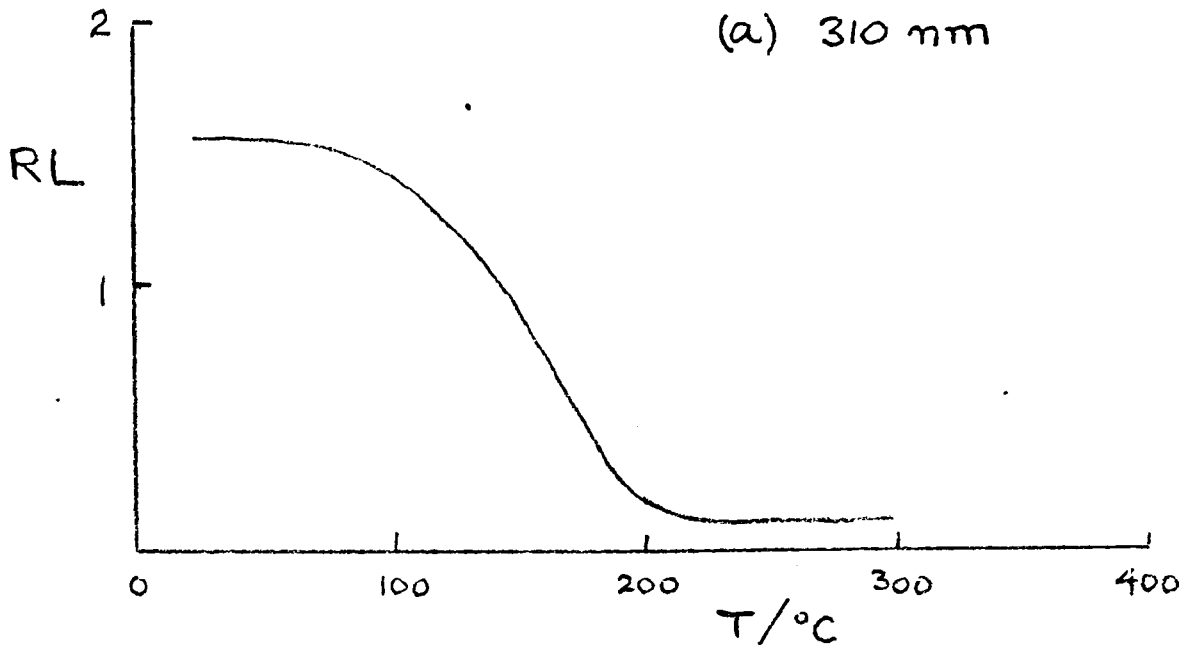

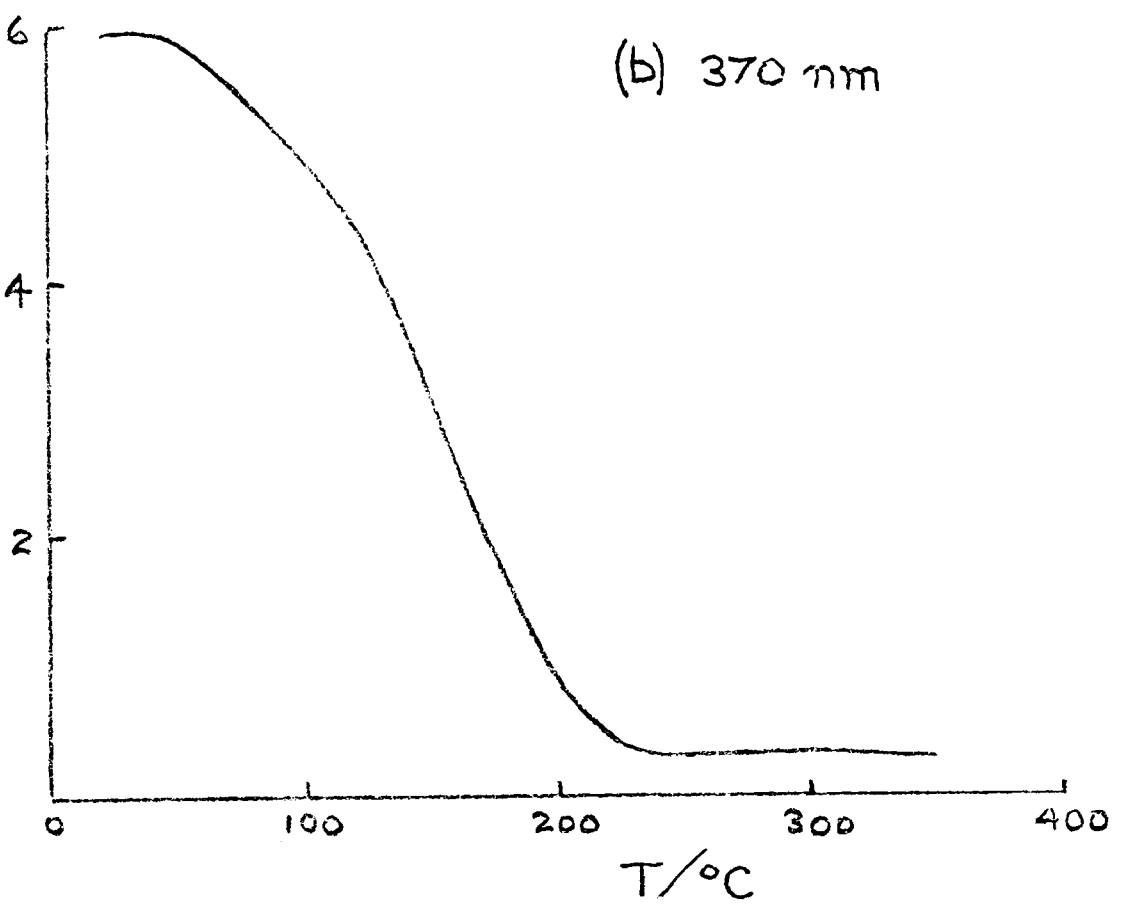

Fig. 5.14 RL as a function of temperature

NB These are experimental results and the intensities have not been corrected for filter transmission characteristics.

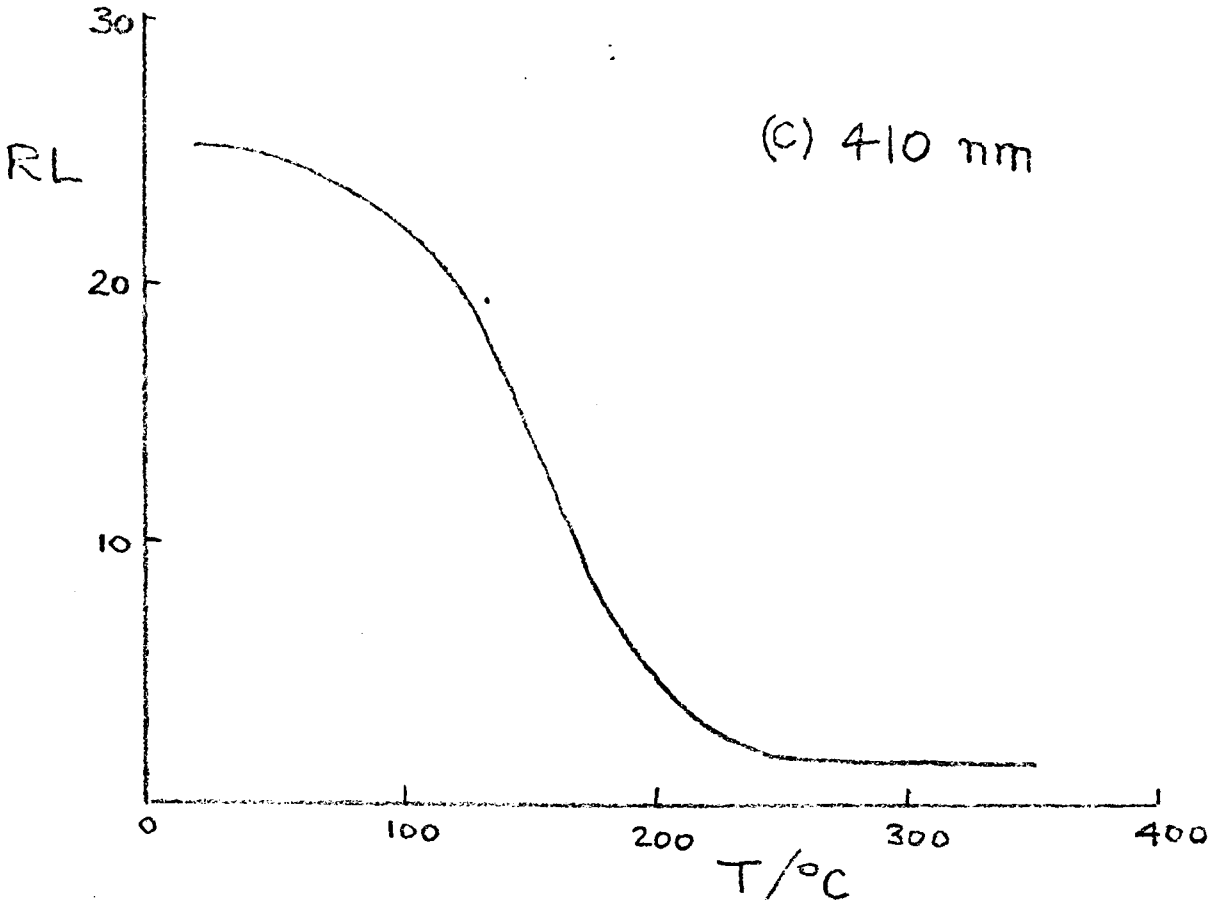

Fig. 5.14 RL as a function of temperature

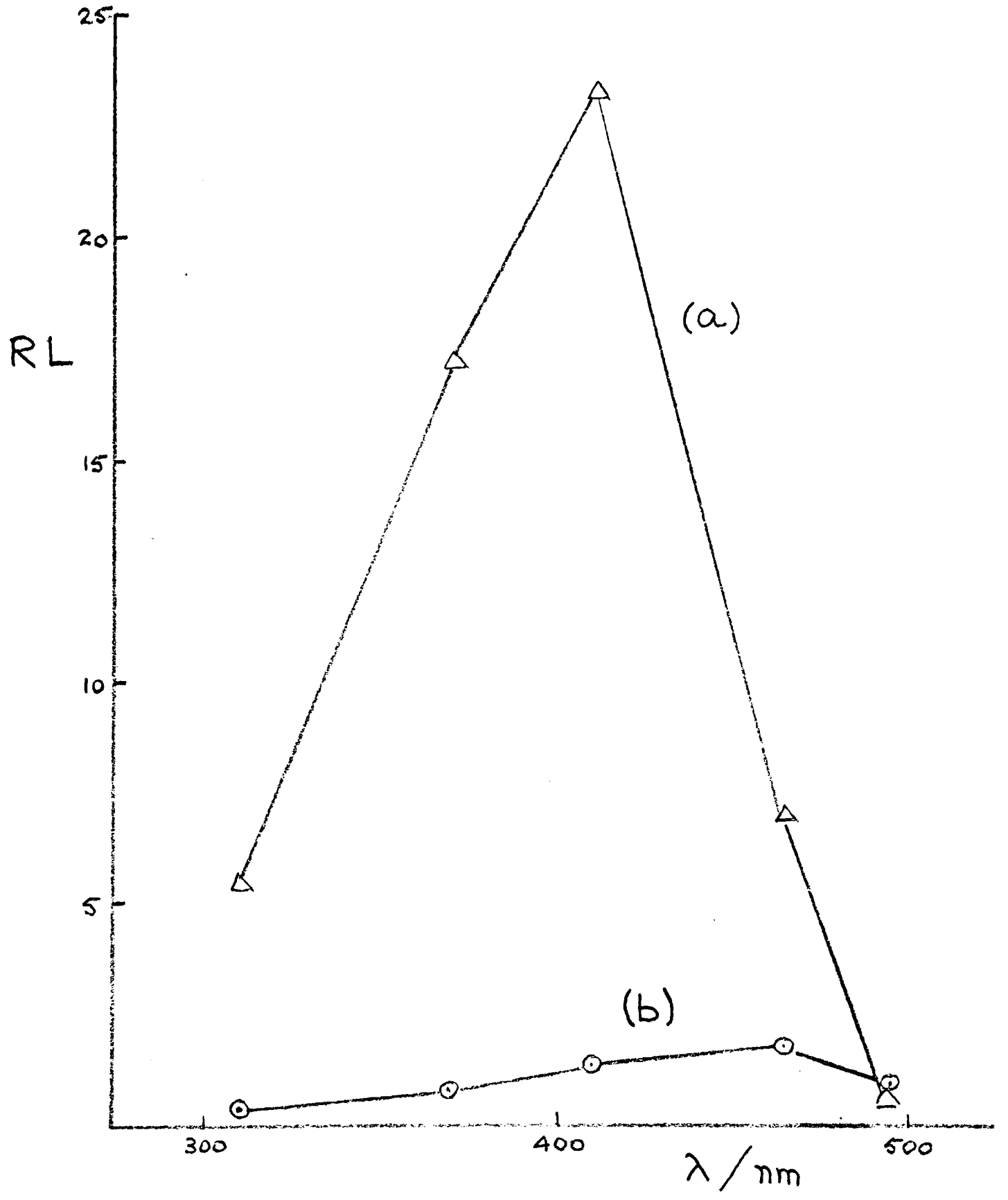

Fig. 5.15 Emission spectra of RL at 50°C

(a) component that shows thermal quenching

(b) steady component

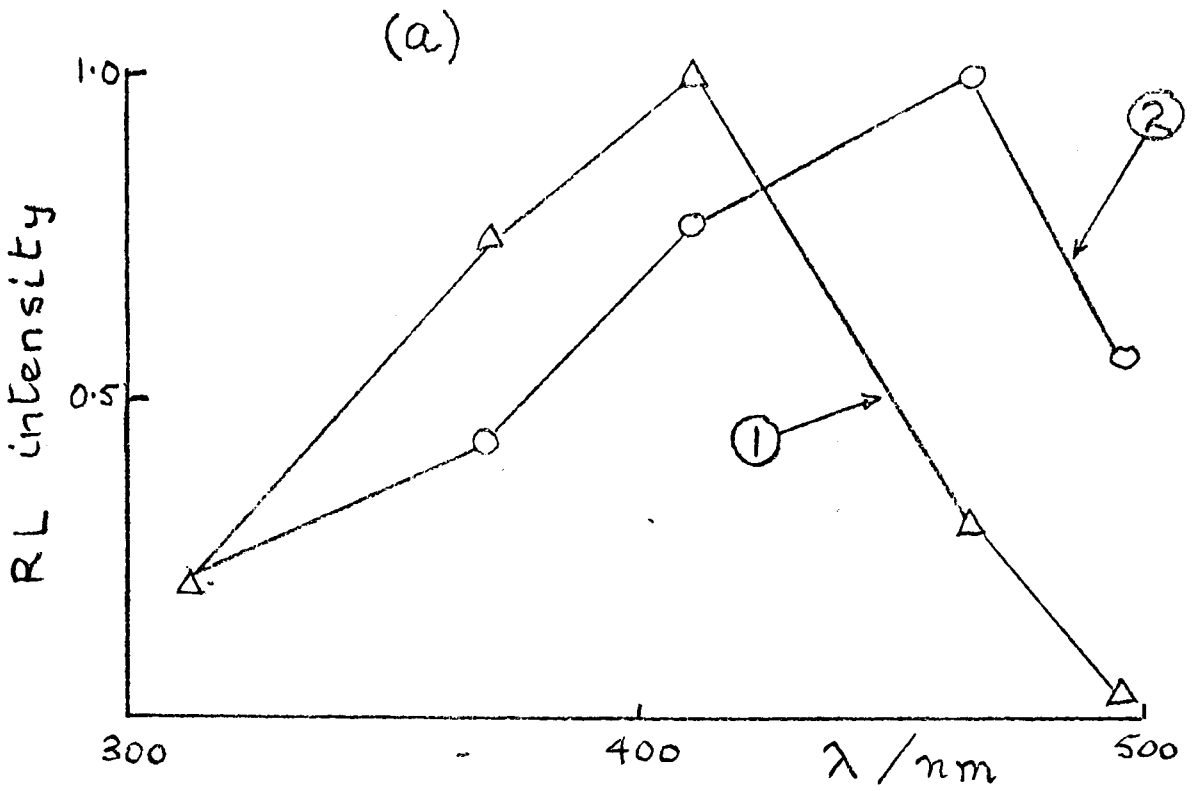

Fig. 5.16 Emission spectra

(a) normalised RL spectra at 50°C;
(1) component that shows thermal quenching at higher temperatures, (2) steady component

(b) normalised TL spectra;
(1) 110°C peak, (2) 350°C peak

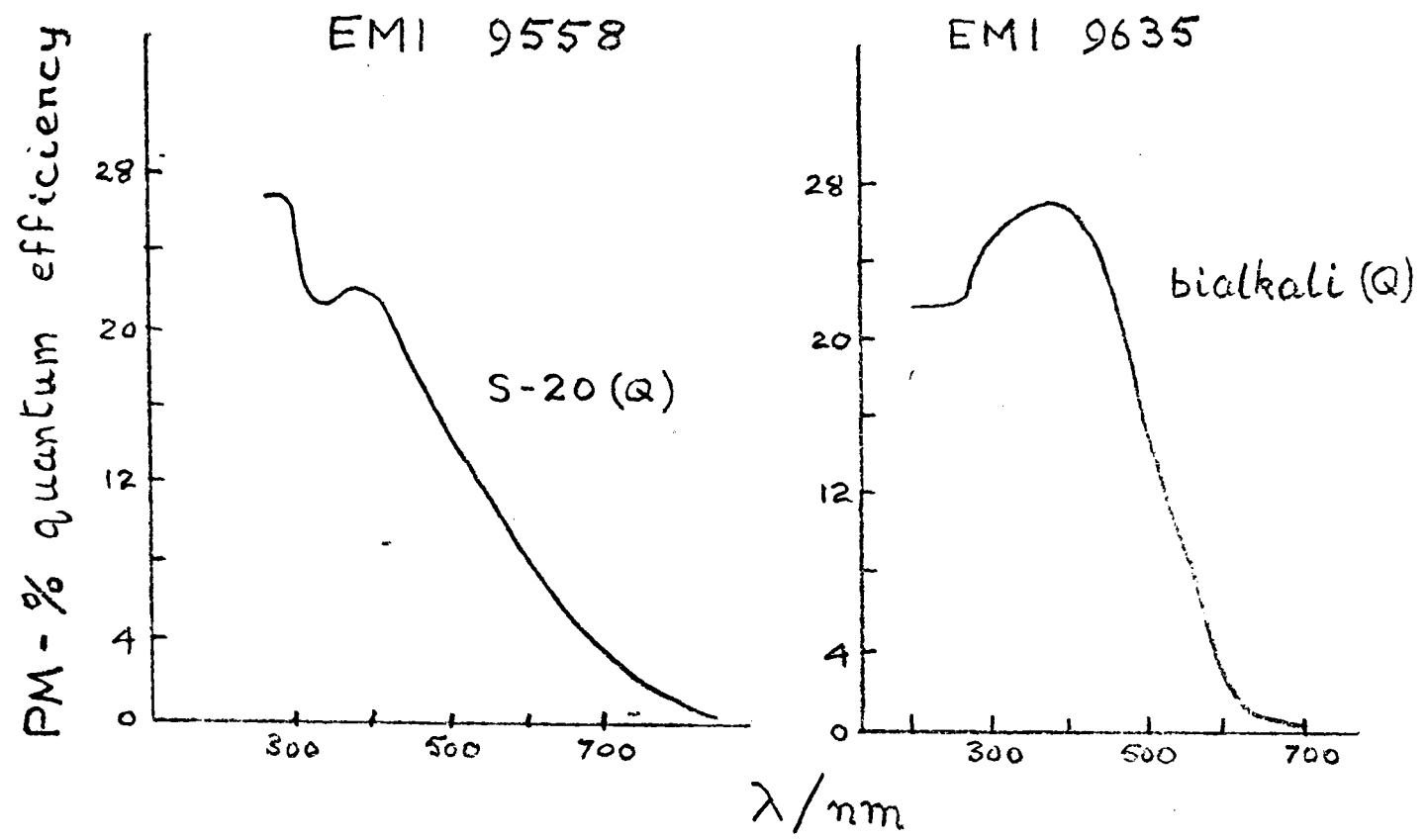

Fig. 5.17 Quantum efficiency of photomultipliers and colour filter characteristics

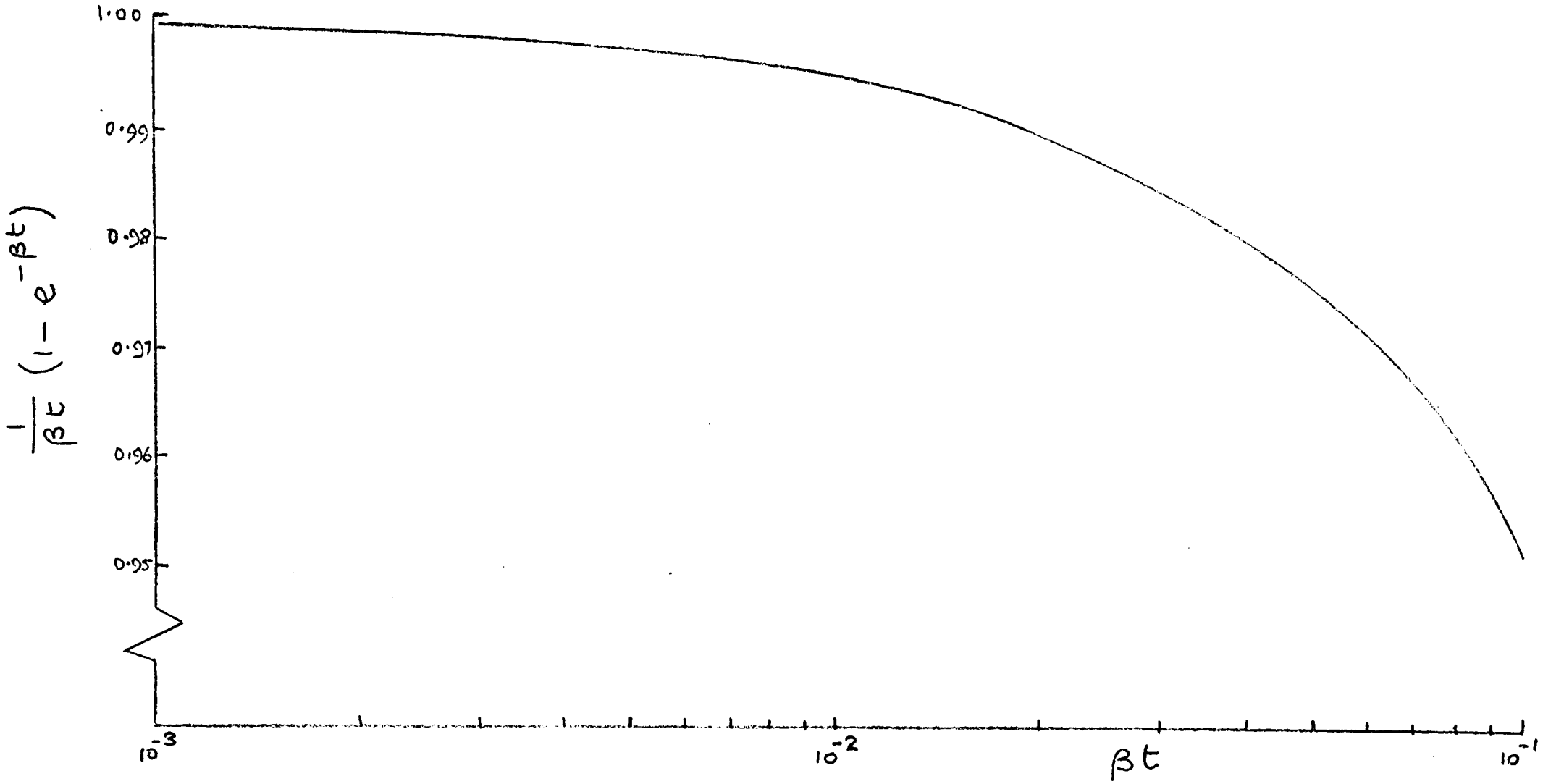

Fig. 5.18 Plot of $\frac{1}{\beta t}(1 - e^{-\beta t})$ vs log βt for $\beta t < 0.1$

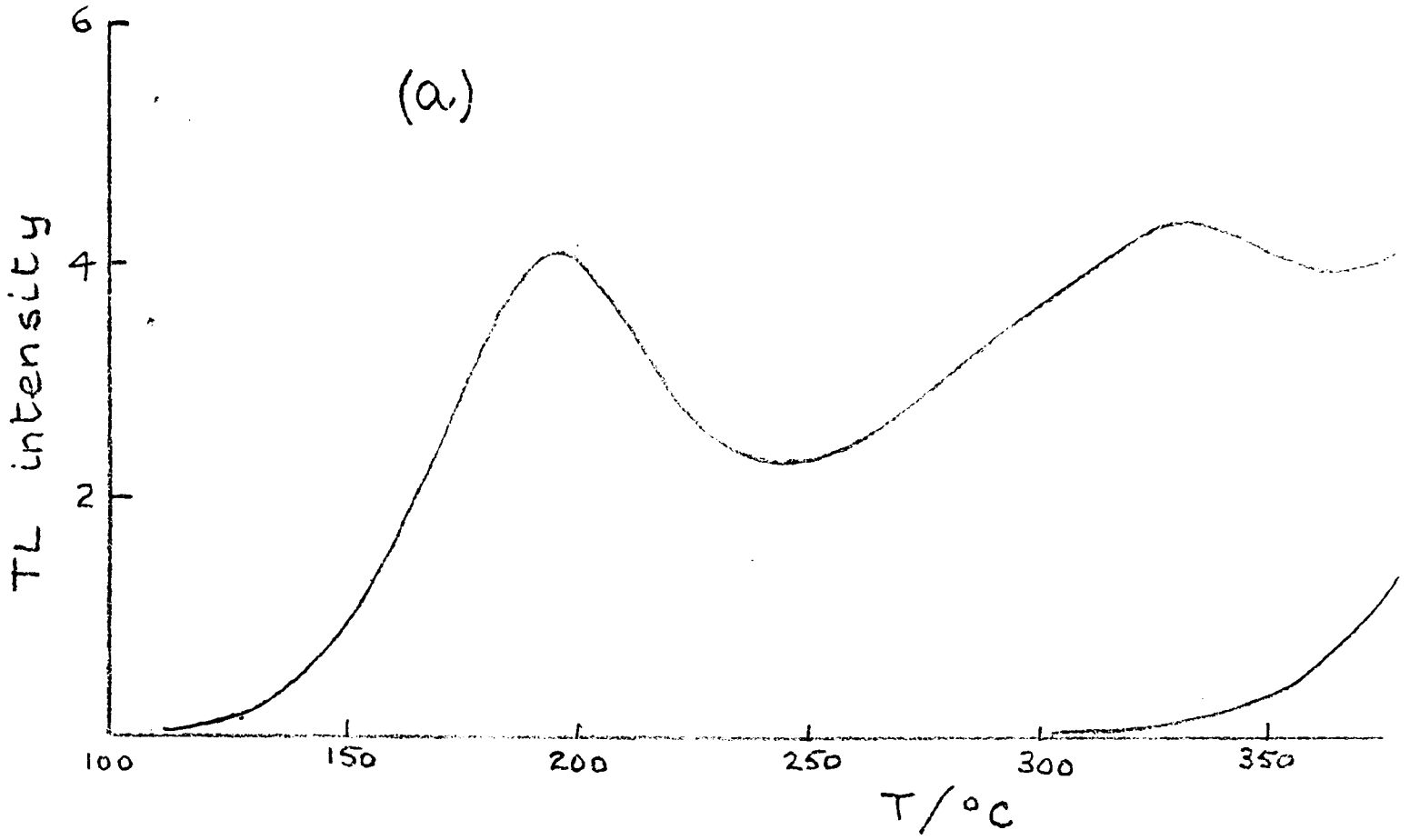

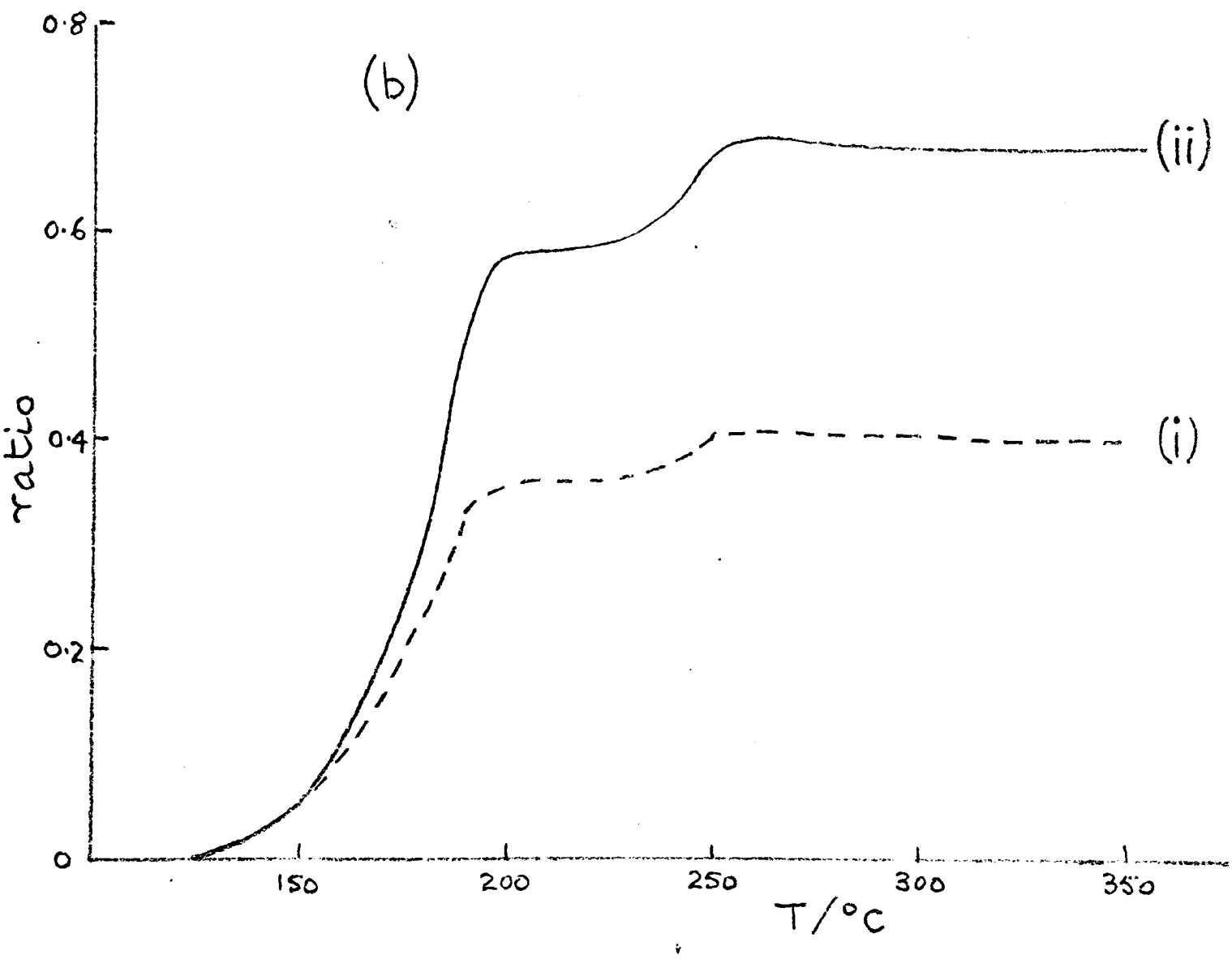

Fig. 5.19 Quartz 71 a2 inclusion dating:

(a) natural glow curve

(b) plateau test, (i) $N/(N+\beta)$, (ii) $N/\{(N+\beta)-N\}$

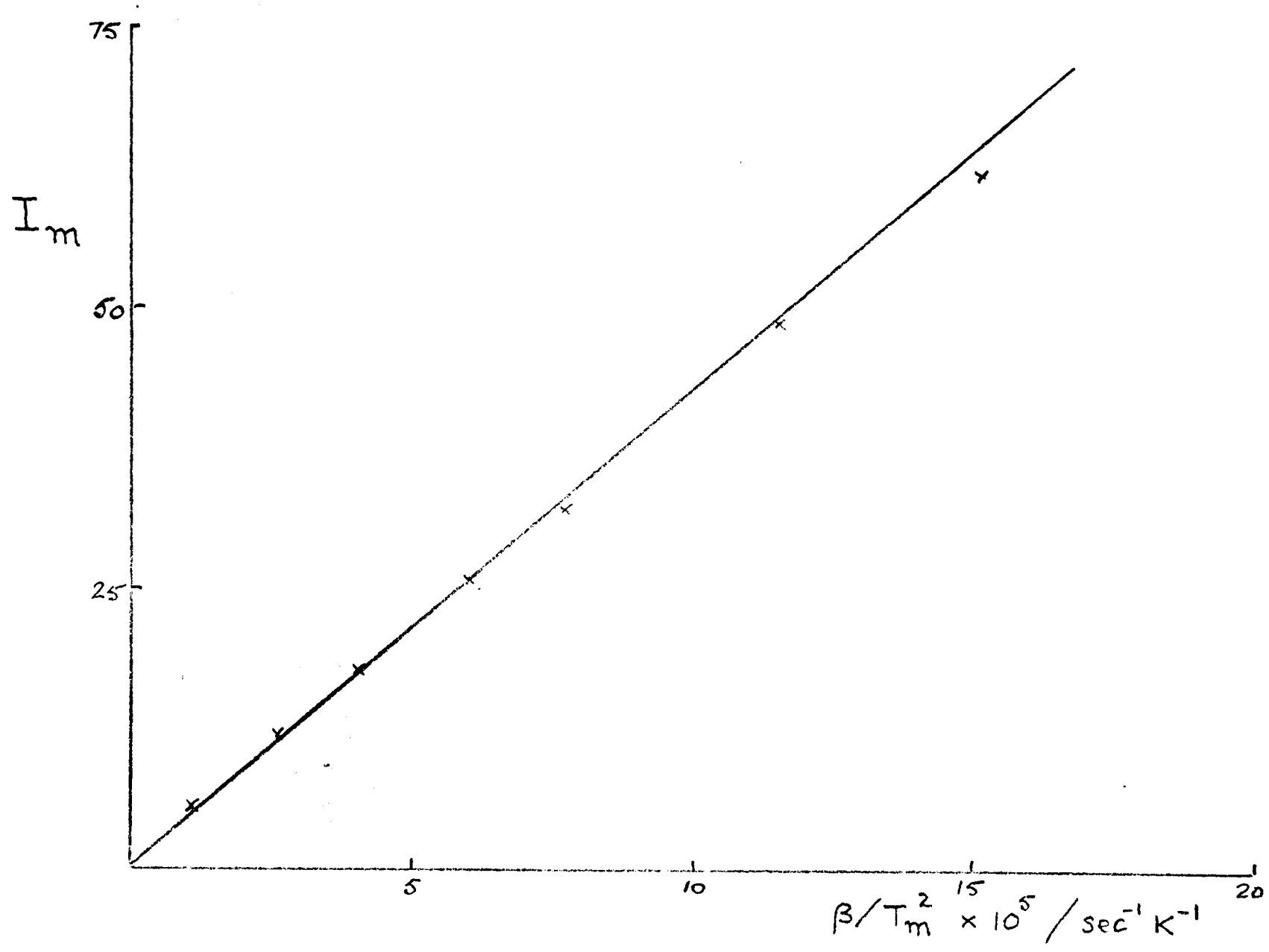

Fig. 5.20 110°C peak in quartz; peak intensity I_m vs β/T_m^2

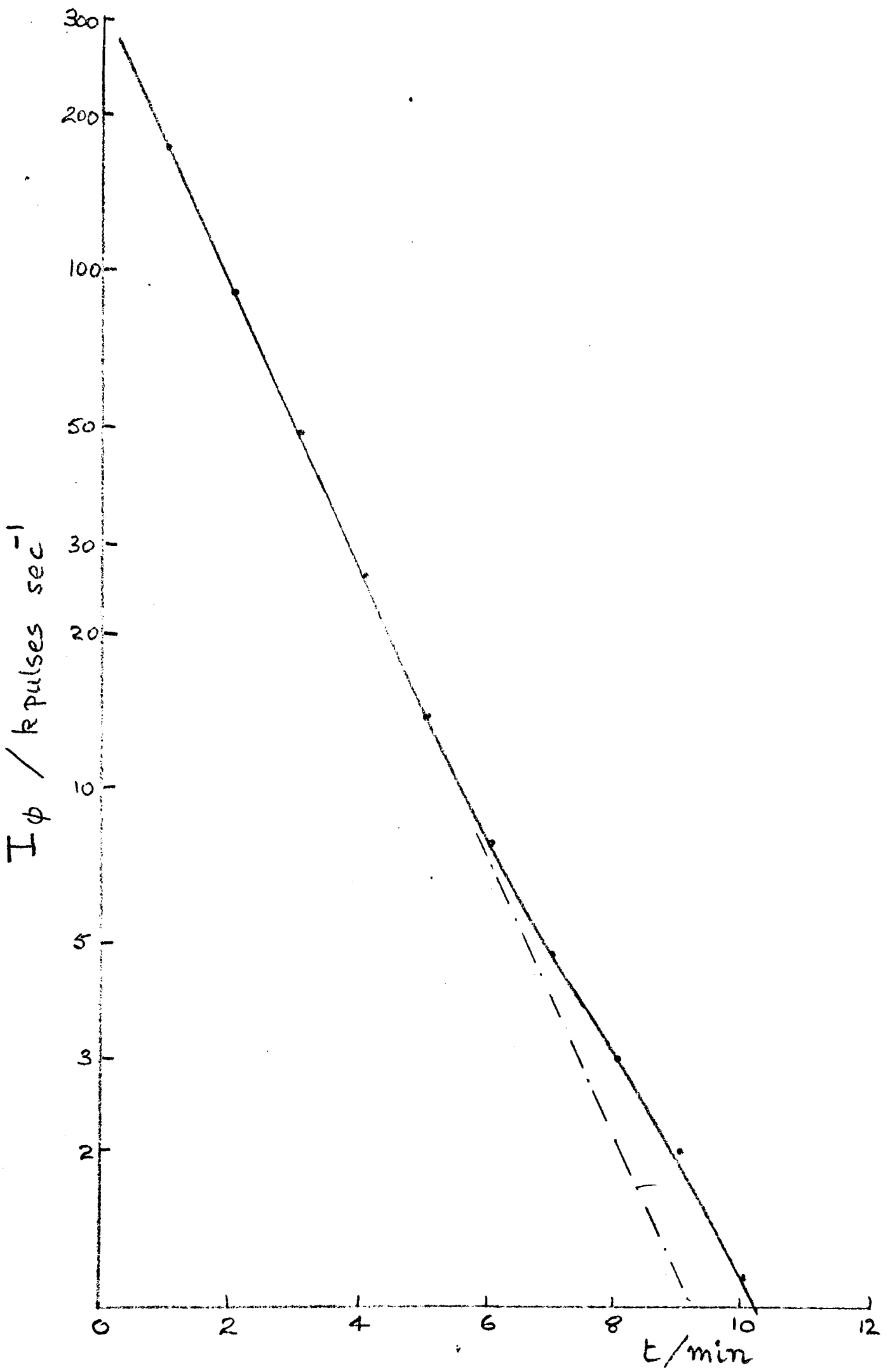

Fig. 5.21 Quartz: decay of phosphorescence at 57°C for 110°C peak

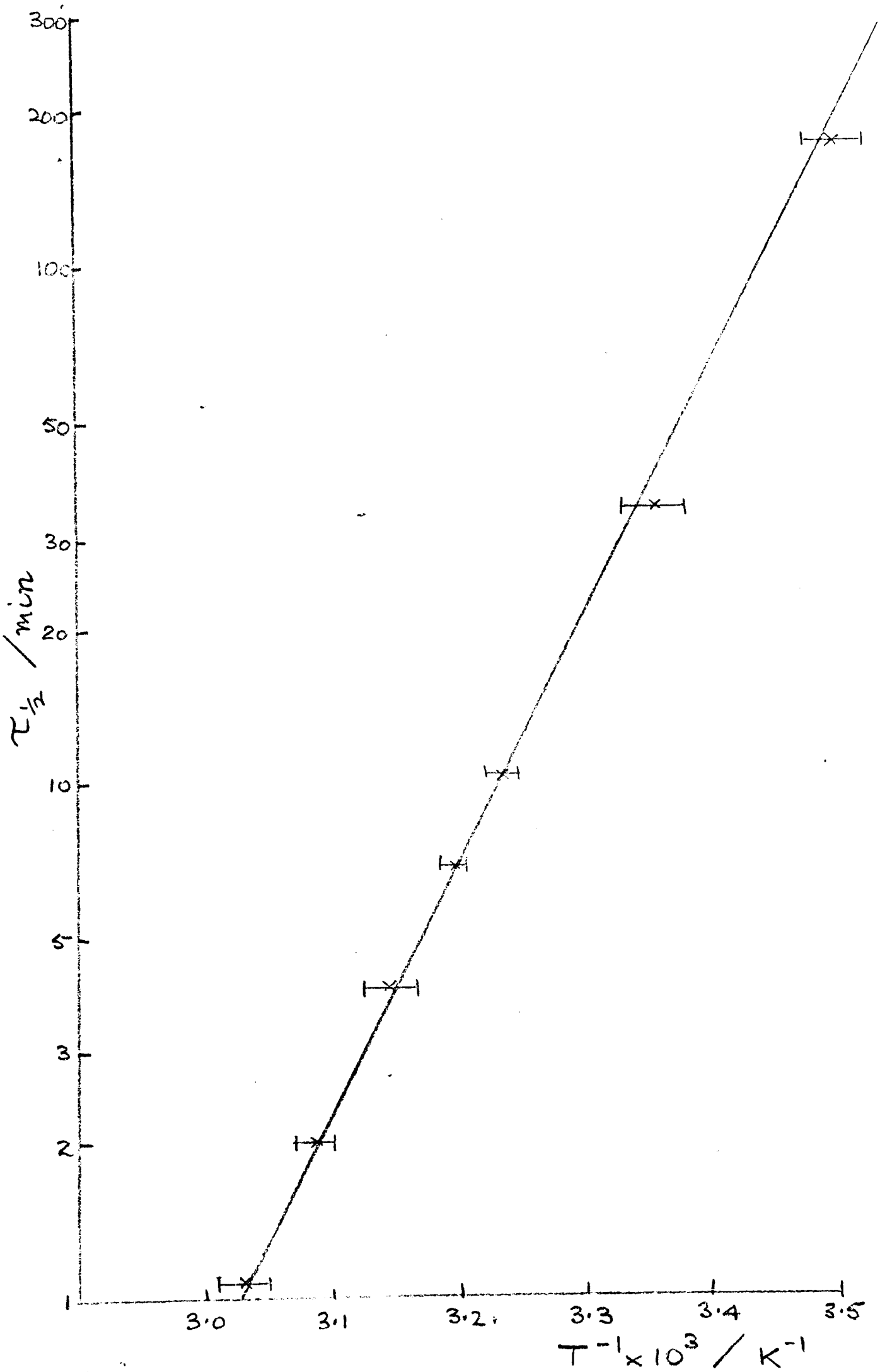

Fig. 5.22 Predosed quartz, phosphorescent decay of 110°C peak

CHAPTER 6 KINETIC STUDIES ON LIMESTONE

6.1 INTRODUCTION

In order to investigate the possibility of abnormal fading in limestone on a much longer timescale than that of the experiments described in Chapter 7, samples of limestone were obtained that had been heated at some known time in antiquity, either by man or by volcanic activity. The date of heating of the archaeological samples had been established by the radiocarbon dating of associated charcoal. The much earlier heating dates for the geological samples were ascertained by TL dating using a peak already shown to be stable for the archaeological samples. The electronic stability inferred from the fading characteristics of the samples was compared with that derived from laboratory measurements of E and s values.

6.2 TRAPS AND EMISSION CENTRES IN LIMESTONE

The emission centres in calcite have been studied by doping synthetic samples during precipitation; the most important activator in all carbonates was found to be Mn^{2+} and the presence of Fe^{2+} was found to have a quenching action on the luminescent emission (Medlin, 1968a). This was true for all the glow peaks studied including the 230°C and the 320°C peaks. After studying samples with different concentrations of dopants, Medlin concluded that, though the emission of luminescence occurs at the Mn^{2+} ion, it is not itself the recombination centre; the site of recombination is more likely to be a lattice defect and luminescent recombination will only take place if the defect is within one or two nearest neighbour distances of a Mn^{2+} ion. This accounts for the large variations in luminescence

efficiency and such variations have been used to study the infilling of secondary calcite and carbonate rocks (Sippel and Glover). The infilled mineral often gives banded luminescence due to the variations in concentration of the activator ions or quenching ions in the circulating ground water.

Medlin's study of the luminescent emission enabled him to construct a configurational coordinate diagram for Mn^{2+} in calcite. In this diagram the curves for the ground state and lowest excited state do not cross or approach each other closely and hence a radiative transition from this excited state to the ground state is much more likely than a non-radiative one.

Such a system predicts that thermal quenching of the observed luminescence will not occur. The curves for the higher excited levels are shallow however and intersect the curve of the lowest excited state near their minima; hence non-radiative transitions to the lowest state occur before the subsequent radiative transition to the ground state.

6.3 COLOUR OF LUMINESCENT EMISSION

The colour of the luminescence was observed using a filtrometer with band pass filters (see appendix B for filter characteristics). The luminescent emission spectrum of the 320°C TL glow peak is shown in Fig. 6.1(a) where the TL intensity is plotted logarithmically. In spite of the emission being predominantly yellow/green, in measuring low levels of TL it was nevertheless beneficial to use blue filters to cut down the effect of thermal radiation; the best was found to be a Corning (7-59) filter, Fig. 6.1(b).

6.4 DETERMINATION OF 320°C PEAK TRAP DEPTH

(a) The initial rise method

The initial rise method, as described in Chapter 3.3, was used to study the 320°C peak in a piece of archaeologically burnt limestone, 501 m ll. A typical glow curve for the sample is shown in Fig. 6.2; the peak of interest occurs at just above 350°C when the heating rate is 6°C/second.

To determine the trap depth 5 mg of 90-125 micron grains were spread on the plate and given a 5 krad β dose after the sample had been heated to remove the natural TL. It was then heated to 250°C and held at that temperature for 1 minute to remove the peak that forms a shoulder on the low temperature side of the peak. The sample was then heated (at 6°C/second) and cooled repeatedly through a temperature range of about 20°C so that a series of initial rise curves were obtained between 275°C and 425°C; to improve the accuracy of the measurements, the X-axis of the chart recorder was used on an expanded range. The resulting plots of log I versus T^{-1} are shown in Fig. 6.3 and the curves on the lower side of the peak and within 60°C of it give the trap depth to be 1.94 ± 0.04 eV, the 2% error being that in measuring the slope of the plots which have error bars allowing for an error of ± 1°C in temperature measurement.

(b) Hoogenstraaten's method

To check the validity of the initial rise determination and confirm that no significant thermal quenching was present, a plot of log β/T_m^2 versus T^{-1} was obtained. Only three different heating rates were available experimentally, Fig. 6.4, but these were sufficient to yield a trap depth of 2.0 ± 0.2 eV. The error in T_m is estimated to be ± 2°C. This confirms the more accurately determined initial rise value.

(c) Johnson's study of the 320°C peak

In 1965 Johnson studied the isothermal decay of the natural TL of a piece of limestone at various temperatures (Johnson, 1965). He found that the decays, observed for four different temperatures, could be split into two exponential components and from them he derived two sets of values of E and s which are given in Table 6.1(a), along with those values of E obtained in the previous section.

6.5 PREDICTED ELECTRONIC STABILITY

Using the equation

$$\frac{E}{k T_m^2} = \frac{s}{\beta} \exp - \frac{E}{k T_m^2}$$

and the fact that $T_m = 352^{\circ}C$ for $\beta = 5.7^{\circ}C$, s was determined and Table 6.1(b) shows the predicted mean lives at 20°C for Johnson's data and for the value of E determined by the initial rise method. The table emphasises the effect of only a 0.04 eV error in the determination - the mean life is doubled.

The large difference between the initial rise results and the isothermal decay results of Johnson needs to be explained. Because the 320°C peak is common to nearly all limestones it is likely to be due to the same defect and is therefore likely to have the same trap depth in different limestones. A more likely source of the discrepancy is the interpretation of the isothermal decay curves Johnson obtained. From his glow curves the peak can be seen to be composite and the isothermal decay curves show a peak shift to higher temperatures with longer storage time. This was found to happen experimentally in sample 501 m 11 and for this reason I did not use this method for trap depth determination.

TABLE 6.1

(a) VALUES OF E AND S DETERMINED FOR THE 320 °C PEAK IN LIMESTONE

Johnson's results obtained from isothermal decay of natural TL

E/eV	s/sec^{-1}
1.68	2.4×10^{12}
1.66	7.3×10^{12}

Initial rise method on limestone 501 m 11

$E = 1.94 \pm .04$ eV $s = 1.4 \times 10^{15}$ sec^{-1}

Hoogenstraaten's method

$E = 2.0 \pm 0.2$ eV $s = 4.5 \times 10^{15}$ sec^{-1}

(b) MEAN LIVES AT 20 °C CONNECTED WITH THE ABOVE VALUES OF E

Johnson's data

$$\tau_{20} = 200 \pm 50 \times 10^{6} \text{ years}$$

Initial rise data

E/ev	τ_{20}/years
1.90	22×10^{9}
1.94	50×10^{9}
1.98	113×10^{9}

6.6 DOSE RESPONSE OF THE 320°C PEAK

Having checked the theoretical stability of the 320°C glow peak in limestone, the linearity of the growth response curve was then investigated. A set of fine grain discs were deposited and their natural TL was removed by heating to 500°C; they were then given β irradiations of between 50 rads and 10^5 rads. The growth curve for the peak is shown on a log-log plot in Figure 6.5 along with that of the 415°C ordinate, which was found to be non-linear. The linearity of the 320°C peak up to at least 10^5 rads and its long half life make it a very useful peak for dating purposes and it is used in the following section to date archaeologically fired limestone and to compare the result with radiocarbon dates of the same archaeological level.

In the course of these experiments it was noted that there was no shift in peak temperature with increasing dose, i.e. the peak obeys first order kinetics.

6.7 DATING OF ARCHAEOLOGICALLY FIRED LIMESTONE USING THE 320°C PEAK

Small pieces of limestone, about 3 cm in diameter, were collected from a Mesolithic occupation site on Portland Bill, Dorset. The site contained two hearths of burnt limestone, parts of which were removed for archaeomagnetic studies. There was no pottery on the site, but fragments of charcoal had been recovered for radiocarbon dating. A capsule containing natural CaF_2 (MBLE type S) was buried on the site and left for a year enabling the total environmental dose rate (cosmic + radiogenic) to be determined, averaging the seasonal fluctuations (Aitken).

The samples 501 b3, 501 m 11 and 501 m1 were prepared by scraping off the outer 2 mm and crushing gently in a vice. The grains were sieved and the 8-50 μ, 50-150 μ and 150-300 μ grains were extracted, as well as the 1-8 μ fine grains which were deposited on Al discs.

When using a heating rate of 6°C/second a plateau was obtained between the 300°C and 375°C ordinates for the fine grain for the sample 501 b3 but the intensity ratio curve dropped above 375°C, Fig. 6.6. This can be explained by the non-linearity of the TL above the 375°C ordinate, as was shown in the growth curve in Fig. 6.5 for the 415°C ordinate, giving rise to an underestimate of the natural dose.

The method of additional doses (Aitken and Fleming, 1973) was used to calculate the equivalent dose for the TL at the 320°C peak, Fig. 6.7. The alpha sensitivity of the peak was obtained by additional alpha doses with a ^{242}Cm source and the effective k value was thus calculated. Similar measurements were carried out on the fine grains of two other pieces of limestone and the results are summarised in Table 6.2.

An estimate of the natural TL of the other grain sizes was obtained by comparing the natural TL at the 320°C peak with that of a second glow monitor dose. The ratios of these two measurements are shown in Table 6.3 along with the equivalent doses for the 1-8 micron grains and the 50-150 micron grains; the ratio of the slopes of the 1st and 2nd growth curves for these two samples is also shown.

The results suggest that the fine grains do receive a larger dose rate than the larger grain sizes and therefore the distribution of radioactivity is not uniform as might be thought because of the apparent homogeneity of limestone. It was therefore decided that the fine grains would be used for dating.

The uranium and thorium activity was measured by thick source alpha counting and the potassium content measured by flame photometry. The uranium and thorium activities were assumed constant over archaeological time as the limestone had been formed about 200 million years ago. Because limestone has such a low radioactivity the effect of the environmental

TABLE 6.2

TL DATING ANALYSIS OF THREE PIECES OF LIMESTONE FROM PORTLAND BILL

	501 b3	501 m11	501 m1
% K_2O	0.08	< .03	0.53
α counts/ksec			
1. background	.05 ± .05	.02 ± .02	.04 ± .04
2. immediately sealed			
total count	3.19 ± .09	1.72 ± .06	6.30 ± .19
pairs	.030 ± .008	not significant	0.062 ± .019
3. delayed 14 days			
total count	3.37 ± .13	1.74 ± .08	6.32 ± .25
TL data in rads			
Equivalent dose	1710 ± 100	1100 ± 50	3390 ± 120
k_{eff}	0.35	0.25	0.31
internal dose rates in mrad/year			
α eff	155	56	276
total β	24	11	73
total γ	28	14	91
environmental dose rates in mrad/year			
dose rate allowing for attenuation and internal dose rate	73	72	77
TL Age/years	6780 ± 540	7870 ± 660	7950 ± 810

TABLE 6.3

GRAIN SIZE VARIATION OF EQUIVALENT DOSE IN LIMESTONE, 501 m11

grain size /microns	Natural/ 2nd glow β	ED by add β/Krad	S1/S2
150 - 300	1.00 ± .03	-	-
50 - 150	0.97 ± .03	0.955	.96
8 - 50	0.95 ± .03	-	-
1 - 8	1.55 ± .05	1.10	1.27

Second glow β dose = 0.90 Krad

dose rate is far more important than it is in most pottery dating when soil and pottery often have similar activities. As mentioned earlier 50 mg of natural fluorite was buried in a black nylon capsule in a related layer on site for about a year. The dose rate for this site was found to be 77 ± 2 mrad/year, of which 15 mrad/year will be due to the cosmic ray flux. Because the pieces of the limestone are 3 cm in diameter a small correction was applied for attenuation of the environmental dose; Table 6.2 shows the correction to be less than 3% even for samples 501 b3 and 501 m11 which have very low self activity. If one considers a sphere of radius r of non-radioactive but attenuating medium surrounded by an infinite uniformly emitting and similarly attenuating medium, then the % γ dose at the centre of the sphere is $e^{-\mu r}$ where μ is the total linear attenuation coefficient. This function is plotted in Fig. 6.8, where the value of μ used is that for a 1.2 MeV γ ray in aluminium; the calculated average attenuation coefficients for the γ rays of the ^{238}U and ^{232}Th series are within 1% of this value (Fleming, 1969) and the density of aluminium is close to that of both quartz and limestone.

The age of the context was given as

$$7{,}170 \text{ years BP} \quad \pm 390 \quad \pm 640$$

where the two error limits represent the standard error on the average age and the standard error obtained by including the individual error terms respectively (Aitken and Alldred). The uncalibrated radiocarbon dates obtained from charcoal from the same level are

$$7{,}150 \pm 135 \text{ BP} \qquad \text{(BM 473)}$$

$$7{,}101 \pm 97 \text{ BP} \qquad \text{(BM 960)}$$

These have been obtained using the Libby half life (5568 years) and ignoring the long term variation of radiocarbon production. Damon, Long and Wallick

suggest that the long term error varies sinusoidally with a peak amplitude of about 370 years for their data, which only goes back to 6542 BP, (conventional radiocarbon date using the Libby half life), and with a period of about 10,000 years. Extending their sine wave back another 600 years indicates a correction of 500 $\pm$ 100 years. Combining this term and the correction due to the revised half life (5730 $\pm$ 40 years), the corrected ages in years before 1970 are

$$7{,}877 \pm 178$$

and

$$7{,}827 \pm 148$$

The error on the revised radiocarbon age is given as

$$t_1^{*} = \frac{T_{\frac{1}{2}}^{*}}{T_{\frac{1}{2}}} \left[\left\{ t \cdot \frac{\sigma\,(T_{\frac{1}{2}})^{*}}{T_{\frac{1}{2}}^{*}} \right\}^2 + t_1^{\,2} \right]^{\frac{1}{2}}$$

where t is the conventional age,

$\frac{T_{\frac{1}{2}}^{*}}{T_{\frac{1}{2}}}$ is the ratio of the revised half life over the Libby half life,

$\sigma\,(T_{\frac{1}{2}}^{*})$ is the error on the conventional age (personal communication, M.F. Barbetti). The error quoted is that obtained by combining t_1^{*} and the uncertainty in the extrapolation of the sine wave.

The TL dates for samples 501 m11 and 501 m1 agree well with the corrected radiocarbon dates. The mean age was brought down by that for sample 501 b3 which was about 14% low; there is no immediate explanation for this.

Only three samples could be dated even though many more were collected. Some were found to be unburnt and gave a geological equivalent dose; others were found to have been burnt but had little TL sensitivity. As the weak response to a laboratory test dose was similar to that of the unburnt limestone, experiments involving the heating of limestone at 500°C

(i.e. above the aragonite/calcite transition temperature), at 770°C and 1,000°C (i.e. above the temperature at which CO_2 is driven off to leave quick lime) for 24 hours were carried out, but the 320°C TL peak could not be induced.

An X-ray diffraction study, using a Guinea camera with Cu K_α radiation was kindly carried out by Dr. Whittaker, Mineralogy Department, Oxford on two of the dated samples, two burnt but insensitive samples and two unburnt samples. All the samples were found to be predominantly calcite with a very small amount of quartz. No correlation was found with the TL properties, which could not therefore be attributed to the presence of different minerals.

Minor element analysis by optical emission spectroscopy was carried out by F. Schweitzer. Manganese and iron were studied because of their well documented effect on the luminescence of calcite as discussed in section 6.2. Magnesium was included as it can also replace calcium ions in the hexagonal calcite lattice (Deer, Howie and Zussman). The results are given in Table 6.4 and again there is no apparent correlation with the TL properties.

The most likely explanation is that the sensitive samples originally came from a different limestone bed to the others and perhaps had a different geological stress history. These samples emphasise the point that each carbonate sample must have its TL sensitivity checked individually before dating can be considered.

The TL dating carried out on the three sensitive samples is the first application of TL to archaeologically burnt limestone. The agreement with the radiocarbon dates is considered satisfactory and it gives confirmation of the laboratory observations that limestone is not subject to abnormal fading. It is therefore to be expected that the mean lives predicted from

TABLE 6.4

MINOR ELEMENT ANALYSES OF LIMESTONE SAMPLES FROM PORTLAND BILL

Sample	Mg O	% Fe_2O_3	Mn O
burnt, with good TL			
501 m11	.670	.0285	.052
501 b3	.950	.750	.058
burnt, with low TL sensitivity			
501 b2	.700	.170	.051
501 b7	1.10	1.20	.094
unburnt, with low TL sensitivity			
501 b5	1.07	1.14	.066
501 b6	.910	.470	.110

the E and s values will be valid and in a later section direct confirmation of this is obtained for the 230°C peak.

6.8 DETERMINATION OF THE 230°C PEAK TRAP DEPTH

In Fig.6.2 a small peak can be seen at about 285°C; this peak is identified as that designated the 230°C peak by Johnson (Johnson, 1965). In a piece of geologically heated limestone 126 el on which TL analysis was done, this peak was more prominent, Fig.6.9, and its luminescent emission, Fig.6.10, was similar to that of the 320°C peak in 501 mll shown in Fig.6.1.

(a) The initial rise method

5 mg of the sample was spread on the heater plate, thermally drained of its natural TL and given a 25 krad β dose. It was then heated to 200°C and held at that temperature for 5 minutes to remove the low temperature TL. Three of the plots of log I versus T^{-1} obtained from the subsequent initial rise curves are shown in Fig.6.11. Given that the temperature of the peak occurs at 283°C for the heating rate used, the three curves in the temperature range 230°C to 275°C give a trap depth E = 1.52 ± .03 eV. The error bars on the points are the error in temperature measurement of ± 1°C.

(b) Hoogenstraaten's method

The sample was drained of its natural TL and repeatedly given a 1 krad β dose which was glowed at different heating rates; a plot of $\log \beta/T_m^2$ versus T^{-1} was thus obtained which give a value of E = 1.6 ± .1 eV, Fig.6.12. The errors indicate an uncertainty of ± 2°C in the measurement of T_m.

(c) Johnson's study of the 230°C peak

By studying the isothermal decay of the natural TL in the 230°C peak

Johnson obtained two exponential decays and hence two values of E and s. These are shown in Table 6.5(a) along with those determined in sections 6.8(a) and 6.8(b).

6.9 PREDICTED ELECTRONIC STABILITY

The mean lives assuming 1st order kinetics predicted by the various values of E and s are given in Table 6.5(b); there is a two orders of magnitude difference between Johnson's results and those obtained for limestone 126 el. Table 6.6 gives the variation of mean life with temperature.

6.10 JOHNSON'S DATING OF A CONTACT-METAMORPHOSED LIMESTONE

Where a lava dyke has penetrated an older sedimentary limestone, the TL of the surrounding limestone will have been affected by the localized heating to an extent depending on the temperature of the magma and the thermal conductivity of the limestone. Johnson attempted to determine the magma temperature by using the appropriate TL decay equations and heat conduction theory in conjunction with the TL at different distances from the lava-limestone interface (Johnson, 1966). In an earlier paper he had obtained an age of 47,500 years $\pm$ 22% for the same contact-metamorphosed limestone from the Uinkaret lava field near the Grand Canyon National Monument, Arizona (Johnson, 1963); he then used the relative stabilities of the 230°C and the 320°C peaks to calculate the maximum ambient temperature since the metamorphic event, which he gave as 20°C (Johnson, 1965).

There were several acknowledged sources of error in the measurements. The most serious of them were (a) that the natural TL equivalent dose was obtained by integrating all the TL including the 230°C peak which was known

TABLE 6.5

(a) VALUES OF E AND S DETERMINED FOR THE 230 ^{o}C PEAK IN LIMESTONE

Johnson's results obtained from isothermal decay of natural TL

E/eV	s/sec^{-1}
1.44	8×10^{11}
1.42	4×10^{12}

Initial rise method on limestone 126 e1

$E = 1.52 \pm .03$ eV $s = 2 \times 10^{13}$ sec^{-1}

Hoogenstraaten's method

$E = 1.6 \pm 0.1$ eV $s = 1 \times 10^{14}$ sec^{-1}

(b) MEAN LIVES AT 20 ^{o}C CONNECTED WITH THE ABOVE VALUES OF E

Johnson's data

$\tau_{20} = 9 \pm 2 \times 10^{3}$ years

Initial rise data

E/eV	τ_{20}/years
1.49	130×10^{3}
1.52	230×10^{3}
1.55	380×10^{3}

TABLE 6.6

VARIATION OF MEAN LIFE WITH STORAGE TEMPERATURE

FOR 230 ^{o}C PEAK (E = 1.52 eV)

T/^{o}C	mean life/years
10	1877×10^3
15	645×10^3
20	230×10^3
25	85×10^3

to be decaying (b) that no allowance was made for the different TL sensitivity of α particles i.e. no k value was obtained (c) that the γ dose from the lava flow itself was ignored.

On receiving samples of limestone and lava from the same contact zone, more detailed studies were carried out and are reported in the next section. The initial idea had been to date the lava flow by TL but the discovery of 'anomalous fading' as reported in Chapter 4 precluded this study.

6.11 DATING OF GEOLOGICALLY HEATED LIMESTONE USING THE 320°C PEAK

Limestone sample 126 e1 (Johnson's reference D 52) was two inches from the lava interface. It was crushed gently in a vice and the fine grains 1-8 μ were deposited on aluminium discs. Experiments were not carried out on other grain sizes because of the length of the irradiation times needed which were of the order of 10 hours. The method of additional doses was used to obtain the equivalent dose and alpha sensitivity at the 320°C peak in the same way as for the archaeologically burnt limestone in section 6.7. The results of the TL analysis and radioactivity analysis of the limestone and the neighbouring lava are shown in Table 6.7. Also included is the analysis of sample 126 e6 (Johnson's reference D 51) which is a piece of limestone 30 cm from the lava interface and which therefore receives its γ dose entirely from the limestone. For 126 e1 the γ dose from the lava is estimated to be 50% of that from an infinite half space; Fig.6.13 shows the theoretical plot for radiation from an infinite half space through an absorbing layer of thickness h and of density 2 gm/cm^3 obtained using the King function

$$\mathbb{K}(\mu h) = \exp(-\mu h) - \mu h \int_{\mu h}^{\infty} e^{-t} \frac{1}{t} \, dt$$

which has a more rapid initial decrease than the more simple attenuation

TL DATING ANALYSIS OF LIMESTONES 126 e1 AND 126 e6 AND RADIOACTIVITY ANALYSIS OF LAVA 126 e5

	126 e1	126 e5	126 e6
% K_2O	< 0.1	1.01	< 0.1
α-counts in counts/Ksec			
1. background	0.0	0.1 ± .1	0.13 ± .04
2. immediately sealed total count	4.15 ± .25	10.2 ± .3	2.80 ± .03
pairs	not significant	.19 ± .04	not significant
3. delayed 14 days total count	4.21 ± .16		2.60 ± .13
TL data (320 °C peak)			
Equivalent dose	50,000 ± 5,000 rads (10%)		55,000 ± 5,000
k eff	0.115		0.35
internal dose rates in mrad/year			
α eff	68		135
total β	31		22
environmental dose rate in mrad/year			
cosmic	15		15
$\frac{1}{4}$ x lava γ	31		
$\frac{3}{4}$ x limestone γ	33		limestone γ 29
Total dose rate in rad/year		.178 ± .017 (10%)	.202 ± .010 (5%)
Age	280,000 ± 40,000 years (14%)		270,000 ± 30,000 years (10%)

NB The 10% error in the dose rate for 126 e1 includes the error in the lava γ dose which allows for the sample to be anywhere within a foot of the lava/limestone interface.

factor for a parallel beam of γ rays, $e^{-\mu h}$, (Alekseev, Grammatov, Nikonov and Tafeev). For h = 5 cm (i.e. 2 inches), $I/I_o \approx 0.5$ and hence 0.25 X the infinite source lava γ dose + 0.75 X the infinite source limestone γ dose should be the appropriate γ dose received by the sample.

As with the archaeologically burnt limestone, the uranium and thorium decay chains were assumed to be delivering a constant dose rate to the sample since it was heated. There might have been some disequilibrium in the lava but this would have needed much more detailed radioactive analysis by α spectrometry. Combining the TL and radioactivity results, an age of 275,000 $\pm$ 30,000 years was obtained for the metamorphic event which is almost an order of magnitude greater than that obtained by Johnson, 47,500 $\pm$ 10,500 years. Comparing his results and those obtained in this study, it can be seen from Table 6.8 that applying a reduced α efficiency of 0.1 to his results, an age of about 220,000 years is obtained. As both his equivalent dose and his recalculated (k_{eff} = 0.1) dose rate are under half the values that I obtained but the age agrees within experimental error, the most likely reason for the discrepancies is that the samples were not in fact the same. The age of 275,000 ($\pm$ 30,000) years is still consistent with the geological information that the lava dyke was Pleistocene i.e. less than 2 million years old.

The agreement of the ages determined for 126 e1 and 126 e6 is made more interesting when one considers that, even though the equivalent doses are similar, the dose rates obtained for each are made up from quite different components as is emphasised in Table 6.9; the variations are caused by the differing α activities and TL α efficiencies and by the effect of the lava on the γ dose rate for 126 e1.

TABLE 6.8

COMPARISON OF JOHNSON'S RESULTS AND THOSE OBTAINED FOR 126 e1 AND 126 e6

	126 e1	126 e6	Johnson (a)	Johnson (b)
U equivalent/ppm(1)	2.34 ± 6%	4.77 ± 4%	1.22 ± 22%	1.22 ± 22%
% K_2 0	< .1	< .1	< .1	< .1
natural ED/Krad	50 ± 10%	55 ± 9%	17.7 ± 3%	17.7 ± 3%
α efficiency	0.115	0.35	1	0.1
calculated rad/yr	0.178 ± .017	0.202 ± .010	0.373 ± .082	0.080 ± .015
age/years	280,000 ± 14%	270,000 ± 11%	47,500 ± 22%	220,000 ± 22%

NB

Johnson (a) are results taken for sample B, Johnson, 1963, p.612-613

Johnson (b) are as for Johnson (a) but with α efficiency = 0.1 instead of 1

(1) U equivalent is the uranium content assuming all the α-counts were from the U decay chain i.e. no thorium decay products present.

TABLE 6.9

COMPARISON OF DOSE RATES FOR 126 e1 AND 126 e6

dose rates/mrad yr^{-1}	126 e1	126 e6
α effective	68	135
β	31	22
γ	64	29
cosmic	15	15
Total	178	201
U equivalent/ppm	2.34	4.77
k_{eff}	0.115	0.35

6.12 ELECTRONIC STABILITY OF THE 230°C PEAK AS IMPLIED BY THE DATING OF LIMESTONE 126 e1

As in quartz, the presence of a higher temperature, thermally stable peak permits calculation of the mean life of electrons in a lower peak at the ambient temperature. Assuming a linear build-up of TL with dose and first order kinetics for the trap emptying, then for the lower peak at 230°C

$$\frac{dn}{dt} = \alpha - \beta n$$

and integrating gives

$$n_1(t) = \frac{\alpha}{\beta}(1 - e^{-\beta t})$$

For the 320°C peak which has not decayed,

$$\frac{dn}{dt} = \alpha' \text{ and } n_2(t) = \alpha' t$$

Hence

$$\frac{n_1(t)}{n_2(t)} \frac{\alpha'}{\alpha} = \frac{1}{\beta t}(1 - e^{-\beta t})$$

where α and α' relate the dose received to the TL sensitivities of the two peaks. In this sample the 230°C and 320°C peaks had different α sensitivities as is shown in Table 6.10. The change in sensitivity between first and second glow curves, S/S_o, also differed but this was not important as the equivalent doses were found by the additional dose method and the second glow intercept was not significant.

The ratio $\frac{n_1(t)}{\alpha} \times \frac{\alpha'}{n_2(t)}$ is simply the ratio of the ages that are determined for the two peaks, taking into account the different α sensitivities. This gives

$$\frac{1}{\beta t}(1 - e^{\beta t}) = 0.71 \pm .14$$

TABLE 6.10

COMPARISON OF 230 °C AND 320 °C PEAKS IN LIMESTONE 126 e1

	230 °C	320 °C
ED_β/krad	39 ± 4	50 ± 5
k_{eff}	0.14	0.115
S/S_o	1.49	1.11
α_{eff} in mrad/year	83	68
β, γ + cosmic "	110	110
total dose rate in rad/year	.193	.178
Age/years	200,000 ± 30,000	280,000 ± 40,000

$$\frac{\text{Age (230 °C)}}{\text{Age (320 °C)}} = 0.71\ (\pm\ 20\%)$$

i.e. range of $\frac{1}{\beta t}(1 - e^{-\beta t}) = 0.57$ to 0.85

Hence $\beta t = 0.73$; the error range being 0.33 to 1.25

and hence β^{-1}, the mean life, $\approx$ 380,000 years with error limits of 220,000 to 850,000 years.

which from Fig.6.14 is found to give $\beta t = 0.73$, with limiting values of 0.33 and 1.25. Using the age t = 280,000 as determined for the 320°C peak, the mean life, β^{-1}, is found to be 380,000 years within the error limits of 220,000 to 850,000 years. Comparing these values with those derived from the experimentally derived values for E and s in Table 6.6, the effective mean temperature of the limestone is in the range 14°C to 20°C which is considered reasonable for the limestone studied. This implies that the values of E and s obtained for the 230°C peak are consistent with the geological evidence.

6.13 CONCLUSION

The results reported in this chapter indicate that the 320°C peak is suitable for dating limestone that was heated during the past million years or so, in respect of both the linearity of dose response and thermal stability. Now that the suitability of the 320°C peak in calcite has been established, TL becomes a promising potential tool for dating the formation of limestone and other forms of calcite; according to the mean life predicted by the E and s values the method is useful up to about 10^9 years, but as mentioned earlier the age limitation will probably be due to TL saturation; the data for Fig.6.5 indicates linearity of acquisition up to at least 10^5 rads, typically equivalent to about half a million years.

The 230°C peak is likely to be less useful because of its relatively short mean life at ambient temperature, $\sim 10^5$ years; remembering that provided samples are younger than 0.1 τ the error in the age obtained will be less than 5%, dating is practicable on samples up to 10^4 years old. However its main use is likely to be in the study of recent carbonate samples from the ocean bed where the temperature is such that the mean life is at least 10^6 years.

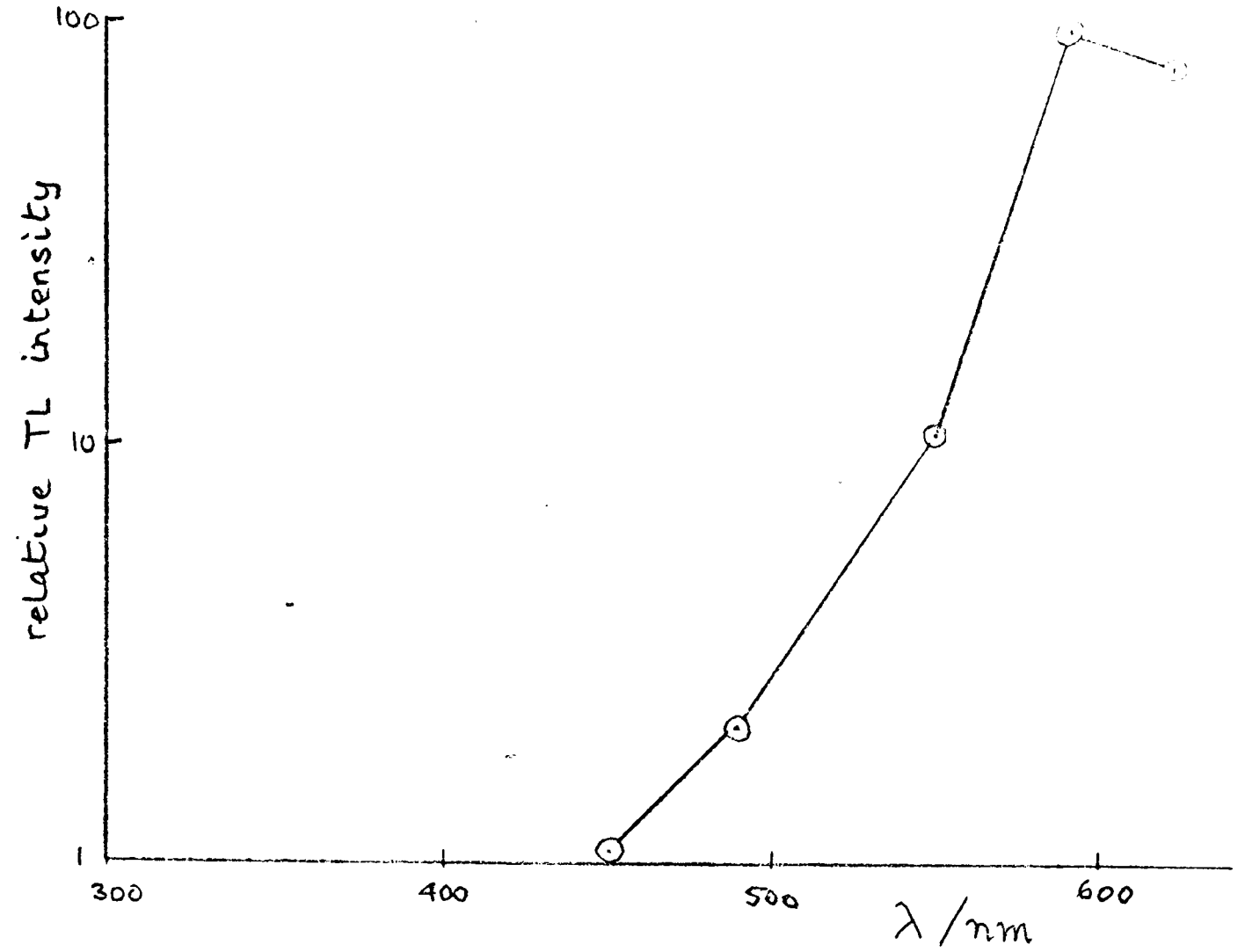

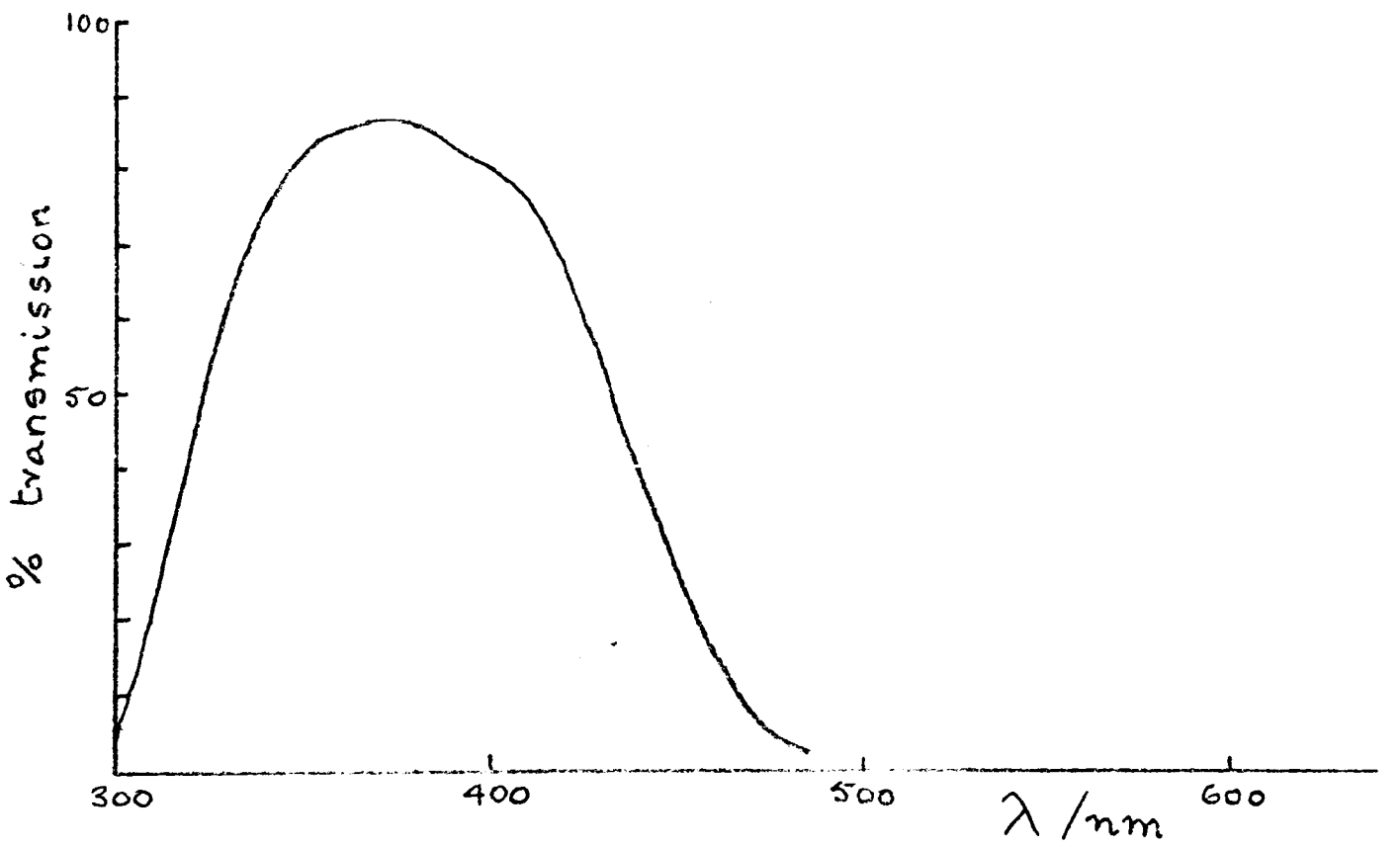

Fig. 6.1a Limestone 501 m11, emission spectrum of the 320°C peak

6.1b transmission characteristics of Corning (7-59) violet filter

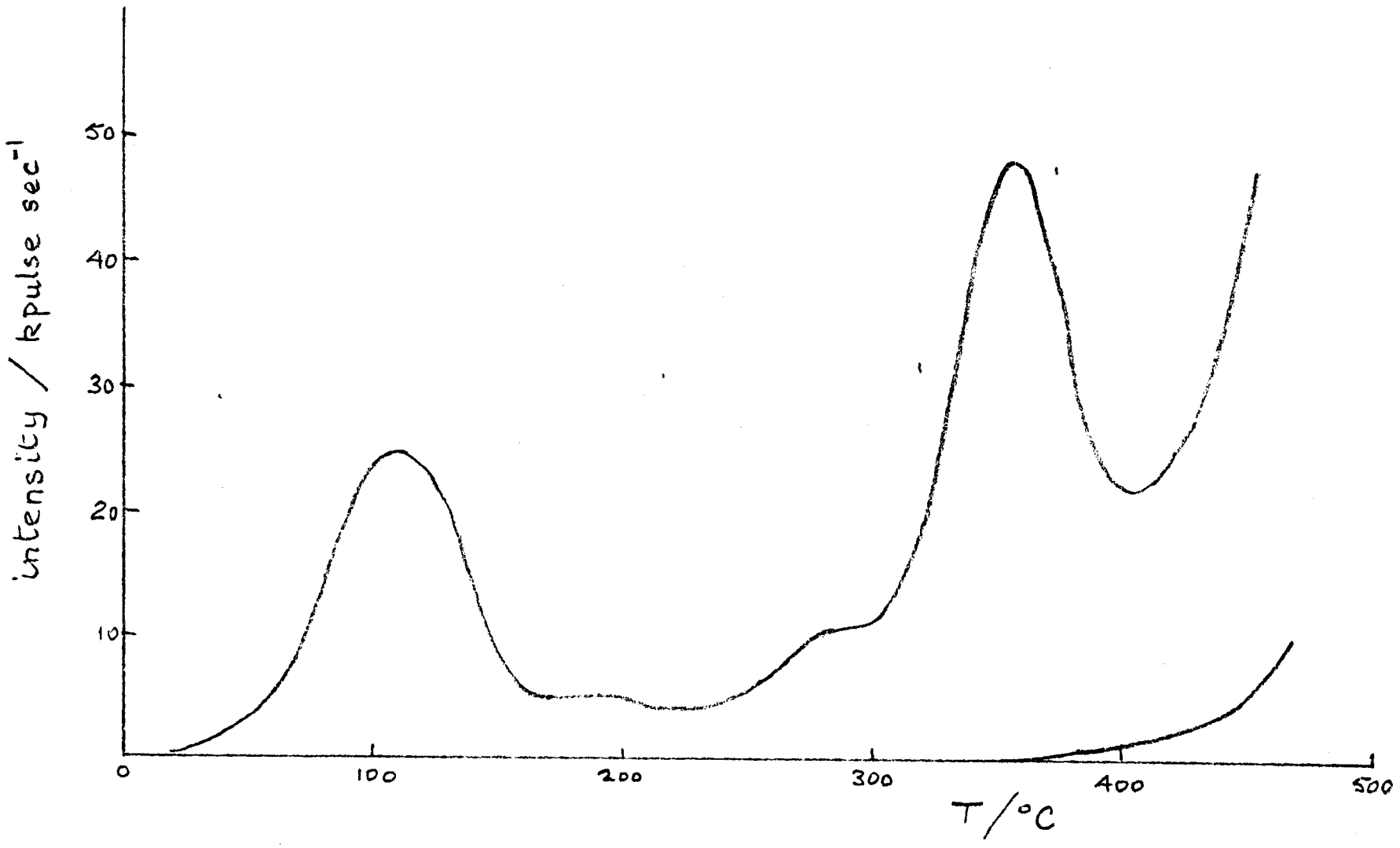

Fig. 6.2 Limestone 501 mll; response to a 1 krad β dose observed using a 7-59 blue filter

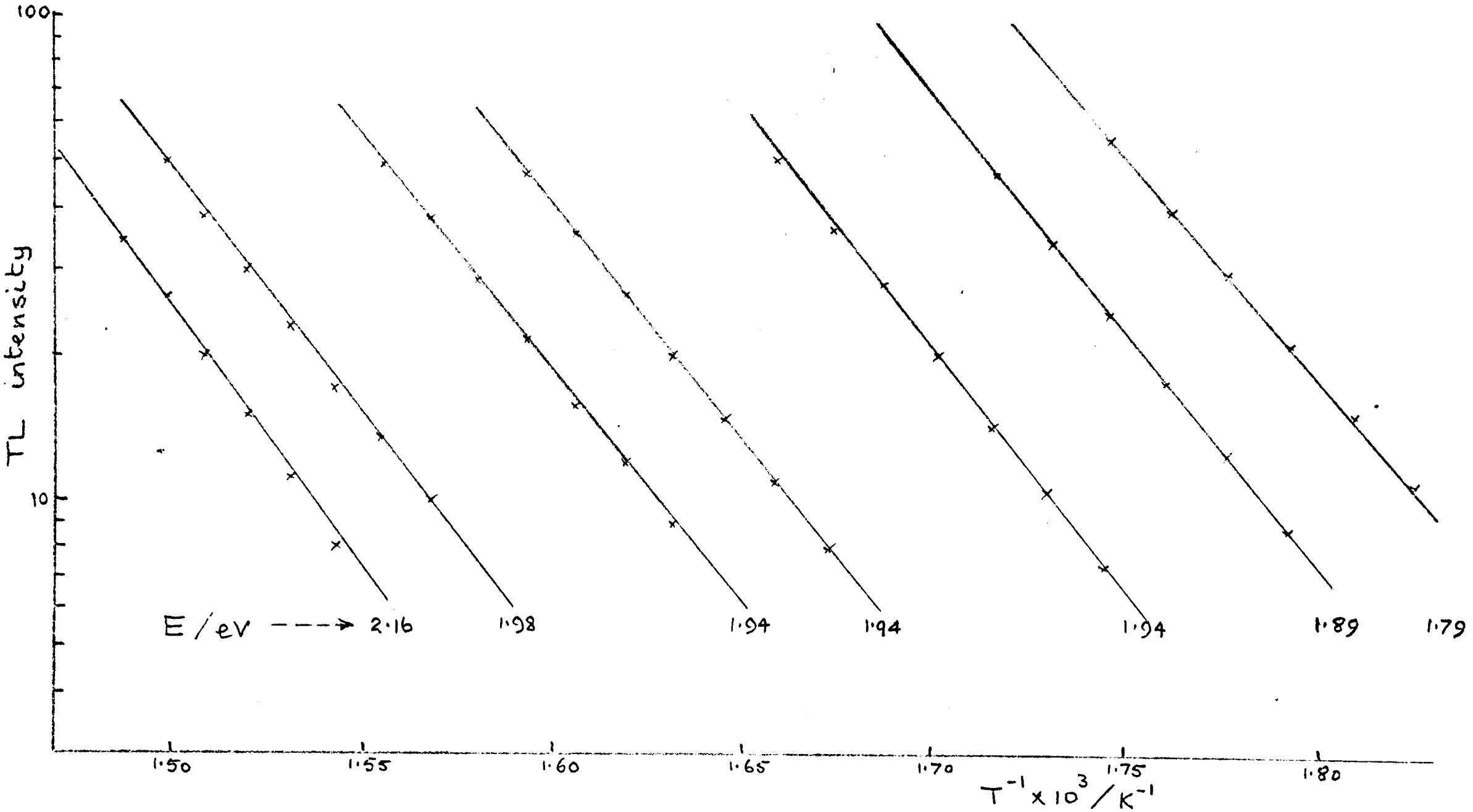

Fig. 6.3 Limestone 501 m11; initial rise results for high temperature peak

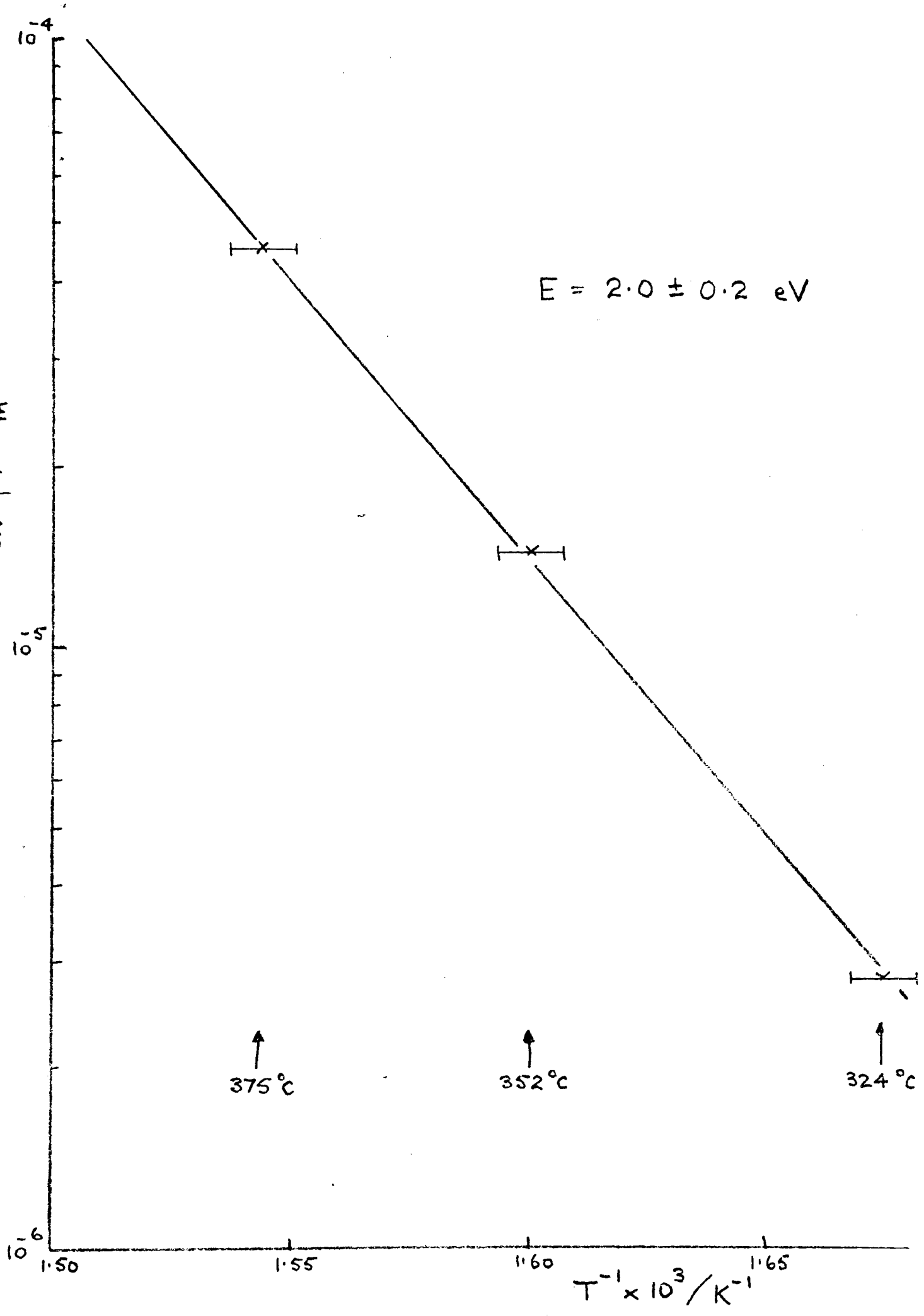

Fig. 6.4 Limestone 501 m11; 320°C peak, plot of $\ln \beta / T_m^2$ vs T^{-1}

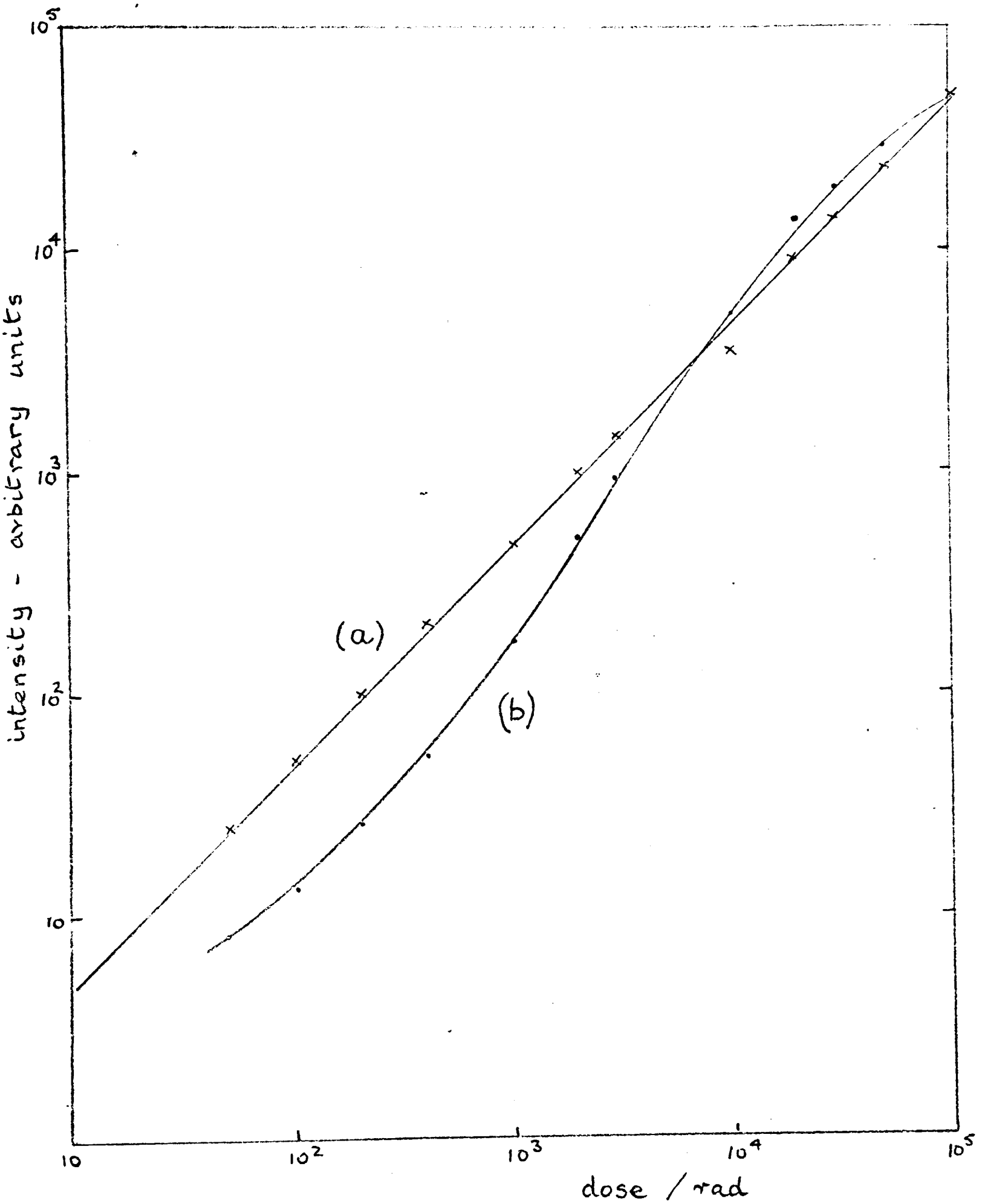

Fig. 6.5 Limestone 501 m11

Second glow β growth curves for peaks at (a) 320°C ordinate, (b) 415°C ordinate

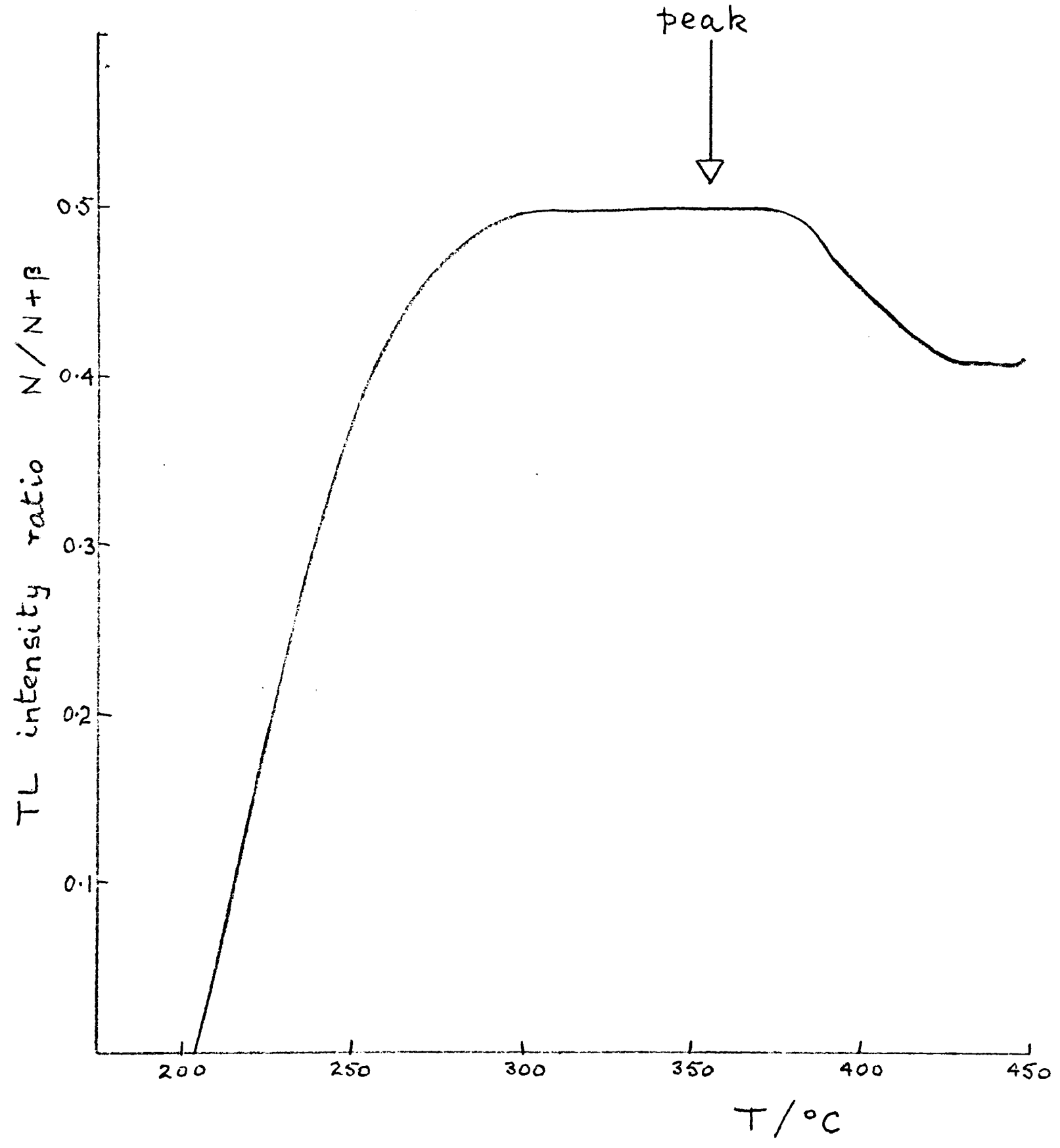

Fig. 6.6 Burnt limestone 501 b3, plateau test

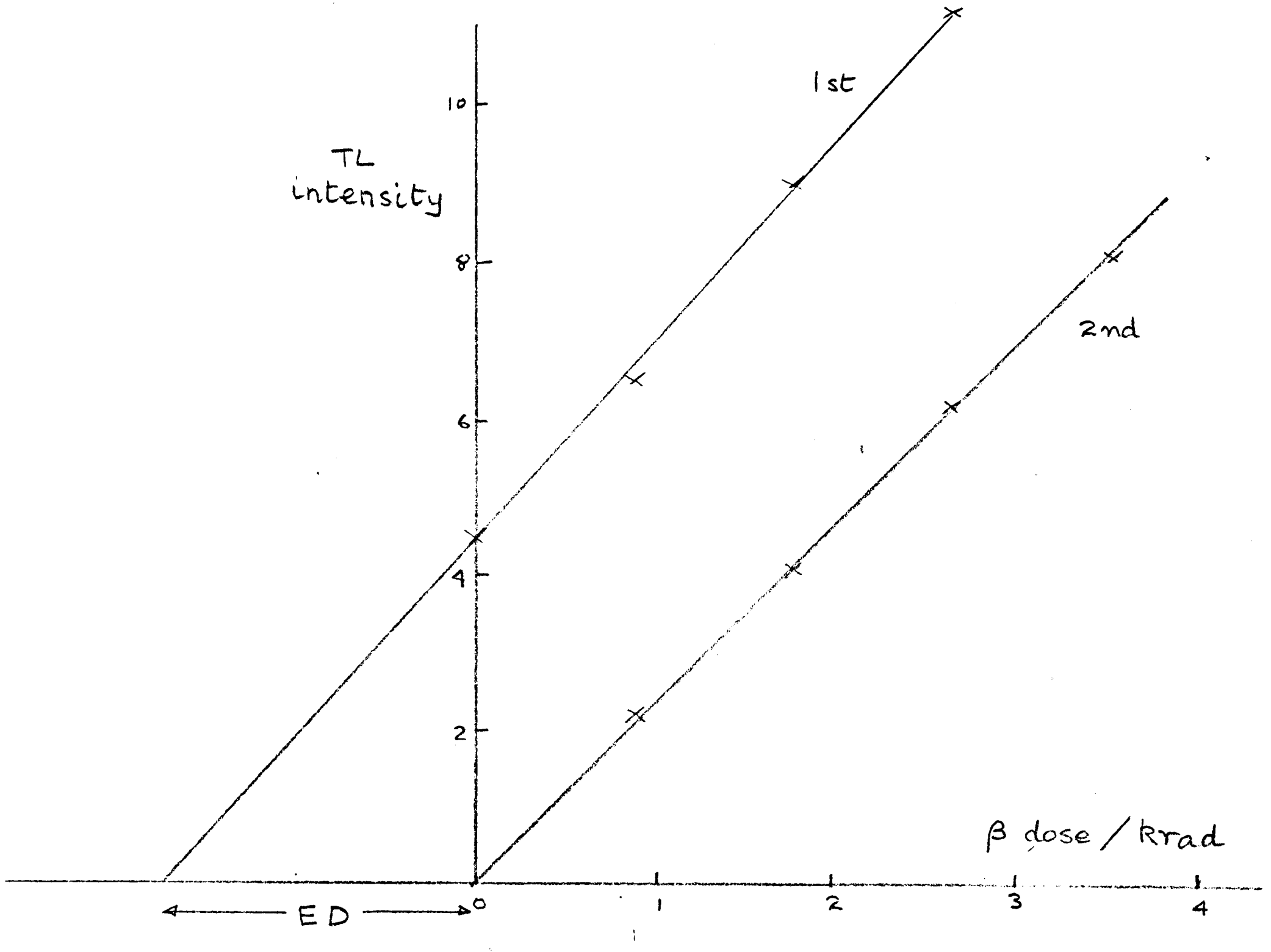

Fig. 6.7 Limetsone 501-b3: β growth curves

Fig. 6.8 Attenuation as a function of distance (μ = 0.15 cm^{-1})

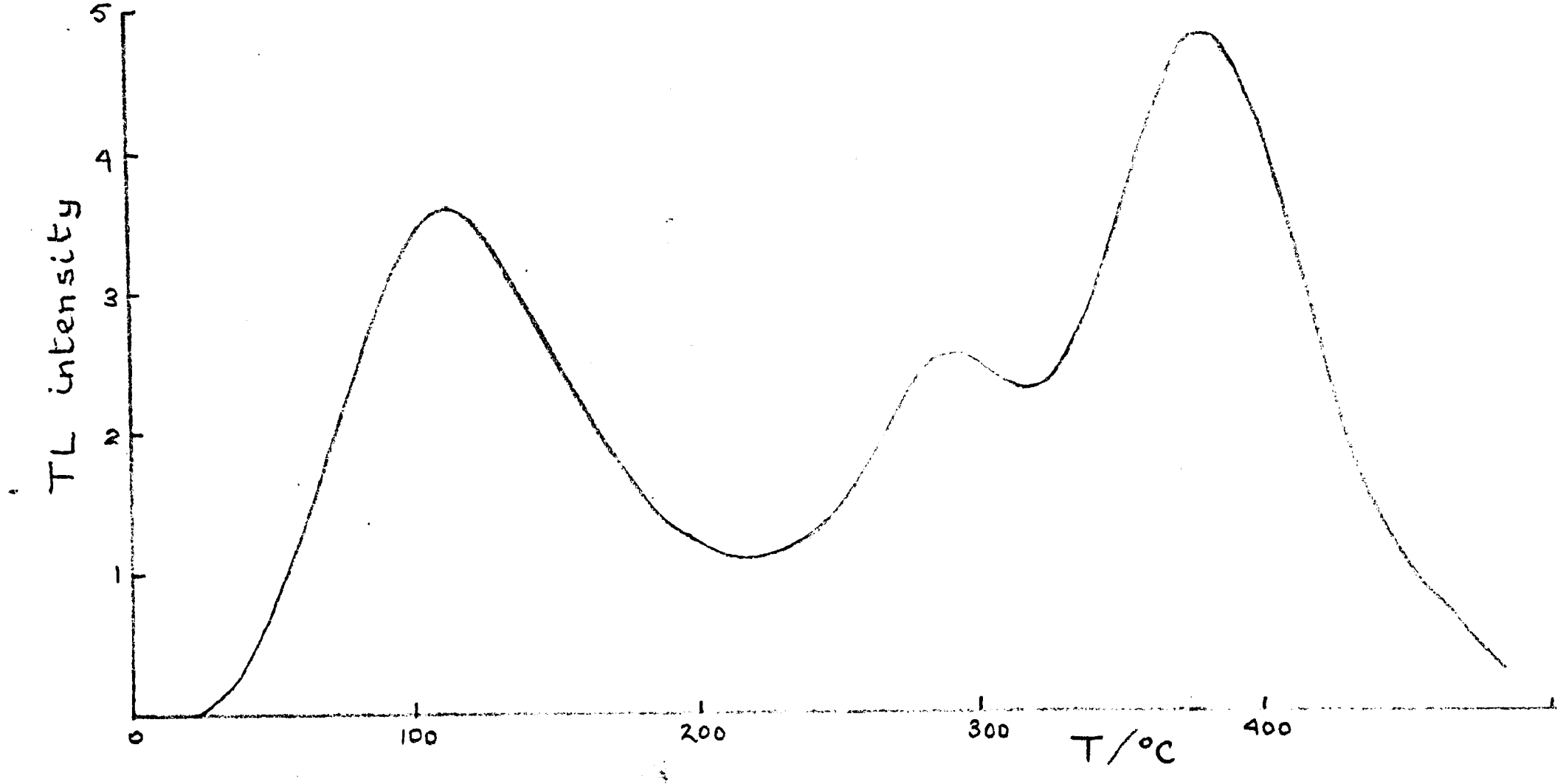

Fig. 6.9 Limestone 126 el: response to a large β dose, observed using a 5-60 blue filter and a heating rate of 6°C/sec

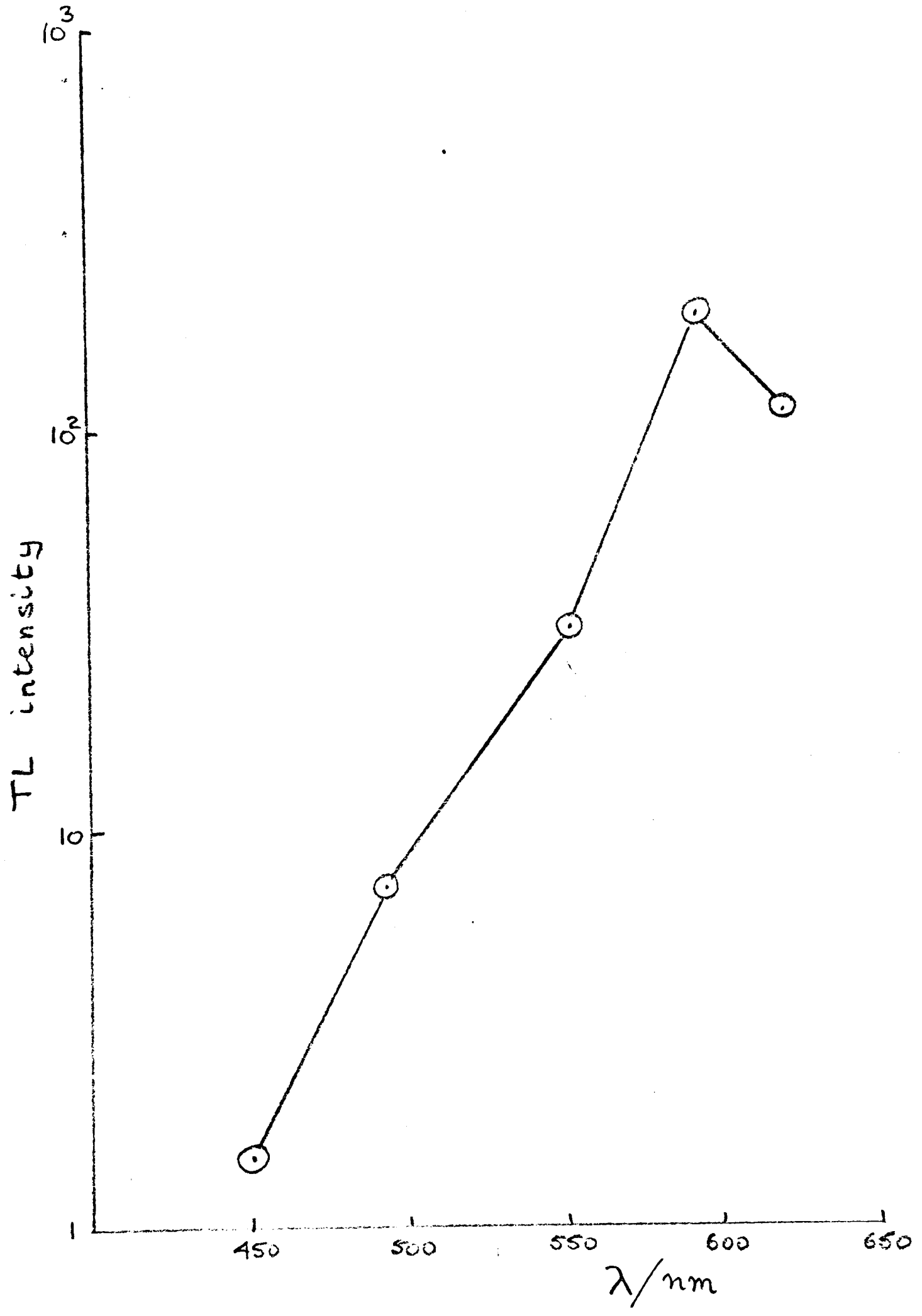

Fig. 6.10 Limestone 126 el:
luminescent emission of 230°C peak

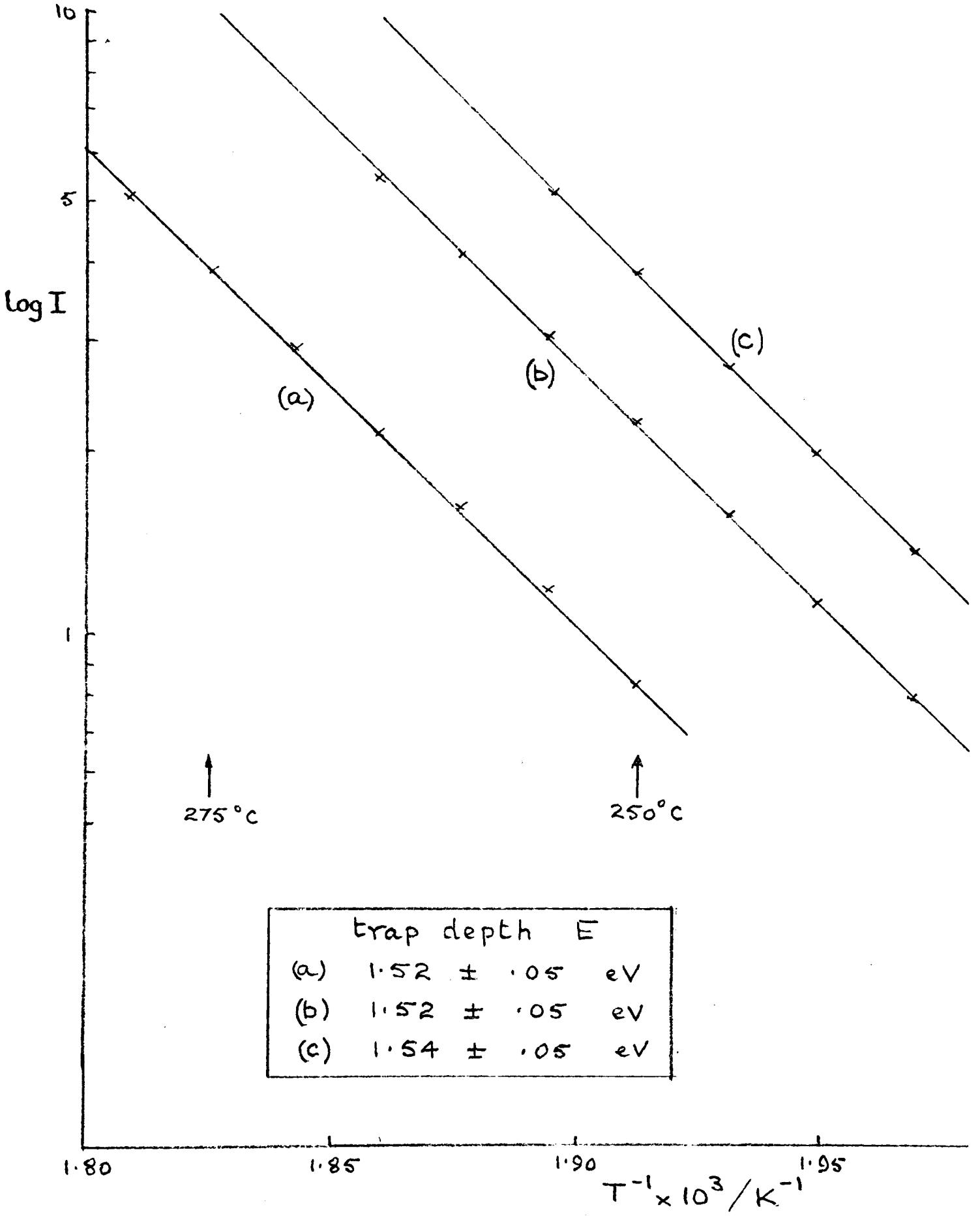

Fig. 6.11 Limestone 126 el: initial rise results for 230°C peak, heating rate 6°C/sec

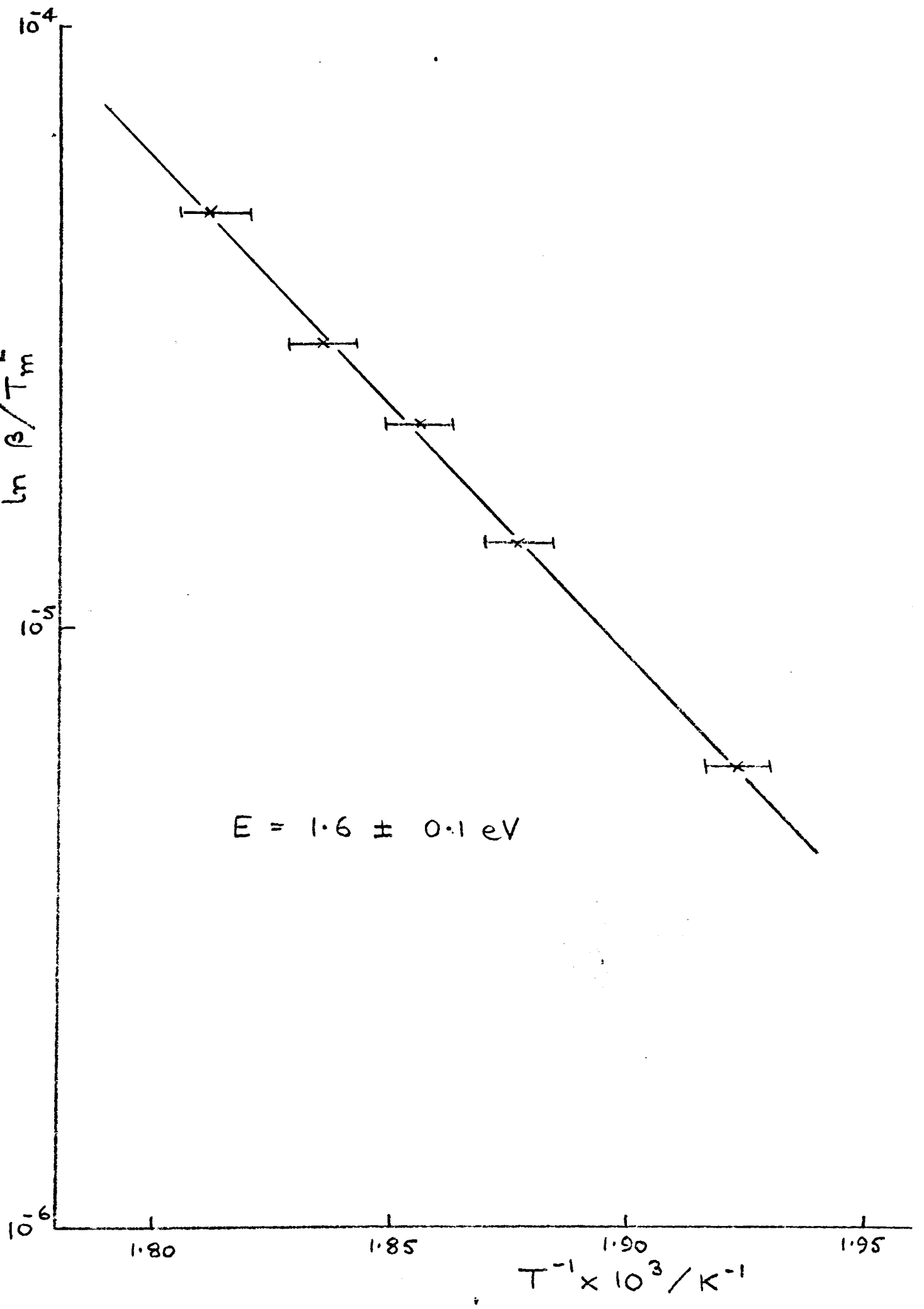

Fig. 6.12 Limestone 126 e1, 230°C peak, plot of $\ln \beta/T_m^2$ vs T^{-1}.

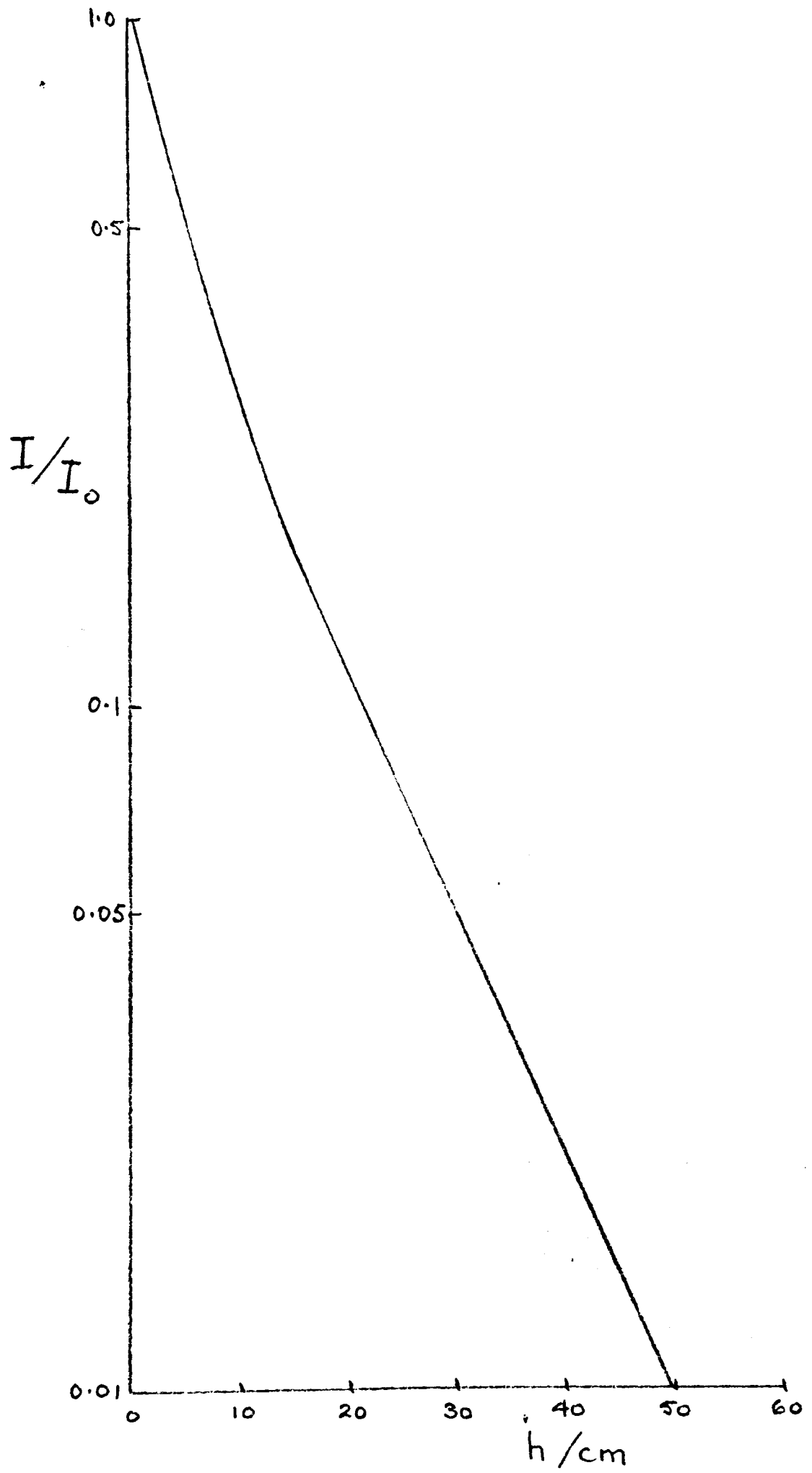

Fig. 6.13 $I/I_o = \Phi(\mu h)$ as a function of h

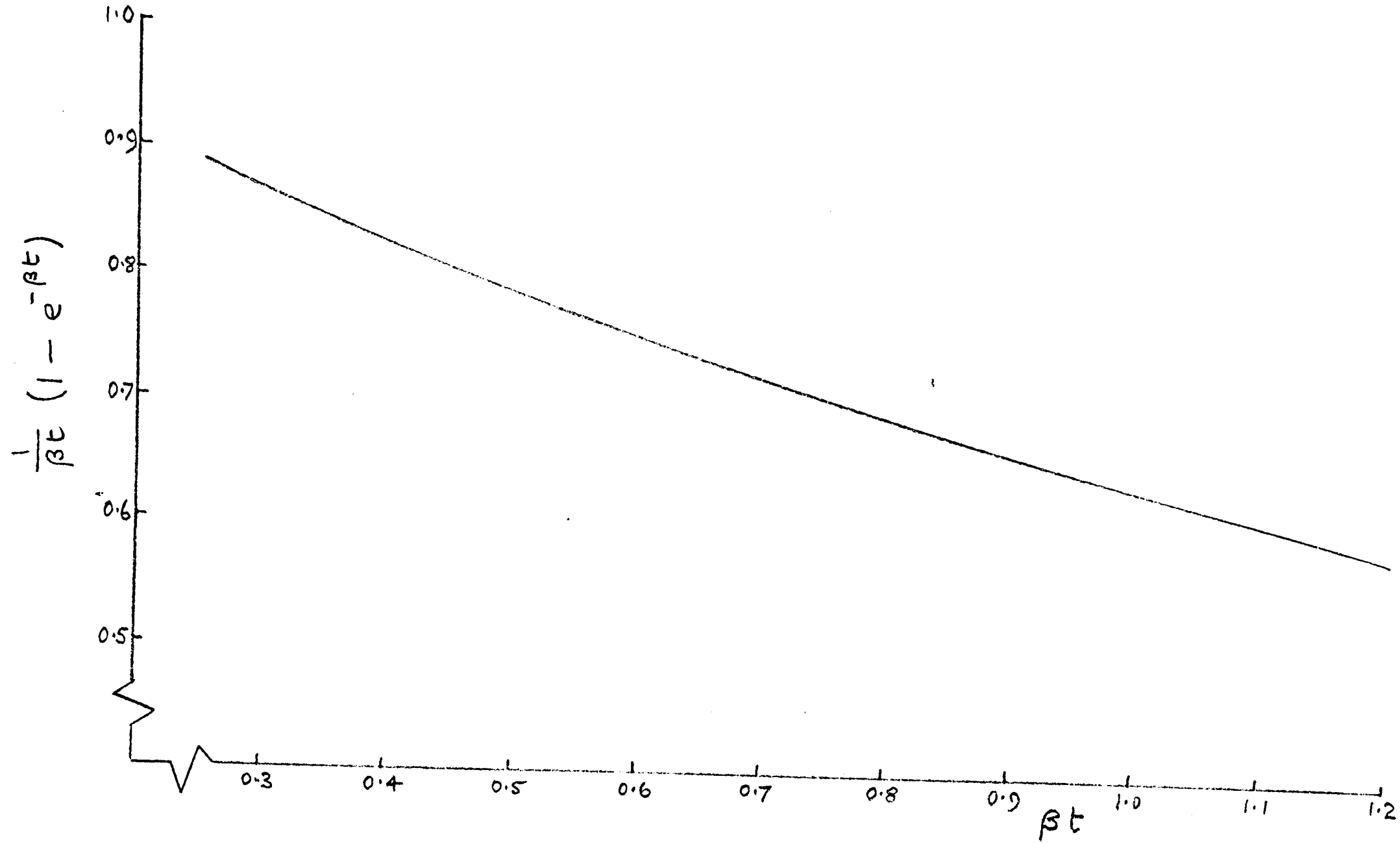

Fig. 6.14 Plot of $\frac{1}{\beta t}(1 - e^{-\beta t})$ vs βt for βt from 0.3 to 1.2

PART III

The discovery of 'anomalous fading' in lava prompted the study of a variety of TL sensitive minerals which were likely to be used for dating material of chronological importance. Various experiments were carried out to characterize the phenomenon and in spite of the complexity of naturally occurring minerals with regard to the amount and type of impurities present, an explanation of the phenomenon was sought with the aim of finding a way round the problem as regards dating.

CHAPTER 7 EXPERIMENTAL STUDY OF ANOMALOUS FADING

7.1 INTRODUCTION

Following the discovery of the short term instability of high temperature TL in the lava samples studied in Chapter 4, various minerals were acquired from Dr. F.B. Atkins of the University Museum and V. Mejdahl of the Danish Atomic Energy Commission Research Establishment, Riso. These included various feldspars, both alkali and plagioclase, zircon and apatite. These minerals are known to be amongst the most sensitive TL minerals. Feldspars have been studied with a view to their use as nuclear accident dosimeters (Ichikawa and Tanida; Ichikawa, Fukuda and Higashimura) and have also been used in the relative TL dating of pottery from Danish archaeological sites (Mejdahl). Zircon has been suggested for use in dating because of its high internal radioactivity (Zimmerman, 1971(c)) and fluorapatite was studied for the same reason.

A sample of mullite was obtained from Dr. B. Butler, Geology Department, Oxford University; it was considered of interest because it has been shown by X-ray diffraction to be the characteristic mineral in hard paste porcelains, stonewares and high fired earthenwares (Bimson). It is formed by heating clay minerals, such as the kandite and illite groups, above 1050°C. Also it can be observed under the microscope as fine needle-like crystals at glaze-body interfaces for several porcelains (Insley and Frechette) and also in fused china clay (Ford).

Norwegian α quartz (BDH chemicals) and limestone sample 126 e1 were also

tested for abnormal fading.

The results of a preliminary survey are shown in Table 7.1, where the repeatability is within ± 3%. The samples were subjected to the same procedure as the lava samples:

(i) irradiate

(ii) store in darkness at room temperature

(iii) measure TL

(iv) irradiate

(v) measure TL immediately

A $^{90}Sr/^{90}Y$ β source was used for the irradiations and doses of about 5 kilorad were given at a dose rate of about 1 kilorad/minute.

7.2 TIME DEPENDENCE

The results in Table 7.1 indicate the range of fading found in the minerals studied. About twenty different feldspar samples were tested; in five the fading was less than 5% after four weeks storage and in the remainder the behaviour was intermediate between this and the fading of the six feldspar samples quoted in the table. Because of the repeatability error of ± 5% no further experiments were carried out on the samples showing only slight fading.

In Chapters 5 and 6 the archaeologically determined electronic stability of the high temperature TL in quartz and limestone has been shown to agree with that predicted by kinetic theory and implies that no long term anomalous fading has occurred in these samples. These two samples are not discussed further in this chapter.

In Chapter 4 lava samples were irradiated and left for times up to several months at room temperature; their decay was found to be most

TABLE 7.1

ROOM TEMPERATURE FADING OF MINERALS

mineral	abscissa	TL lost	
zircon	350 °C	16% in	17 hours
apatite	400	40	15 "
mullite	400	11	12 days
Feldspars			
labradorite(i)(BA6)	350	40	15 hours
andesine(i)(BA7)	350	16	16 hours
bytownite	350	10	8 days
labradorite(ii)	350	15	7 days
andesine(ii)	350	28	17 "
sanidine	300	25	4 hours
quartz	above 350	< 3%	2 years
limestone	at 380 peak	< 3%	2 months

conveniently expressed by plotting the log of the fraction of TL left at a particular glow curve temperature versus the log of the storage time. This section describes the results of similar room temperature decay measurements carried out on particular minerals. The samples were thermally drained to remove their natural TL and 100-150 μ grains were used for the fading tests. Irradiations were carried out using a $^{90}Sr/^{90}Y$ 40 mc beta source.

(a) Plagioclase feldspar (Lab.ref. BA6)

This feldspar was described as labradorite as it had a 50% anorthite composition. A typical glow curve after artificial β irradiation is given in Fig. 7.1(a). There was no change in sensitivity with heating or pre-dose and no change in fading rate with heating and hence many measurements could be carried out on a relatively small number of samples which reduces errors occurring in normalization between samples. Typical ratio plots showing the amount of TL remaining at each glow curve abscissa after storage at a temperature of 10°C for different lengths of time are shown in Fig. 7.1(b). Below 150°C the ratio drops sharply to zero due to the thermal emptying of the low temperature traps as expected (see Chapter 3). Figs. 7.2(a) and 7.2(b) show the decay of the 300°C glow curve ordinate at 10°C; Fig. 7.2(a) suggests that the decay may be made up of a few discrete exponential decays, but this information is obscured in Fig. 7.2(b) where log(% TL left) versus log t is plotted, as was done for the lava samples.

(b) Plagioclase feldspar (Lab.ref. BA7)

This sample had a 43% anorthite composition and was therefore considered to be andesine. It also showed rapid fading and a plot of the % TL left at each temperature abscissa after 10 days storage at 10°C is given in Fig. 7.3(b); the plateau given above the 250°C abscissa is even better

than that for feldspar BA6. The decay over fifteen days is shown on a log-log plot in Fig. 7.3(c).

(c) Fluorapatite $Ca_{10}(PO_4)_6F_2$

A typical glow curve after an artificial β irradiation of 500 rads is shown in Fig. 7.4(a); an optical system favouring the blue part of the spectrum (PM EMI 9635 + Chance-Pilkington HA-3 + Corning 5-60) was used so that the response to thermal radiation was low and hence the glow curve could be studied up to 450°C . The fading at 10°C storage temperature is shown in Fig. 7.4(b). Fading of the 270°C peak is shown as a function of t and log (t) in Figs. 7.5(a) and (b).

(d) Zircon $ZrSiO_4$

A typical glow curve is shown in Fig. 7.6(a); the optical system has no colour filter and the high temperature thermal radiation has been subtracted. Unlike the previous three samples there appears to be no further fading at the 300°C abscissa after 100 hours storage at 10°C.

(e) Mullite $3Al_2O_3.2SiO_2$

A typical glow curve is shown in Fig. 7.7(a) and Fig. 7.7(b) shows the fading for TL above the 250°C abscissa due to storage at 10°C. The long term fading is shown in Fig. 7.7(c).

These five samples show that anomalous fading occurs in several different minerals. There is no significant correlation with glow curve shape; fading takes place throughout the glow curve and in some cases is such that a good plateau is given even though there has been 30% loss in only 10 days e.g. Fig. 7.3(a). This means that the 'plateau test' as has been applied to archaeological specimens is not a sufficient criterion for the stability of the trapped electrons that give rise to high temperature TL.

The form of the loss at any particular abscissa appears to be caused by a sum of several exponential decays; although this was only clearly demonstrated for feldspar BA6.

7.3 TEMPERATURE DEPENDENCE

In an attempt to remove the unstable electrons so that dating would be possible, the effect of increasing the storage temperature was studied and in the case of one sample, feldspar BA6, an activation energy for the initial exponential fading was obtained. However, the breakdown of this exponential temperature dependence was found for storage at very low temperatures.

(a) Plagioclase feldspar (BA6)

Samples were irradiated at a given temperature and then held at that temperature for various lengths of time before the glow curve was measured. A check was made between each measurement to ensure that no change in sensitivity had occurred. This involved a similar irradiation followed by taking an immediate glow curve.

Because the fading was not a single exponential decay as was demonstrated in Fig. 7.2(a), two methods of determining an effective activation energy E were used, assuming a relationship of the form

$$\tau^{-1} = A \exp(-E/kT) \qquad (7.1)$$

where A has the dimensions of $[T^{-1}]$ and T is the storage temperature. Firstly the time τ^1 taken to obtain 22% fading at the 300°C glow curve ordinate was obtained for four different temperatures. These are given in Fig. 7.8; the slope of the curve gives E = 0.19 ± .01 eV. The error bars represent a ± 2°C uncertainty in the storage temperature and a ± 5% error on τ^1.

TABLE 7.2

Times needed to give 22% loss of TL at 300 °C ordinate for different storage temperatures for feldspar BA6

Time	Storage Temperature/°C
$2\frac{3}{4}$ hours	- 18
$1\frac{1}{4}$ hours	10
30 mins	45
5 mins	157

TABLE 7.3

Half lives of the initial fast decay in feldspar BA6 as a function of storage temperature;

Half life $\tau\frac{1}{2}$/mins	Storage Temperature/°C
45	10
18	45
3	157

More detailed curves were obtained for the decays at 10°C, 45°C and 157°C, e.g. Fig. 7.9; they were analysed as being due to the sum of three components, one having a very long mean life which made up 36% of the total TL, one having an intermediate mean life and being 31% of the total TL and the third decaying rapidly and making up 33% of the total TL. The half lives obtained for the fastest fading component are given in Table 7.3 and log $\tau_{\frac{1}{2}}$ versus T^{-1} is plotted in Fig. 7.8(b); the activation energy is 0.19 ± .01 eV. Extrapolation of the curve back to $T^{-1} = 0$, gives an intercept $A \approx 1\ sec^{-1}$. A plot of log $\tau_{\frac{1}{2}}$ versus T^{-1} is shown for the second component in Fig. 7.10; the activation energy obtained from the slope of the plot is 0.31 ± .01 eV. In section 7.4 these values of activation energy are compared with that obtained by the initial rise method.

Extrapolation of log $\tau_{\frac{1}{2}}$ versus T^{-1} for the initial decay implies that at 77K the half life should be about 10^{12} minutes i.e. ~ 10^{6} year. To check whether such an extrapolation is valid, some samples in aluminium dishes, 1 cm diameter, were irradiated at room temperature and immediately placed in an aluminium capsule fastened to a German silver hollow rod to reduce conduction of heat to the sample. The capsule was then immersed in liquid nitrogen (77K). The total handling time at room temperature was less than two minutes after a one minute irradiation. The decay at -196°C, i.e. 77K, is shown in Fig. 7.11 along with those at 10°C and 45°C. The time taken to reach a 22% loss at 77K is about 10 hours.

Such a disagreement between the predicted half life at 77K and that observed experimentally implies that the simple exponential decays no longer hold. This was checked by storing samples in liquid hydrogen (20K) for 190 hours, facilities being provided by Dr. H. Rosenberg of the Clarendon Laboratory; if the simple exponential relationship was still holding then

the half life at 20K should be 40 orders of magnitude longer than that at 77K. The fading in 190 hours at 20K was found to be 28 ± 4% i.e. not significantly different from that at 77K. The exponential relationship appears to break down at some temperature between 77K and 255K, though it appears to be valid between 255K and 430K.

(b) Fluorapatite - low temperature oven

Similar isothermal decay experiments were carried out on samples of fluorapatite. No exponential analysis was possible, but the decay of the TL at the 400°C abscissa during storage at 10°C and 100°C is shown in Fig. 7.12. If, as for feldspar BA6, a plot is made of the time taken for there to be 75% TL left at the 400°C abscissa versus reciprocal temperature then an activation energy of 0.21 ± .01 eV is obtained from the slope and a time of 500 ± 30 hours is predicted for storage at -100°C, Fig. 7.13.

Because the peak structure between 100°C and 300°C of fluorapatite is relatively well defined, a special oven was designed to allow irradiation and storage at -100°C, Fig. 7.14. The oven itself was made of Permali, a relatively poor heat conductor and a good electrical insulator. A conventional nichrome heater plate was attached to two copper blocks which were immersed in a tank of liquid nitrogen. The heater leads, fitted with giant crocodile clips were in place only whilst taking a glow curve to minimise heat loss and were clipped on to soft lead terminals. The photomultiplier tube was also only in position during a glow curve and the oven was for the rest of the time blanked off to prevent ice forming on the sample. Dry nitrogen was passed continuously through the oven. The oven and the liquid nitrogen reservoir were surrounded by blocks of expanded polystyrene and spaces were filled in with expanded vermiculite. In spite of this there was considerable heat loss and a temperature of 173K could only be maintained

for a few hours.

Five hour fading experiments were carried out on fluorapatite samples which were irradiated and then held at 173K. Repeatability was not good because ice on the lead terminals prevented good electrical contact; however, for 5 hour storage there was fading of 20 ± 10% throughout the glow curve above 50°C . This means that, as for feldspar BA6, the exponential temperature dependence above room temperature breaks down at low temperatures. A more detailed study of the deviation would need the construction of a more complicated oven specifically designed for use down to 77K.

7.4 COMPARISON OF ISOTHERMAL DECAY DETERMINATION OF THE ACTIVATION ENERGY AND THAT DETERMINED BY THE INITIAL RISE METHOD

In the previous section two activation energies 0.19 ± .01 eV and 0.31 ± .01 eV were obtained from isothermal decay measurements on feldspar BA6 at storage temperatures well below the peak. The activation energy for the untrapping of an electron at a temperature near to the peak was studied using the initial rise method of trap depth determination as described in Chapter 3. The sample was given a 30 krad β dose and then alternately heated and cooled in 15°C steps between 100°C and 350°C. For each initial rise curve a plot of log I versus T^{-1} was made e.g. Fig. 7.15, and the values of E obtained for each curve are shown as a function of temperature in Fig. 7.16(a); the temperature at which a peak would occur in a glow curve is about 50°C above the measurement temperature. Above 200°C the trap depths are about 1.6 ± .2 eV and this is consistent with traps that empty above 250°C . It is very different however to the activation energies of 0.19 and 0.31 eV determined by isothermal decay in the previous

section.

In Chapter 5 thermal quenching was shown to upset initial rise measurements in quartz. To check whether this was happening in feldspar BA6, the prompt luminescence during β irradiation was observed as a function of temperature, Fig. 7.16(b). There is a slight decrease in the intensity with increasing temperature but there is not the characteristic sharp decrease as was found for quartz. Hence the values of E determined by the initial rise method were considered correct. No check could be made using first order kinetic techniques as the peaks were far too broad.

7.5 DEPENDENCE ON GLOW CURVE ABSCISSA

Fading is characterised by loss of TL right through the glow curve above the abscissa at which there should be no loss of TL due to thermal emptying of traps. Looking at Figs. 7.1, 7.3(a), 7.4, 7.6, 7.7 and the similar curves obtained for lavas in Chapter 4, there is no apparent correlation between the shape of the glow curve i.e. the distribution of traps, and the rate or amount of anomalous fading in the high temperature part of the glow curve.

One thing that can be noted is the fact that in some cases the fading is the same at each glow curve ordinate e.g. Figs. 7.3(a) and 7.7, for short term laboratory fading tests. If this was true over archaeological or geological time, such samples would give rise to plateaux and would normally be considered suitable for dating. An example of such behaviour occurs in lava 129 e15 which gave a low age and showed short term fading in spite of passing the plateau test.

Other samples show different rates of fading at different glow curve abscissae e.g. Fig. 7.4, and the other lava samples. Such behaviour, where the TL at lower abscissae fades faster, destroys the plateau and such samples

would normally be rejected from a dating programme for this reason. More unusual behaviour is shown by feldspar BA6, Fig. 7.1, where the TL at 180°C appears less susceptible to fading than that at 300°C.

7.6 WAVELENGTH DEPENDENCE

Having been unable to show any positive correlation with glow curve shape, i.e. with particular electron traps, the question of whether only particular luminescence centres are involved must be looked at. To facilitate this study the emission spectra of several minerals that showed short term fading were obtained at different glow curve abscissae.

(a) Feldspar BA6

The spectrum of the TL at the 300°C glow curve abscissa was obtained using the filtrometer (Appendix Bi), Fig. 7.17, and the maximum emission was seen to be about 400 nm. The spectrum of the 100°C peak is also shown and this is slightly more green; the emissions are normalized. A spectrum was also obtained for the 300°C abscissa of a sample that had been left to fade for 21 hours at room temperature and had lost 45% of its TL at that abscissa; the spectrum was the same as that shown for the unfaded sample within the experimental error of ± 5%.

(b) Fluorapatite

The immediate glow curve after a 500 rad β dose shown in Fig. 7.4(a) has peaks at 100°C, 200°C and 270°C and their relative emission spectra are shown in Fig. 7.18. The 100°C peak is seen to have its main emission at a wavelength greater than 500 nm, whereas the 200°C and 270°C peaks also have a significant emission around 380 nm.

It is of interest to note that Mn and rare earth ions substituting for Ca are considered to give rise to the luminescence spectra of natural

apatites (Portnov and Gorobets; Mitchell and McGavock). Portnov and Gorobets found that some apatites showed a broad luminescence peaking in the yellow at 580 nm which was very similar to that in synthetic apatite doped with Mn^{2+}. This could be the luminescence centre connected with the 100°C peak. The violet peak could be caused by Ce^{3+} which gives a broad peak centred at 365 nm but without a detailed luminescence spectrum it is impossible to say.

Fading tests were then repeated using an optical system biased towards the yellow emission, EMI PM tube 6255 + Corning (4-96). Within the experimental repeatability of ± 5% the fading loss was the same as for the violet emission observed in section 7.2. Also when the fading above 50°C was observed using the low temperature oven, the fading was the same at 100°C as at 300°C. This implies that the fading is not connected with any particular luminescence centre.

(c) Zircon

The emission spectrum of the high temperature TL in the region of the 280°C peak was studied using both the filtrometer and a Bausch and Lomb spectrometer (used at the University of Sussex with the assistance of Dr. P.D. Townsend - Appendix Bii). The two spectra are shown in Fig. 7.19. It can be seen that using the filtrometer the peak at 480 nm dominates the spectrum whereas the spectrometer shows the presence of a discrete emission peak at 575 nm; the resolution was 15 nm.

7.7 TO DETERMINE WHETHER THE FADING PROCESS IS RADIATIVE

In order to find out whether the fading takes place radiatively or non-radiatively, the phosphorescence from three fast fading minerals was observed continuously during the initial fading period. The modified

optical system, but without the colour filter described in Chapter 4, was used in conjunction with a 'photon integrator' so that the background pulses were less than 1% of the expected phosphorescence.

Each sample was given a 5 krad β dose, thermally washed at 150°C for 5 minutes to remove the electrons trapped in shallow traps that would otherwise empty thermally during the observation period and give rise to luminescence. The sample was then cooled and held at 10°C whilst fading occurred. The TL was then measured with the same optical system in the usual way and compared with a monitor glow curve for the same sample which had undergone similar thermal washing but had not been stored. The number of pulses equivalent to the difference between the TL glow curves was then compared with the total number of pulses above the dark current counted during the period of storage at 10°C. The results are given in Table 7.4. In all cases the phosphorescence was found to be not more than 5% of the TL lost due to storage i.e. the fading is predominantly non-radiative.

Earlier attemps to observe phosphorescence with an unmodified optical system were inconclusive as the level of tube noise was comparable with the phosphorescence being observed. Also the larger doses given by a Co-60 γ beam at the Department of Biochemistry, Oxford being used to overcome this, caused sensitivity changes which upset the comparative TL measurements and they were not accurately reproducible.

It is in fact most likely that the fading process is totally non-radiative; the phosphorescence observed could be due to insufficient thermal washing. It must be emphasised that the term non-radiative means that no luminescence is seen in the region of photomultiplier sensitivity i.e. 300 nm - 550 nm; a longer wavelength emission is not ruled out.

TABLE 7.4

COMPARISON OF TL LOST DURING FADING

WITH THE TOTAL PHOSPHORESCENCE, ϕ ,

OBSERVED DURING THE PERIOD OF STORAGE

	TL lost (pulses)	ϕ (pulses)	ϕ/TL lost/%
fluorapatite	1.4×10^5	1.4×10^3	1
BA 6	10^5	5×10^3	5
Sanidine	1.5×10^6	6×10^3	0.4
Mullite	2×10^5	10×10^3	5

7.8 DEPENDENCE ON TYPE OF RADIATION

In many thermoluminescent phenomena e.g. the form of the TL growth curve, different types of ionizing radiation have different effects; for example the effective sensitivity of a given material is the same for β and γ radiation but is about an order of magnitude less for α irradiated samples. This has been explained by considering an α-track to have a core which is in saturation (Zimmerman, 1972). If the fading is increased by the mutual proximity of filled traps and centres (to each other), then it would be expected that the rates and perhaps the extent of the fading would be affected by using α irradiation instead of β irradiation.

Fine grains (1-8 μ) were deposited on aluminium discs and fading experiments using α, β and γ irradiations similar in dose rate and total dose were carried out. For mullite the α and β decay measurements were within 5% of each other but it is worth noting that the α irradiated discs seemed to have faded somewhat more over the whole range of storage times. Similar results were obtained for other minerals and a typical result is shown in Fig. 7.20 in this case for an orthoclase feldspar (Lab.ref. Z1), $KAlSi_3O_8$. It fades more slowly than the other minerals discussed; this means there is little loss of trapped electrons during the 15 minute journey from the Co-60 γ source in the Biochemistry Department. Given the experimental reproducibility is $\pm$ 5% there is not a significant difference between the rate of decay of the α irradiated samples and those irradiated by β or γ irradiation. To check that the initial decay of the α irradiated sample has not been increased so much that it takes place before even the monitor glow curve can be taken, the α sensitivity was looked at and found to be about 0.1 x the β sensitivity. This is about the value for the high temperature TL in non-fading minerals

(e.g. quartz and limestone) and hence it is unlikely that any very rapid fading of the α irradiated samples has occurred.

7.9 DOSE DEPENDENCE AND DOSE-RATE DEPENDENCE

Having observed a slightly faster decay for an α irradiated than for β and γ irradiated samples, an experiment was set up to observe the fading in a large single crystal of fluorapatite after a 1 Mrad dose of X-rays. The dose was given using a source of primary X-rays with a filament current of 30 mA and voltage of 50 kV with the sample at a distance of 1 cm from the collimator to provide uniform irradiation. The optimum position was checked by exposing pieces of film at various distances from the collimator. The exposure lasted 5 minutes so that the results could be compared with the fading after 500 rad β irradiations also given in 5 minutes to the same sample. The resulting decay curves are shown in Fig. 7.21; the fading is slightly faster for the heavily irradiated sample.

This could be due to either a total dose or a dose rate effect, but as all irradiations have to be carried out in an identical time period, so that the effect of fading during irradiation is the same, the difference cannot be determined. This is also true for the alpha irradiation experiments since, although the effective total dose is the same as for the beta irradiation, the centre of the track is in fact in saturation.

7.10 THE EFFECT OF IR ON FADING

In an attempt to remove the fading component so that dating would be made possible, the effect of exposing a freshly irradiated sample to infrared radiation of the appropriate energy was considered. For a thermal activation energy of 0.2 eV, the associated wavelength needed to optically

activate the electron is likely to be about 2 μ and certainly less than 6 μ i.e. in the near infra-red.

Freshly β irradiated samples were placed under a IR lamp (Philips 300E/479 Infraglow) which has the spectrum shown in Fig. 7.22. The samples were contained in small aluminium planchettes which could be transferred directly to the heater plate in the TL glow oven. Half the samples were exposed directly to the lamp at a distance of 30 cm; the others were shielded by aluminium discs. The samples were placed close together on an aluminium sheet to ensure that the planchettes were at the same temperature. Fig. 7.23 shows the TL remaining for each type compared with that stored in the dark at 10°C. The shielded sample seemed to have reached a higher temperature, as is shown by the greater loss of TL below 200°C, than the unshielded sample but the latter has a greater loss of TL between 200°C and 300°C.

This suggests that the unstable TL might be removed by appropriate wavelength IR but more systematic bleaching experiments using an IR monochromator would be necessary to do this efficiently.

7.11 THE EFFECT OF AN APPLIED ELECTRIC FIELD

Another attempt to enhance the fading rate was made by applying a high field across a sample to try and distort the potential wells in the region of the traps and luminescent centres. This has been seen to enhance phosphorescence in organic materials in which a similar decay is taking place (A. Charlesby, personal communication).

A modification was made to the TL glow oven so that an electric field could be applied to the sample in situ, Fig. 7.24. An evacuated chamber was constructed so that a pressure of $< 10^{-2}$ torr could be maintained whilst

a voltage of 3 kV supplied by a Brandenburg EHT unit was applied. The sample of fluorapatite fine grains, 1-8 μ diameter, was deposited on a 1 cm diameter aluminium disc. The disc was placed on the glow oven heater plate which was earthed and a brass electrode 1 cm in diameter was placed on a piece of 25 μ thick Melinex on top of the grains. The Melinex had a specified dielectric strength of 3×10^6 volts/cm. No change in either the rate or extent of fading was noticed.

However because the dielectric constant of the fluorapatite is not known, the strength of the field across the actual grains was not known and might not have reached the 10^5 volts/cm considered likely to be capable of distorting the field in the lattice of the fluorapatite grains.

7.12 THE EFFECT OF FIRING AT 950°C

As all the experiments described so far have been carried out on geological samples, some minerals were fired in air in a furnace at 950°C for three days to simulate an archaeological firing. The results are seen in Table 7.5. In most cases the fading rates have changed but we must also note that the glow curve shape has also changed. Sanidine is the only mineral showing an increase in fading after its firing. Fig. 7.23 shows the rate of fading in fluorapatite before and after firing; it must be noted that there was no definable change in the shape of the decay curves for the two sets of measurements.

It seems then that the lack of evidence (in the form of low dates) for fading in pottery may be due to the heating that took place when it was archaeologically fired but is just as likely to be due to the lack of fading that would have occurred in the original minerals from which the pot was made.

TABLE 7.5

CHANGES IN ROOM TEMPERATURE FADING DUE TO 950 ^{o}C FIRING

Mineral	Ordinate/^{o}C	Storage Time	% TL lost Unfired	% TL lost fired	Shape change
zircon	350	17 hrs	16	12	yes
fluorapatite	400	15 hrs	40	22	yes
sanidine	300	4 hrs	25	50	yes
labradorite BA6	350	1 day	48	6	yes
mullite	400	3 days	10	10	no

7.13 THE EFFECT OF RECRYSTALLIZATION

In a final attempt to change the fading characteristics of various minerals, three fading minerals were recrystallized after being subject to a pressure of 1 kilobar at a temperature of 830°C for 3 days. The samples were heated in gold capsules to prevent contamination. They were cooled to 25°C within about 2 minutes, the first 100°C drop occurring in about 5 seconds. Two samples of each mineral were prepared, one dry and one with water vapour present; there was no difference between the results for the two treatments. The recrystallization was carried out by Graham Norris of the Department of Geology, Manchester University.

The samples studied were labradorite BA6, sanidine and orthoclase; the latter recrystallized as sanidine, as could be seen from the glow curve and as was verified by X-ray diffraction. The results on the other two minerals are given in Table 7.6. The labradorite fades at a slower rate and to a lesser extent after recrystallization; the sanidine also fades at a slower rate.

Three feldspars (126f) were obtained from non-volcanic deposits in Scandanavia by V. Mejdahl and they showed less than 5% fading in two months storage at room temperature. They were recrystallized under similar conditions and tests showed that the fading of the recrystallized samples in the same period was also less than 5%.

7.14 CONCLUSIONS

Anomalous fading in the region of the high temperature TL was found to be present in many different minerals, with the exception of quartz and limestone. In this chapter the results of various experiments designed to elucidate the nature of the phenomenon have been described and the results

TABLE 7.6

COMPARISON OF UNFIRED AND RECRYSTALLIZED MINERAL RT FADING

		% TL lost at 350 °C ordinate	
Mineral	time stored	unfired	recrystallized
labradorite BA6	24 hours	48	25
	170 hours	57	27
sanidine	24 hours	70	27
	170 hours	-	46

are summarized below -

(a) The fading is characterized by a loss of TL throughout the glow curve; consequently the occurrence of fading in a sample for dating is not necessarily shown up by the plateau test. There does not appear to be any correlation with either glow curve shape or any particular luminescence centre; there was no change in the spectrum after fading had occurred.

(b) For one particular mineral (feldspar BA6) the temperature dependence of the fading was found to have an activation energy of about 0.2 eV, whereas the activation energy obtained from glow curve analysis was 1.6 eV. This suggests that the mechanism involved in the untrapping of an electron during fading is different to that during a glow curve.

Because the low activation energy of fading makes the process relatively insensitive to storage temperature, it is difficult to achieve the removal of all the fading components by thermal washing in a conveniently short time without serious thermal drainage. Since at 157°C the first component has a half life of 4 minutes and the second component has a half life of about an hour (Figs. 7.8(b) and 7.10), these components could be eliminated by storage at this temperature for several hours but one can never be sure that the remaining component that had been considered stable is in fact so and does not have a mean life that is not obtainable from a laboratory experiment but is still important in the decay of the natural TL. Such comments are even more pertinent to materials where the decay is less susceptible to analysis.

Results of section 7.3 also showed that the simple exponential temperature dependence, that held over the temperature region -18°C to 157°C, no longer held when experiments were carried out at 77K and 20K.

(c) For the four most rapidly fading minerals the fading at room temperature

was found to be non-radiative in the visible part of the spectrum.

(d) Fading still occurred in samples that had been heated at 950°C in air and also in some that had been recrystallized; although the fading was not removed by these treatments it was noted that in three cases out of four the fading was reduced after heat treatment.

(e) There was a slight dependence on either total dose or dose-rate.

(f) Attempts to accelerate the fading by means of an applied electric field were not successful, but there was some indication that it can be accelerated by application of IR radiation.

(g) Although it was not specifically discussed earlier, it is to be noted that no apparent correlation was found between fading and the intrinsic luminescent sensitivity. The high temperature TL of quartz and most of the feldspars, e.g. BA6 and those from the lavas studied in Chapter 4, were considered to have relatively low TL response to a given β dose; on the other hand limestone, sanidine (which faded very rapidly), and feldspars 126f (which showed negligible fading) were considered to be several times more sensitive.

7.15 IMPLICATIONS FOR POTTERY DATING

As much of the TL from fine grains used in the dating of pottery is thought to be from feldspars, the question as to whether fading has occurred in pottery samples must be reconsidered. The first criterion that must still be satisfied before the dating is accepted as reliable is whether the high temperature TL satisfies the plateau test. However the nature of anomalous fading as established in this chapter has shown that this is not a sufficient test of the electronic stability.

A series of tests designed to look specifically for fading are now also

used routinely for all pottery submitted to this laboratory for dating by the fine grain technique. The procedure is laid out in Table 7.7; the natural high temperature TL is used if necessary to normalize the results of the second glow measurements. The two delayed measurements (2) and (3) are then compared with the immediate measurement obtained for disc (1); if there is more than 10% loss in the high temperature TL of either (2) or (3) the sherd is rejected from the dating programme. In most cases it has been found that the fading shown by (2) and (3) are not significantly different (personal communication, E. Whittle and S.J. Fleming). This might suggest that there exists a short term fading component only, in which case dating could be carried out after making allowance for it. However, there is not sufficient accumulated experience of work carried out on pottery to allow such corrections to be made.

There is also uncertainty as to whether the fading tests should be carried out on a sample that has been thermally drained of its natural TL in taking the initial glow curve or whether fading should be looked for in the TL induced by an additional β irradiation in a sample that has not been thermally drained. There is evidence that the fading differs for the two different sets of measurements (personal communication, S.G.E. Bowman). The above systematic tests on fine grain pottery samples are also complicated by supralinearity and sensitivity changes due to heating.

TABLE 7.7

PROCEDURE FOR CHECKING FOR ANOMALOUS FADING IN POTTERY SAMPLES

	DISC 1	DISC 2	DISC 3
1.	glow out natural	glow out natural	glow out natural
2.	β irradiate	β irradiate	β irradiate
3.	glow immediately	store overnight	store for 2 months
4.		glow	glow

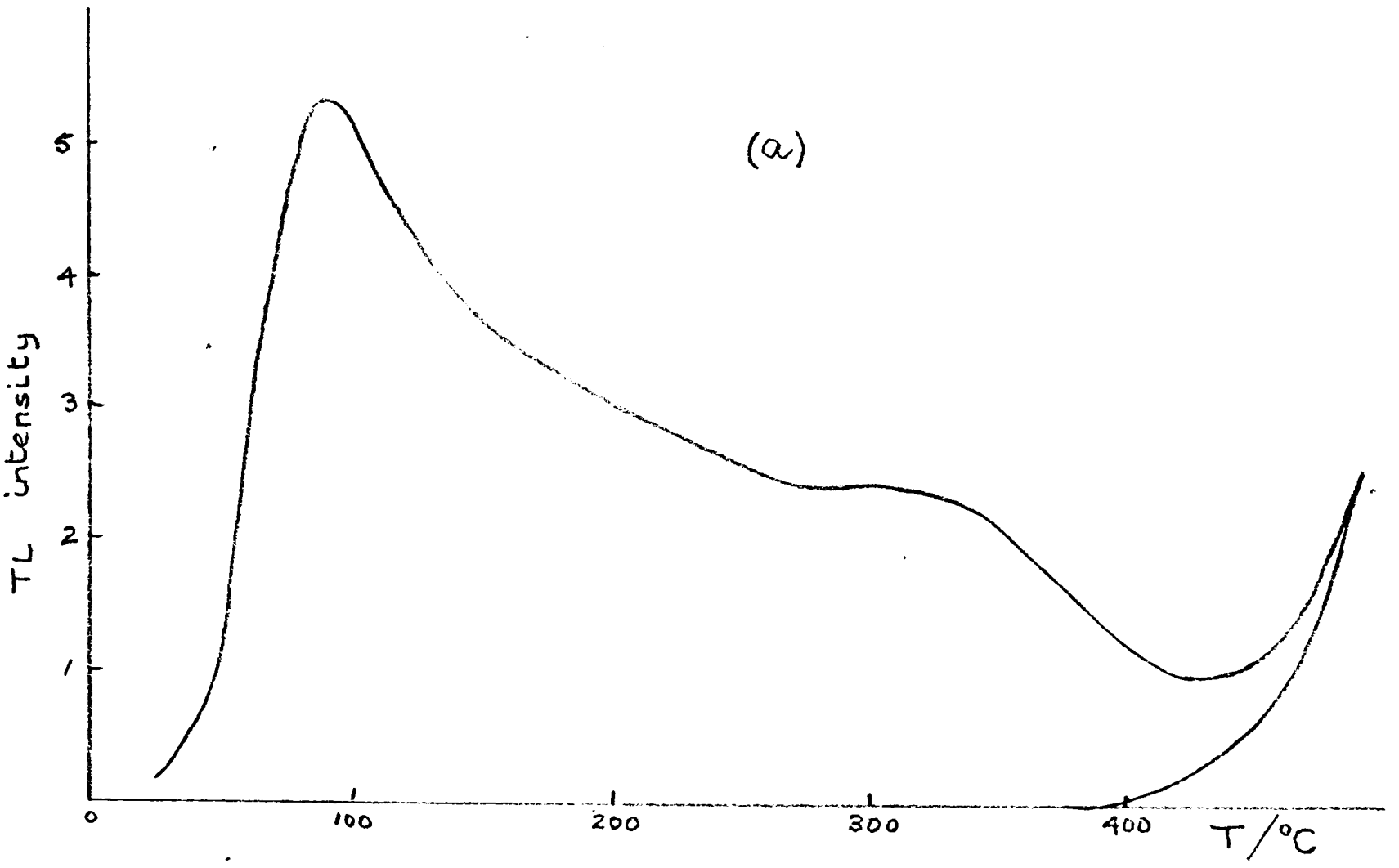

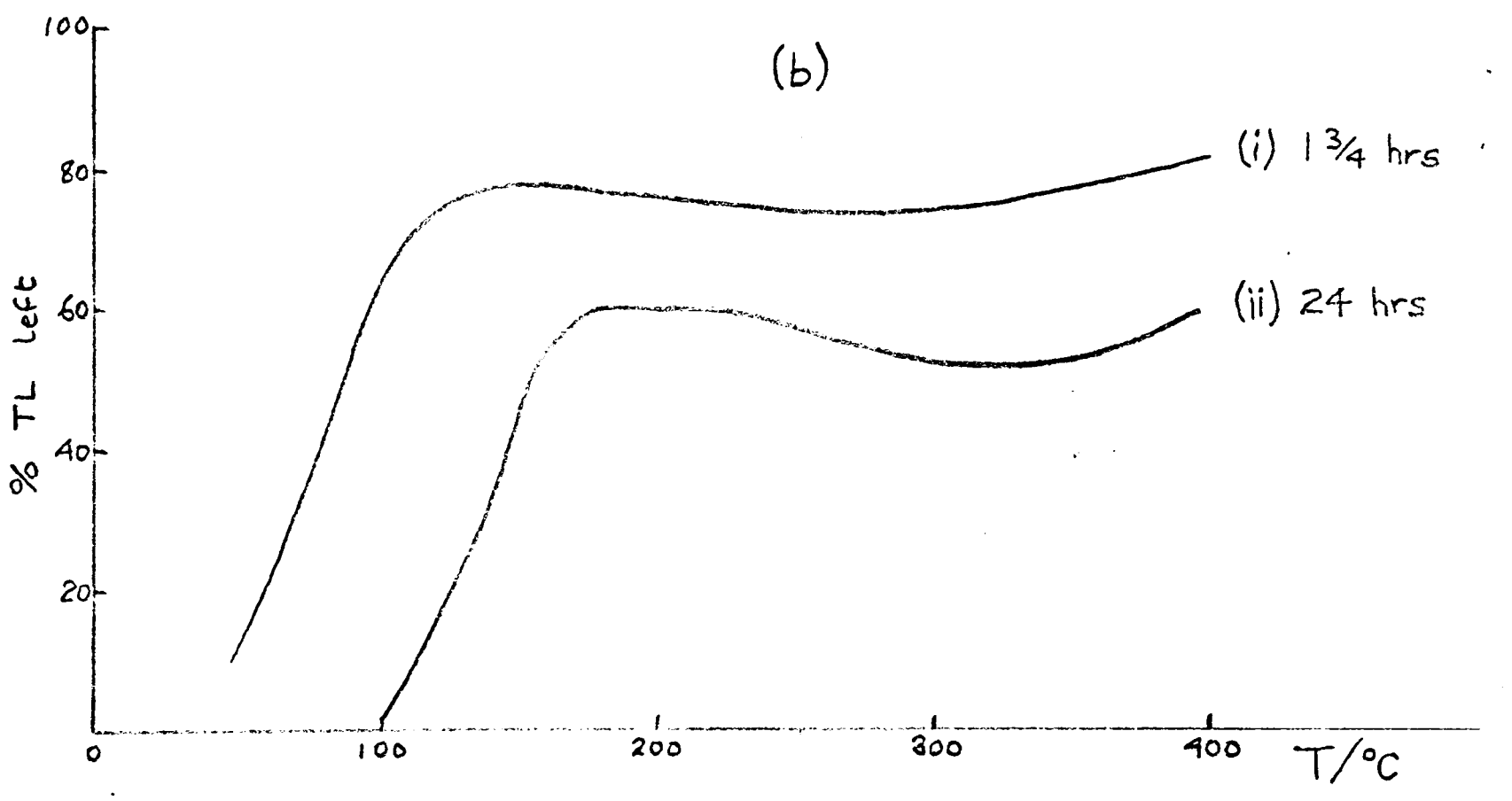

Fig. 7.1 Labradorite (BA6)

(a) TL glow curve after artificial β irradiation
(heating rate 6°C/s, PM EMI 9635, filters HA3 + 7.59)

(b) % TL left after storage at 10°C,
(i) for $1\frac{3}{4}$ hours, (ii) for 24 hours

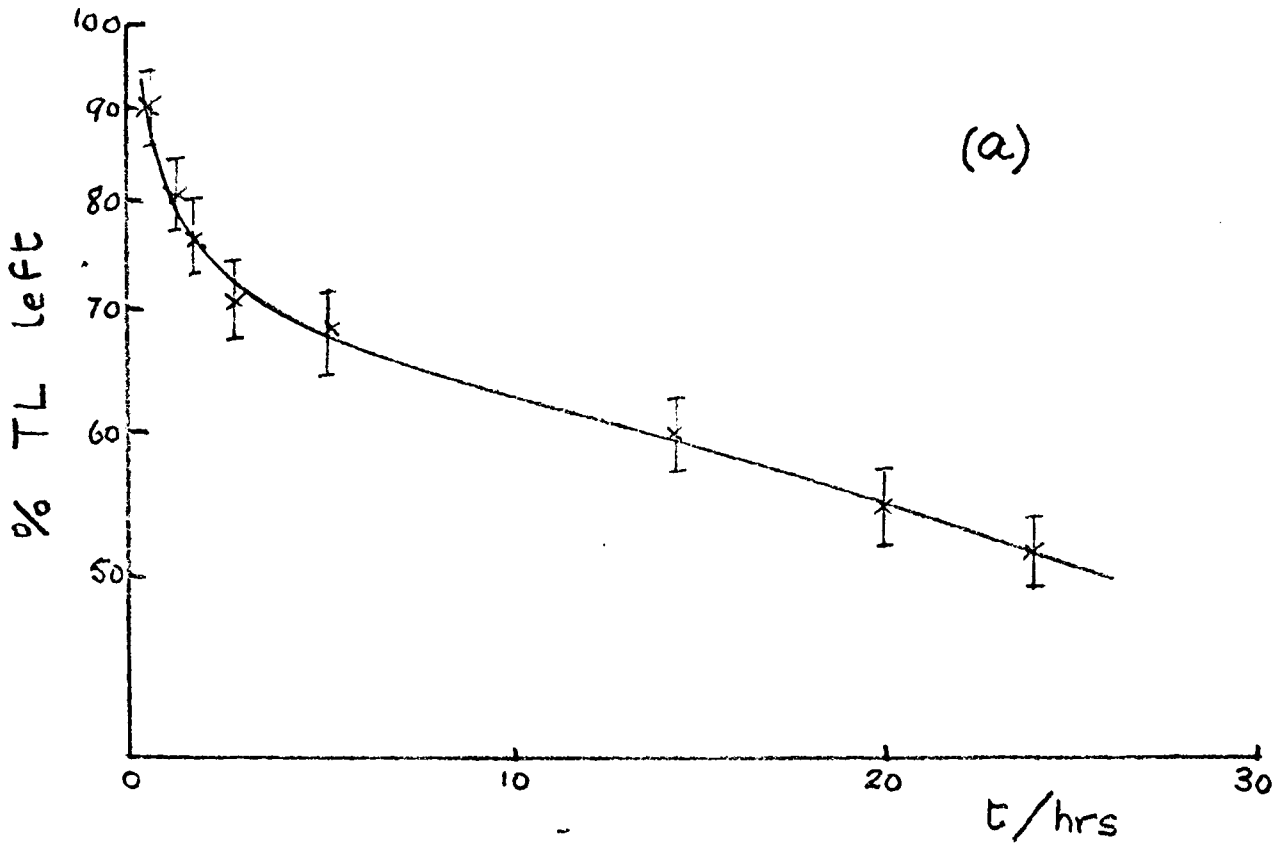

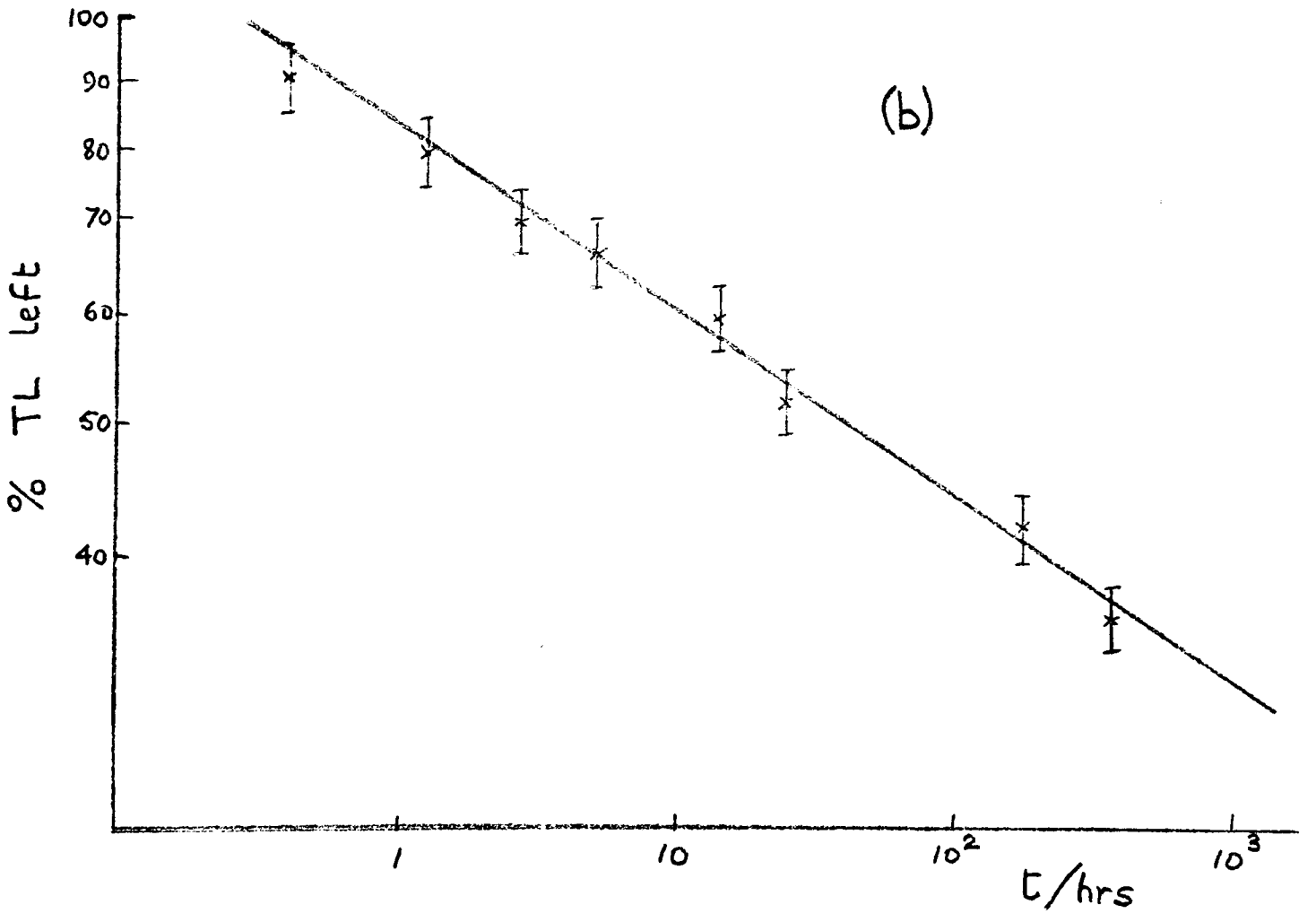

Fig. 7.2 Labradorite (BA6) fading

% TL left at 300°C abscissa vs. storage

time at 10°C, (a) log/linear, (b) log/log.

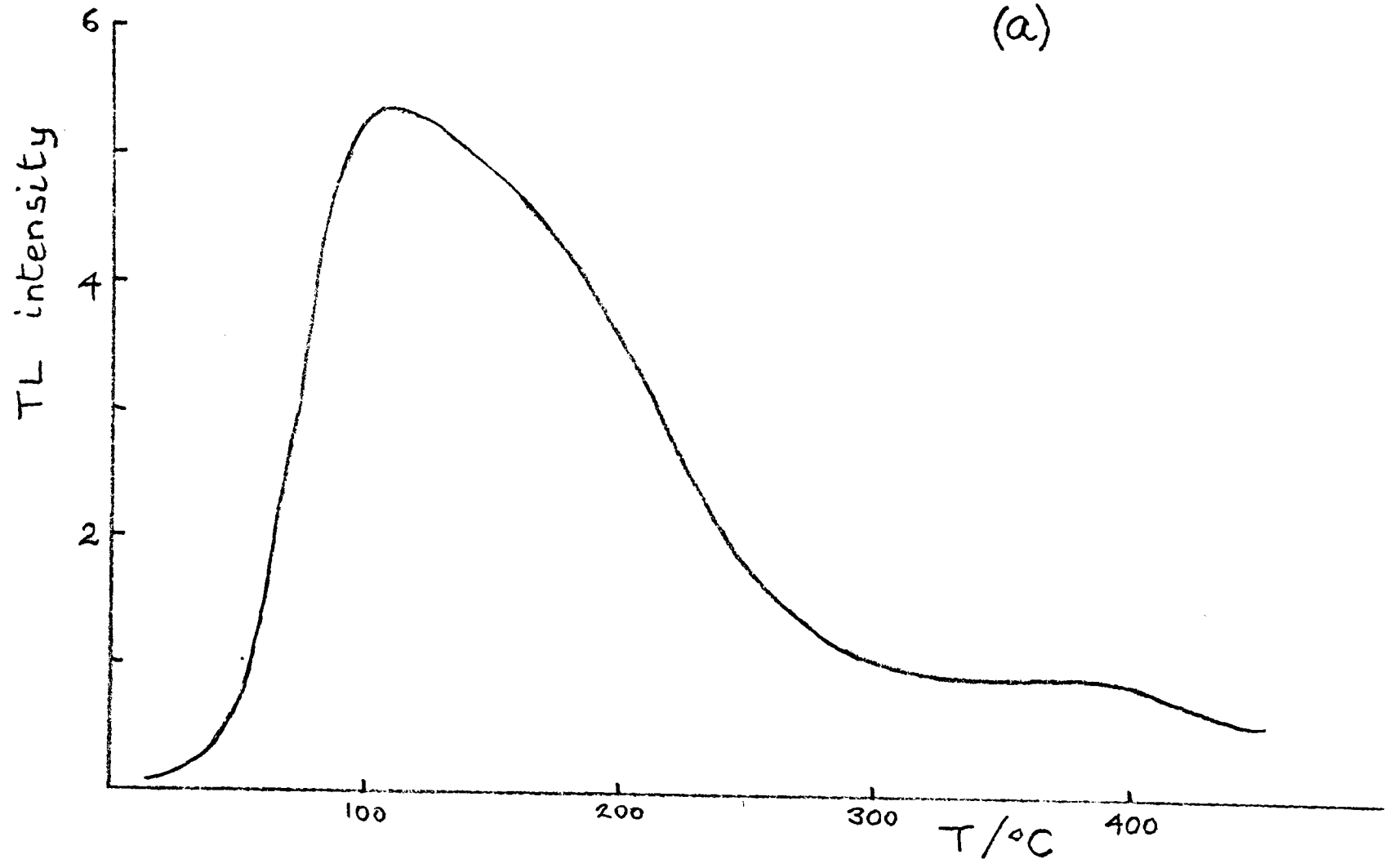

Fig. 7.3 Andesine (BA7)

(a) TL glow curve after artificial β irradiation

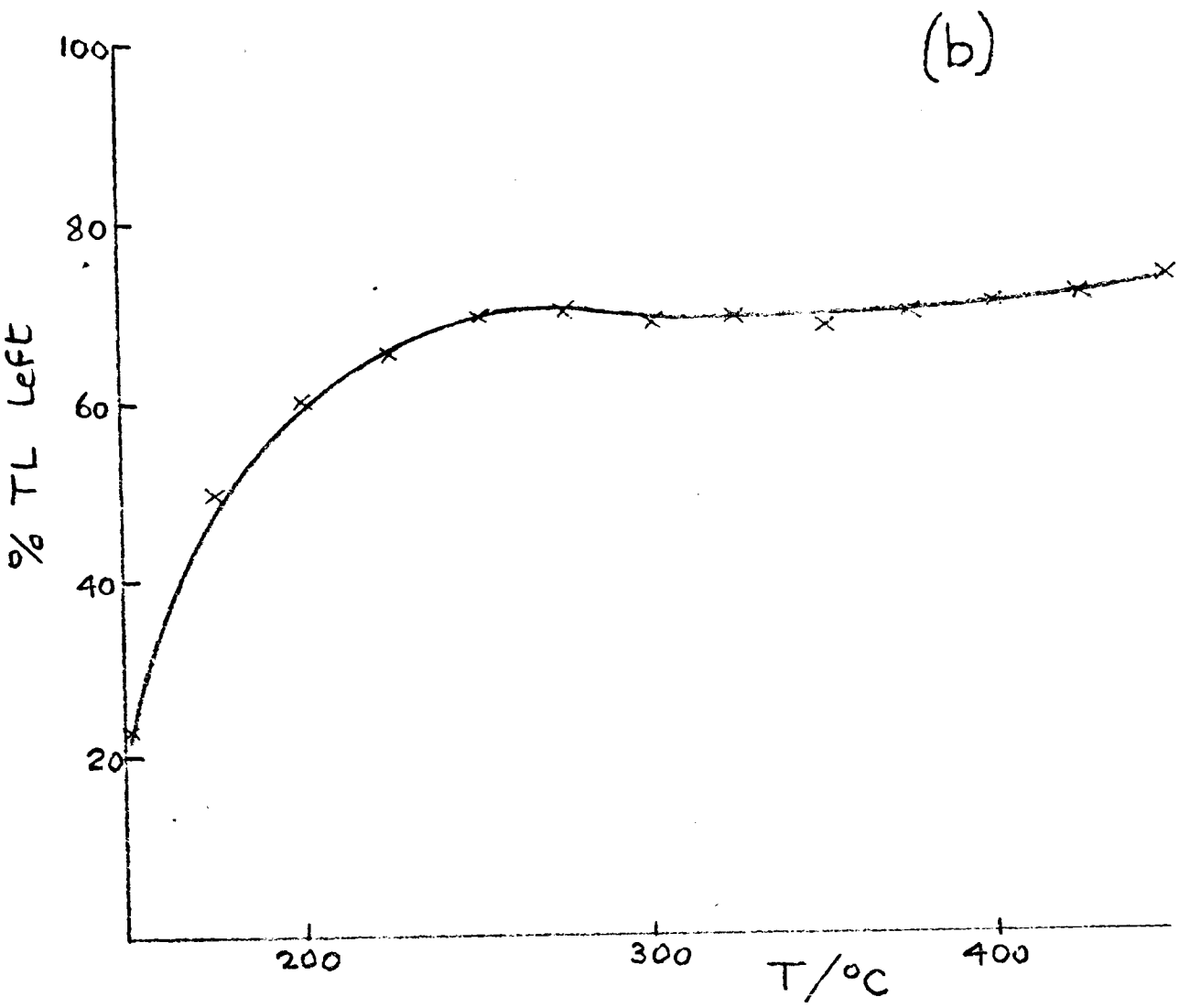

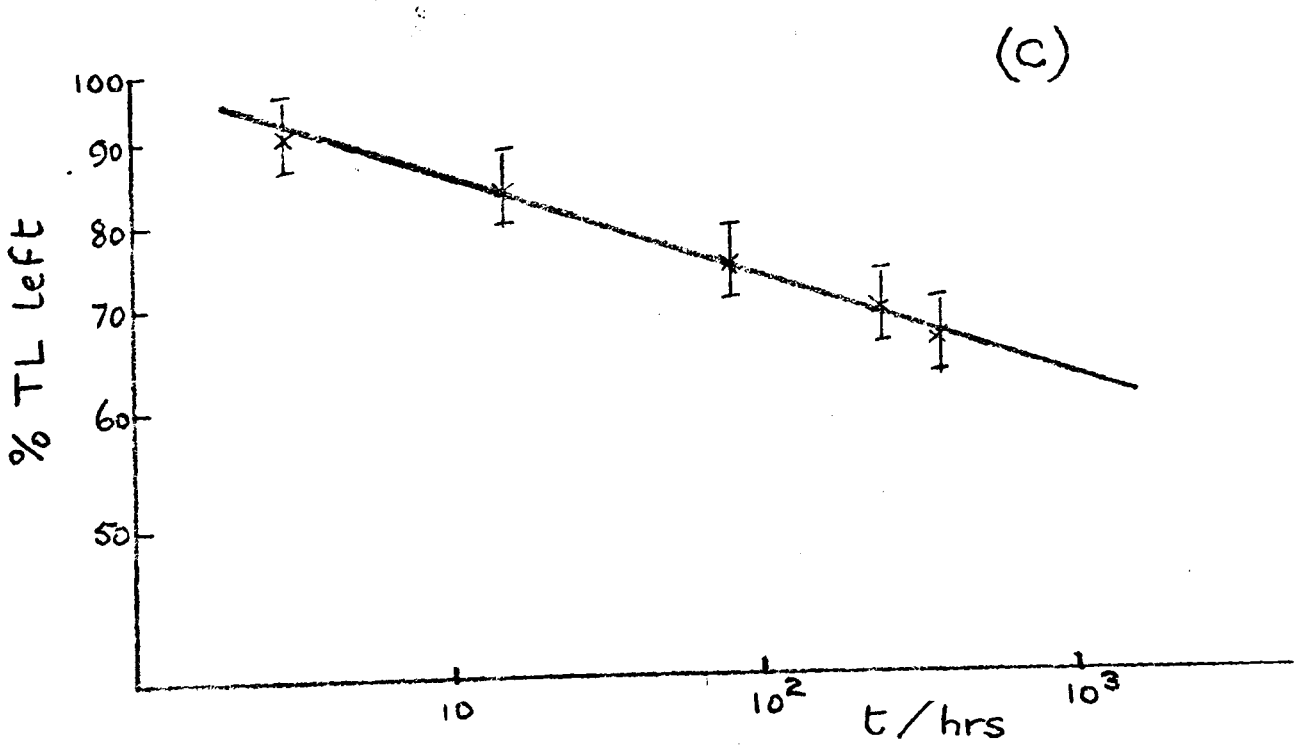

Fig. 7.3 Andesine (BA7)

(b) % TL left after 10 days storage at 10°C

(c) % TL left at 350°C abscissa vs. storage time at 10°C

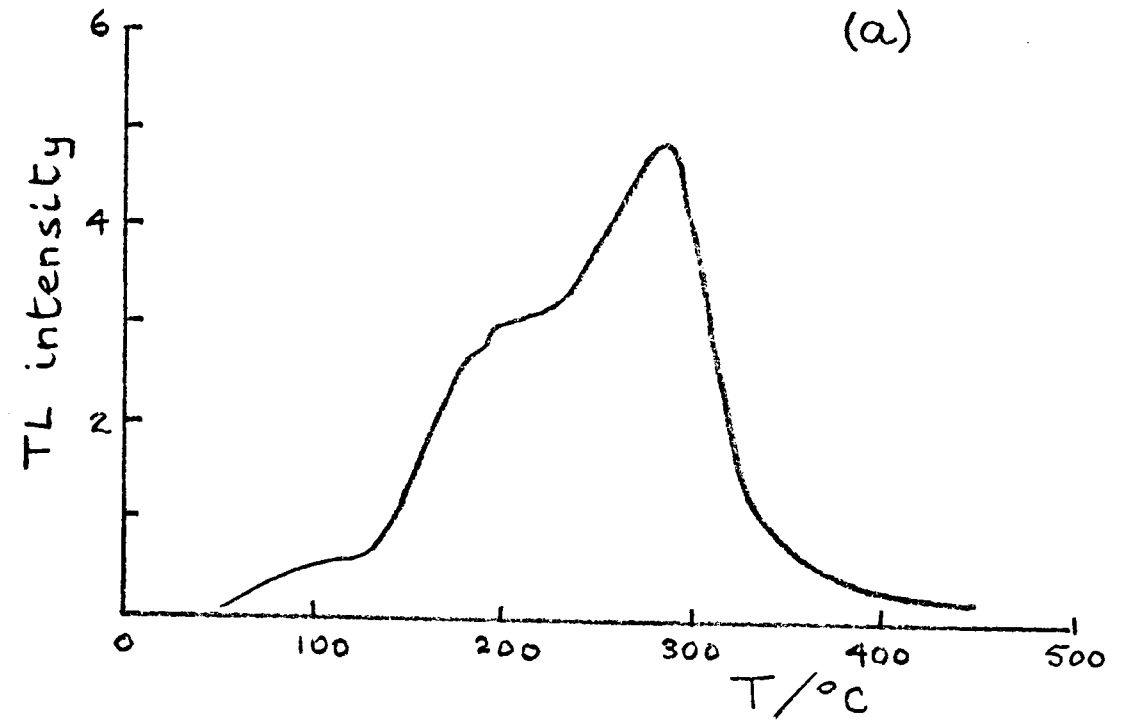

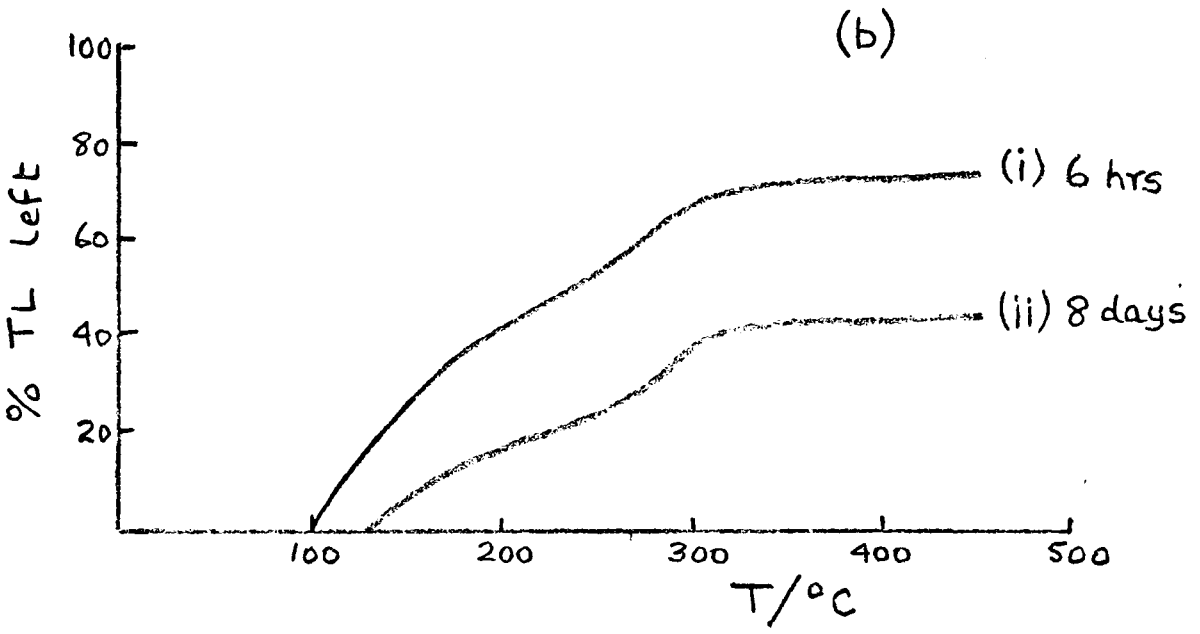

Fig. 7.4 Fluorapatite

(a) TL glow curve after 500 rad β dose,
(heating rate 6°C/s, PM EMI 9635, filter HA3 + 5-60)

(b) % TL left after storage at 10°C,
(i) for 6 hours, (ii) for 8 days

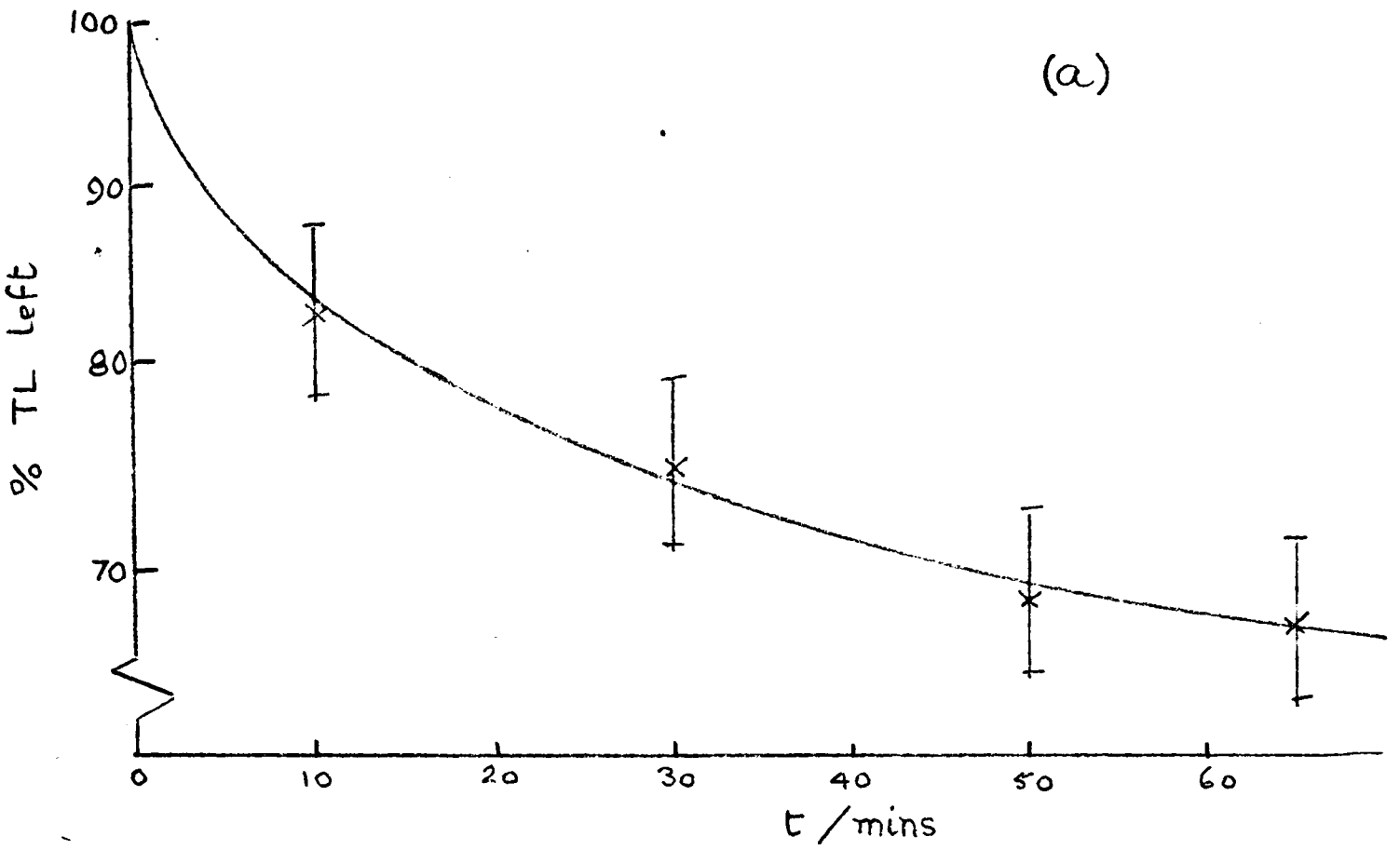

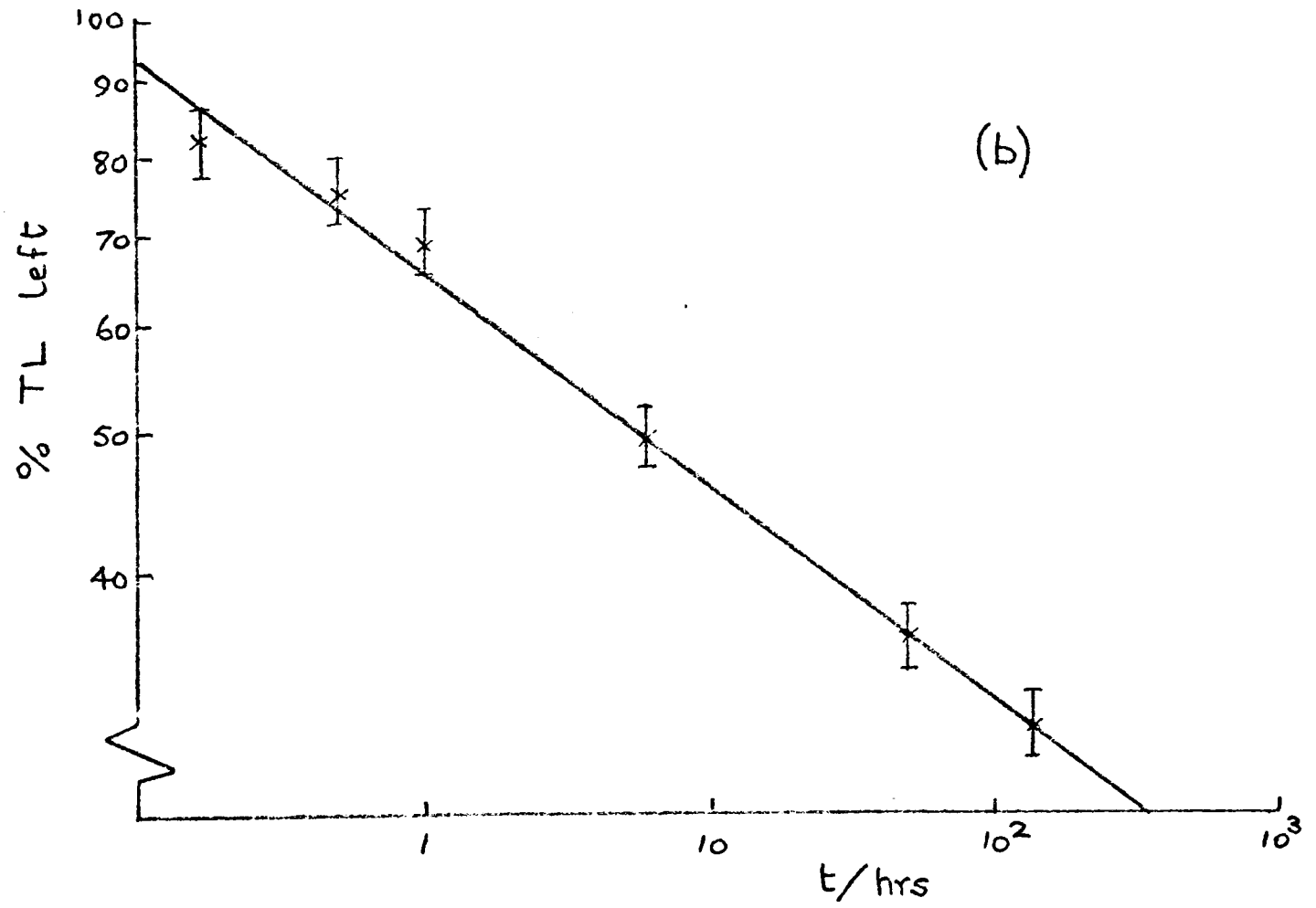

Fig. 7.5 Fluorapatite fading

% TL left at 270°C abscissa vs. storage time at 10°C, (a) log/linear, (b) log/log.

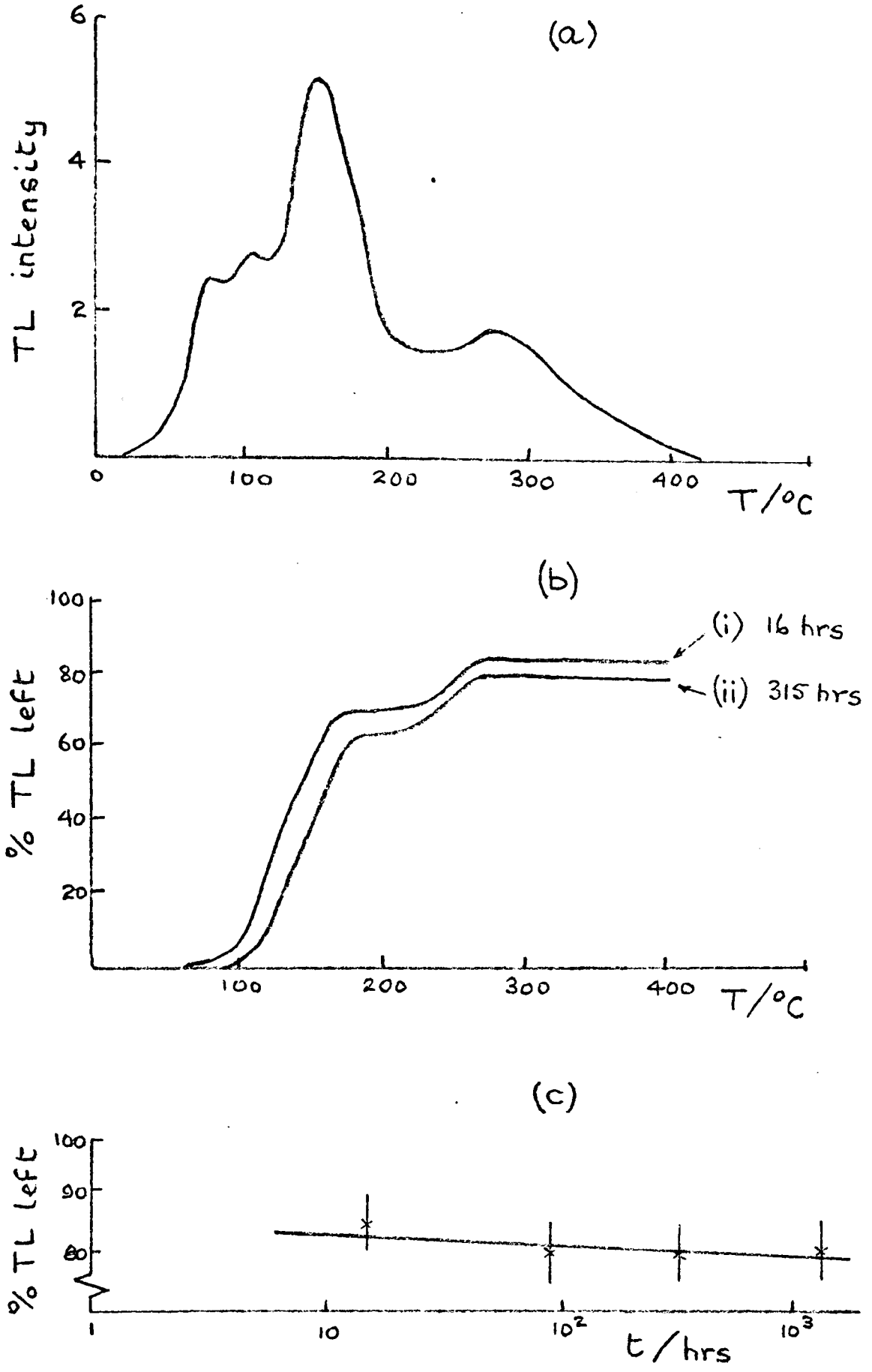

Fig. 7.6 Zircon

(a) TL glow curve after 1 krad β dose (heating rate 6°C/s, PM EMI 6225, filter HA3)

(b) % TL left after storage at 10°C (i) for 16 hours, (ii) for 315 hours

(c) % TL left at 300°C abscissa vs. storage time at 10°C (log/log)

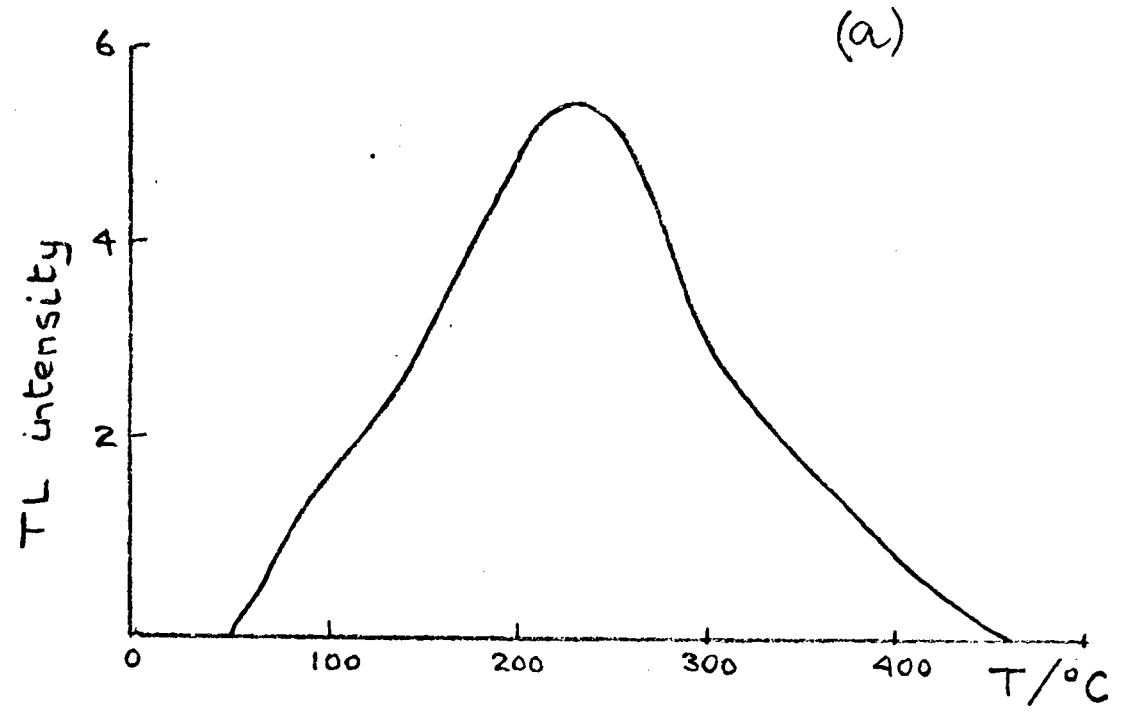

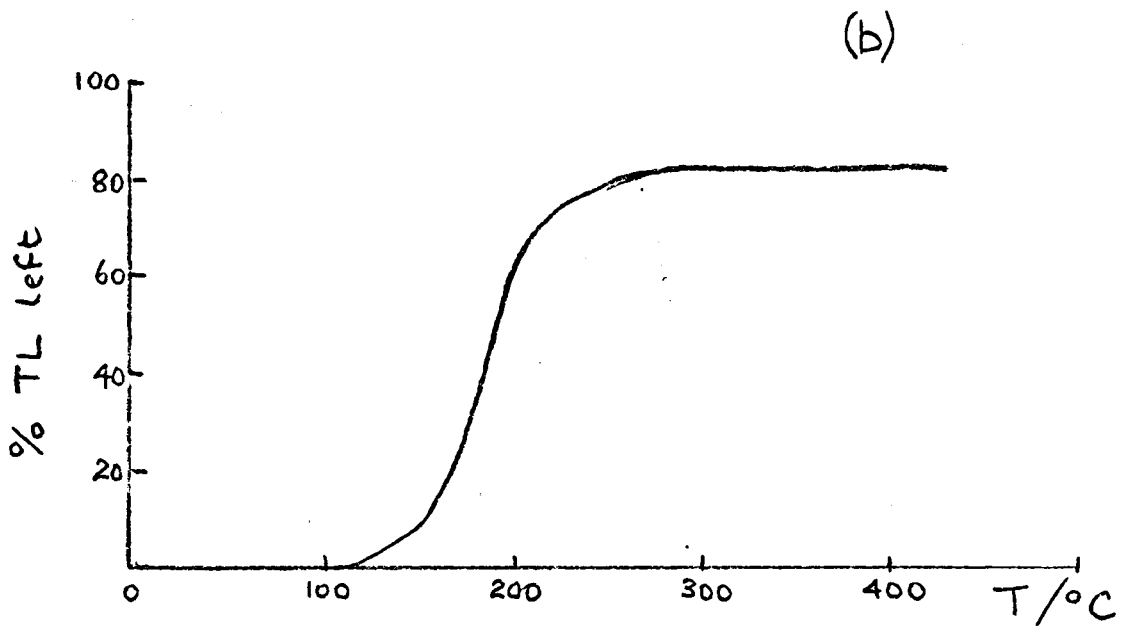

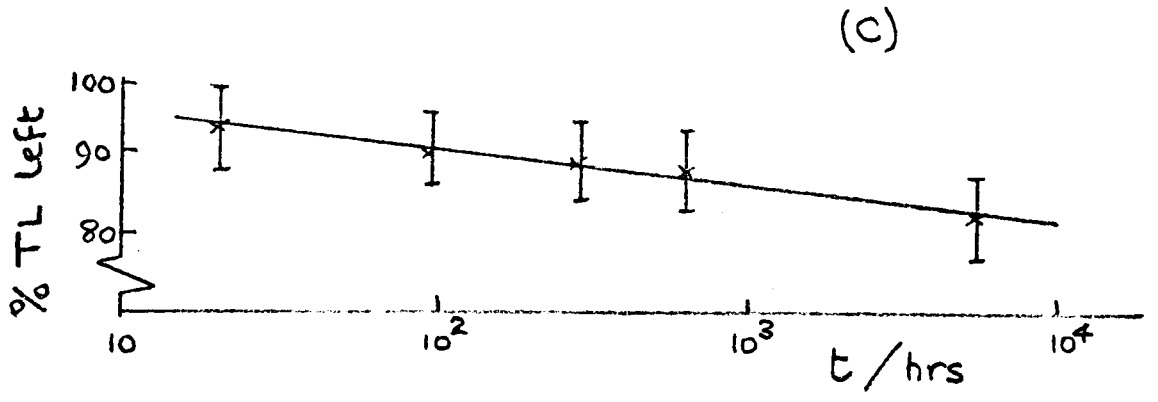

Fig. 7.7 Mullite

(a) TL glow curve after 100 rad β dose (heating rate 6°C/s, PM EMI 6255, filters HA3 + 5-60)

(b) % TL left after storage at 10°C for 220 days

(c) % TL left at 350°C abscissa vs. storage time at 10°C (log/log)

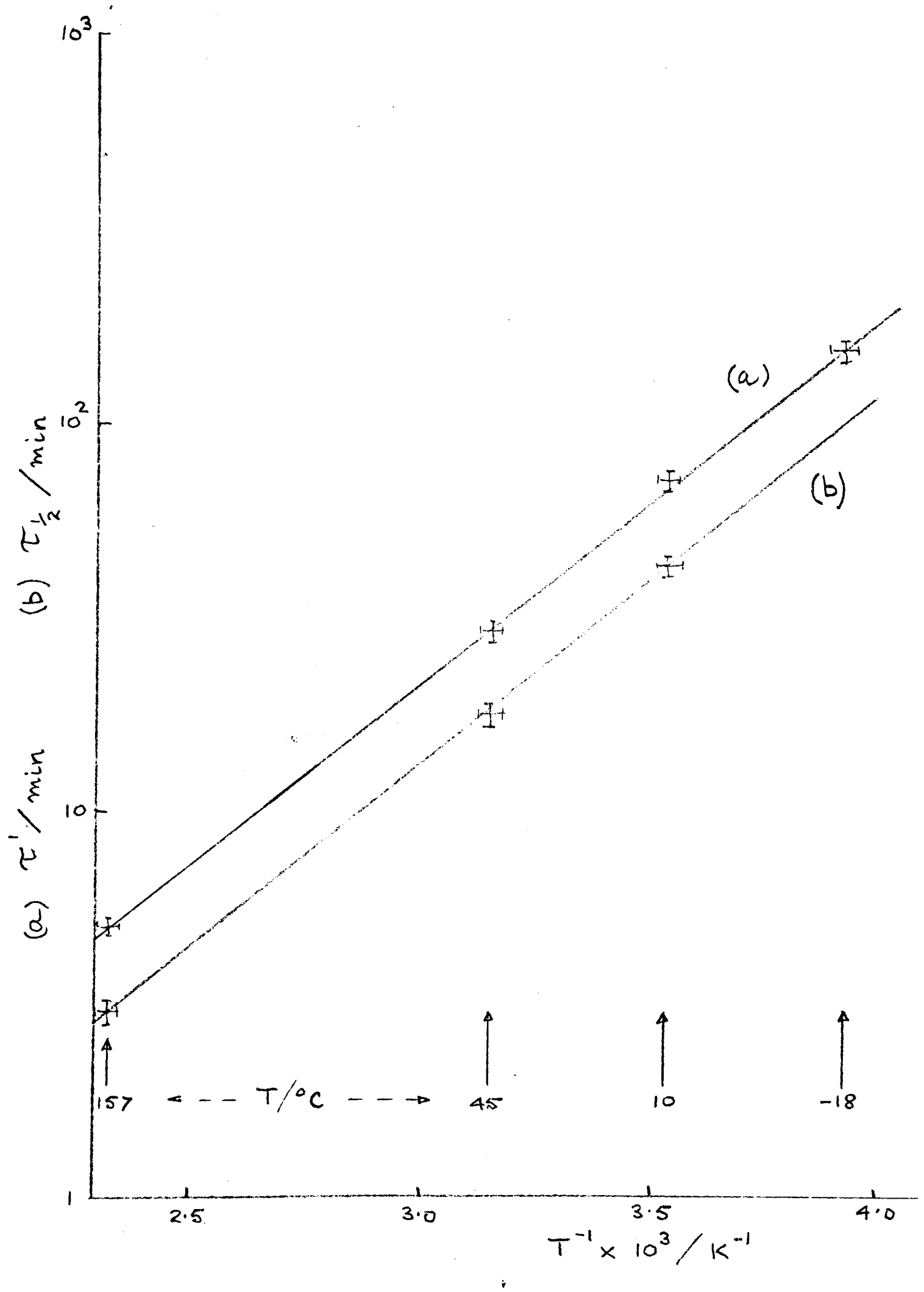

Fig. 7.8 Labradorite BA6, isothermal decay of TL at 300°C abscissa ; (a) log τ^{1} vs T^{-1}, (b) log $\tau_{\frac{1}{2}}$ vs T^{-1}

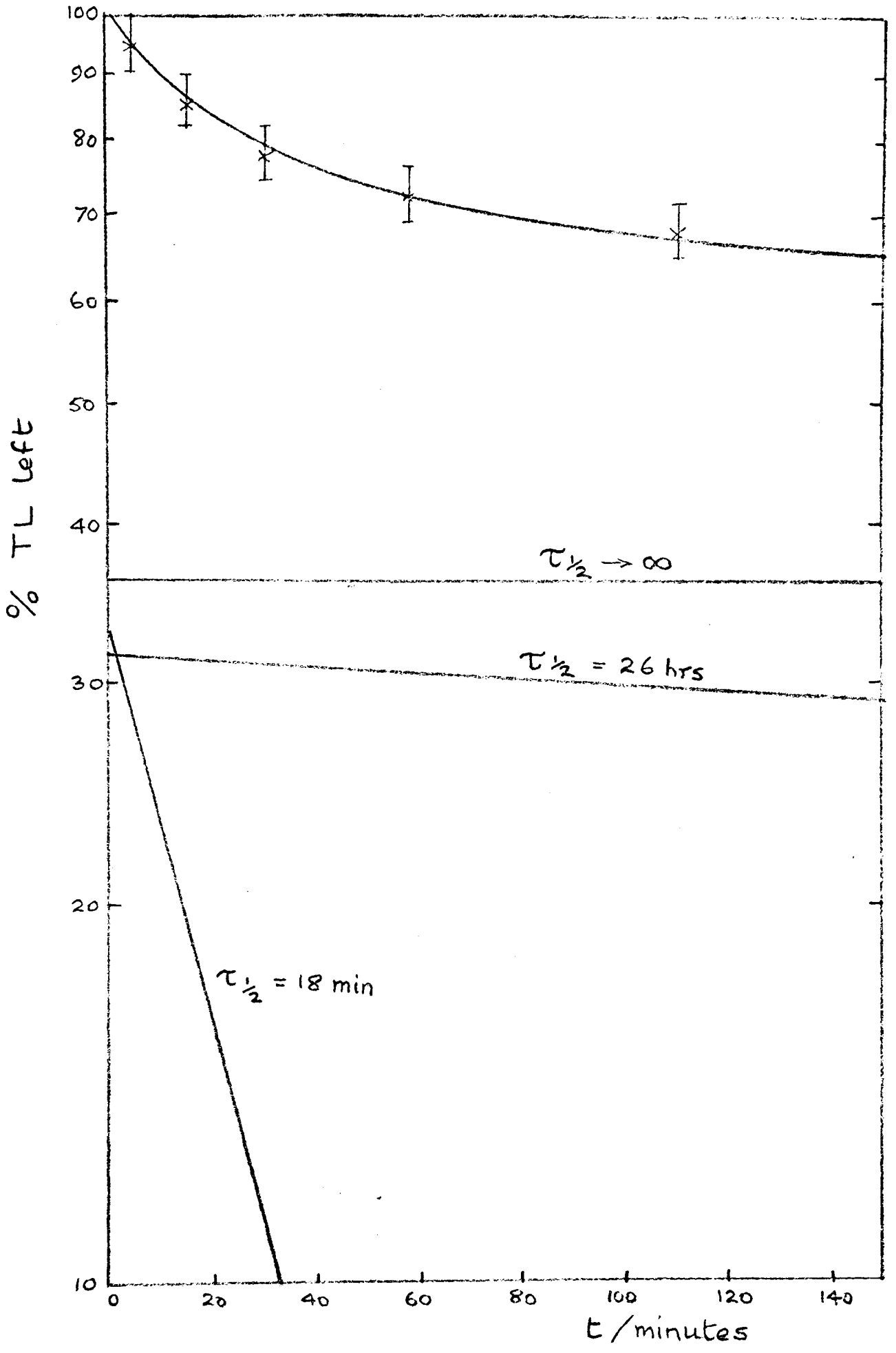

Fig. 7.9 Labradorite (BA6)

Isothermal decay of TL at 300°C abscissa vs. storage time at 45°C. The upper curve is the sum of the three exponential components.

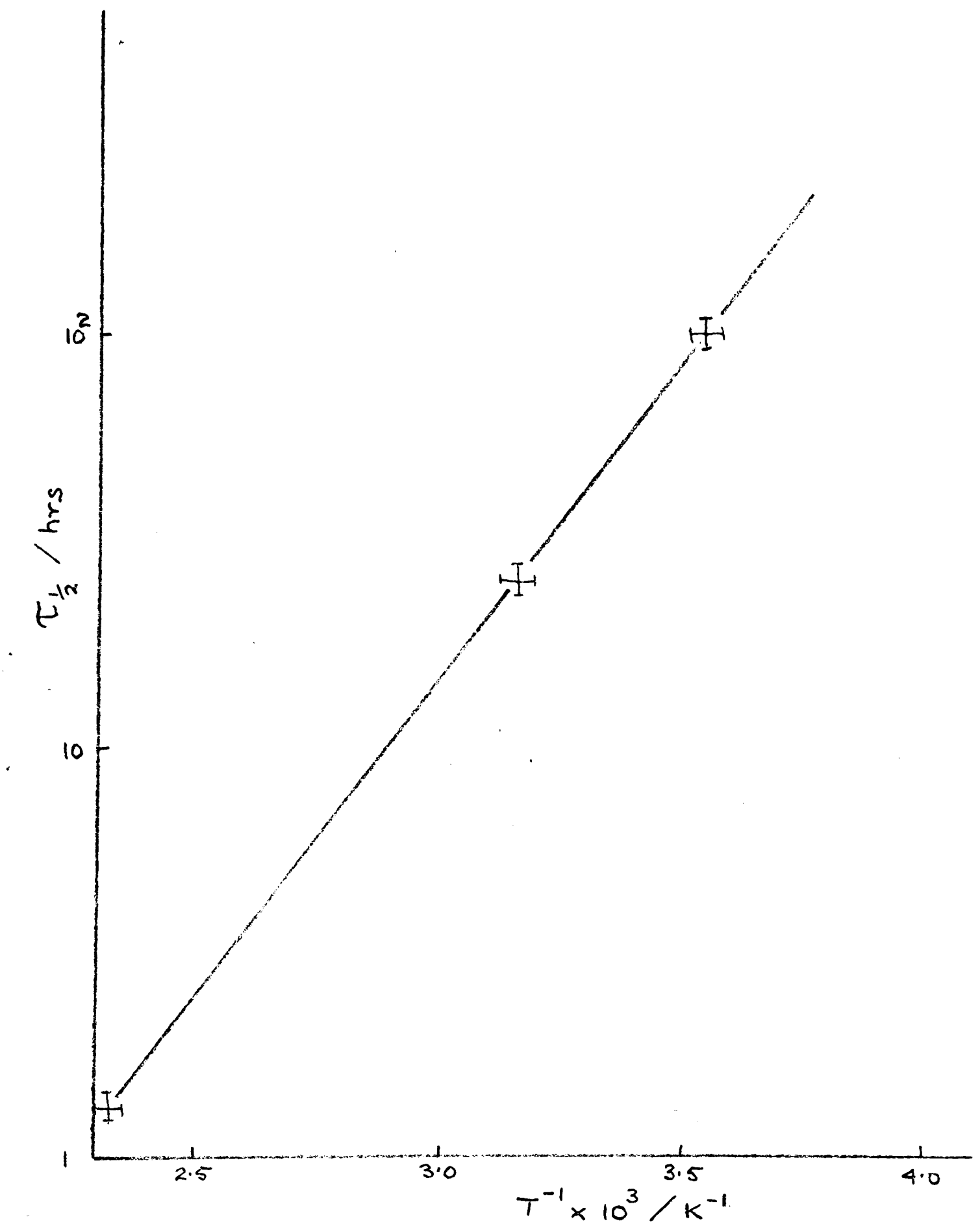

Fig. 7.10 Labradorite BA6; log $\tau_{\frac{1}{2}}$ vs T^{-1} for second fastest decay component

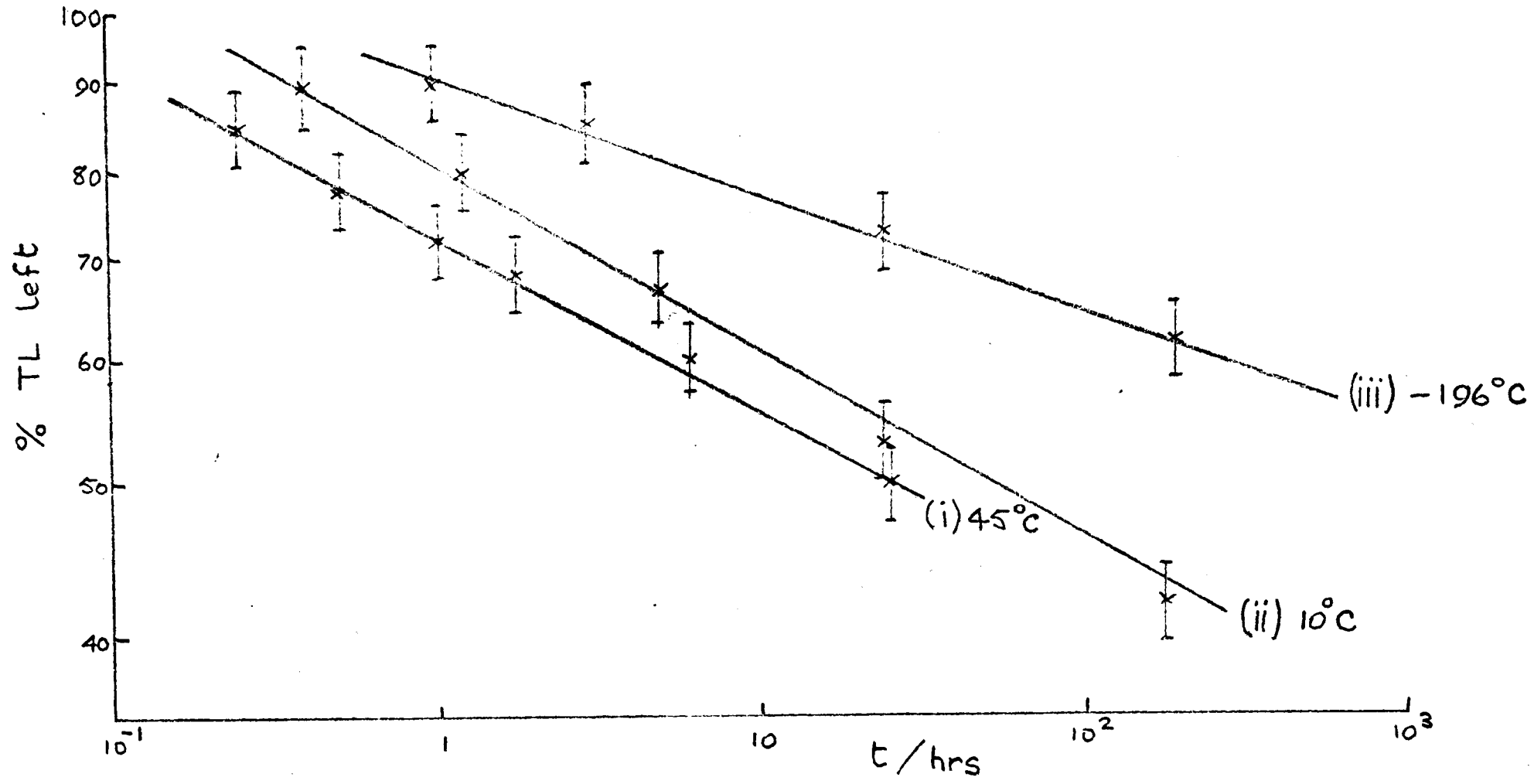

Fig. 7.11 Feldspar (BA6) fading

% TL left at 300°C ~~abscissa~~ vs. storage time at (i) 45°C, (ii) 10°C, (iii) -196°C

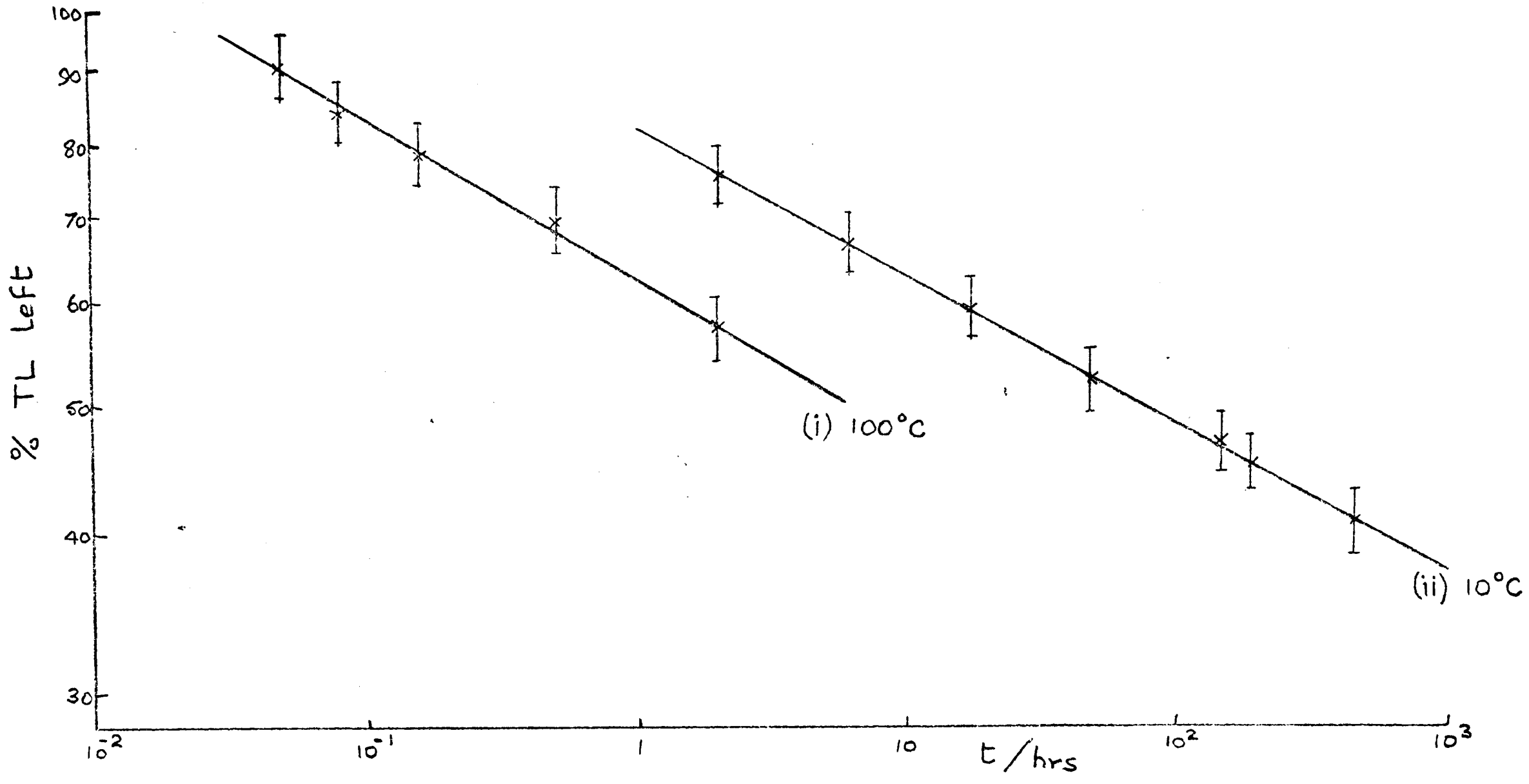

Fig. 7.12 Fluorapatite fading

% TL left at 400°C abscissa vs. storage time
at (i) 100°C, (ii) 10°C

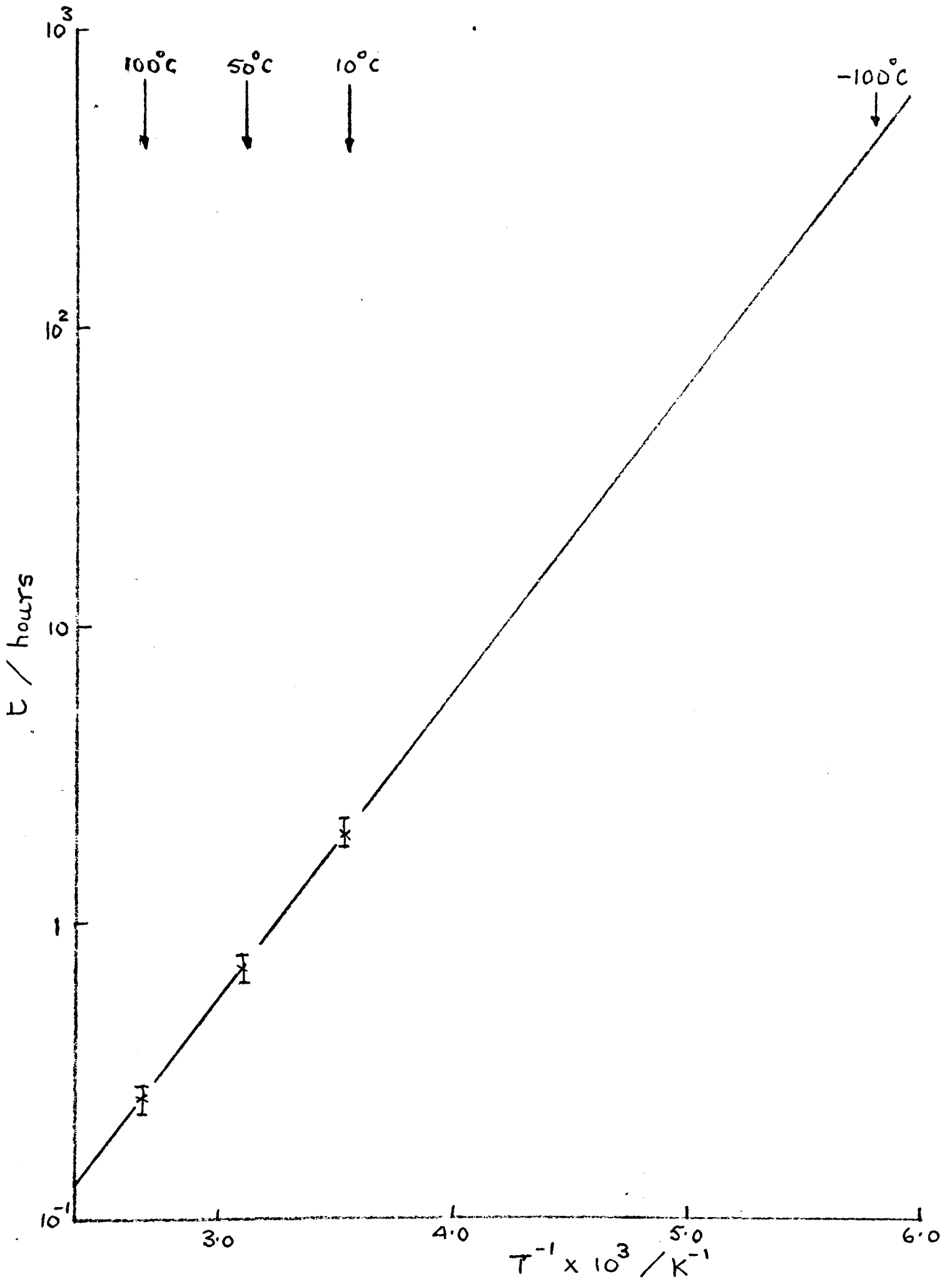

Fig. 7.13 Fluorapatite; log t vs T^{-1}, where t is the time taken for the TL at the 400°C abscissa to decay by 25%

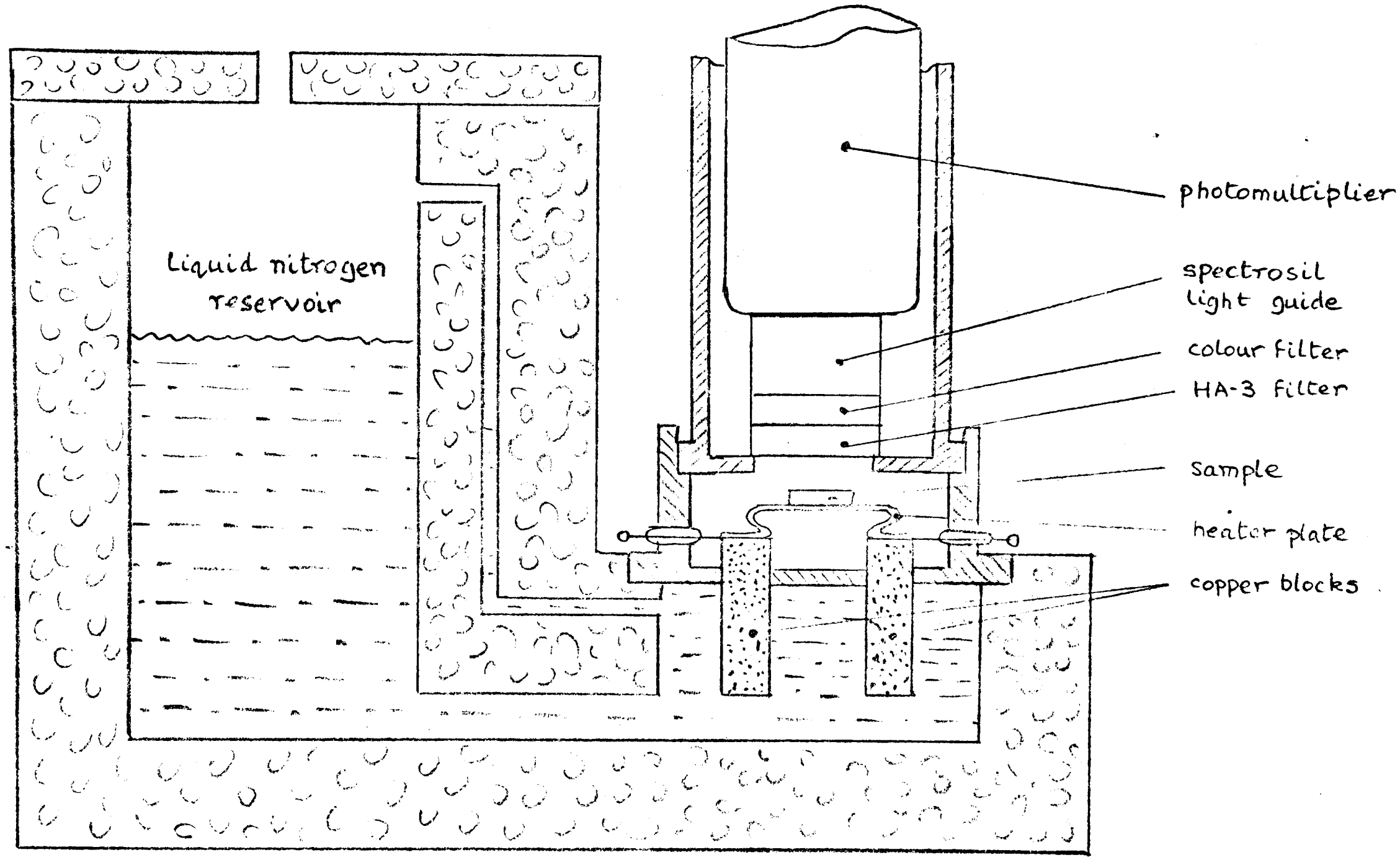

Fig. 7.14 Low temperature oven

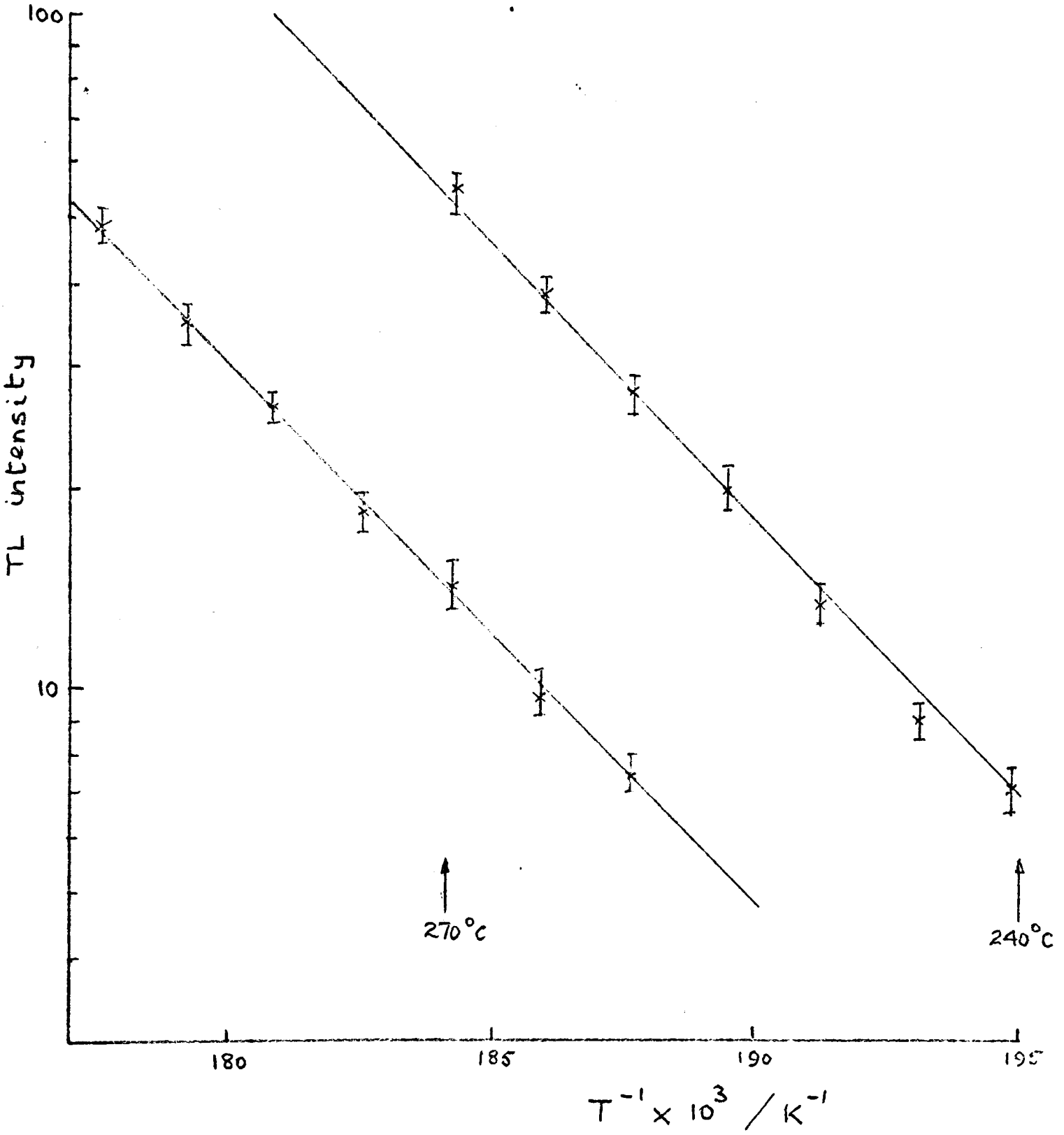

Fig. 7.15 Feldspar BA6, initial rise plot of log I vs T^{-1}

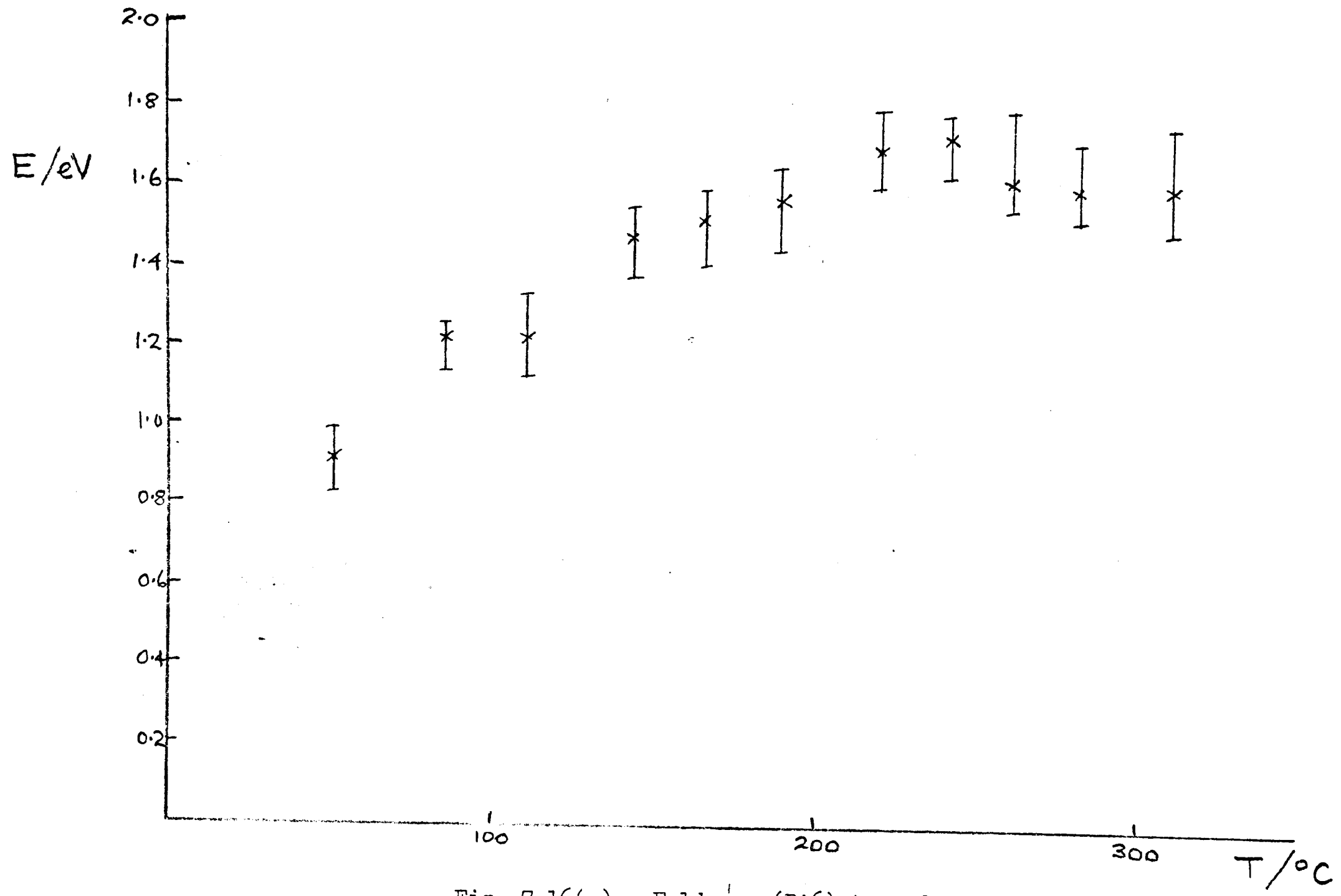

Fig. 7.16(a) Feldspar (BA6) trap depth

trap depth E (determined by initial rise method) vs. measurement temperature.

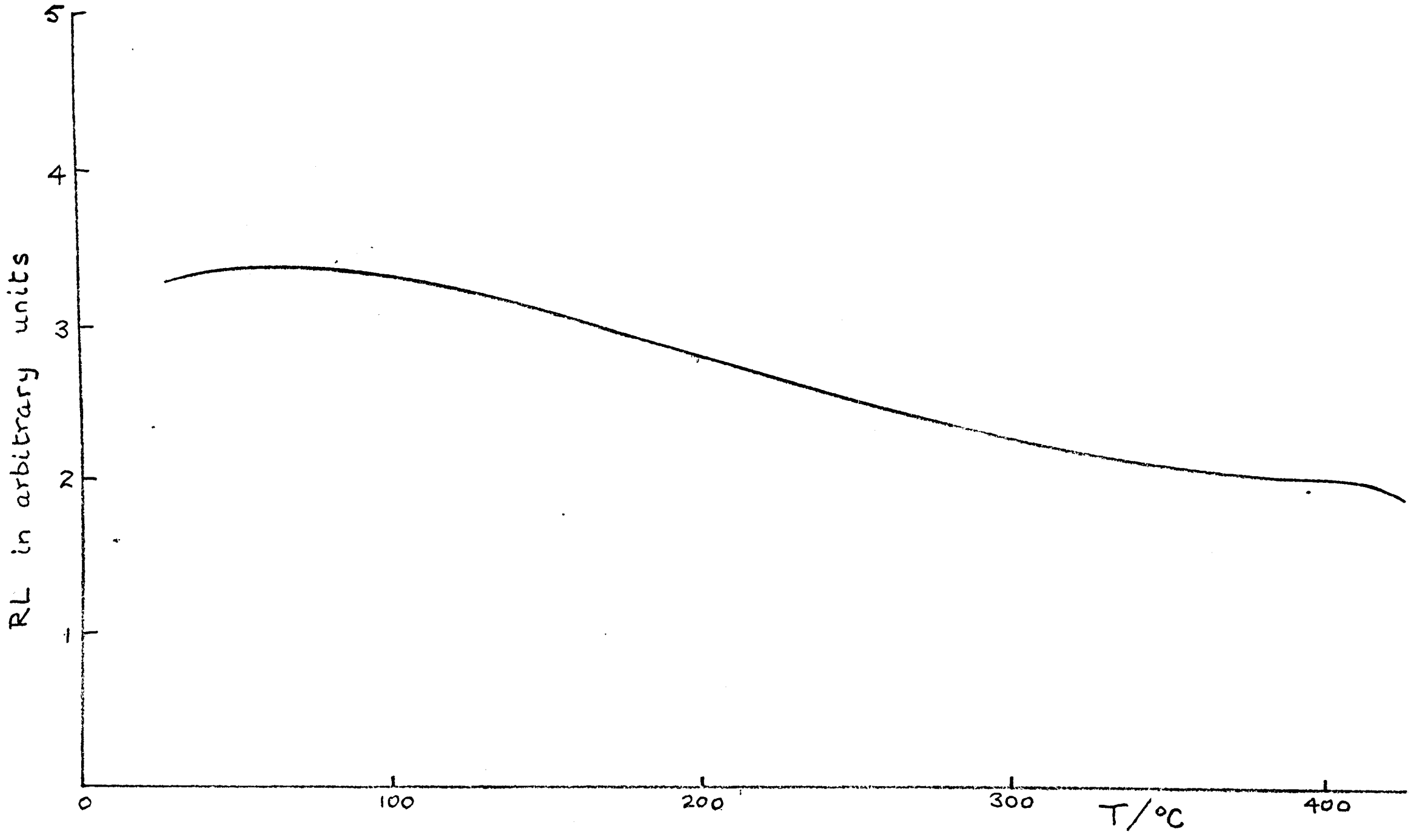

Fig. 7.16(b) Feldspar (BA6) radioluminescence

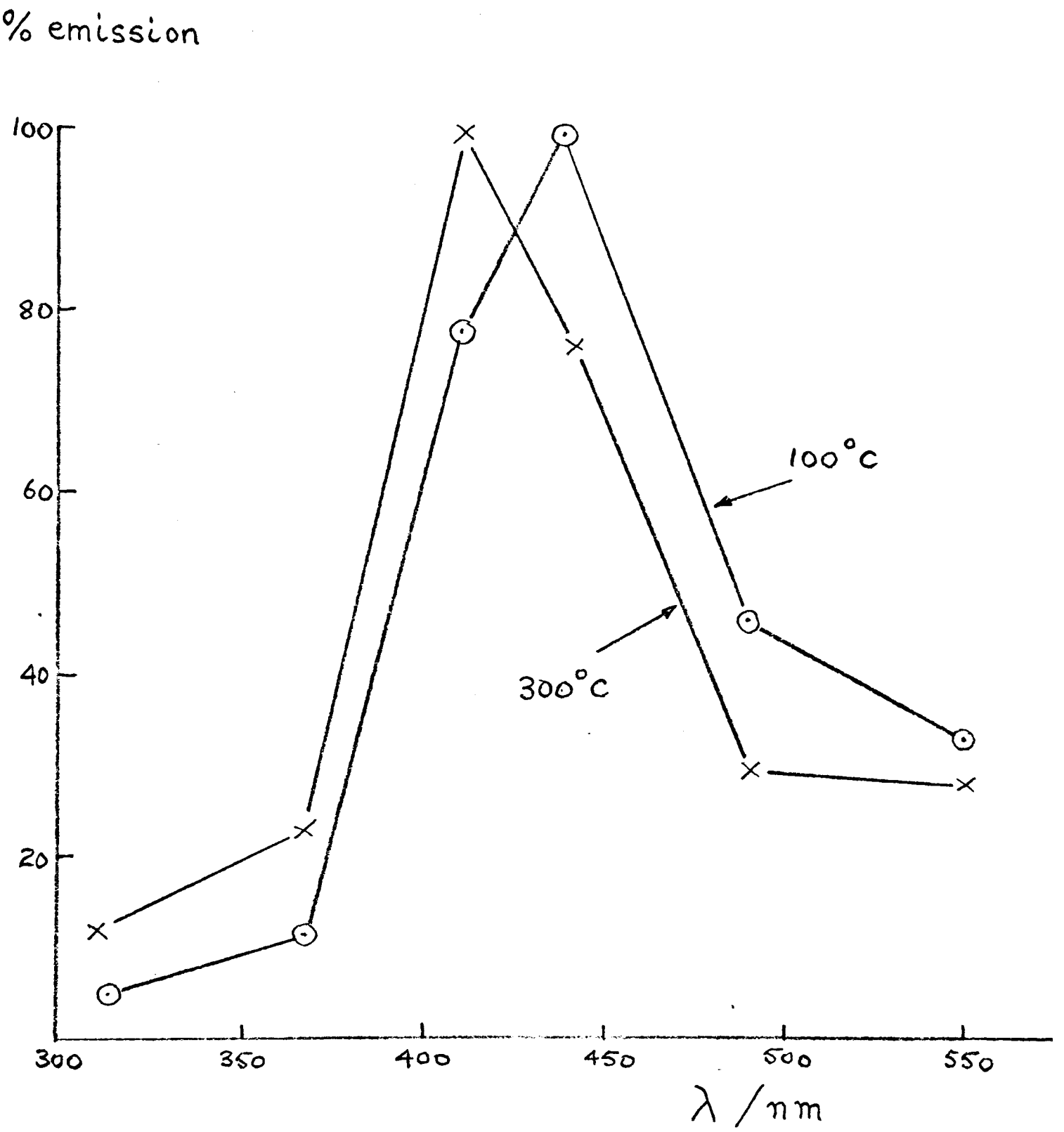

Fig. 7.17 Feldspar (BA6) TL emission

normalized emission spectrum, circles 100°C, crosses 300°C

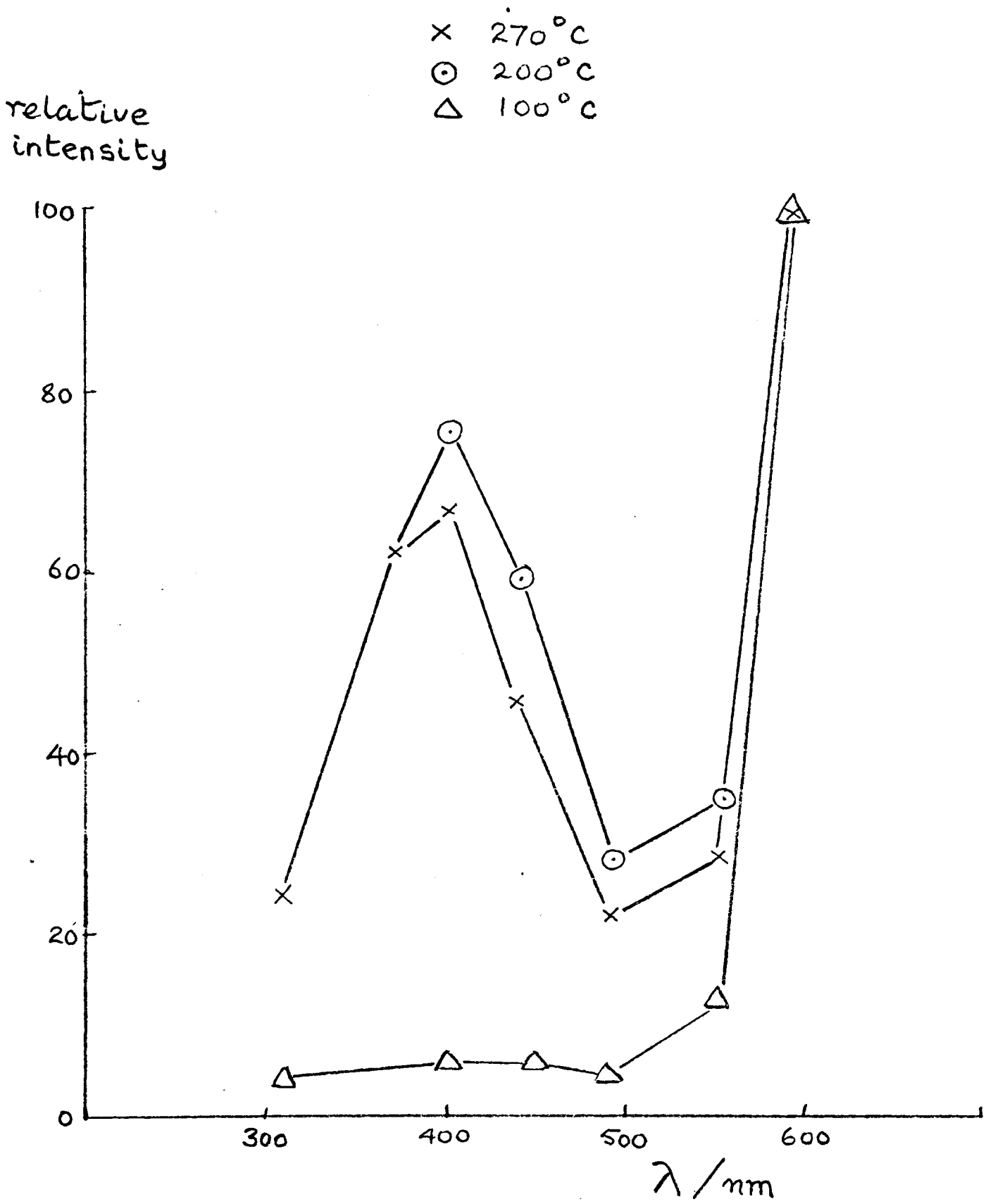

Fig. 7.18 Fluorapatite TL emission

relative emission spectrum of various peaks, crosses 270°C, circles 200°C, triangles 100°C

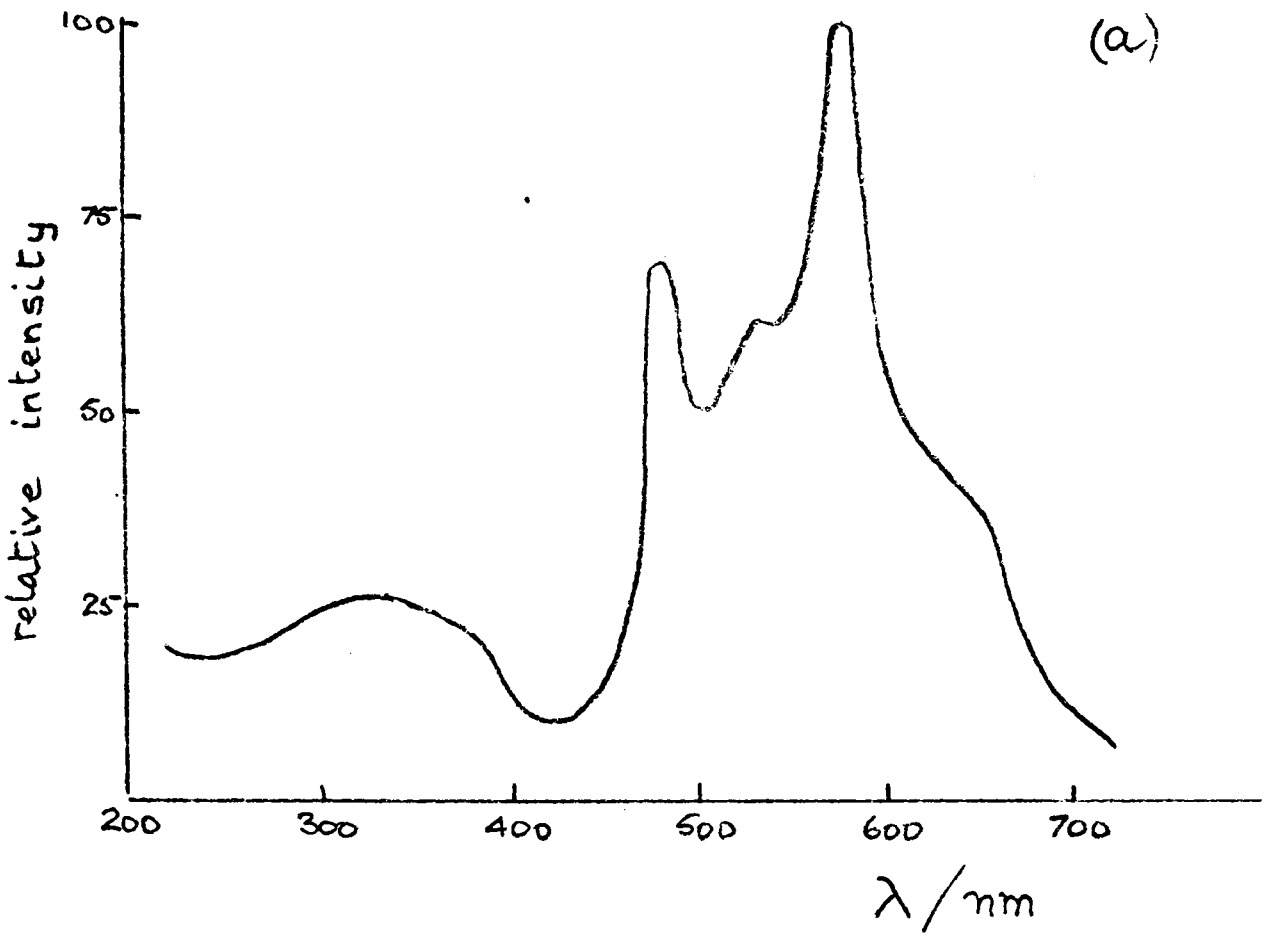

Fig. 7.19 Zircon, 280°C peak

emission spectra using (a) a spectrometer, (b) the filtrometer.

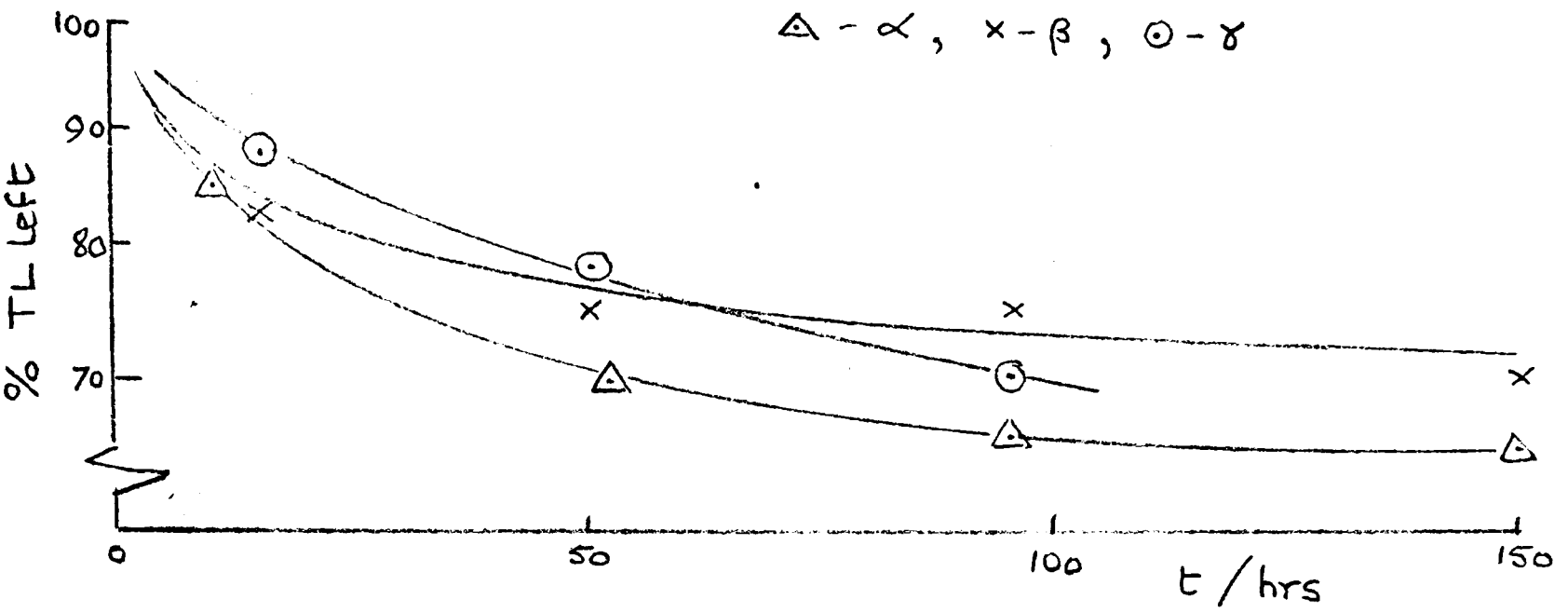

Fig. 7.20 Orthoclase .. Decay of TL at 300°C ordinate vs. storage time at 10°C after different type of irradiation; triangles - alpha, crosses - beta, circles - gamma.

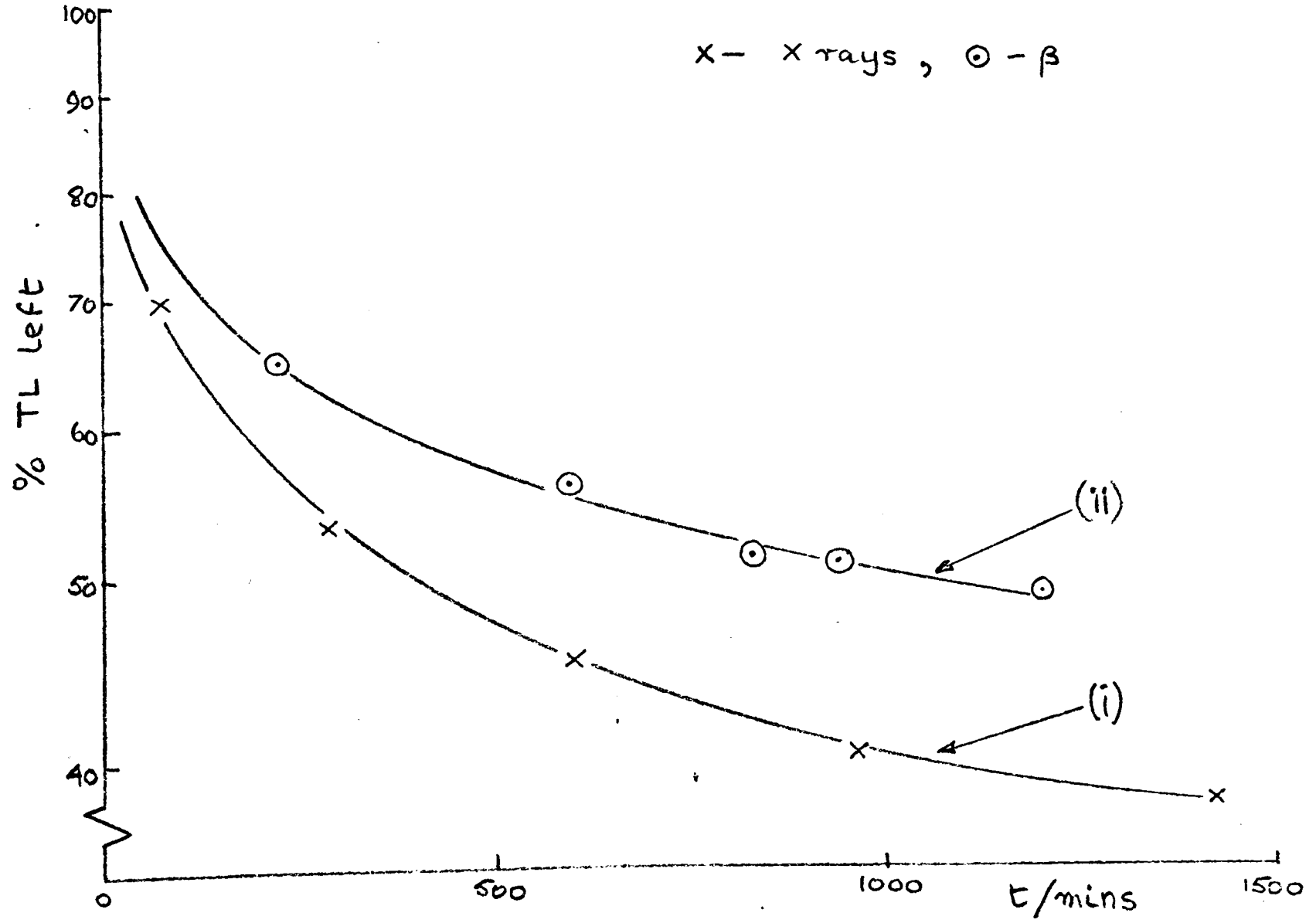

Fig. 7.21 Fluorapatite (large crystal) .. Decay of TL at 300°C ordinate vs. storage time at 10°C; after irradiation by (i) 1 Mrad X-rays, (ii) 500 rad β

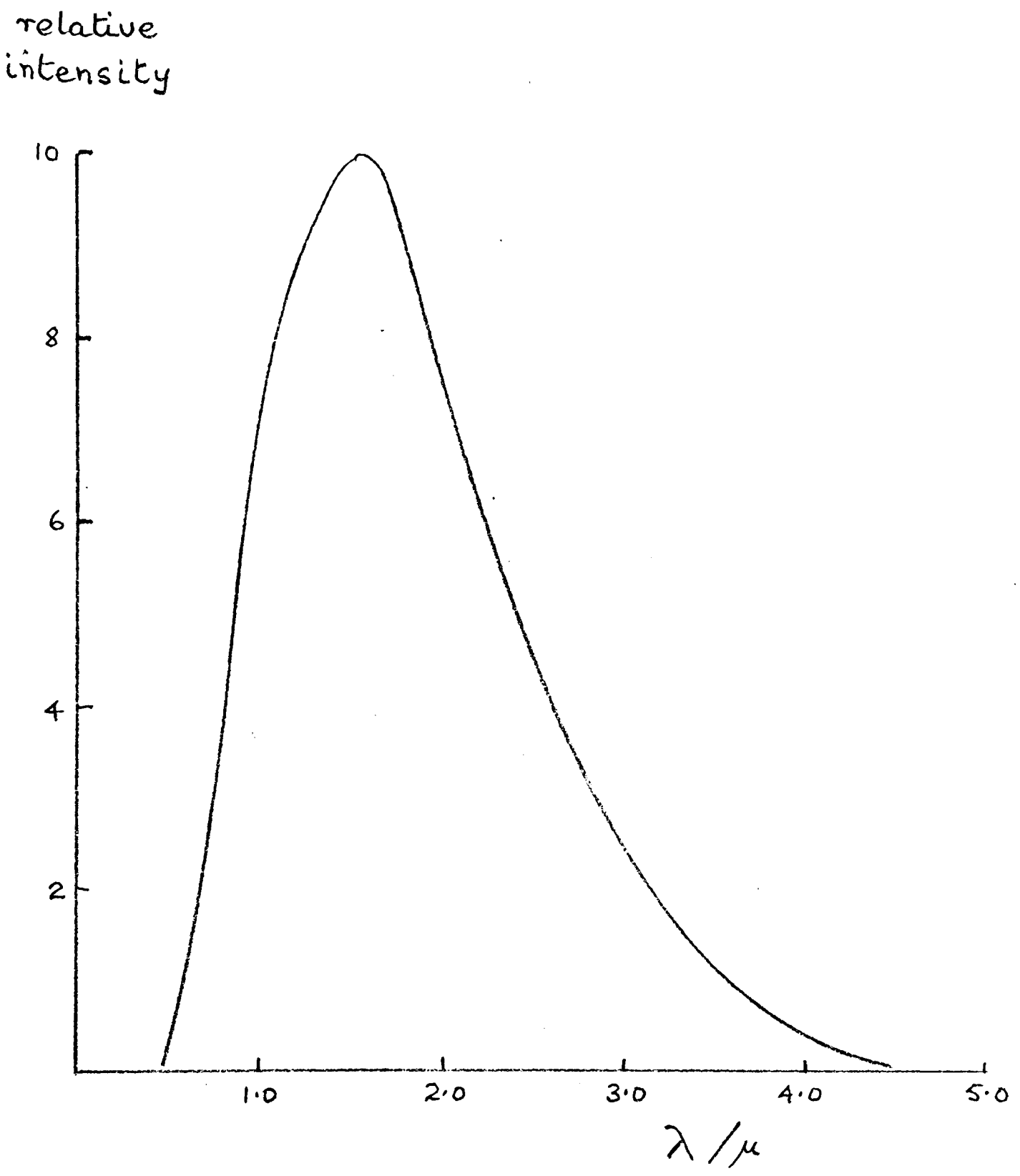

Fig. 7.22 Emission spectrum of I.R. lamp

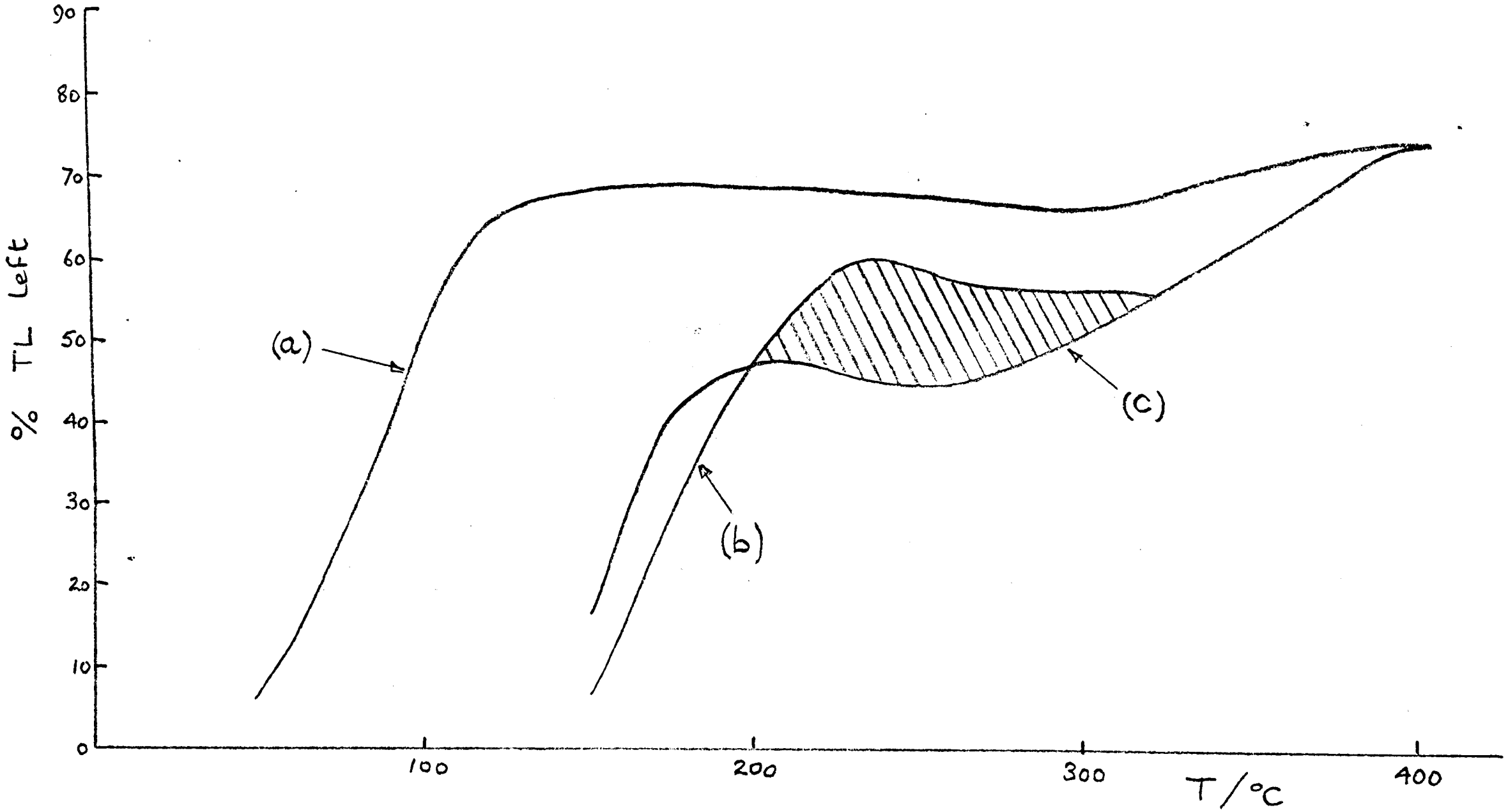

Fig. 7.23 Feldspar (BA6) .. Effect of $2\frac{3}{4}$ hour I.R. exposure after β irradiation; (a) no I.R., (b) planchette covered with Al, (c) planchette exposed to I.R.

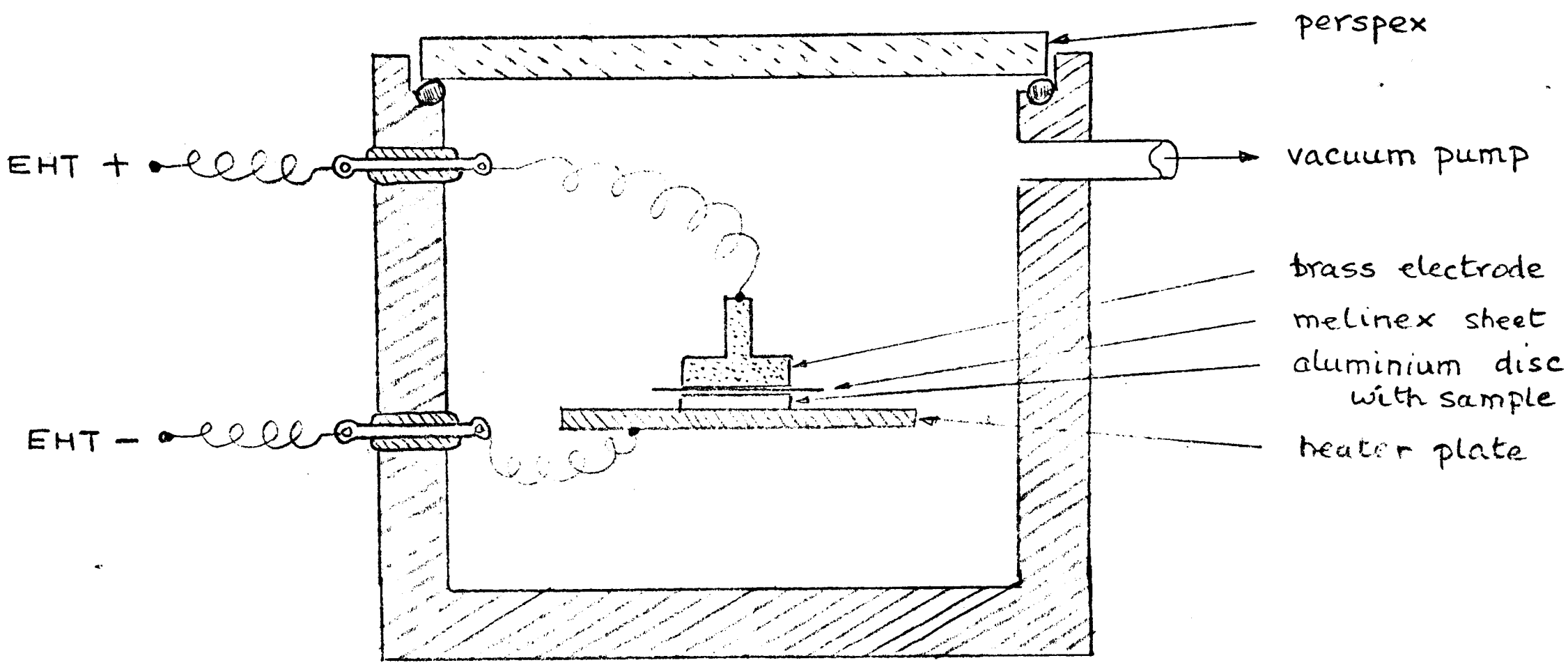

Fig. 7.24 Oven modification to permit application of electric field

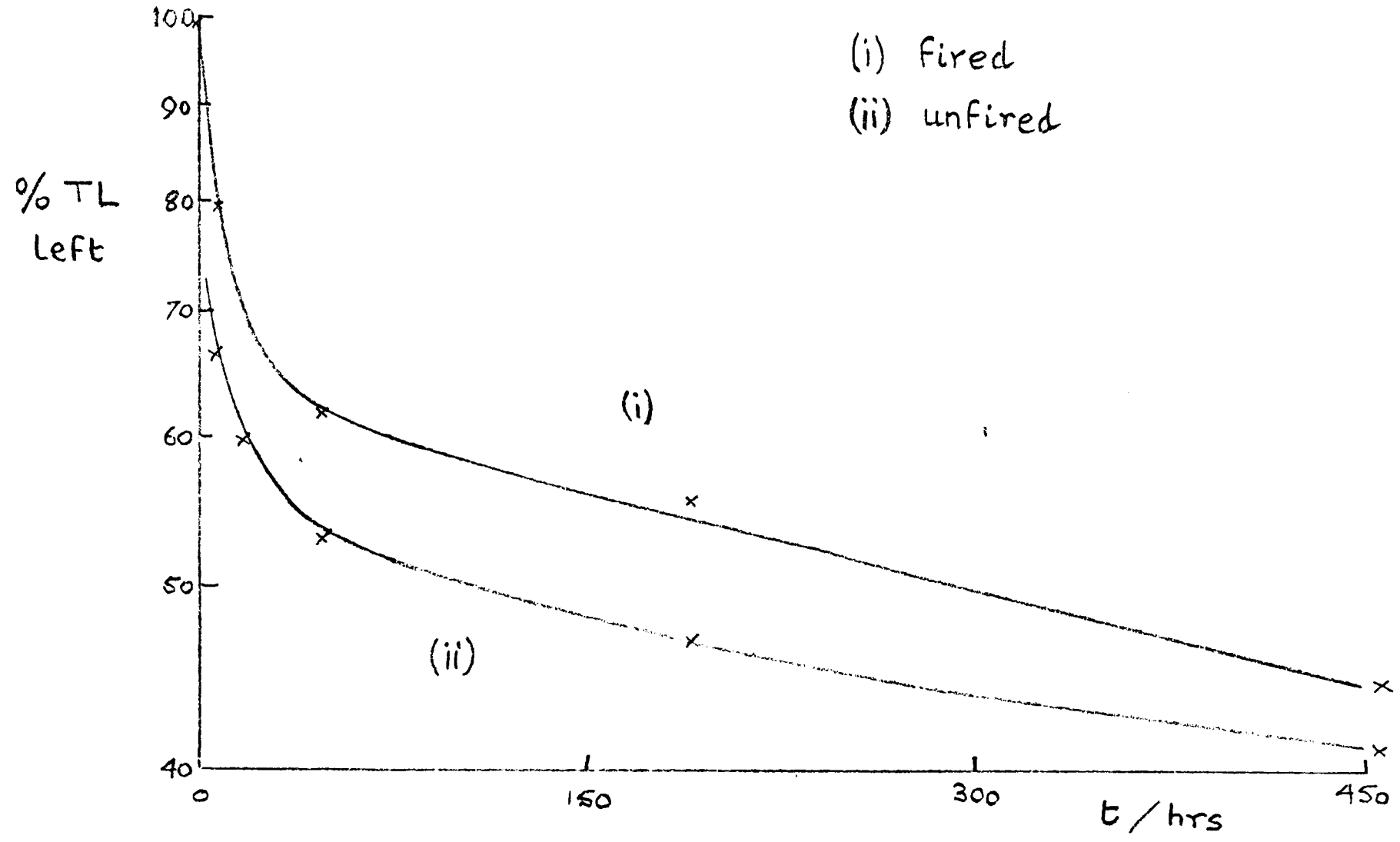

Fig. 7.25 Fluorapatite fading

% TL left at 400°C [illegible] vs storage time at room temperature,

(i) fired, (ii) unfired

CHAPTER 8 ANOMALOUS FADING - POSSIBLE MECHANISMS

8.1 INTRODUCTION

In Chapter 4 the failure to obtain meaningful dates for volcanic lava was shown to be due to anomalous fading. In Chapter 7 several different minerals that exhibited anomalous fading were studied experimentally in an attempt to understand the phenomenon and see whether its effect on dating could be avoided. In this chapter I shall review anomalous fading as reported for lunar material and discuss similar phenomena in other materials which help to throw light onto possible mechanisms.

8.2 ANOMALOUS FADING IN LUNAR SAMPLES

In early studies of TL of lunar samples, the magnitude of the natural TL was many orders of magnitude below that expected from the accumulated dose of excitation from radioactive and cosmic ray sources on the lunar surface (Garlick and Robinson)., An explanation for this lack of natural TL could be seen when studies were made on artificially irradiated samples from the Apollo 11 and 12 missions (Hoyt et al, 1970; Dalrymple and Doell); various results are summarized in Fig. 8.1 which includes the results of an experiment carried out on a terrestrial plagioclase, labradorite (Garlick et al, 1971). From this diagram it can be seen that at room temperature the decay of trapped electrons in lunar samples is very similar for the different glow curve selected. The decays shown for the labradorite are much faster but again have the same slope for two different glow curve

However when the storage temperature is raised the shallower traps lose their electrons by the more usual, strongly temperature dependent thermal activation processes described in Chapter 3.

Similar results have been reported on samples of Apollo 14 rock which have been irradiated with 160 MeV protons and stored at -196°C (Blair, Edgington, Chen and Jahn); traps at 0°C, 50°C, 85°C and 110°C showed considerable decay within a few hours. Their preliminary results indicated an initial exponential decay superimposed on a steady component.

The effect of anomalous fading on the natural TL of lunar fines from the Apollo 12 and Apollo 14 missions has already been mentioned in Chapter 4. One grain in fifteen was shown to produce the natural TL, whereas some of the grains that gave no natural TL contributed substantially to the artificially induced TL (Hoyt et al, 1972). This could be explained by substantial anomalous fading having occurred in the majority of the grains. If this is the case then the use of the artificially induced TL of a bulk sample for normalization of the natural TL is likely to be misleading. This was indeed found to be so - no systematic variation of the 300°C to 400°C natural TL with depth below the lunar surface had been obtained when bulk samples had been used, but considerable improvement had been shown when single grain measurements were used.

8.3 TEMPERATURE INDEPENDENT FADING IN INORGANIC MATERIALS

(a) Diamond

An early example of temperature independent fading of TL was reported in 1950 for UV stimulated diamond (Bull and Garlick). The two peaks at 400K (127°C) and 520K (247°C) given on heating at 2.5°C/second were found to give rise to a lower light sum if stored at 90K (-183°C) for 6 hours

before glowing than if glowed immediately after UV excitation. Repeating the storage but at 289K (13°C), the effect of normal thermal activation became apparent as well. The mean life of the temperature independent component was about 10^5 seconds, whereas that predicted by kinetic analysis was about 10^{20} seconds.

(b) Photochromic materials

It has been found that there is an upper limit to the optical absorption coefficient that can be obtained in photochromic materials e.g. CaF_2, sodalite and $SrTiO_3$. The limit is reached when the concentration of photochromic centres is sufficiently high that the average time before an electron tunnels back to the recombination centres becomes short compared to the observation time (Faughnan; Faughnan, Staebler and Kiss).

Using the model shown in Fig. 8.2 of an electron removed from site A and trapped at site B a distance R away, Faughnan calculated the transition probability of the electron tunnelling from the trap at energy E_t to an excited state of the recombination centre of energy level E_e for which there is overlap of wave function with the trap level E_t. Using a square potential well Faughnan calculated the transition probability from time dependent perturbation theory and in the case of $SrTiO_3$ obtained numerical values of the tunnelling decay rate as a function of distance, Table 8.1. For $R < 40$ Å the tunnelling decay is so fast that closely spaced pairs will not contribute to the observed induced optical density.

Faughnan also showed that the decay of the optical density is proportional to log t and the slope of this is determined by the concentration of recombination centres, N_o. Values of N_o determined from experimental decay curves for $SrTiO_3$ and $CaTiO_3$ agree with values of N_o obtained from other measurements. The decays were found to be independent of storage

TABLE 8.1

TUNNELING DECAY RATE AND ASSOCIATED MEAN LIVES AS A FUNCTION OF THE DISTANCE R BETWEEN A TRAPPED ELECTRON AND ITS ASSOCIATED RECOMBINATION CENTRE

R/Å	$\tau_R^{-1}/\text{sec}^{-1}$	τ_R/sec
10	10^{13}	10^{-13}
20	10^{9}	10^{-9}
30	10^{5}	10^{-5}
40	10	0.1
42	1.6	0.6
43	1.0	1.0
44	.25	4
46	.04	25
50	10^{-3}	10^{3}
60	10^{-7}	10^{7}

temperature; for a Ni doped $SrTiO_3$ sample the decay at 4.2K was found to be identical to that at 77K.

(c) Zinc sulphide phosphors

It has been reported that traps of depth 0.1 eV in ZnS are emptied on storage at 4.2K and that the process is accompanied by strong luminescence, termed 'tunnel afterglow' (Riehl). The difference in area between two delayed glow curves was found to be equal to the difference in the two phosphorescent decays i.e. the decay process was 100% radiative. Since the decay was radiative he was able to show that there was the expected red shift of the emission spectrum of the afterglow with delay time; this is predicted if the photon energy is given as

$$E(h\nu) = E_g - (E_c + E_T) + \frac{e^2}{\epsilon_o r} \qquad (8.1)$$

where r is the spatial separation of the trap and recombination centre, ϵ_o is the static dielectric constant, E_g is the band gap energy and E_T and E_c are the depths of the trap and recombination centre respectively. The energy level diagram is shown in Fig. 8.3. If the probability for an electronic transition from the trap to the centre is expressed as

$$W(r) = W_o \exp(-r/r_o) \qquad (8.2)$$

where r_o is half the effective Bohr radius of the trap, there is good agreement with the experimental afterglow decay curve.

(d) TL dosimetry phosphors

Fading has been reported in many different phosphors but collation of results by different authors is made difficult by their use of integrated glow curves which include thermal fading of low temperature peaks (Webb; Fowler). Another difficulty is the relatively small amount of fading, e.g. a few % or less in a month's storage at room temperature, and hence decay

curves have large experimental errors.

CaF_2:Mn, a widely used phosphor, has a broad peak centred at 250°C when heated at 1°C/minute (315°C at 10°C/second) which should be stable at room temperature. This is not so; it appears to lose about 10% of its TL at the peak in four weeks if measured at heating rates of 1°C/second or greater (Schulman). The amount of fading has been found to be dependent on the heating rate used (Schulman, Ginther, Gorbics, Nash, West and Attix) and this has been shown to be connected with thermal quenching occurring in the region of a peak which contains a distribution of trap depths (Gorbics et al, 1968(b)).

8.4 TEMPERATURE INDEPENDENT FADING IN ORGANIC MATERIALS

(a) Methylcyclohexane

When methylcyclohexane (MCH) doped with biphenyl has been γ irradiated at 77K, an isothermal luminescence (ITL) has been recorded over several hours (Kieffer, Meyer and Rigaut). Further irradiations were carried out at 4.2K and decays on storage at 4.2K, 66K and 77K were observed to be similar; in fact if the decay curves are normalized by their initial intensities the curves can be superimposed and it can therefore be assumed that the method of recombination at the three different temperatures is the same. Thermal untrapping of electrons at 4.2K ($kT \approx 3.6 \times 10^{-4}$ eV) is extremely unlikely and electron tunnelling has been suggested as the mechanism giving rise to the deferred luminescence (Kieffer, Magat, Meyer and Rigaut). Application of a simple quantum mechanical model, similar to that used by Riehl for zinc sulphide, gave agreement with the detailed experimental results (Meyer).

(b) Tryptophan in ethylene glycol/water glass

The luminescence afterglow of UV irradiated tryptophan in EG/H_2O glass

has been observed to give a decay that is linear on a log I/I_o versus log t plot (Moan). The process of recombination is thought to be due to a temperature dependent effect connected with the viscosity of the material and an electron tunnelling effect which dominates the lower temperatures.

8.5 DEFECT DIFFUSION

The effect of diffusion of defects in materials being considered for TL dating is usually ignored but it has been suggested that over long periods of time at environmental temperatures a diffusion process with a low activation energy could be more important than electronic activation processes with higher activation energies (Townsend). In several cubic alkali halides the diffusion of defects is well known; in CaF_2 doped with a rare earth the diffusion of interstitial F^o atoms with an activation energy of about 0.8 eV has been shown to give rise to the 330K glow peak (Merz and Pershan). The aggregation of divalent ion-vacancy pairs have also been observed e.g. in LiF:Mg (Dryden and Shuter) and in NaCl and KCl doped with lead (Dryden and Harvey). The rate-limiting process is taken as the diffusion of the dipoles through the lattice and for Pb^{++}-vacancy pairs in NaCl and KCl the activation energies obtained are about 0.8 eV.

In fluorapatite theoretical analysis of anion vacancy diffusion has given activation energies of 0.77 eV and 2.0 eV for Fe^- and $O^=$ vacancies respectively (Welch and Royce) but the authors comment that vacancy diffusion in a real crystal would be easily blocked by impurities. Experimental studies of diffusion of Ca^{2+}, PO_4^{3-} and OD^- ions in fluorapatite have been carried out at high temperatures, but on extrapolation to ambient temperature the diffusion coefficients obtained predict movement of about 1 Å in 10^{20} years (den Hartog, Welch and Royce). This implies that ion diffusion is highly

unlikely to give rise to fading.

8.6 DISCUSSION

(a) Type of materials exhibiting anomalous fading

As described in the previous chapter, the fading appears to be an intrinsic property of the material exhibiting it and is not connected with the method of sample preparation i.e. there is no grain size effect. Further evidence of the intrinsic nature of the phenomenon is shown by the fact that recrystallation of various feldspars that exhibited fading did not remove the effect; the slight changes in fading rate that did occur can be explained by a rearrangement of the relevant traps and centres.

These results suggest that the origin of the minerals is important in deciding whether they are likely to exhibit anomalous fading or not. Feldspars formed under conditions of rapid cooling e.g. in lava, are likely to contain more impurities than those igneous rocks that have formed much more slowly beneath the surface of the earth by consolidation from the magma, i.e. plutonic rocks, and it is highly likely that the anomalous fading is related to the presence of impurities. Most clay minerals are formed by the weathering of plutonic rocks and hence one would expect to find little or no anomalous fading in pottery made from such clay. However clay from a volcanic region is likely to contain minerals of volcanic origin and, in some cases, deliberate 'gritting' of the clay with volcanic rock by the potter is known. Hence pottery from a volcanic region must be thought likely to exhibit anomalous fading.

The fading does not appear to be connected with any particular trap as this would have shown up in TL loss connected with a particular glow peak, rather than loss throughout the glow curve often occurring at the same rate

for a few hundred degrees span of the glow curve . Similarly, assuming there are several types of centre present, it does not appear to be connected with any particular luminescent centre as the fading rates are negligibly different when the glow curves are taken using different filter systems. The occurrence of fading in many different minerals, feldspars (K, Na, Ca silicates), zircon ($ZrSiO_4$) and fluorapatite ($Ca_{10}(PO_4)_6F_2$), together with the above evidence suggests that the fading is connected with the number and arrangement of defects in the lattice rather than with the nature of the host material.

(b) Possible mechanisms

From the experimental data presented in Chapter 7, it is clear that in certain materials two processes are responsible for the loss of trapped electrons. There is the thermal activation process which follows a Boltzmann type probability relation

$$p = s \exp(-E/kT) \qquad (8.3)$$

This predicts the loss of electrons from a given trap of depth E to be strongly temperature dependent, and there is another process which allows electrons to 'leak away' from traps which should be deep enough to be assumed completely stable at the temperatures of observation. This process is not entirely 'non-thermal' as was first thought; for instance, section 7.3(a) shows that around room temperature a characteristic energy of 0.2 eV can be obtained for a component of the decay in plagioclase feldspar BA6, the energy being much less than that associated with the thermal activation of the electron from its trap (~ 1.6 eV). However at much lower storage temperatures fading still occurred and at a rate faster than predicted by even the lower activation energy (section 7.3).

From the studies of related phenomena in various materials in sections 8.2 to 8.6, two mechanisms are outstanding as likely explanations for

anomalous fading; these are -

(i) Defect diffusion - allowing non-radiative escape of trapped electrons when the diffusing defect encounters a trapping site;

(ii) Wave mechanical tunnelling - allowing direct transfer of an electron from a trap to an adjacent centre.

In addition to these two, a third possibility (discussed later) should be borne in mind -

(iii) Thermal decay of available activated luminescence centres i.e. decay of the probability for the production of luminescence by an electron when released from its trap in the course of a glow curve.

(c) Discussion of mechanisms

(i) Defect diffusion - From section 8.5 it seems unlikely that, in materials as impure as those that were studied in Chapter 7, defects are capable of diffusing at room temperature. It must also be remembered that in most materials the degree of fading did not allow analysis into two or three simple exponentials but were most simply expressed on a log-log plot and could be considered to be due to the sum of a large number of exponential decays. If this is to be explained by diffusion one must propose that there are as many defects capable of diffusing in the appropriate temperature range as there are exponential decay components. Also, one must allow for the fading at very low temperatures (77K, 20K) to be due to a defect diffusing with a very low activation energy indeed. The evidence seems to suggest that diffusion is not the cause of the anomalous fading observed in Chapter 7.

(ii) Tunnelling - This mechanism agrees far better with the exponential evidence though the straightforward tunnelling as suggested by Garlick and Robinson can hardly account for the temperature dependence observed in

feldspar BA6. That the decay is linear on a log-log plot is adequately explained in terms of a sum of exponential components corresponding to a distribution in the value of the separation r between trap and adjacent centre, the transition probability being given by

$$W = W_o \exp(-r/r_o) \qquad (8.4)$$

where r_o is half the effective Bohr radius of the trap.

However although the tunnelling process will exhibit a small temperature dependence due to change of lattice spacing and therefore of wave function overlap, it can hardly account for the marked temperature dependence shown by feldspar BA6 between -18°C and 150°C (Fig. 7.8). In this region, assuming a Boltzmann like temperature dependence

$$p = \tau^{-1} = A \exp(-B/kT) \qquad (8.5)$$

the value of B obtained is of the order of 0.2 eV which is well below the thermal activation energy obtained when the electron is thermally released during a glow curve. Also the value of the pre-exponential factor, A, was many orders of magnitude below those associated with the normal thermal activation process; typically $A \approx 10^0 = 1\ sec^{-1}$ compared with $s \approx 10^{14} sec^{-1}$.

One simple model which could describe such a system is shown in Fig. 8.4; (a) shows thermal activation of the electron out of its trap of depth E, as determined for instance by the initial rise method, followed by radiative recombination at the adjacent luminescence centre; (c) shows the tunnelling that takes place from the low energy states of the trap through the base of the potential barrier between the trap and the centre; (b) shows how the same model can allow for the thermal dependence of the fading as given by equation (8.5). In the intermediate temperature region, the electron can be thermally excited to an energy state from which it can tunnel through

the barrier to the adjacent centre and recombine, the energy of recombination being lost non-radiatively for the process as shown. Equation (8.5) should therefore be rewritten

$$p = W s \exp(-B/kT) \qquad (8.6)$$

where B is the characteristic energy, s is a pre-exponential factor $\sim 10^{14}\,sec^{-1}$ and W is a number $\sim 10^{-14}$, which is related to the probability of an electron tunnelling through the barrier once it has received sufficient thermal energy to reach a state $\geq$ B. This can be thought of as <u>thermally assisted tunnelling</u>.

A variety of values of B and W, and hence p, are possible depending upon the distortion of the lattice near a trap centre pair and this gives rise to the log-log time dependence of the fading at a given storage temperature

$$I/I_o = \sum_i n_i \exp(-p_i t) \qquad (8.7)$$

(iii) <u>Decay of activated luminescence centres</u> - For this mechanism it is postulated that some of the luminescence centres are only about 0.2 eV above the valence band and have a pre-exponential factor, s, of only $\sim 1\ sec^{-1}$. These values fit the observed temperature dependence of the fading (e.g. feldspar BA6) and the low value of s allows a substantial proportion of the centres that are 'unfaded' at the beginning of a glow curve to remain available for producing luminescence as the temperature is raised in the course of a glow curve. To explain this very low value of s one must postulate a very high degree of retrapping of holes at the luminescencc centre with a very low but finite probability of the hole being trapped at a nearby non-radiative centre, see Fig. 8.5.

This explanation still needs to invoke tunnelling to explain the observed decay at very low temperatures; this could be either a contribution to the

fading from mechanism (ii) or it could be in terms of mechanism (iii) i.e. from non-radiative centre to luminescence centre as shown in Fig. 8.5(c).

The experimental result that the fading does not appear to be connected with any one luminescence centre is not incompatible with this mechanism; it can be explained by all the luminescence centres having an energy state about the same height above the valence band. This model can also explain why in some minerals there is an almost equal loss of TL throughout the glow curve; the fading depends only on the presence of activated luminescence centres and is unconnected with the different traps that are emptied in that part of the glow curve.

(d) Spatial distribution of traps and centres

One other piece of related information obtainable from the results of Chapter 7 is the implication that the fading takes place between spatially related trap-centre pairs. If the traps and centres were randomly distributed throughout the lattice, there would be an increase in fading rate with an increase in the total dose given due to the increased chance of a trapped electron finding an activated luminescent centre within a distance that permits tunnelling. In section 7.9 it was shown that for fluorapatite there was only a slight increase in fading rate due to giving the sample a Megarad dose using an X-ray source compared with that after giving a krad dose to the same sample with a $^{90}Sr/^{90}Y$ beta source. Similarly the rate of fading for alpha irradiated samples, where the heavily ionized tracks will be in saturation, has only a slightly faster fading rate. If the fading had taken place very rapidly (i.e. before a measurement could have been made) then the effect would have been shown up by an anomalously low k value (ratio of α sensitivity/β sensitivity); the k values were quite normal however, about 0.1. This also supports the pairing of the traps with their associated luminescence centres.

8.7 IMPLICATIONS

It is now appropriate to consider whether either of the most likely mechanisms (ii) and (iii), have any practical implications for dating. Probably the most important implication is from (iii); since traps are not involved, an alternative way of determining the trapped electron population should be immune to fading if this mechanism is dominant. Possible techniques are electron spin resonance (ESR), thermally stimulated exoelectron emission (TSEE) and thermally stimulated current (TSC). The first of these is several orders of magnitude too insensitive for the level of radiation dosage involved. The third has been tried by Hwang and Fremlin but appears to be impractical because the effect of ion-vacancy annealing predominates (Hwang and Fremlin). The second remains a possibility but at the time of writing the reliability of TSEE measurements is insufficient for it to be considered as an accurate dating technique whether or not subject to fading.

As regards TL dating itself a critical question is whether measurement of short-term fading can be used to predict long-term fading; is it even possible that samples which show negligible short-term fading can nevertheless have a substantial long-term fading component? Unfortunately neither mechanism allows a conclusive denial of this possibility, nor do the results given in Chapter 7. In mechanism (ii) the closest separation of any trap-centre pair could be such that the mean life of the thermally assisted tunnelling is of the order of hundreds of years. There is also nothing in the model to say what percentage of the total trap-centre pairs is at this separation; for example in the case of feldspar BA6, there were three roughly equal components, but other materials appeared to have a larger number of small components. Similarly in the other model, (iii), there is nothing to say that the height of the luminescence centre that is closest to

the valence band has an associated mean life of the order of hundreds of years.

Hence the fact that a sample passes a short-term fading test cannot be taken as conclusive evidence that no fading has occurred during archaeological time, though such a sample is more likely to give a correct date than a sample that shows short-term fading. It is also implicit in the above discussion that samples in the latter category must be rejected and that any attempt to make a correction for fading is likely to be unreliable.

In view of this pessimism it is appropriate, in conclusion, to review the arguments for accepting the reliability of any TL dates. The source of the pessimism is the discovery that for feldspar samples the mean lifetime of trapped electrons may be several orders of magnitude less than the value predicted by laboratory measurement of the trap parameters E and s. However the results of Chapters 5 and 6 indicate that for quartz and limestone the observed mean lifetimes are not inconsistent with the predicted values. The reliability of quartz is substantiated by the test programme reported by Fleming in which the TL ages for the quartz inclusions from some twenty Romano-British pottery fragments agreed with the known archaeologic ages with a standard deviation of less than 6% (Fleming, 1970).

Hence it is reasonable to accept the reliability of TL dates based on quartz and probably also those based on limestone. For other minerals a necessary criterion is that the sample does not exhibit short-term fading. A second and obvious criterion is that samples from the same age context should give the same TL age, since it is unlikely that all will have suffered the same degree of anomalous fading.

Since a test programme on pottery of known age (Zimmerman, 1971(a)) gave reliable TL dates for unseparated mineral constituents, these being

probably dominated by feldspars, it must be assumed that the above criteria were satisfied although the first was not checked. In the initial work on lava reported in Chapter 4 of this thesis, the test programme showed that the TL dates were in violent disagreement with the geological ages and the subsequent work described here shows that this was due to the minerals violating these two criteria.

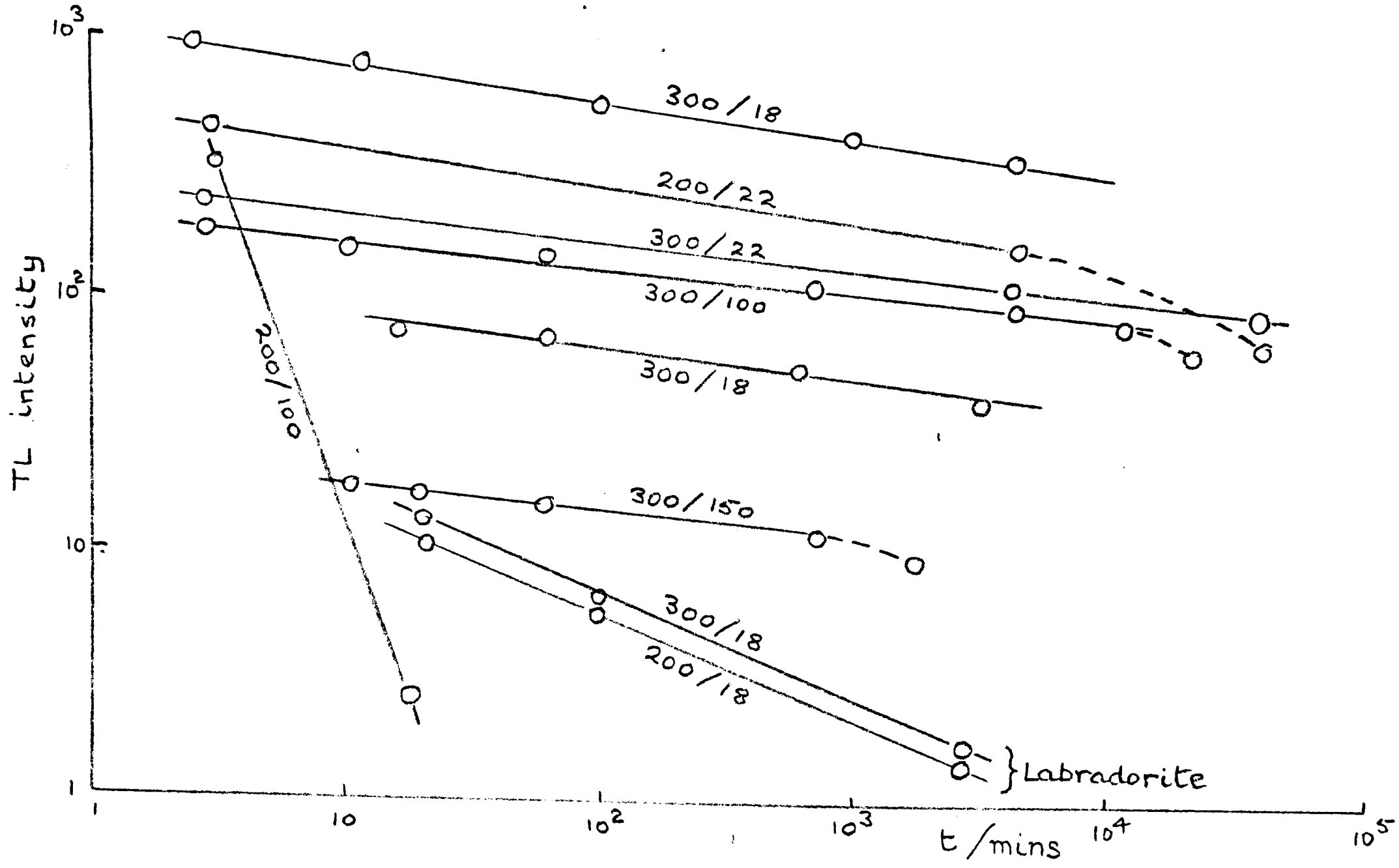

Fig. 8.1 TL decay in Apollo 11 samples vs. storage time. The first number on the curves is the TL abscissa in ^{o}C, the second the storage temperature in ^{o}C

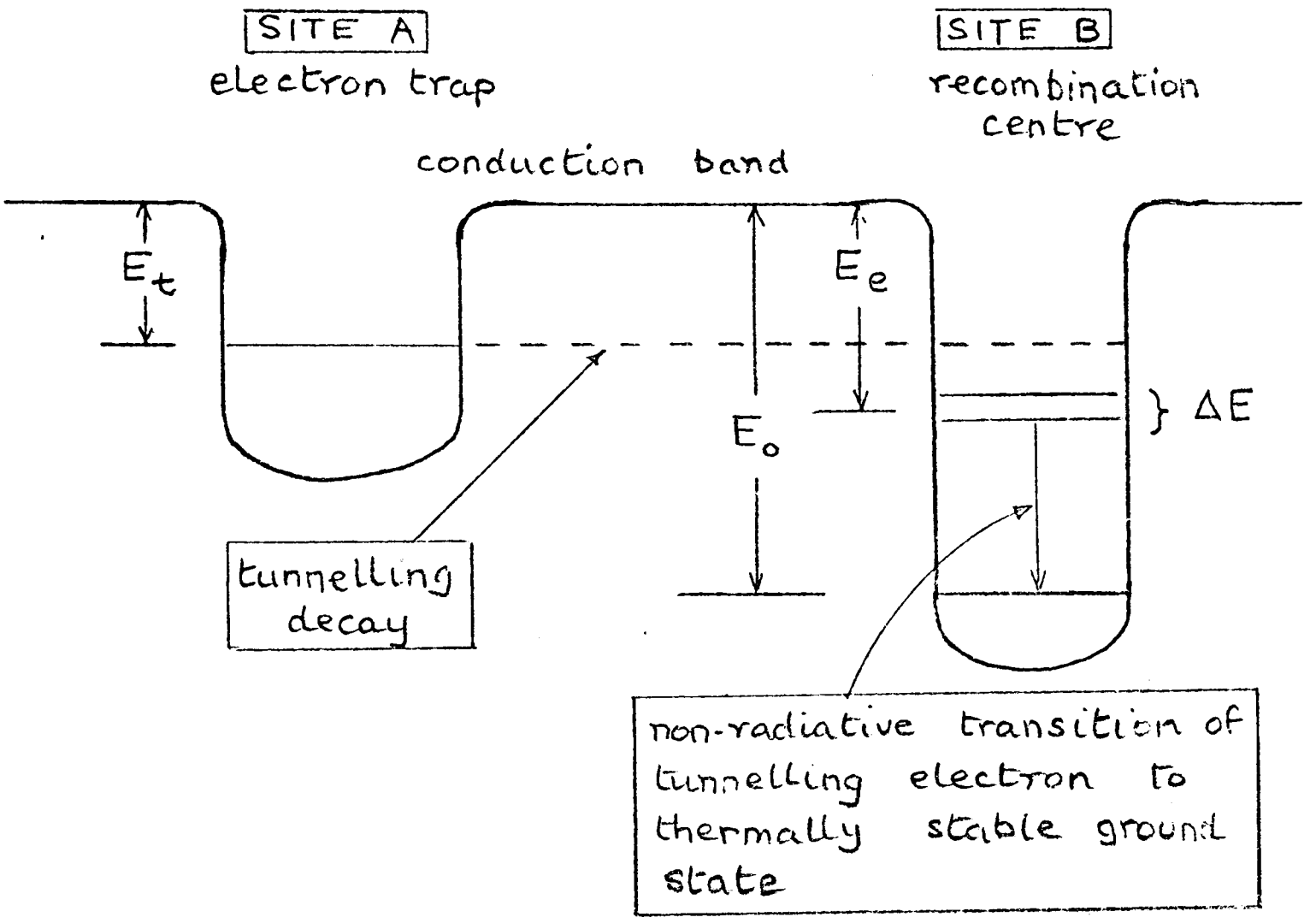

Fig. 8.2 Energy level diagram for tunnelling in photochromic materials (after Faughnan)

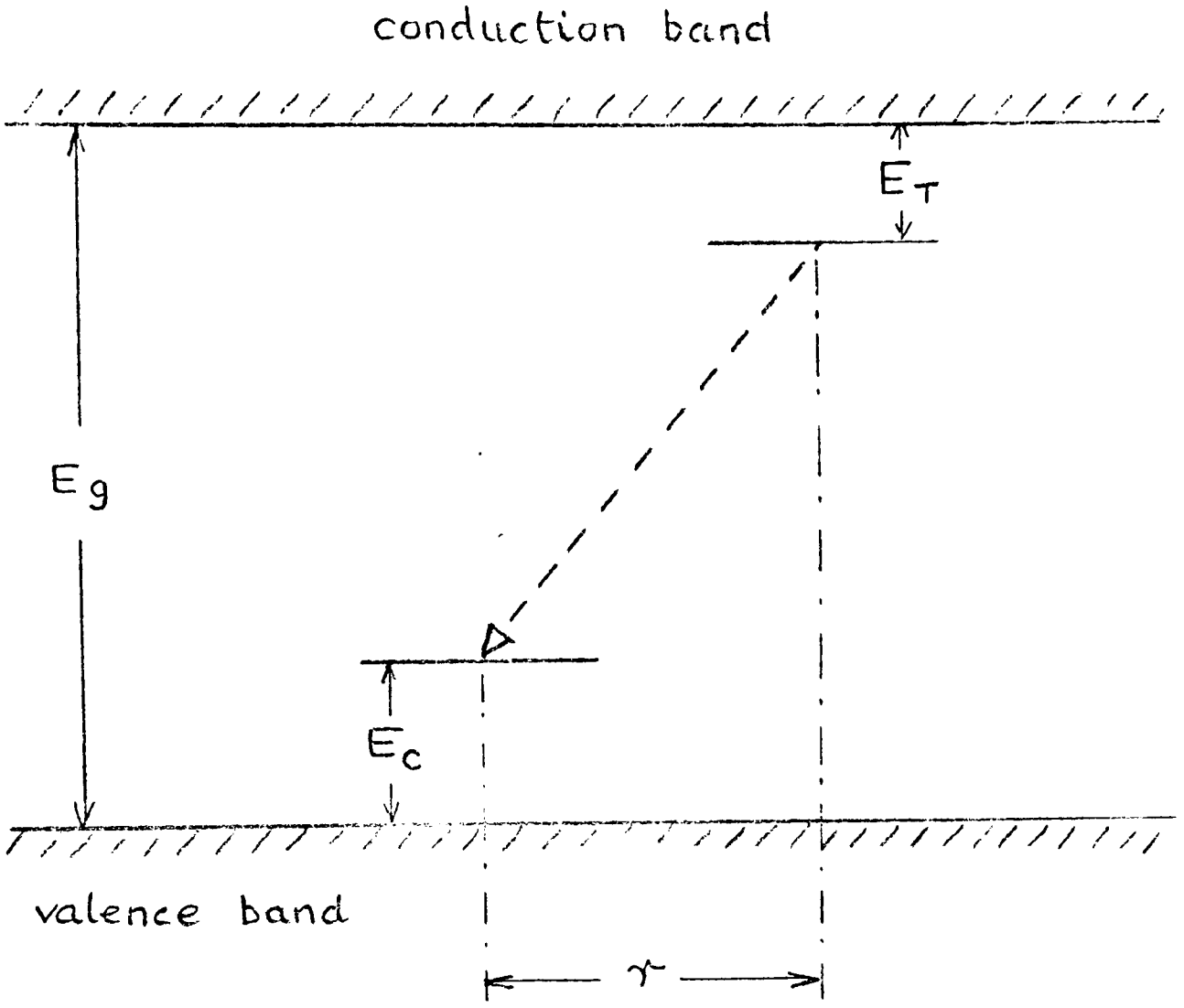

$$E\,(h\nu) = E_g - (E_c + E_T) + e^2/\epsilon_o r$$

Fig. 8.3 Direct transfer of electron from trap to centre

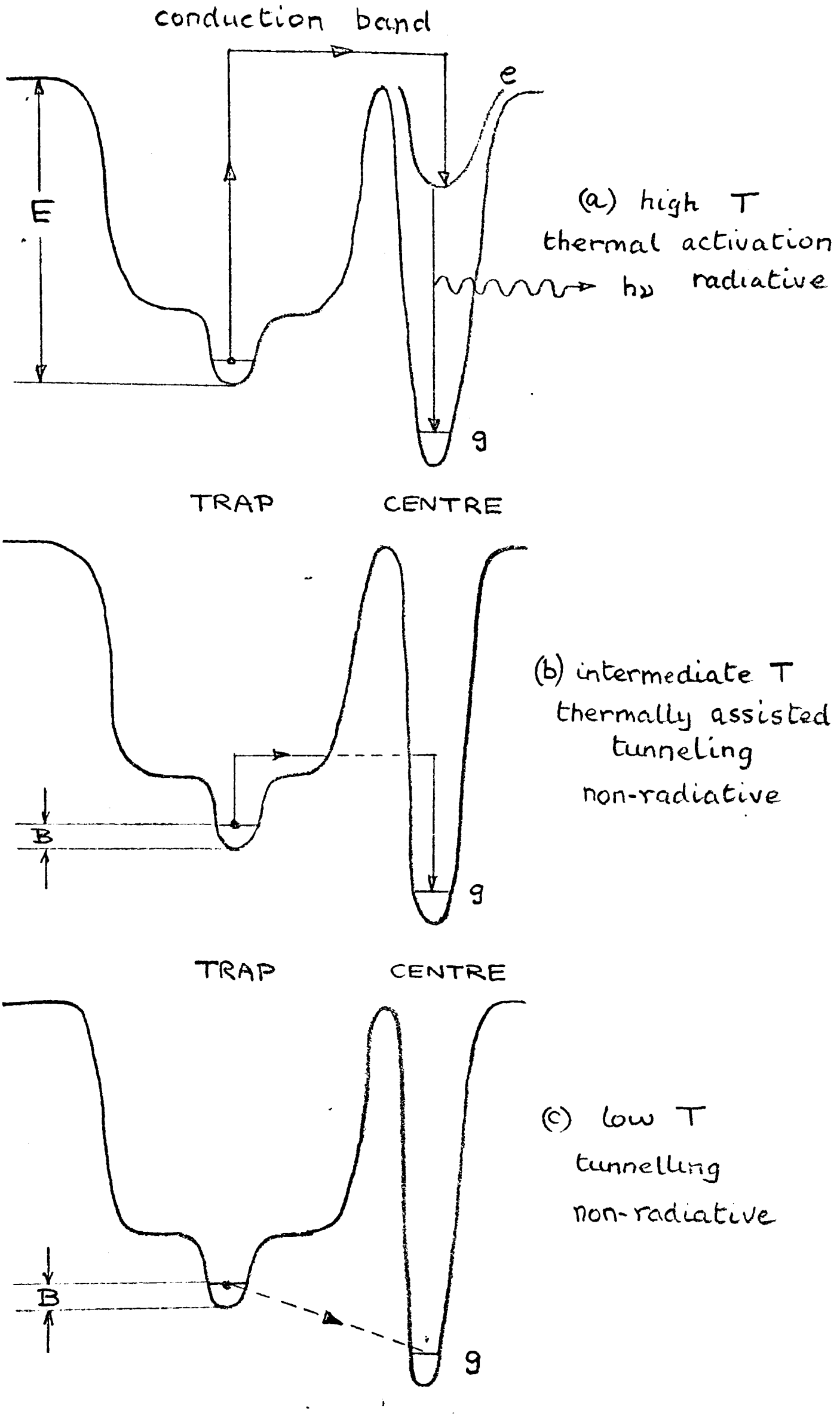

Fig. 8.4 Model A for anomalous fading, involving the trapped electron and the activated luminescence centre

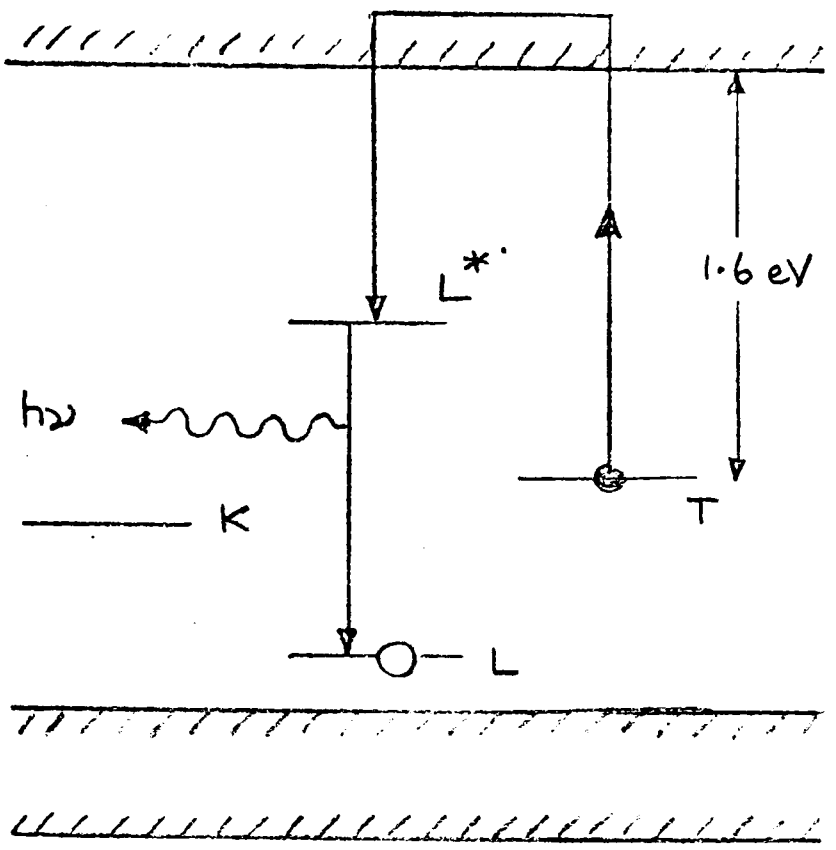

(a) high T

thermal activation

radiative

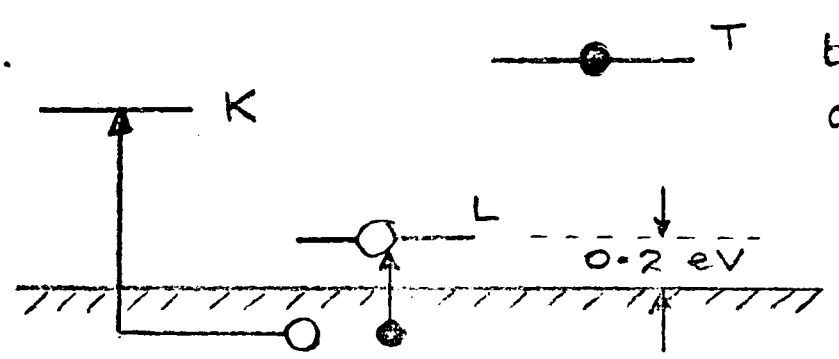

(b) intermediate T

thermal untrapping of hole traps with high retrapping

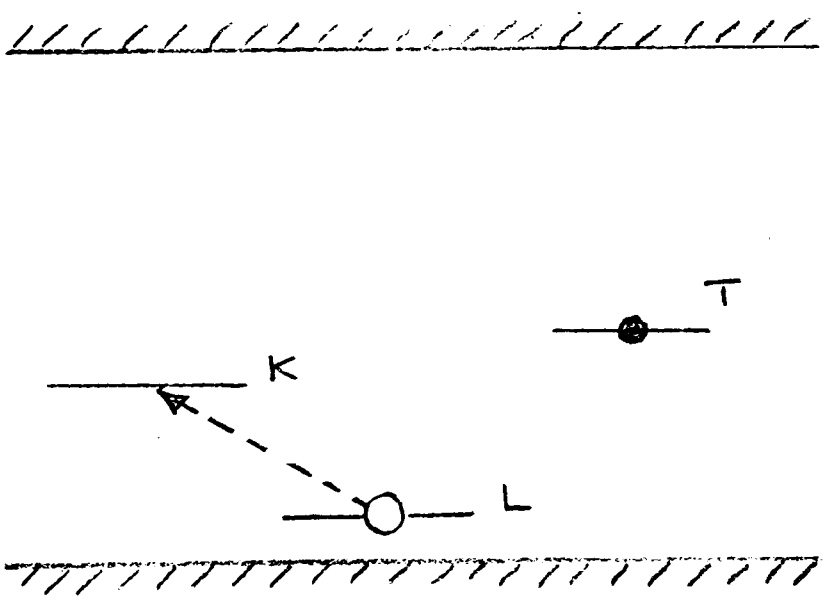

(c) low T

tunnelling

Fig. 8.5 Model B for anomalous fading, not involving the trapped electron

APPENDIX A

EFFECT OF RADIOACTIVE DISEQUILIBRIUM

(a) Let us consider the effect of disequilibrium of ^{226}Ra on the determination of the age of a sample by TL dating when the radioactivity is estimated from the measured ^{238}U content. At a time t after the disequilibrium has occurred, laboratory measurement of the ^{226}Ra and ^{238}U activities would give an activity ratio

$$\frac{A(^{226}Ra)}{A(^{238}U)} = F(t) \qquad (A.1)$$

where $F(t) \neq 1$ and the activities are given as

$$A(^{238}U) = U(t)\lambda_u = U_o\lambda_u \exp(-\lambda_u t) \qquad (A.2)$$

where U_o is the number of uranium atoms at $t = 0$ and λ_u is the uranium decay constant and

$$A(^{226}Ra) = R(t)\,\lambda_R \qquad (A.3)$$

The total number of atoms of ^{226}Ra at time t after the introduction of the disequilibrium is given as

$$R(t) = \frac{\lambda_u}{\lambda_R - \lambda_u} U_o \left[\exp(-\lambda_u t) - \exp(-\lambda_R t)\right] + R_o \exp(-\lambda_R t) \qquad (A.4)$$

Combining these equations we can obtain an expression for the initial total number of ^{226}Ra atoms,

$$R_o = \frac{\lambda_u}{\lambda_R} F(t)\, U_o \exp(\lambda_R - \lambda_u)t - \frac{\lambda_u}{\lambda_R - \lambda_u} U_o \left[\exp(\lambda_R - \lambda_u)t - 1\right] \qquad (A.5)$$

We are now in a position to be able to calculate the number of disintegrations due to the excess ^{226}Ra ($F(t) > 1$),

$$\Delta Ra = \left[R_o - R(t)\right]_{F(t)>1} - \left[R_o - R(t)\right]_{F(t)=1}$$

$$= U_o \frac{\lambda_u}{\lambda_R} \left[\exp(\lambda_R - \lambda_u)t - \exp(-\lambda_u t)\right] \left\{F(t) - 1\right\} \qquad (A.6)$$

This can be simplified as $\lambda_u \ll \lambda_R$, i.e.

$$\Delta Ra = U_o \frac{\lambda_u}{\lambda_R} \left[\exp(\lambda_R t) - 1\right] \left\{F(t) - 1\right\} \qquad (A.7)$$

Also the number of parent ^{238}U atoms that have decayed in a time t is

$$U_{eq} = U_o \lambda_u t \qquad (A.8)$$

Hence in a time t the fractional excess dose X received by the sample above the equilibrium dose rate will be given as

$$X = \frac{\text{Dose } \Delta Ra}{\text{Dose } U_{eq}} = \frac{e^{\lambda_R t} - 1}{\lambda_R t} \left\{F(t) - 1\right\} \left[\frac{kE\alpha + E\beta + E\gamma}{kE\alpha' + E\beta' + E\gamma'}\right] \qquad (A.9)$$

where $E\alpha$, $E\beta$, and $E\gamma$ are the total alpha, beta and gamma energies associated with each complete disintegration (right hand column of Table A.1) and $E\alpha'$, $E\beta'$ and $E\gamma'$ are the energies of the complete decay after ^{226}Ra (centre column of Table A.1) and k is the alpha efficiency (this is in the range 0.05 to 0.3). Substituting these values in equation A.9, one obtains

$$X = \frac{\text{Dose } \Delta Ra}{\text{Dose } U_{eq}} = 0.719 \frac{e^{\lambda_R t} - 1}{\lambda_R t} \left\{F(t) - 1\right\} \qquad (A.10)$$

For example if the present day activity ratio F(t) is 1.1 and if the sample is 4,800 years old $\lambda t = 3$ and hence the dose ratio X = 0.46,

indicating a 46% error in the total dose received by the sample due to the ^{238}U chain if equilibrium with ^{238}U is assumed. A present day activity ratio $F(t) = 1.1$ would have been caused by an initial disequilibrium $F(0) = 3.0$; this is given by the equation

$$F(t) - 1 = (F(0) - 1) \exp(-\lambda t)$$

Hence an age that is 23% too high would be evaluated if the uranium chain is responsible for half the dose and if its dose rate is calculated assuming equilibrium.

(b) Let us also consider the total dose that would be obtained if a thick source alpha count was measured and secular equilibrium was assumed. Turner, Radley and Mayneord made the simplifying assumption that the mean range of α particles for the complete series ^{238}U to ^{206}Pb is the same as for the shorter series ^{226}Ra to ^{206}Pb and hence the α counting formula is simply

$$8(U) + 5(\Delta Ra) = 8(U') \qquad (A.11)$$

where (U') is the calculated activity of a uranium series in equilibrium and (ΔRa) is the activity of the excess ^{226}Ra.

The present day disequilibrium is defined as

$$F(t) = \frac{(Ra)}{(U)} = 1 + \frac{(\Delta Ra)}{(U)}$$

and hence

$$(\Delta Ra) = (U)\{F(t) - 1\} \qquad (A.12)$$

Combining equations A.11 and A.12, one obtains

$$(U') = (U)(1 + \tfrac{5}{8}\{F(t) - 1\}) \qquad (A.13)$$

The error in the total dose rate obtained using this value for the uranium activity is given as

$$E = \frac{\text{Dose } \Delta Ra + \text{Dose } Ueq - \text{Dose } U'}{\text{Dose } U'} \qquad (A.14)$$

and using equations A.7, A.8 and A.13, equation A.14 becomes

$$E = \left[U_o \frac{\lambda_u}{\lambda_R} \left\{ \frac{\exp(\lambda_R t) - 1}{} \right\} \left\{ \frac{F(t) - 1}{} \right\} f(E') - \tfrac{5}{8} \frac{U_o \lambda_u t \{F(t) - 1\}}{} f(E) \right] \Big/ U_o \lambda_u t \left[1 + \tfrac{5}{8} \{F(t) - 1\} \right] f(E)$$

$$= \frac{\left[\exp(\lambda_R t) - 1 \right] \{F(t) - 1\}}{\lambda_R t \left[H \tfrac{5}{8} \{F(t) - 1\} \right]} \frac{f(E')}{f(E)} - \tfrac{5}{8} \frac{\{F(t) - 1\}}{\left[1 + \tfrac{5}{8} \{F(t) - 1\} \right]}$$

$$= \frac{\{F(t) - 1\}}{\left[1 + \tfrac{5}{8} \{F(t) - 1\} \right]} \left[\frac{\exp(\lambda_R t) - 1}{\lambda_R t} \frac{f(E')}{F(E)} - \tfrac{5}{8} \right]$$

where $$\frac{f(E')}{f(E)} = \frac{kE\alpha + E\beta + E\gamma}{kE\alpha' + E\beta' + E\gamma'} = 0.719$$

TABLE A1

ENERGIES IN MeV ASSOCIATED WITH EACH COMPLETE

DISINTEGRATION OF THE URANIUM CHAIN

Type	Pre ^{226}Ra	Post ^{226}Ra	Total
α	13.62	29.25	42.87
β	.88	1.12	2.00
γ	.07	1.85	1.93
Effective energy	2.31	5.90	8.21

APPENDIX B

i. OPTICAL EMISSION DATA USING FILTROMETER

The filtrometer was constructed by S.J. Fleming for observation of spurious TL in dosimetry phosphors (Fleming, 1968). Fig. B1 shows the calibrated EMI 6256 PM tube receiving light via interchangeable interference filters. The Balzers broad band interference filters used are shown in Fig. B2. A monitor channel using a similar PM tube with two OB-10 (blue) filters was used to check for reproducibility.

The effective detection efficiency of the system was derived by taking the transmission spectrum of each filter at 10 nm intervals and multiplying it by the corresponding cathode quantum efficiency at each wavelength. These products were then summed for each filter. The measured PM tube response divided by the effective detection efficiency approximates to the actual emission spectrum.

ii OPTICAL EMISSION SPECTRA USING A SPECTROMETER

The sample was in the form of a crystal about 0.3 ins in diameter and about 0.15 in thick. The largest opposing faces were ground and polished to improve thermal contact and to enhance the light output. After irradiation it was placed on the heater cylinder and heated at 20^{o}C/minute in the evacuated sample chamber. The light emitted by the sample passed through a quartz window and on to a mirror which reflected the light through a quartz

lens and on to the entrance slit of a Bausch and Lomb spectrometer, Fig. B3. The slit width was set at 15 nm pass width and the light was observed using an EMI extended S-20 photomultiplier which was cooled by passing cold N_2 gas through the housing. A small percentage of the total light output passed through a scratch in the mirror and was observed by another S-20 photo-multiplier tube. This was used to compensate for the signal decay whilst scanning the main signal at a fixed temperature. The scanning rate was 100 nm per minute. The intensities were measured using DC amplifiers and the outputs were fed to chart recorders, a third being used to monitor the temperature as observed by the chrome-alumel thermocouple. The X-ray dose rate was 10^4 R/minute and the sample was irradiated for 20 minutes before starting the optical measurements.

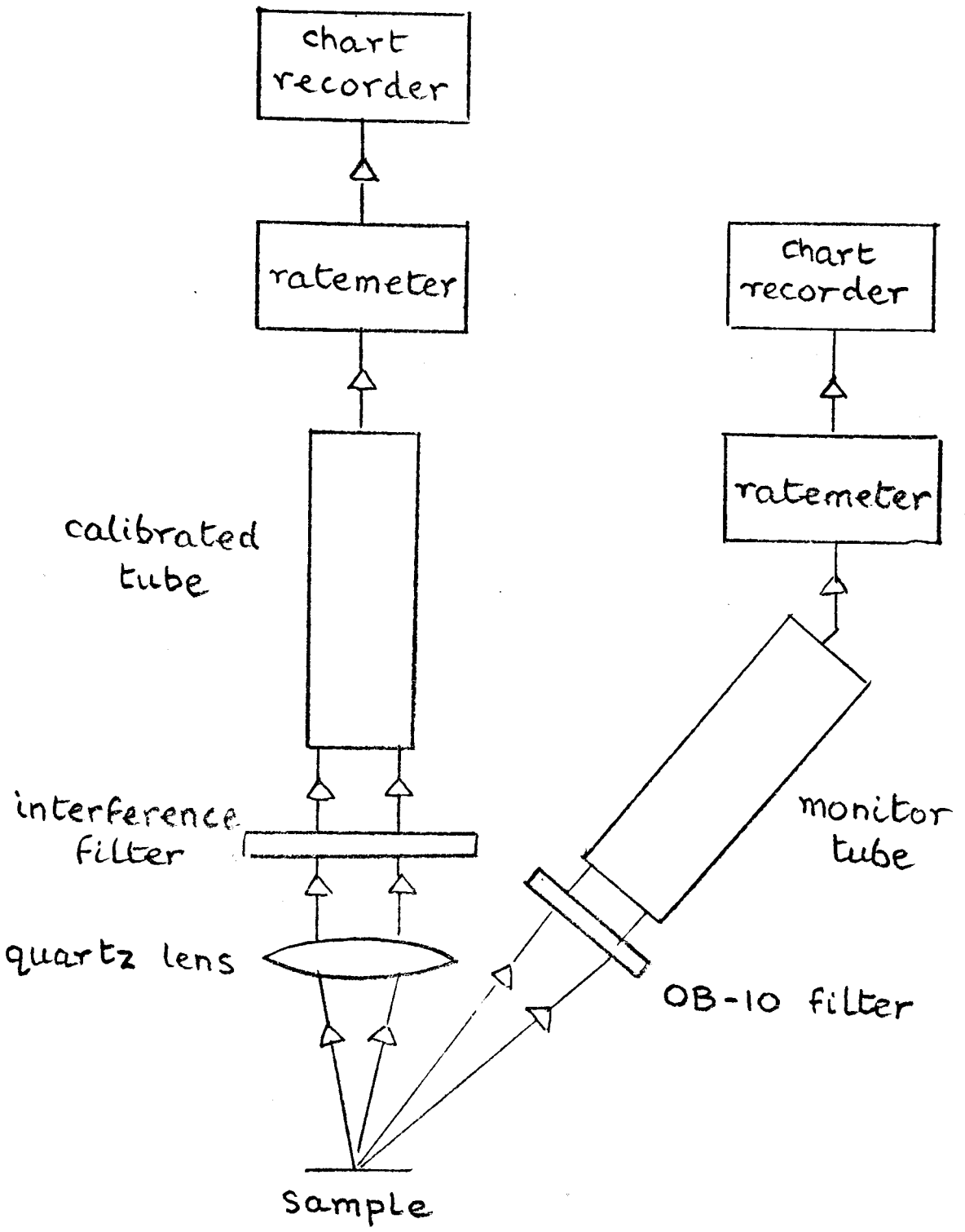

Fig. B.1 Block diagram of filtrometer

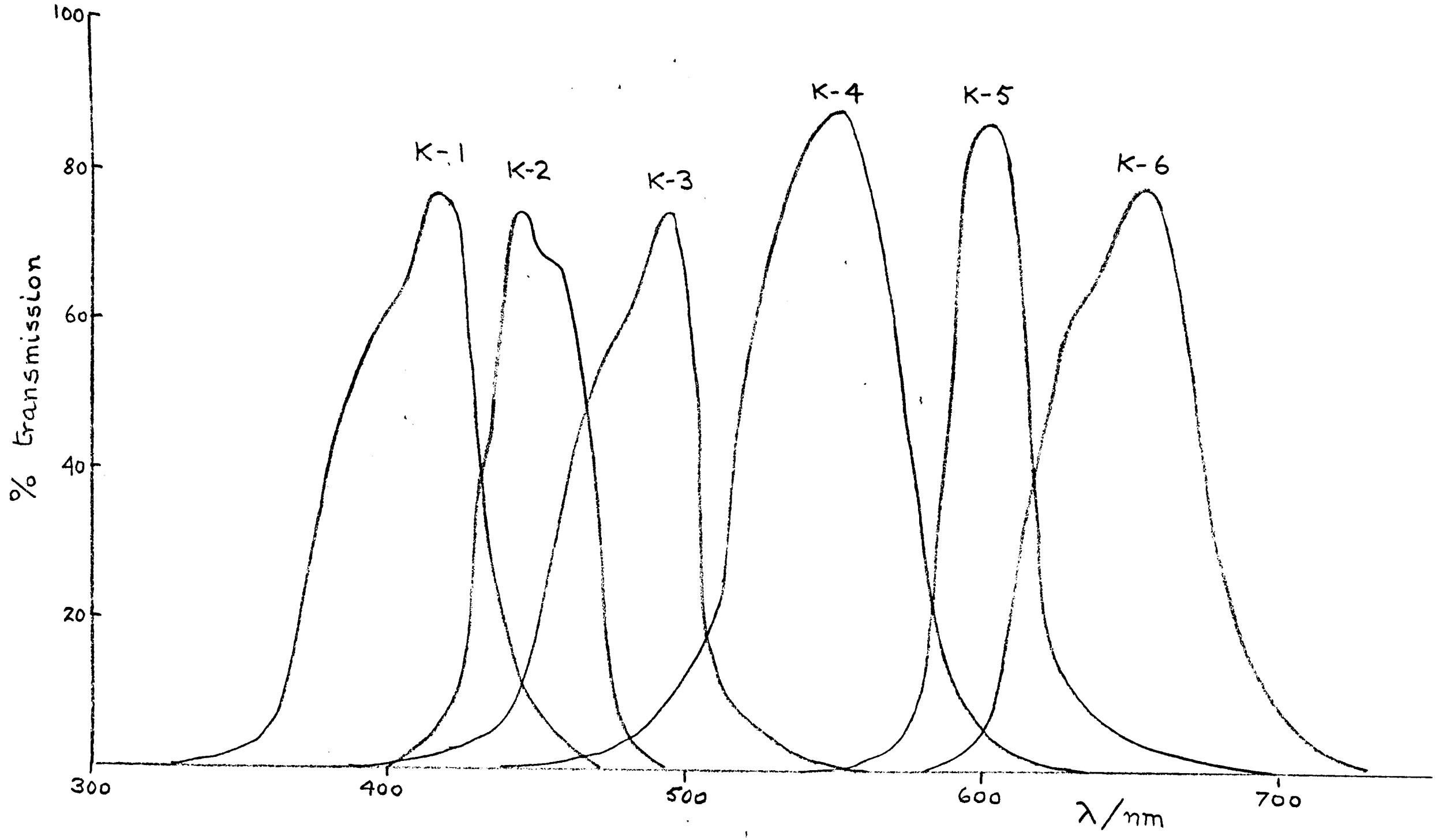

Fig. B.2 Transmission spectra of interference filters

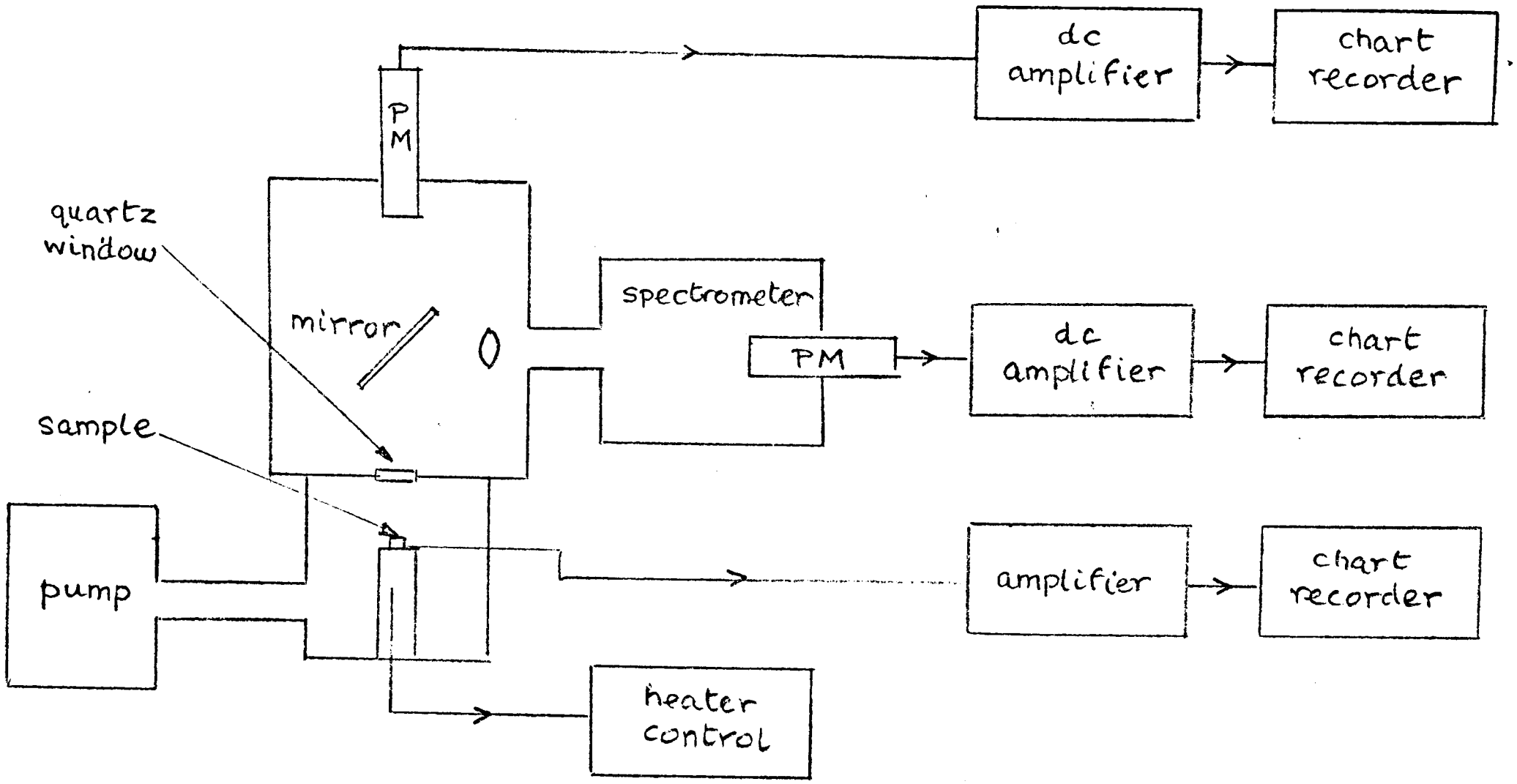

Fig. B.3 Optical transmission equipment

ACKNOWLEDGEMENTS

I thank Dr. M.J. Aitken for his advice and encouragement throughout the project. I also wish to thank J.C. Alldred for many helpful discussions. Useful discussions were also held with Dr. I.M. Blair, Prof. A. Charlesby, Prof. G.F.J. Garlick, Dr. S. Moorbath, Dr. P.D. Townsend and Dr. D.W. Zimmerman.

I also thank Prof. Sigugeirsson for his hospitality whilst collecting lava in Iceland and Dr. G.W. Grindley for collecting samples in Italy. I thank Dr. F.B. Atkins of the University Museum, Oxford, and Dr. B. Butler for giving me samples from their collections. I thank Mrs. Susanne Palmer for the burnt limestone from Portland Bill, Dorset, and Dr. N.M. Johnson for the contact metamorphosed limestone.

I thank Mrs. G. Huxtable for performing all the potassium analyses in this thesis and R. Curtis for technical assistance.

Financial assistance from the N.E.R.C. is gratefully acknowledged.

I finally wish to thank my typist Mrs. E.N. Farr and everyone else who helped in the preparation of this thesis.

.....

REFERENCES

AITKEN, M.J. (1969) Archaeometry, 11, 109

AITKEN, M.J., TITE, M.S., REID, J. (1963) Archaeometry, 6, 11

AITKEN, M.J., THOMPSON, J., FLEMING, S.J. (1968) Proc.Int.Conf.Lumin. Dosim., 2nd, Gatlinburg, Tenn., 364

AITKEN, M.J., FLEMING, S.J., DOELL, R.R., TANGUY, J.C. (1968(a)) in TL of Geological Materials (ed. D.J. McDougall), Academic Press, 359

AITKEN, M.J., FLEMING, S.J., REID, J., TITE, M.S. (1968(b)) in TL of Geological Materials (ed. D.J. McDougall), Academic Press, 133

AITKEN, M.J., FLEMING, S.J. (1971) The 1st International Scientific Congress on the Volcano of Thera, 293

AITKEN, M.J., ALLDRED, J.C. (1972) Archaeometry, 14, 257

AITKEN, M.J. FLEMING, S.J. (1973) in Topics in Radiation Dosimetry, Supplement 1, (ed. F.H. Attix) Academic Press, 1

d'ALBISSIN, M., FORNACA-RINALDI, G. (1968) in TL of Geological Materials (ed. D.J. McDougall), Academic Press, 241

ALEKSEEV, V.V., GRAMMAKOV, A.G., NIKONOV, A.I., TAFEEV, G.P. (1957) Radiometric methods in the prospecting and exploration of uranium ores, Ministry of Geologyand Mineral Resources Conservation, USSR

ALLMAN, M., LAWRENCE, D.F. (1972) Geological laboratory techniques, Pub. Blandford Press, London

BERRY, A.L. (1973) J.Geophys.Res., 78, 6863

BETTINALI, C., FERRARESSO, G. (1968) in TL of Geological Materials (ed. D.J. McDougall), Academic Press, 143

BIMSON, M. (1969) Studies in Conservation, 14, 83

BLAIR, I.M., EDGINGTON, J.A., CHEN, R., JAHN, R.A. (1972) Proc. Third Lunar Sci.Conf. Geochim.Cosmochim.Acta, Suppl.3, 3, 2949

BONHOMMET, N., ZÄHRINGER, J. (1969) Earth and Planetary Science Letters, 6, 43

BOTHNER, M.H., JOHNSON, N.M. (1969) J.Geophys.Res., 74, 5331

BRÄUNLICH, P. (1967) J.Appl.Phys., 38, 2516

BRÄUNLICH, P. (1968) in TL of Geological Materials (ed. D.J. McDougall), Academic Press, 241

BROECKER, W.S., BENDER, M.L. (1972) in Calibration of Hominoid Evolution, (ed. W.W. Bishop and J.A. Miller), Scottish Academic Press, 19

BULL, C., GARLICK, G.F.J. (1950) Proc.Roy.Soc.Lond., 63, 1283

CHEN, R., HABER, G.A. (1968) Chem.Phys.Lett., 2, 483

CHEN, R., WINER, S.A.A. (1970) J.Appl.Phys., 41, 5227

CHERRY, R.D. (1964) in 'The Natural Radiation Environment' (J.A.S. Adams and W.M. Lowder, eds.), 407, University of Chicago Press

CHRISTODOULIDES, C., ETTINGER, K.V. (1971) Modern Geology, 2, 235

CHRISTODOULIDES, C., FREMLIN, J.H. (1971) Nature, 232, 257

CURIE, D. (1963) Luminescence in Crystals (Methuen, London)

DALRYMPLE, G.B. (1968) Earth and Planetary Science Letters, 3, 289

DALRYMPLE, G.B., DOELL, R.R. (1970), Proc.Apollo 11 Lunar Sci.Conf. Geochim.Cosmoschim.Acta Suppl.1, 3, 2081

DAMON, P.E., LONG, A., WALLICK, E.I. (1972) Proc.Eighth Int.Radiocarbon Dating Conference, A28

DEER, W.A., HOWIE, R.A., ZUSSMAN, J. (1966) An Introduction to the Rockforming Minerals, Pub.Longman

DELIBRIAS, G., GUILLIER, M.T., LABEYRIE, J. (1972) Radiocarbon, 14, 304

DESAI, V.S., AITKEN, M.J. (1974) Archaeometry, 16, 95

DRYDEN, J.S., HARVEY, G.G. (1969) J.Phys.C: Solid State Phys., 2, 603

DRYDEN, J.S., SHUTER, B. (1973) J.Phys.D: Appl.Phys., 6, 123

DUPLESSY, J.C., LABEYRIE, J., LALOU, C., NGUYEN, H.V. (1970) Nature, 226, 631

FAUGHNAN, B.W. (c.1970) R.C.A. reprint

FAUGHNAN, B.W., STAEBLER, D.L., KISS, Z.J. (1971) Applied Solid State Science, Advances in Materials and Device Research, 2, (ed. R. Wolfe), 107

FLEISCHER, R.L., HART, H.R. (1972) in Calibration of Hominoid Evolution (ed. W.W. Bishop and J.A. Miller), Scottish Academic Press, 135

FLEMING, S.J. (1968) Proc.Int.Conf.Lumin.Dosim., 2nd, Gatlinburg, Tenn., 266

FLEMING, S.J. (1969) Unpublished D.Phil. thesis, Oxford University

FLEMING, S.J. (1970) Archaeometry, 12, 133

FLEMING, S.J. (1974) New Scientist, 61, 808

FORD, D.C., THOMPSON, P., SCHWARCZ, H.P. (1971) in '2nd Guelph Symposium on Geomorphology' (eds. E. Yatsu and A. Falconer), 247

FORD, W.F. (1967) 'The effect of heat on ceramics', Maclaren and Sons, Ltd., 128

FOWLER, J.F. (1965) Nature, 207, 997

GARLICK, G.F.J., GIBSON, A.F. (1948) Proc.Phys.Soc., 60, 574

GARLICK, G.F.J., LAMB, W.E., STEIGMANN, G.A., GEAKE, J.E. (1971) Proc. Second Lunar Sci.Conf., Geochim.Cosmochim.Acta Suppl.2, 3, 2277

GARLICK, G.F.J., ROBINSON, I. (1972) The Moon (eds. S.K. Runcorn and H.C. Urey), I.A.U., 324

GOBRECHT, H., HOFMANN, D. (1966) J.Phys.Chem.Solids, 27, 509

GORBICS, S.G., NASH. A.E., ATTIX, F.H. (1968(a)) Proc.Int.Conf.Lumin.Dosim. 2nd, Gatlinburg, Tenn., 568

GORBICS, S.G., NASH, A.E., ATTIX, F.H. (1968(b)) Proc.Int.Conf.Lumin.Dosim. 2nd, Gatlinburg, Tenn., 587

HALPERIN, A., BRANER, A.A. (1960) Phys.Rev., 117, 408

HALPERIN, A., BRANER, A.A., BEN-ZVI, A., KRISTIANPOLLER, N. (1960) Phys. Rev., 117, 416

HALPERIN, A., CHU, W.Y., HABER, G.A., DROPKIN, J.J. (1967) International Conference on II-VI Semiconducting Compounds (Benjamin Press), 68

DEN HARTOG, H., WELCH, D.O., ROYCE, B.S.H. (1972) Phys.Status Solidi B, 53, 201

HOOGENSTRAATEN, W. (1958) Philips Res.Rep., 13, 515

HOYT, H.P., KARDOS, J.L., MIYAJIMA, M., SEITZ, M.G., SUN, S.S., WALKER, R.M., WITTELS, M.C. (1970) Proc.Apollo 11 Lunar Sci.Conf.Geochim. Cosmochim. Acta Suppl 1, 3, 2269

HOYT, H.P., WALKER R.M., ZIMMERMAN, D.W., ZIMMERMAN, J. (1972) Proc.3rd Lunar Sci.Conf., Vol.3, 2997

HUTCHISON, C.S. (1965) NZ Journal of Science, 8, 431

HWANG, F.S.W. (1970) Nature, 227, 940

HWANG, F.S.W., FREMLIN, J.H. (1970) Archaeometry, 12, 67

HWANG, F.S.W., GOKSU, H.Y. (1971) Modern Geology, 2, 225

ICHIKAWA, Y., TANIDA, M. (1969) Bull.Inst.Chem.Res., Kyoto University, 47, 23

ICHIKAWA, Y.,FUKUDA, S., HIGASHIMURA, T. (1970) Bull.Inst.Chem.Res., Kyoto University, 48, 40

INSLEY, H., FRECHETTE, V.D. (1955) 'Microscopy of Ceramics and Cements' Academic Press, 94

JAMIESON, J.C. (1953) J.Chem.Phys., 21, 1385

JOHNSON, N.M. (1960) J.Sediment.Petrology, 30, 305

JOHNSON, N.M. (1963) Journal of Geology, 71, 596

JOHNSON, N.M. (1965) J.Geophys.Res., 70, 4653

JOHNSON, N.M. (1966) Journal of Geology, 74, 607

JOHNSON, N.M., BLANCHARD, R.L. (1967) Amer.Mineralogist, 52, 1297

JOHNSON, P.D., WILLIAMS, F.E. (1952) J.Chem.Phys., 20, 124

KAUL, I.K., GANGULI, D.K., HESS, B.F.H. (1972) Modern Geology, 3, 201

KIEFFER, F., MAGAT, M., MEYER, C., RIGAUT, J. (1971) Nature (Phys.Sci.) 232, 130

KIEFFER, F., MEYER, C., RIGAUT, J. (1971) ChemPhys.Letters, 11, 359

KIGOSHI, K. (1967) Science, 156, 932

KLASENS, H.A. (1946) Nature, London, 158, 306

MEDLIN, W.L. (1961) Phys.Rev., 122, 837

MEDLIN, W.L. (1963(a)) J.Opt.Soc.Am., 53, 1276

MEDLIN, W.L. (1963(b)) J.Chem.Phys., 38, 1132

MEDLIN, W.L. (1968(a)) in TL of Geological Materials (ed. D.J. McDougall), Academic Press, 193

MEDLIN, W.L. (1968(b)) in TL of Geological Materials (ed. D.J. McDougall), Academic Press, 91

MEJDAHL, V. (1972) Archaeometry, 14, 245

MERZ, J.L., PERSHAN, P.S. (1967) Phys.Rev., 162, 217

MESOLELLA, K.J., MATHEWS, R.K., BROECKER, W.S., THURBER, D.L. (1969) J.Geol., 77, 250

MEYER, C. (1972) Thesis (unpublished), Universite de Paris-Sud, Centre d'Orsay

MITCHELL, R.S., McGAVOCK, E.H. (1960) Rocks and Minerals, 35, 553

MOAN, J. (1973) J.Luminescence, 6, 256

McDOUGALL, D.J. (1968) in TL of Geological Materials (ed. D.J. McDougall), 527, Academic Press

NICHOLAS, K.H., WOODS, J. (1964) Brit.J.Appl.Phys., 15, 783

NISHIMURA, S. (1970) Earth and Planetary Science Letters, 8, 293

OVERSBY, V.M., GAST, P.W. (1968) Earth and Planetary Science Letters, 5, 199

PORTNOV, A.M.,GOROBETS, B.S. (1969) Dokl.Akad.Nauk.SSSR, 184, 199 (transl. 184, 110)

RANDALL, J.T., WILKINS, M.H.F. (1945) Proc.Roy.Soc.London A, 184, 366

RAO, D.R., BOSE, H.N. (1971) Phys.Rev.B, 4, 2746

RAPOLLA, A., VITOZZI, P. (1967) IUGG Symposium on Physical Volcanology, 1

RIEHL, N. (1970)J.Luminescence, 1, 1

ROSHOLT, J.N., EMILIANI, C., GEISS, J., KOCZY, F.F., WANGERSKY, P.J. (1961) J.Geology, 69, 162

ROSHOLT, J.N., NOBLE, D.C. (1969) Earth and Planetary Science Letters, 6, 268

SABELS, B.E. (1962) in Symposium of Radioactive Dating (IAEA, Vienna) 87

SCHULMAN, J.H. (1965) 1st Int.Conf.on Luminescence Dosimetry, Stanford University, 21

SCHULMAN, J.H., GINTHER, R.J., GORBICS, S.G., NASH, A.E., WEST, E.J., ATTIX, F.H. (1969) Int.J.Appl.Radiat.Isotopes, 20, 523

SHALGAONKAR, C.S., NARLIKAR, A.V. (1972) J.Mater.Sci.GB, 7, 1465

SIPPEL, R.F., GLOVER, E.D. (1965) Science, 150 1283

SOMAYAJULU, B.L.K., TATSUMOTO, M., ROSHOLT, J.N., KNIGHT, R.J. (1966) Earth and Planetary Science Letters, 1, 387

TALIBUDEEN, O. (1964) Soils and Fertilizers, 27, 347

TANNER, A.B. (1964) in 'The Natural Radiation Environment' (J.A.S. Adams and W.M. Lowder, eds) 161, University of Chicago Press

THURBER, D.L. (1971) in Calibration of Hominoid Evolution (eds W.W. Bishop and J.A. Miller) Scottish Academic Press, 1

TITE, M.S., WAINE, J. (1962) Archaeometry, 5, 53

TOWNSEND, P.D. (1968) in TL of Geological Materials (ed. D.J. McDougall) 51, Academic Press

TURNER, R.C., RADLEY, J.M., MAYNEORD, W.V. (1958) Brit.J.Radiol., 31, 397

VAN DER PLAS, L. (1966) The Identification of Detrital Feldspars: Developments in Sedimentology, 6, Pub.Elsevier

VITA-FINZI, C. (1973) Recent Earth History, Macmillan

VOLCHOK, H.L., KULP, J.L. (1957) Geochimica et Cosmochimica Acta, 11, 219

WEBB, G.A.M. (1967) Brit.J.Appl.Phys., 18, 7

WELCH, D.O., ROYCE, B.S.H. (1973) Phys.Status Solidi B, 57, 193

WILKENING, M.H. (1974) Science, 183, 413

WILLIAMS, G.E., POLACH, H.A. (1969) Earth and Planetary Science Letters, 7, 240

WINTLE, A.G. (1973) Nature, 245, 143

WINTLE, A.G., OAKLEY, K.P. (1972) Archaeometry, 14, 277

ZELLER, E.J., WRAY, J.L., DANIELS, F. (1955) J.Chem.Phys., 23, 2187

ZIMMERMAN, D.W. (1971(a)) Archaeometry, 13, 29

ZIMMERMAN, J. (1971(b)) J.Phys.C: Solid St.Phys., 4, 3265

ZIMMERMAN, D.W. (1971(c)) Science, 174, 818

ZIMMERMAN, D.W. (1972) Radiation Effects, 14, 81